PCM enhanced ventilated window- Configuration and control strategy development

Hu, Yue

Publication date:
2020

Document Version
Publisher's PDF, also known as Version of record

PCM ENHANCED VENTILATED WINDOW- CONFIGURATION AND CONTROL STRATEGY DEVELOPMENT

BY
YUE HU

DISSERTATION SUBMITTED 2020

AALBORG UNIVERSITY
DENMARK

PCM ENHANCED VENTILATED WINDOW- CONFIGURATION AND CONTROL STRATEGY DEVELOPMENT

by

Yue Hu

AALBORG UNIVERSITY
DENMARK

Dissertation submitted

Dissertation submitted: March 2020

PhD supervisor: Prof. Per K. Heiselberg,
Aalborg University

PhD committee: Associate Professor Tine Steen Larsen (chairman)
Aalborg University

Professor Marco Perino
Politecnico di Torino

Professor Guilherme Carrilho da Graca
University of Lisbon

PhD Series: Faculty of Engineering and Science, Aalborg University

Department: Department of Civil Engineering

ISSN (online): 2446-1636
ISBN (online): 978-87-7210-622-9

Published by:
Aalborg University Press
Langagervej 2
DK – 9220 Aalborg Ø
Phone: +45 99407140
aauf@forlag.aau.dk
forlag.aau.dk

Printed in Denmark by Rosendahls, 2020

CV

Personal details

Name: Yue Hu

Date of birth: 26-06-1990

Nationality: Chinese

Tel: +45 52827174

Email: huyuefeiyue@163.com

Education

10.2016- 02.2020	Aalborg University, Denmark, Architecture Engineering, PhD study
09.2013-05.2016	Chongqing University, China, Heating, Gas Supply, Ventilating and Air Conditioning Engineering, Master study
09.2009-07.2013	Zhengzhou University, China, Building Environment and Equipment Engineering, Bachelor study

Project experiences

- Iceiling project- Intelligent cooling and heating ceiling with energy storage (10. 2019-now)
- EU Horizon 2020 ReCO2ST project- PCM enhanced ventilated window (01.2018-now)
- Denmark horning company PCM ventilated window project (10. 2016-01.2018)
- Master project-Testing the night ventilation of office building in Guizhou (05. 2015-06.2015)
- Master project-Existing office building reconstruction project (09. 2014 - 12. 2014)
- Chinese Academy of Sciences IHEP Reconstruction Project (07. 2014 – 09.2014)

ENGLISH SUMMARY

Low energy and sustainable buildings use renewable energy for building energy conservation and building energy flexibility. The conventional ventilated window (VW) is efficient in decreasing the building heating energy demand, but has the disadvantage of low heating/cooling efficiency. PCM as a high energy storage material, can be used for ventilation heating/cooling purposes. However, it has been a challenge to efficiently apply PCM for both heating and cooling purposes and to integrate it with building components for existing and new buildings.

This thesis proposes a PCM enhanced ventilated window (PCMVW) to improve the thermal and energy performance of the original VW. In summer, the PCM works as a heat sink during the nighttime and is cooled down by the relatively cold ambient air. It cools down the ventilated air during the daytime when ventilation pre-cooling is needed. In winter, the PCM stores solar energy during the sunny daytime. It pre-heats the ventilated air when the air needs to be preheated.

The research work firstly revolves around the PCM properties for PCM selections. It suggests that the melting/freezing temperature of the selected PCM is limited by the purpose of the application. The geometry of the PCM heat exchanger is also limited considering the low thermal conductivity of the PCM in general. The research continues with the study of the temperature hysteresis of the PCM and the necessity in thermal and energy modeling.

The thesis then focuses on the development of the PCM heat exchanger by experimentally and numerically studying the heat transfer mechanism of the PCM heat exchanger. The development and tests of PCM heat exchanger with/without artificial sun are done in the climate chamber. The numerical models are built and verified by the experimental data.

The configuration optimization of the PCM heat exchanger is conducted so as to optimize the heat storage density and the charge/discharge speed for both solar energy storage and night cooling applications. The optimized configuration for the night cooling application is 10 mm plate thickness. The optimized configuration for the solar energy storage application is 6 mm air gap thickness and 90 mm plate depth.

The PCM heat exchanger with the optimized configuration is then used to enhance the thermal effect of the VW. The PCMVW is built and tested in the façade lab, and compared with a conventional VW. The conclusion is that the PCMVW can significantly improve the energy performance compared to the VW for both heating and cooling purposes. However, the cooling ability of night cooling application is limited without advanced ventilation design and shading control.

A numerical model is built in EnergyPlus for further thermal and energy investigation of the system. The PCMVW is compared with 2 other ventilation systems to examine its thermal and energy performances. The study then compares different control strategies including adding absorption/reflection shades, ventilating directly from the PCM heat exchanger to the room, separately adjusting the ventilation schedule for the ventilated window and the PCM heat exchanger. The thesis provides the developed operation control strategy for the system in buildings under Danish climate conditions.

DANSK RESUME

Lavenergibygninger og bæredygtige bygninger bruger vedvarende energi for at opnå energibesparelse samt at opnå fleksibilitet i bygningsenergi. Det konventionelle ventilerede vindue (VW) er effektivt til at reducere energibehovet til bygningens opvarmning, men har en lav opvarmnings / køleeffektivitet.

PCM som et oplagringsmateriale med høj energitæthed kan bruges til ventilationsopvarmning / køling. Det har dog været udfordrende at anvende PCM effektivt til både opvarmnings- og køleformål samt at integrere det med bygningskomponenter til eksisterende og nye bygninger.

Denne afhandling foreslår et PCM-forbedret ventileret vindue (PCMVW) til at forbedre den termiske og energimæssige ydeevne for det originale VW. Om sommeren fungerer PCM som et kølelegeme i løbet af natten og afkøles af den omgivende luft med lav temperatur. PCM afkøler den ventilerede luft i løbet af dagen, når ventilations for-køling er nødvendig. Om vinteren lagrer PCM solenergi i løbet af de solrige dagtimer. Det forvarmer luften, når ventilations forvarmning er nødvendig.

Forskningsarbejdet undersøger først PCM-egenskaber for at udvælge PCM-kandidater. Det antyder, at smelte / frysetemperaturen for det valgte PCM er begrænset på grund af formålet med applikationen. Geometrien for PCM-varmeveksleren er også begrænset i betragtning af den lave termiske ledningsevne i PCM generelt. Forskningen fortsætter med studiet af temperatur hysterese af PCM og dets nødvendighed i termisk og energimodellering.

Specialet fokuserer derefter på udviklingen af PCM-varmeveksleren ved eksperimentelt og numerisk at studere varmeoverførselsmekanismen i PCM-varmeveksleren. Udvikling og test af PCM varmeveksler med / uden kunstig sol udføres i klimakammeret. De numeriske modeller er bygget og verificeret af de eksperimentelle data.

Konfigurationsoptimering af PCM-varmeveksleren udføres for at optimere varmelagringsdensiteten og opladnings- / afladningshastigheden for både applikationer med solenergilagring og natkøling. Den optimerede konfiguration til natkøling har en pladetykkelse på 10 mm. Den optimerede konfiguration til anvendelse i solenergilagring har en luftspaltetykkelse på 6 mm og en pladedybde på 90 mm.

Herefter bruges PCM-varmeveksleren med den optimerede konfiguration til at forbedre den termiske effekt af VW. PCMVW er bygget og testet i facadelaboratoriet ved at sammenligne det med et konventionel VW. Der konkluderes, at PCMVW kan forbedre energiydelsen markant over VW til både opvarmnings- og køleformål. Men

samtidig er køleevnen til anvendelse i natkøling begrænset uden avanceret ventilationsdesign og skyggekontrol.

En numerisk model er opbygget i EnergyPlus til yderligere termisk og energi-undersøgelse af systemet. Undersøgelsen sammenligner derefter forskellige kontrolstrategier inklusiv tilføjelse af absorptions- / reflektionsvinduer, ventilering direkte fra PCM-varmeveksleren til rummet samt separat justering af ventilationsplanen for det ventilerede vindue og PCM-varmeveksleren. Specialet giver strategien for den optimerede driftskontrol for systemet i bygninger i dansk klima.

ACKNOWLEDGMENTS

The studies present in this thesis is a PhD project financed by the EU Horizon 2020 research and innovation program under grant agreement NO. 768576(ReCO2ST). Special thanks to the company Horn Vinduer for their great suggestions of the development of the PCM enhanced ventilated window and their development and technical support of the tested subjects.

I would express my great thanks to my supervisor Per K. Heiselberg, the project leader and the mentor of my academic career. It is him who leads me into the door of research world and shows me the artistic and methodology of research, and fascinates me with the challenges and sense of accomplishments in the research field. This thesis is not just an ending of a PhD project, but more like a node in my future academic career.

Thanks to all my nice and dedicated colleagues in Civil Engineering department and especially from the division of Architectural Engineering. I am glad I have the honor to work in a nice, open and supportive working environment surrounded by all of you. Special thanks to Michal Z. Pomianowski, Chen Zhang, Mingze liu, Rui Guo for the great help of sharing their knowledge of building physics and building modeling experiences. Thanks to Rasmus L. Jensen, Rui Guo, Hicham Johra, Kim T. Jønsson for all the support and help, especially in the lab. Thanks to the girl's office and PhD office for your kindly care and support, which keeps me warmed and inspired, especially during the straggling days of my PhD.

Thanks to my family in China. Without your so many years' support I wouldn't have gone so far. Thanks to my new family in Denmark, especially Karsten Jakobsen. You made me feel accepted and loved in a second home town. Thanks to all my friends in China and in Denmark, for the caring and support you brought for me.

Yue Hu

February 2020

TABLE OF CONTENTS

Chapter 1. Introduction 19
1.1. Background: status of building energy consumption 19
1.2. Thermal energy storage and phase change material 20
1.3. Ventilated window 21
1.4. PCM enhanced ventilated window 23
1.5. Objectives of the thesis 25
1.6. Outline of the thesis 25
Chapter 2. Basics of PCM properties and PCM in building simulation 27
2.1. PCM properties 27
2.2. PCM temperature hysteresis 29
2.3. DSC measurement 29
2.4. PCM modeling and hysteresis effect on modeling accuracy 31
2.5. PCM selection for building applications 33
2.6. Conclusions 35
Chapter 3. PCM heat transfer study based on the configuration optimization of a PCM heat exchanger 37
3.1. Experimental study of the PCM heat exchanger 37
3.1.1. Experiment setup 37
3.1.2. Experimental results 41
3.2. Numerical study of the PCM heat exchanger 51
3.2.1. The night cooling application 51
3.2.2. The solar energy storage application 53
3.2.3. Model validation 54
3.3. Configuration optimization of the PCM heat exchanger 54
3.3.1. Night cooling application 54
3.3.2. Solar energy storage application 57
3.4. Conclusions 59
Chapter 4. The effect of PCM enhanced ventilated window on the energy performance of the system 60

4.1. Experimental study of the PCM enhanced ventilated window 60
4.1.1. Experimental setup 60
4.1.2. Experimental results 61
4.2. Numerical study of the PCMVW in an apartment 70
4.2.1. Model description 70
4.2.2. Model validation 72
4.2.3. The PCMVW performance 74
4.3. Control strategy development 76
4.3.1. Summer night cooling application control strategy development 76
4.3.2. Winter solar energy storage application control strategy development 79
4.4. Conclusions 81
Chapter 5. Conclusions 83
Chapter 6. Future works 85
Literature list 86
Publications for the thesis 95
Appendices 97

TABLE OF FIGURES

Figure 1-1 The working principle of the ventilated window. 22
Figure 1-2 Summer night cooling application working principle [27]. 24
Figure 1-3 Winter solar energy storage application working principle [27]. 24
Figure 2-1 The enthalpy gained from latent heat compared with sensible heat. (a) PCM with single phase transition temperature. (b) PCM change phase in a temperature range. 27
Figure 2-2 The temperature hysteresis of paraffin wax 22. (a) Heat capacity curves. (b) Enthalpy curves.[44]..... 29
Figure 2-3 The influence of heat rate on the hysteresis of enthalpy. 30
Figure 2-4 The local sensitivity index of phase transition temperature and hysteresis on the building energy demand.[44] 33
Figure 2-5 The requirement of PCM for building opponents. 34
Figure 2-7 The heat capacity of the PCM used in the night cooling application. Data obtained from DSC measurement.[65]..... 35
Figure 3-1 The setup of hot box and cold box experiment.[65]..... 38
Figure 3-2 The setup of the artificial sun. 39
Figure 3-3 The details of the climate chamber control.[78] 40
Figure 3-4 The thermocouples for temperature measurement inside the PCM heat exchanger.[65]..... 40
Figure 3-5 The inlet and outlet air temperature of the PCM heat exchanger. 41
Figure 3-6 The PCM temperature at different positions of the plates (average of all the measured plates)..... 42
Figure 3-7 The PCM temperature in the heat exchanger with the same height. [65]42
Figure 3-8 Solar radiation distribution on the surface of the heat exchanger. 43
Figure 3-9 The temperature inside the cold box. 44
Figure 3-10 PCM temperature measurements at different heights of the heat exchanger plates during the experimental test..... 45
Figure 3-11 Heat storage capacity of PCM in the two experimental modes..... 47
Figure 3-12 The temperature distribution in the air gap..... 49
Figure 3-13 The energy release rate and release energy of the heat exchanger during ventilation preheating mode. 50
Figure 3-14 The calculation domain of the numerical model. 52
Figure 3-15 The meshing details of the finite element model..... 53
Figure 3-16 The meshing details of the 3D solar energy storage model. 54
Figure 3-17 The outdoor dry-bulb air temperature of a sever summer day in Copenhagen.[65]..... 55
Figure 3-18 The total discharged heat of the PCM for the heat exchanger with different plate thicknesses in the night cooling period.[65]..... 56
Figure 3-19 The outlet air temperature of the PCM heat exchanger in the daytime ventilation pre-cooling period.[65] 57
Figure 3-20 The temperature profile in the PCM plates after 6 hours' charge.[78] . 58

Figure 3-21 The melt fraction of the PCM along with charging time.[78] 58
Figure 3-22 The stored latent heat of the PCM along with charging time.[78] 59
Figure 4-1 The experimental setup of PCMVW and reference VW.[26] 61
Figure 4-2 The working principle of the night cooling application. [26] 62
Figure 4-3 The relations of PCMVW indicators to the outdoor climate conditions. [26] 63
Figure 4-4 The working principle of the solar energy storage application. [26] 64
Figure 4-5 The ventilation performance indicators as functions of the climate parameters. [26] 65
Figure 4-6 The working principle of the VW self-cooling[27]. 66
Figure 4-7 The VW inner surface temperature with and without self-cooling. (a) external surface temperature, (b) top of the internal surface temperature, (c) middle of the internal surface temperature and (d) bottom of the internal surface temperature of the two double windows with and without shading. 67
Figure 4-8 The outdoor wind speed and wind direction. [26]. 68
Figure 4-9 The inner glass surface temperature and outdoor climate. The two windows are under natural ventilation. Window 1 blinds close, reflection side towards outdoor; w2 blinds open. 69
Figure 4-10 The measured outdoor wind speed and wind direction. [26] 69
Figure 4-11 The inner glass surface temperature and outdoor climate. The two windows are under natural ventilation. Window 1 blinds open; w2 blinds close, absorption side towards outdoor. 70
Figure 4-12 The building floor plan for simulation.[27] 70
Figure 4-13 The occupant schedule of the apartment. [27] 71
Figure 4-14 The electricity consumption schedule based on a survey in Denmark. [27] 71
Figure 4-15 The model validation of night cooling application.[27] 73
Figure 4-16 The model validation of solar energy storage application. [27] 73
Figure 4-17 The comparison of PCMVW to 2 other ventilation systems for summer night cooling application.[27]. 74
Figure 4-18 The energy demand of the rooms with 3 different ventilation systems for summer night cooling application.[27] 75
Figure 4-19 The comparison of PCMVW to 2 other ventilation systems for winter energy storage application.[27]. 75
Figure 4-20 The energy demand of the rooms with 3 different ventilation systems for winter energy storage application.[27] 75
Figure 4-21 The summer night cooling control strategy 1. [27] 77
Figure 4-22 The summer night cooling control strategy 2. [27] 77
Figure 4-23 The summer night cooling control strategy 3. [27] 78
Figure 4-24 The HVAC cooling energy demands of the rooms using PCMVW with different summer control strategies. [27] 78
Figure 4-25 Winter solar energy storage control strategy 1. [27] 79
Figure 4-26 Winter solar energy storage control strategy 2. [27] 80
Figure 4-27 Winter solar energy storage control strategy 3. [27] 80

Figure 4-28 The HVAC heating energy demands of the rooms using PCMVW with different winter control strategies. [27] 81

Nomenclature

A	Surface area of the heat exchanger exposed to the solar radiation (m^2)
Cp_{air}	Specific heat capacity of the air (kJ/kg/K)
$E_{recieved}$	Energy received by the PCM (J)
$E_{released}$	Energy released from the PCM to the ventilation system (J)
E_{stored}	Energy stored by the PCM (J)
g	Gravity (m/s^2)
H	Enthalpy (kJ/kg)
I	Average solar radiation received by the surface of the PCM heat exchanger (W/m^2)
T	Temperature (°C)
T_{ext}	External air temperature (°C)
T_{inlet}	Inlet air temperature (°C)
T_l	Melting temperature (°C)
T_{outlet}	Outlet air temperature (°C)
T_s	Freezing temperature (°C)
$T_{s\text{-}l}$	Phase transition temperature (°C)
u	Velocity (m/s)
v	Kinematic viscosity (m^2/s)
Δt	The time of the solar energy storage mode (s)
Greek symbols	
β	Expansion coefficient
δ_M	Momentum boundary layer thickness (m)
η_1	Energy storage efficiency
η_2	Pre-heating efficiency

η_3	Overall energy efficiency
μ	Dynamic viscosity (Pa·s)
ρ	Density (kg/m^3)
Abbreviations	
DSC	Differential scanning calorimetry
HVAC	Heating, ventilation, and air conditioning
LHTES	Latent heat thermal energy storage
PCM	Phase change material
PCMVW	Phase change material enhanced ventilated window
TES	Thermal energy storage
VW	Ventilated window

CHAPTER 1. INTRODUCTION

1.1. BACKGROUND: STATUS OF BUILDING ENERGY CONSUMPTION

Global warming has become a major challenge for the 21st century. With the development of technologies and industry, the massive use of fossil fuels has caused and accelerated many environmental problems such as global warming and climate changes. A warmer climate can reduce the lifespan of building material, aggravate the indoor climate, potentially increase the cooling energy demand and cause some health problems. The extreme weather conditions will require buildings with more energy and equipment resilience. As a consequence, more carbon dioxide will be produced.

The global energy consumption by fuel has doubled in the last 40 years[1] and is still a growing trend. The energy demand is set to grow by more than 25% to 2040[2]. However, the total amount of fossil fuels on earth is limited. Statistics show that with the current, increasing trend of the energy demand, our fossil fuels will drain within a couple of centuries[1].

The building is a large sector for energy consumption. It consists of approximately 40% of the world's total energy consumption and one-third of the greenhouse gas emissions[3]. The space heating and cooling account for 50% of the total building energy demand[4]. Nevertheless, the building energy is an increasing trend with the continued increase in population, in floor area as well as in quality requirements of the indoor environment. Therefore, building energy conservation plays an important role in the aim of decreasing greenhouse gas emissions.

One way for building energy conservation is to improve the building energy efficiency by better management of building energy, such as storing the energy when the electricity price is low, and releasing the stored energy when the electricity price is high. By shifting the building's energy demand to the off-peak hours (normally night time), it lightens the burden of the electricity grid and avoids the waste of the surplus electric power. Other approaches include adopting effective ventilation/HVAC control strategies. Some researchers suggested adjusting the setpoint temperature of air conditioning systems with weather forecasts and electricity prices [5].

Increasing the thermal interior of the building and building envelope can improve the stability of the building indoor environment under different outdoor conditions, especially for some extreme weather conditions. This can be fulfilled either by increasing the thermal mass level or by improving the airtightness of the building. Buildings with high thermal interior levels have the ability of self-adjustment and self-adoptation to the outdoor weather with minimum HVAC energy consumption. Once

the indoor temperature is adjusted to a certain outdoor condition, the energy consumption to maintain it is relatively low. However, achieving a high energy performance building is facing some new challenges due to the increase in thermal insulation and airtightness[6]. One of the big challenges is the increased cooling demand due to solar and internal heat gains, especially in the cooling season. Night ventilation, as well as other ventilative cooling technologies, can potentially decrease the HVAC energy consumption and achieve good indoor environmental quality. The optimized night ventilation control strategy in combination with the right amount of thermal mass level can further improve the night ventilation energy-saving potential[7].

Another promising way of building energy conservation is to replace the building energy source with renewable energy, such as wind energy and solar energy. Solar energy can be stored in thermal energy storage (TES). The conventional storage medium of TES is usually water. The TES with water has the disadvantage of large storage volume due to the low heat capacity of water, which subsequently increases the insolation surface area. Some new materials such as phase change material (PCM) has gained much attention recently[8][9][10]. PCM has the advantage of high heat capacity and high latent heat storage density. As a result, the total storage volume could be decreased using PCM instead of the traditional thermal energy storage material such as water.

1.2. THERMAL ENERGY STORAGE AND PHASE CHANGE MATERIAL

Thermal energy storage (TES) is commonly used for building energy storage[11][12][13][14][15][16]. TES can shift the building energy consumption to off-peak hours. The energy could be converted from electrical power and stored as heat/cold sources during the off-peak hours of the power grid. During peak hours, the stored energy is used for building consumption. TES can also store solar energy during the sunny daytime and use the stored energy during peak hours.

Renewable energy such as wind and solar energy are intermittent energy sources. A large scale usage of such energy sources can have a severe impact on the power network and potentially affect the security of the current power grid[10]. On the other hand, a battery is normally used for small-scale use of renewable energy. However, such battery always has a short lifespan and a bad influence on the environment. Nevertheless, TES for building energy storage has a longer life span and is more flexible in the storage form. It can be a small scale for hourly or daily energy usage, or a large scale for seasonal thermal energy storage, e.g. storing the heat in hot water during the summer for winter usage. It can store thermal energy as sensible energy or latent energy. PCM is popular as the TES for building applications due to its high latent energy storage ability. With the same storage volume, the PCM usually has higher energy storage density than conventional thermal mass such as concrete.

PCMs integrated with building elements can be categorized into passive and active applications. Passive technologies are basically PCMs integrated with construction materials such as gypsum, concrete, bricks, composites and so on. Michal et al.[17] implemented PCM in a hollow-core concrete deck. The results highlighted the potential of using PCM in concrete elements. Guiyin et al. [18] investigated the effect of inserting a PCMs board into building envelopes. Two layers' wallboard with different PCMs is tested. The melting point of the two PCMs is 30.35°C and 26.65°C respectively. They found out that with those PCMs, the time delay of the wall temperature is 2-3 h.

Active applications mainly involve the use of PCMs in glazing, shadings, blinds as well as heat exchangers for room temperature control. Hicham et al. [19] tested a ventilated window with a PCM shading device for preheating the ventilated air. The result is promising in comparison with non-ventilated ones. Diarce et al.[20] tested a ventilated façade with PCM in comparison with other conventional façades, and figured out the working mechanism of the PCM during heat absorption and releasing processes. Alvaro et al.[21] put macro-encapsulated phase change material (PCM) into a ventilated façade in the lab. They found that applying free cooling during the night is the most effective operation strategy to reduce the cooling and heating load of a room. They also found that the thermal resistance of the external envelope has a great influence on the operation of the system.

1.3. VENTILATED WINDOW

The ventilated window was designed as a smart ventilation system for buildings with limited manual fenestration. It is made by two layers of glass surface which form a ventilation cavity. In winter the heat is accumulated in the cavity by solar radiation and the heat transfer from the indoor. The cavity is ventilated to heat up the cold outdoor air before entering into the room. The ventilated window provides the pre-heated air to the indoor room and decreases the heat loss of the window to the outdoor environment. During summer or hot days in winter, the window is cooled down by natural ventilation, to prevent overheating of the indoor room from the overheated window. Meanwhile, the room is ventilated by bypass ventilation. The working principle of the ventilated window is shown in Figure 1-1.

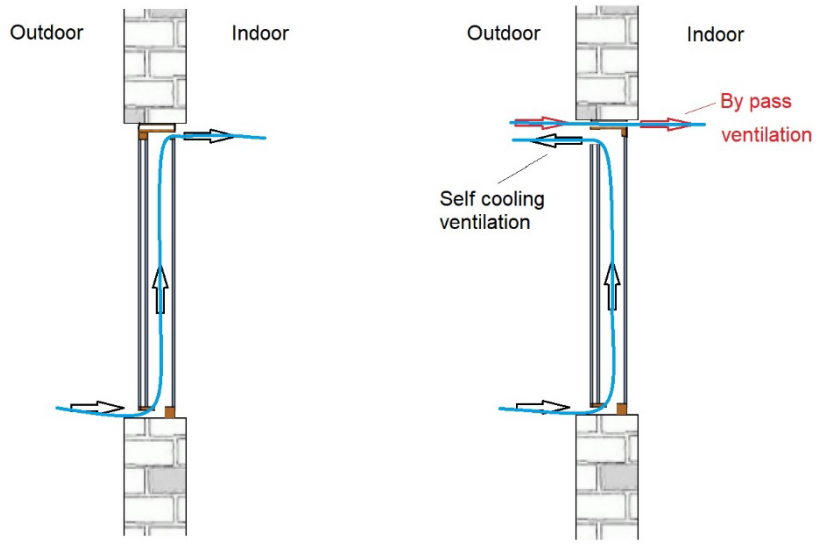

Figure 1-1 The working principle of the ventilated window.

Several researchers have studied the ventilated window numerically and experimentally. One experimental study shows that the ventilated window can heat up the inlet air temperature by 6-12°C [22]. Another study shows that the energy performance of the ventilated window is quite high. It can decrease by 10% of the heating demand [23]. A similar study shows that the ventilated window can achieve good ventilation effect for both the cooling and heating purposes [24]. Other researchers have done the typologies optimization of the ventilated window, and they found that the optimized configuration is with solar control or low emissivity coatings and double penal glazing on the outside of the ventilated cavity in terms of both higher energy conservation and better thermal comfort [25].

The passive heat recovery window was developed in the Energy and Indoor Environment of Building Laboratory in AAU, and now it is available on the market as the Climawin window [26]. The system can automatically control the ventilation airflow distribution by the deviation between the current and desired indoor thermal conditions.

However, based on some studies [22], the inlet air temperature of the VW cannot meet the indoor thermal requirements all the time due to the lack of heat/cold source. The PCM heat exchanger combined with the VW and some other shading technologies

can improve the ventilation performance of the VW and provide a better indoor environmental quality.

1.4. PCM ENHANCED VENTILATED WINDOW

The aforementioned ventilated window may be confronted with low heating efficiency during cold winter. The cooling effect of the summer application is limited by the instant local outdoor air temperature and solar heat gain. To achieve better energy efficiency, it is necessary to combine the ventilated window with some thermal energy storage such as phase change material (PCM).

The PCM applied in the building components improves the building energy flexibility by adding renewable energy to the building energy systems. It reduces building energy consumption from traditional fossil fuels and improves building energy flexibility.

The PCM enhanced ventilated window (PCMVW) is designed to diminish or substitute the energy consumption of the HVAC system for the whole year, even for transition seasons when heating and cooling demands exist during the same day. It can cover both the heating demand and cooling demand of the indoor room. The decentralized ventilation system can provide a good indoor climate for separate rooms, and is competitive to a traditional central ventilation system with extensive and energy-consuming ducts and pipes in the building. The duct-free installation can benefit the new buildings with less floor-to-ceiling height. It can also benefit the energy efficiency renovation projects about existing buildings with normal room heights[27].

The PCMVW is applicable for both summer and winter applications. The two applications have the same configurations, but the working principles and control strategies are different.

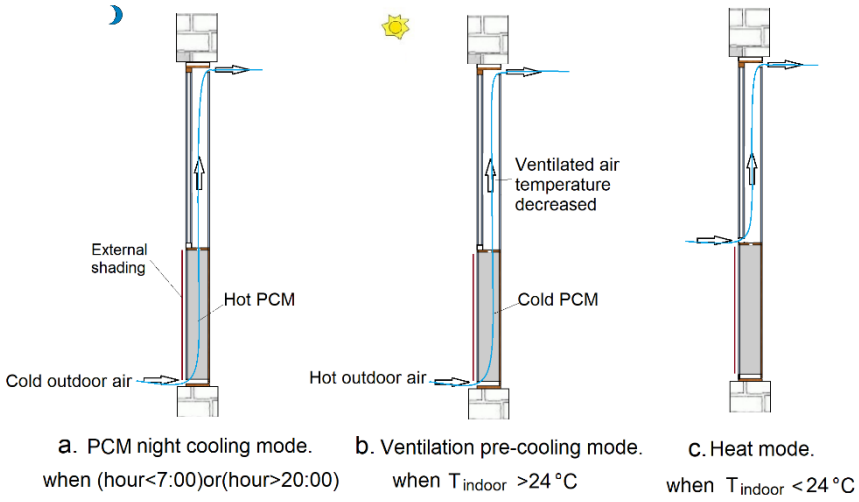

Figure 1-2 Summer night cooling application working principle [28]**.**

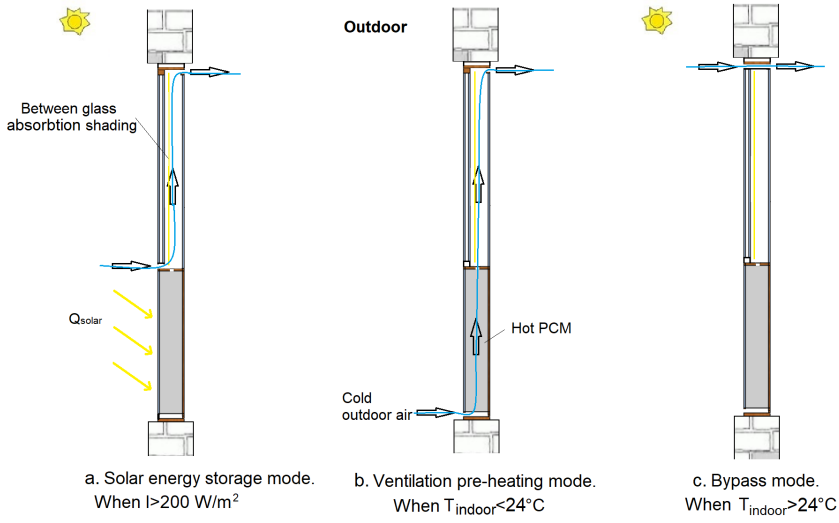

Figure 1-3 Winter solar energy storage application working principle [28]**.**

In the summer night cooling application (Figure 1-2), the PCM works as a heat sink. The cold ambient air is ventilated through the PCM during the night to remove the heat in the PCM in night cooling mode (Figure 1-2 (a)). During the day, the cold PCM

cools down the ventilation when pre-cooled air is needed in ventilation pre-cooling mode (Figure 1-2 (b)). When the indoor air temperature is too low, the PCM is not used to produce heat for the ventilation. Instead, the heating mode is operated (Figure 1-2 (c)), the relatively higher temperature air in the ventilated window (compared to the outdoor air temperature) is ventilated into the room. In winter solar energy storage application (Figure 1-3), the PCM stores solar energy from solar radiation during sunny days in solar energy storage mode (Figure 1-3 (a)). During the ventilation pre-heating mode (Figure 1-3 (b)), it releases the heat into the ventilation when pre-heated air is needed. When the indoor air temperature is too high, the bypass mode is operated (Figure 1-3 (c)), and the outdoor ambient air is ventilated directly into the room.

1.5. OBJECTIVES OF THE THESIS

The concept and working principle of the PCMVW (in chapter 1.4) are proposed at the beginning of the PhD project. The objectives of the thesis are to develop the PCMVW in the best configuration for high energy efficiency and good indoor environmental quality and to improve the energy-saving potential of the PCMVW with good control strategies for both summer and winter applications.

The challenges of this work are as follows:

1. To optimize the design of the PCM heat exchanger to achieve a high energy storage density within the limitation of material properties and facility volume,
2. To combine the PCM heat exchanger with the ventilated window with effective ventilation solutions and test its performance compared to a conventional ventilated window,
3. To develop the accurate numerical models of the system for system behavior and energy consumption prediction, and
4. To develop the control strategies of the system to gain a good indoor environmental quality and improve the building energy efficiency (including advanced shading control strategy).

1.6. OUTLINE OF THE THESIS

Chapter 1 presents the background, working principles of the PCMVW, and the objects and challenges of this PhD study.

Chapter 2 shows the PCM thermal properties, measurement methods and their influence on modeling. It also shows the method of PCM selection for building applications.

Based on the selected PCM, chapter 3 conducts an experimental study of the PCM heat exchanger in the heating/cooling processes with/without an artificial sun. Later

on, based on the heat transfer mechanism found by the experiment, two numerical models are built. The 2D model is used for night cooling application, while the 3D model is used for solar energy storage application. The two models are verified by the experimental results and used to optimize the configuration of the PCM heat exchanger.

In chapter 4, the optimized configuration of the PCM heat exchanger is combined with a ventilated window. The PCMVW is tested in the lab under real weather conditions. Moreover, the numerical models of a 3-room apartment with four PCMVWs are built in Energyplus and verified by experimental results. The models are used for control strategy optimization to achieve better energy performance.

Chapter 5 summarizes the work done in this study and provides some conclusions and guidelines for the configuration of the PCM heat exchanger and control strategies of the building with PCMVW.

Chapter 6 discusses and recommends future research directions.

Appendices A-E present the collection of journal articles related to this PhD study.

CHAPTER 2. BASICS OF PCM PROPERTIES AND PCM IN BUILDING SIMULATION

It is necessary to have an overall knowledge about the material used for thermal energy storage, before the design process of the PCM heat exchanger. This chapter firstly introduces the thermal properties of the PCM and its advantages and disadvantages for thermal energy storage, including the phase transition of the PCM, temperature hysteresis, subcooling, and their influence on the accuracy of building simulation. Later on, the study looks into the potential and requirements for PCM in building applications. Based on that, the PCM used in this project is selected.

2.1. PCM PROPERTIES

PCM is a kind of material that changes its phase in a certain temperature (or temperature range) and release or absorb latent heat simultaneously, as in Figure 2-1. The latent heat during the phase transition process is much higher than the sensible heat, which significantly increases the energy storage ability of the material. Due to its high latent heat storage ability, PCM is largely used as thermal energy storage.

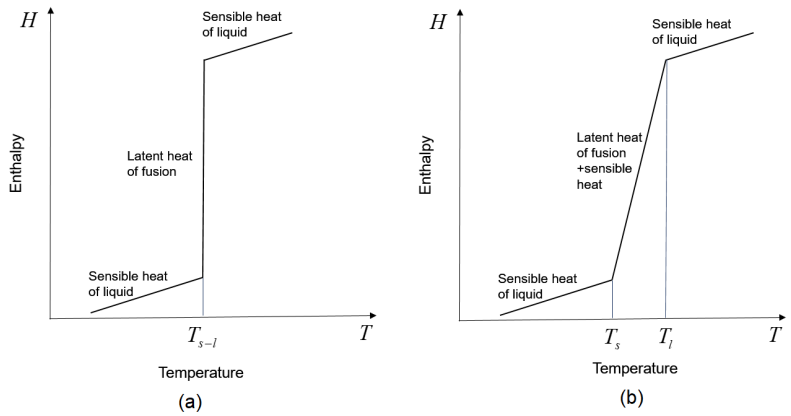

Figure 2-1 The enthalpy gained from latent heat compared with sensible heat. (a) PCM with single phase transition temperature. (b) PCM change phase in a temperature range.

Base on the change of phase, PCMs can be sorted into 4 categories: solid-solid, solid-liquid, solid-gas, liquid-gas[15]. Only solid-liquid PCMs are normally used for Thermal Energy Storage (TES) and building applications. There are some technical limitations to other PCMs. For solid-solid PCMs the heat transfer in the material is slow due to the low thermal conductivity. For solid-gas and liquid-gas PCMs, the facilities need large storage volume and the pressure would be high.

Based on chemical components PCMs could be sorted into 3 categories: Organic, inorganic and eutectic[29]. Organic PCMs have the advantage of stable chemical properties. It is high in latent heat capacity as well[30]. However, there are several drawbacks of organic PCMs, for example low thermal conductivity and leakage problems. Inorganic PCMs have higher latent heat and thermal conductivity than organic PCMs in general, and most of them are non-flammable. Nevertheless, the application is restrained because of their disadvantages include unsteady thermal ad physical properties and subcooling effects. Eutectics are the mixtures of multiple PCMs. It could be divided into organic-organic eutectics, organic-inorganic eutectics, and inorganic-inorganic eutectics. Eutectics usually have sharp melting points, for some mixtures, multiple peaks could be observed. The storage density may be higher than organic PCMs[31].

PCM usually has a quite low thermal conductivity, which makes the heat transfer process slow and potentially limits its application. Many researchers are working on the improvement of the thermal conductivity of the PCMs. One method is to combine PCMs with graphite matrices[32][33] and porous metal foam[34][35]. Another method is to add fins[36], metal spheres[37] or other macro materials to improve the thermal conductivity. Last but not least, nanomaterials, including carbon-based nanostructures, carbon nanotubes, metallic and metal oxide nanomaterials and silver nanowires[38][39]. Another disadvantage of PCM is its leakage problem due to the changed phase. To solve this problem one can incorporate PCM in construction materials or encapsulate PCM in either macro or micro encapsulation[13].

There are already several works considering the disadvantages of PCMs. Belén et al.[40] have tested a heat exchanger with PCMs for building free-cooling propose. The thickness of the encapsulated PCM was set as 15 mm and 25 mm. They found out that the thickness of the PCM encapsulation has the highest influence on the freezing process of the PCM. For the melting process, the most influential parameter is the inlet air temperature. They then gave further consideration of embedding PCM in a porous matrix of graphite[41]. With this method, the PCM plate can be 70% thicker and half of the fan energy can be saved. Based on the researches mentioned above, Xiaoming et al.[42] built a ventilation system with a latent heat thermal energy storage. The thickness of both the PCM layer and the air gap is 10 mm. The results show that the seasonal average cooling energy supply ratio is 85%, and the seasonal average electricity saving ratio is 68%.

Similarly, Yutong et al.[43] evaluated an office building with a cooling unit made by PCM for a window application. It is found out that the optimized thickness of the PCM plates is 5 mm for 8 h activation time.

2.2. PCM TEMPERATURE HYSTERESIS

Many PCMs are showing observable hysteresis and subcooling, especially inorganic PCMs[44]. The hysteresis is observed as the thermal properties of the PCM during the freezing process have some discrepancies compared to that during the melting process, such as heat capacity, enthalpy, viscosity, and thermal conductivity. Take paraffin wax 22 for example. Figure 2-2 shows its heat capacity and enthalpy during the melting and freezing process. The freezing peak of heat capacity is delayed compared to the melting peak. Similarly, the temperature when the phase transition starts during the freezing process has to be lower than the melting temperature, as seen in both the heat capacity curves and enthalpy curves.

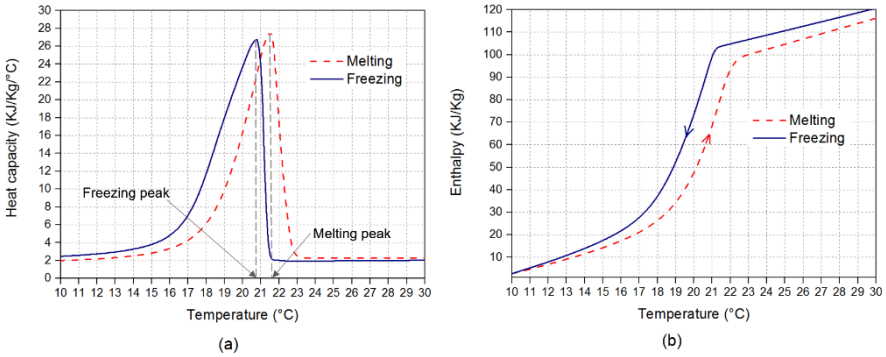

Figure 2-2 The temperature hysteresis of paraffin wax 22. (a) Heat capacity curves. (b) Enthalpy curves.[45]

There are mainly two reasons for the hysteresis phenomenon of PCM. One is the improper measurement methods employed to assess PCM properties, and the other one is the intrinsic properties of the materials and subcooling effect. The first one does not represent the material correctly, and the second one is a material property, which should be modeled in a proper way.

2.3. DSC MEASUREMENT

The PCM thermal properties shown in Figure 2-2 are measured by Differential scanning calorimetry (DSC). DSC is the standard method for the thermal analysis of small material samples. The principle of DSC is based on detecting the difference of enthalpy change between the tested sample and a reference sample subject to the same rate of temperature change. The specific heat capacity of the reference sample is

known so that the specific heat capacity of the tested sample can be deduced. The results of the conventional DSC method (also known as DCS dynamic mode) depend on the sample size and the heating/cooling rate. Too large heating/cooling rates or oversized samples[46] result in temperature inhomogeneity inside the sample, especially if the tested sample has a low thermal conductivity, which is typically the case for PCM. As a consequence, the measured thermal properties will present significant errors [47]. The reduction of sample size will reduce the measurement uncertainty. However, the small sample size is not applicable for non-homogenous materials. Moreover, the subcooling effect in a small sample is more severe than in a large sample. This may result in the over-estimation of subcooling.

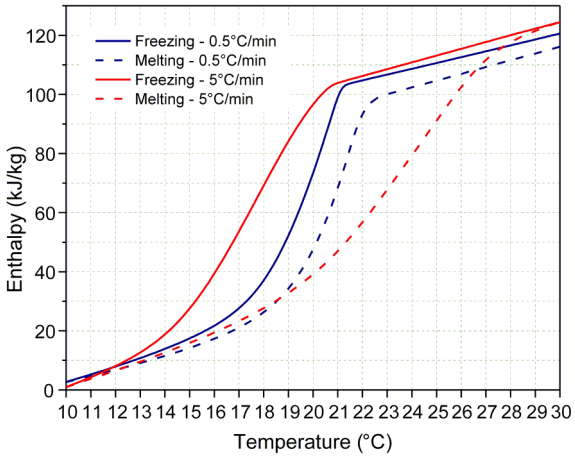

Figure 2-3 The influence of heat rate on the hysteresis of enthalpy.

Figure 2-3 shows that a higher heating and cooling rate increases subcooling, hysteresis, and the phase transition temperature range [46,48,49]. However, a lower heating or cooling rate decreases the magnitude of the DSC signal, which makes it more sensitive to measurement noise. Arkar et al. [50–52] suggested that the properties of the PCM should be determined using the similar heating and cooling rates as the actual temperature change rates of the real application.

The DSC method is applicable for PCMs, which are homogeneous and with no subcooling effect. Methods that are more accurate are required for the thermal analysis of bulk PCM and PCM with subcooling effect. The T-history method can measure the thermal properties of larger size PCM samples with constant heating and cooling temperature instead of temperature ramps. It was first proposed by Zhang et al [53]. The method is based on the comparison of the temperature-history (T-history) of the measured sample and the reference sample. The heat convection rate to the container is considered the same from the tested sample and the reference sample since they are

in the same container. The thermal properties of the reference sample are known so that the thermal properties of the tested sample can be deduced by comparison.

Lázaro et al. [47] have performed a comparison of PCM enthalpy measured by DSC and T-history. The study included Hexadecane, paraffin RT27, and sodium acetate trihydrate graphite compound material. It was found that for materials with hysteresis, the T-history method is more accurate than the DSC. The T-history method is also more accurate for compound materials, because this setup and calculation method are specially designed for those materials. A drawback of the T-history method is that there is no commercial instrument available on the market so the measurement accuracy of each individual setup is hard to evaluate, and it is difficult to compare among the results from different works. Consequently, the reliability of the measured results is uncertain.

The aforementioned problems indicate that it is easy to wrongfully estimate the hysteresis of PCM from the measurements. In addition, each method might not be suitable for the whole range of PCM products. The measurement method should be chosen with great care depending on the material homogeneity, the level of subcooling, the PCM type, the heating/cooling rate, and the temperature range of the LHTES application.

2.4. PCM MODELING AND HYSTERESIS EFFECT ON MODELING ACCURACY

As employing LHTES into building systems is becoming more popular, some of the building simulation tools started to develop modules for phase change material. Some others enable the input of nonlinear thermal properties and hysteresis of the material. Table 2-1 presents the commonly used building simulation tools including PCM models.

Table 2-1 The commonly used models in building simulation software.

Simulation tool	**PCM modeling approach**	**Mathematical method**	**Discretization**	**Hysteresis modeling method**	**Reference**
Energyplus	Heat capacity method	Conduction finite difference(CondFD)	Fully implicit/ Crank-Nicolson	The latest version can model hysteresis and subcooling	[54–59]

Trnsys TYPE204	Heat capacity method	Finite Difference Method	Implicit, semi-implicit	Cannot model hysteresis Parameters like melting/freezing point/range and latent heat are the input to simplify the heat capacity	[60]
Trnsys TYPE399	Enthalpy method	Finite Difference Method	Crank-Nicolson	Hysteresis is considered; linearized enthalpy curves are used	[61]
ESP-r	Heat capacity and heat source method	Finite Difference Method	-	Both simple models without hysteresis and complicated model with hysteresis can be modeled	[62–64]
Fluent	Enthalpy method	Finite Volume Method	-	FLUENT models the heat capacity of the material as a step function	[65]
COMSOL	Heat capacity method	Finite Element Method	-	Hysteresis can be modeled; nonlinear thermal properties can be defined	[66][67]

However, there is less research about the influence of hysteresis on building energy consumption. In this PhD study, 6 PCMs with different hysteresis (the heat capacity and the phase transition temperature are the same) are simulated to test their energy-saving potential for the HVAC system. The PCM is integrated into a PCMVW system for ventilation pre-heating and pre-cooling. In comparison, 6 PCMs with different

phase transition temperatures (the same latent heat and hysteresis degree) are simulated later. The sensitivity analysis is done to see which parameter has a higher influence on the building energy demand. [45]

Figure 2-4 shows the local sensitivity index of phase transition temperature and hysteresis on the building energy demand. It shows that the hysteresis degree has a much higher sensitivity index than the phase transition temperature for both summer energy demand and winter energy demand. However, both phase transition temperature and hysteresis degree have small sensitivity indexes for total energy demand. It is because for summer application, the summer energy demand increases with the increase of PCM phase transition temperature and the hysteresis degree. However, for winter application, the winter energy demand increases with the increase of the phase transition temperature but decreases with the increase of the hysteresis degree. [45]

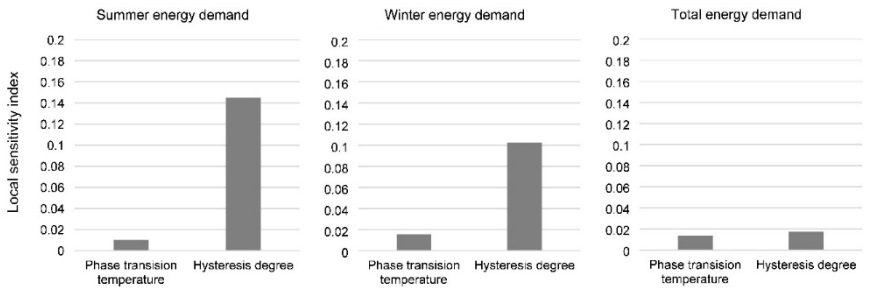

Figure 2-4 The local sensitivity index of phase transition temperature and hysteresis on the building energy demand.[45]

For more information on the model and sensitivity analysis please refer to Appendix E [45]: *"Temperature hysteresis of phase change materials and its impact on building modeling".*

2.5. PCM SELECTION FOR BUILDING APPLICATIONS

There are several requirements for PCM in building applications, as shown in Figure 2-5. Firstly, it should guarantee a thermally comfortable indoor environment. According to ASHRAE Handbook, the comfortable zone for human beings in summer is 23°C-27°C[68]. A temperature difference of 3°C -5°C is necessary for heat transfer[14]. For cooling purposes, the melting temperature range should be 18 °C-24°C accordingly. For comfortable applications in buildings, the melting/freezing

point should be in the range of 20 °C-30°C[69]. Another important factor is the latent heat. The material releases a large amount of heat while changing its phase at an almost constant temperature[70]. With high latent heat, the material could store large amounts of energy with small volume and density, which makes the building lighter. High specific heat is also acclaimed. Other important factors include high thermal conductivity, chemical and physical stability, low volume expansion and no super-cooling effect during solidification[15].

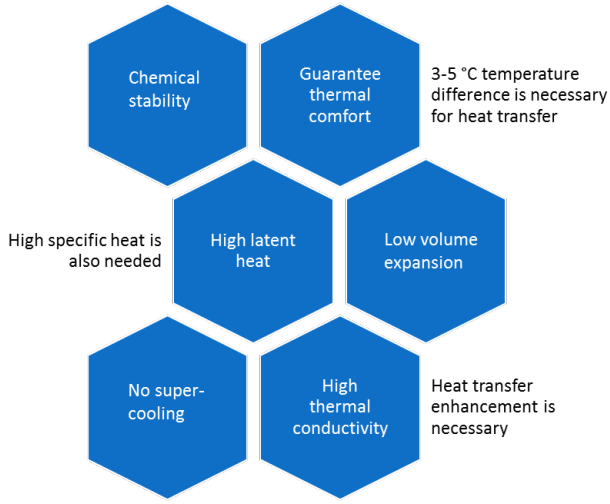

Figure 2-5 The requirement of PCM for building opponents.

As for both cooling and heating purposes, the phase change temperature of PCMs has other limitations. It should be higher than the summer morning temperature and lower than the winter daytime temperature. If the chosen phase change temperature is too low, the PCM may never solidify in summer; if too high, it may never melt in winter, and the heat loss to the ambient is considerable. Some research work also checked this problem. Sayanthan et al.[59]considered 3 different melting temperature PCMs in naturally ventilation buildings in summer, the results indicated that the phase transition temperature of the PCM used in the building should at least be 3-5 °C higher than the indoor air temperature, to guarantee a good thermal comfort indoor environment and improve the PCM efficiency. P.Hoes et al.[71]indicated that the PCM melting temperature should be higher than the minimum outdoor air temperature during summer days. A LTES filled by PCM with embedded heat pipes was developed and tested by Turnpenny et al.[72][73] One of their main conclusions is that the heat transfer rate can be as high as 40 W for 19 h when there is 5 °C difference between the PCM phase transition temperature and the air temperature. Peippo et al.[74] have built and researched a passive solar house in the USA and the results indicated that the optimal phase transition temperature should be 1–3°C higher than the room temperature. Tyagi, Agyenim, et al.[75][76]argued that PCMs used in buildings

should have a phase transition temperature at 20 °C to 32 °C, which is the temperature of the building environment. Some researchers consider the double panel of PCMs as a method for thermal control[77][78]. However, none of them tried to compare the double panel to a single panel to show the necessity of using different layers of PCMs.

For this Ph.D. project, the selected PCM is paraffin wax. The PCM has a melting range of 16 °C -23 °C and a freezing range of 14 °C- 21.5 °C. The melting point is 20.7 °C and the freezing point is 21.5 °C. The total heat capacity of the PCM plates is 117 kJ/kg (for a 10 °C to 30 °C temperature change) [66]. The thermal conductivity of the PCM in the solid-state is 0.18 W/m/k. The PCM is absorbed in a thin fiberboard, to compensate for its low thermal conductivity and to provide encapsulation. The heat capacity of the PCM board measured by DSC is shown in Figure 2-7.

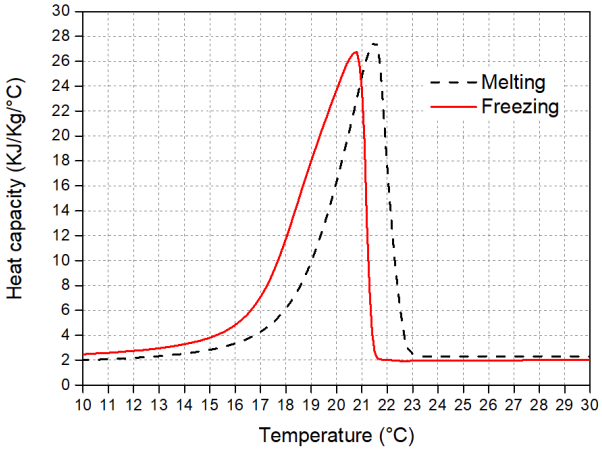

Figure 2-6 The heat capacity of the PCM used in the night cooling application. Data obtained from DSC measurement.[66]

2.6. CONCLUSIONS

The analysis of the PCM thermal properties has the conclusion that the choice of PCM should be based on the temperature requirement of the application. Moreover, the PCM form and thickness should be designed in a way that is good for the heat transfer process. In addition, the hysteresis of PCM should be noticed when doing numerical modeling of PCM.

The sensitivity analysis of the hysteresis degree and phase transition temperature on the building energy demand shows that the hysteresis degree has a higher influence on the summer energy demand and winter energy demand than the phase transition temperature. The summer energy demand increases with the increase of the hysteresis degree, while the winter energy demand decreases with the increase of the hysteresis

degree. Both phase transition temperature and hysteresis degree have less influence on the yearly building energy demand.

For both ventilation heating and cooling purposes, the PCM chosen in this study is paraffin wax 22, which has a melting/freezing point around 22 °C. It is encapsulated in fiberboards, to avoid leakage and make it shape-steady. The measured total heat capacity of the PCM is 117 kJ/kg.

CHAPTER 3. PCM HEAT TRANSFER STUDY BASED ON THE CONFIGURATION OPTIMIZATION OF A PCM HEAT EXCHANGER

This chapter studies the PCM heat transfer mechanism by a case study of the design process of a PCM heat exchanger. The configuration of the PCM heat exchanger is optimized for both summer night cooling application and winter solar energy storage application. The experimental study is firstly presented, to find out the heat transfer mechanism of the PCM heat exchanger, and to provide useful data for the validation of the numerical model. The numerical model is then presented and validated by the experimental results. The model then examined several configurations to decide which one is the best.

3.1. EXPERIMENTAL STUDY OF THE PCM HEAT EXCHANGER

3.1.1. EXPERIMENT SETUP

The aim of the experiment is to study the heat transfer mechanism of the PCM heat exchanger for the summer night cooling application and winter solar energy storage application, and to provide valuable data to validate the numerical model.

For those purposes, a PCM heat exchanger is developed and tested in the climate chamber in the AAU Indoor Environmental Engineering Laboratory. The test equipment includes the hotbox and coldbox to create indoor and outdoor climates, and an artificial sun to create solar radiation[66], as shown in Figure 3-1 and Figure 3-2. Each box is well insulated and includes a cooler and a heater[66]. Fan coils with 0.2 m/s airspeed are used, to provide relatively homogeneous air distribution in the two boxes[66]. They are controlled by proportional–integral–derivative (PID) controller to achieve the desired building climates[66]. The PCM storage is set between the coldbox and hotbox. The two boxes are connected by ducts and a fan, to provide a pressure difference in the two boxes to drive the air goes through the PCM storage[66], see Figure 3-3. The flow rate is measured by an orifice plate. The measurement uncertainty is ± 7.5%. [66]

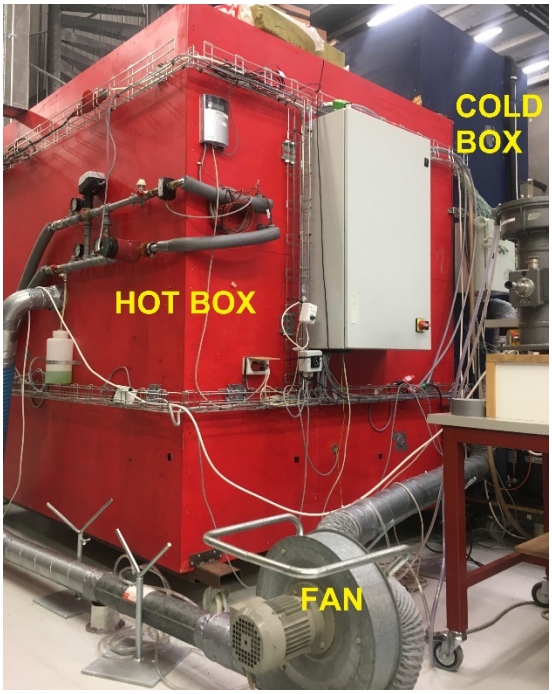

Figure 3-1 The setup of hot box and cold box experiment.[66]

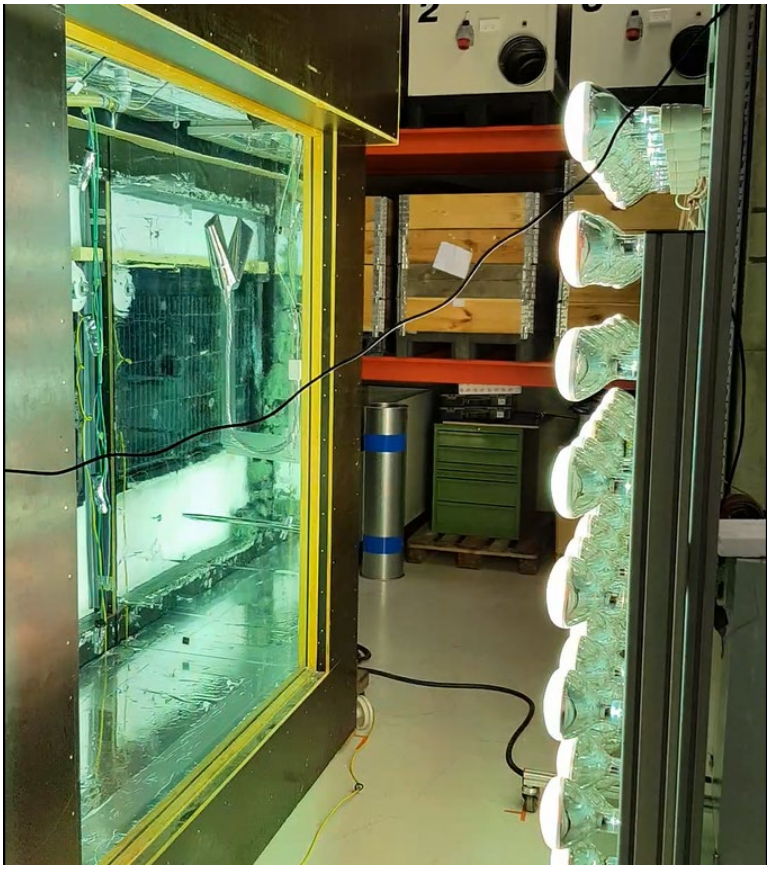

Figure 3-2 The setup of the artificial sun.

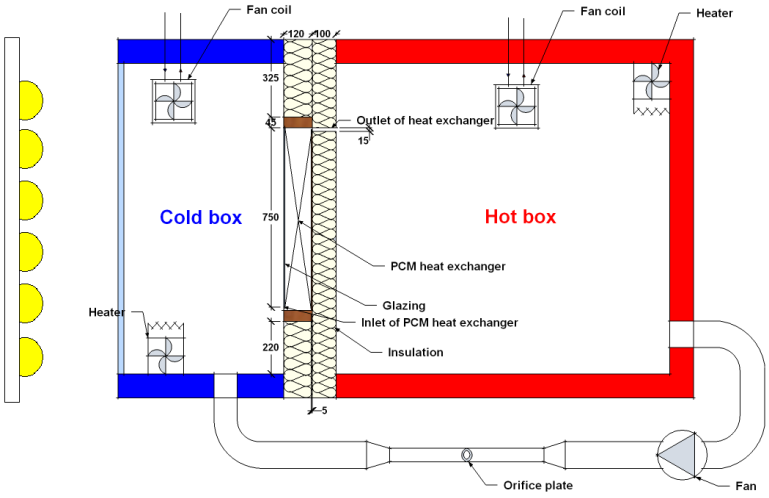

Figure 3-3 The details of the climate chamber control.[79]

The temperature measurement includes the air temperature in the gaps between PCM plates, the air temperature in the inlet and outlet of the PCM heat exchanger, the PCM temperature in different positions of the PCM plates[66]. 56 type K thermocouples are used for the temperature measurement, as seen in Figure 3-4. The uncertainty of the calibration is ± 0.15 °C[66]. A Fluke Helios Plus 2287A data logger is used for the data collection. The logging rate is every 300 s. [66]

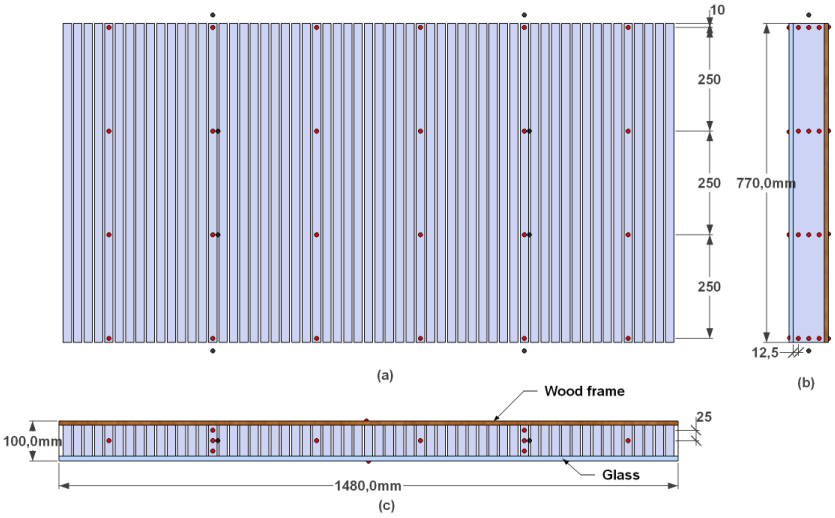

Figure 3-4 The thermocouples for temperature measurement inside the PCM heat exchanger.[66]

3.1.2. EXPERIMENTAL RESULTS

The study consists of two experiment tests, one without the artificial sun and one with the artificial sun. For the test without artificial sun, the PCM is charged by the hot air in the hotbox and then discharged by the cold air in the coldbox. For the test with the artificial sun, the PCM is charged by the solar radiation from the artificial sun, and then discharged by the cold air in the cold box.

3.1.2.1. Without artificial sun

Figure 3-5 shows the air temperature at the top and bottom of the PCM heat exchanger. The air in the hotbox goes into the PCM unit from the top opening to heat up the PCM during 0-7.5 h. The fan switched the direction at 7.5 h. During 7.5 h- 15 h, the air in the cold box goes into the PCM unit from the bottom opening, to cool down the PCM.

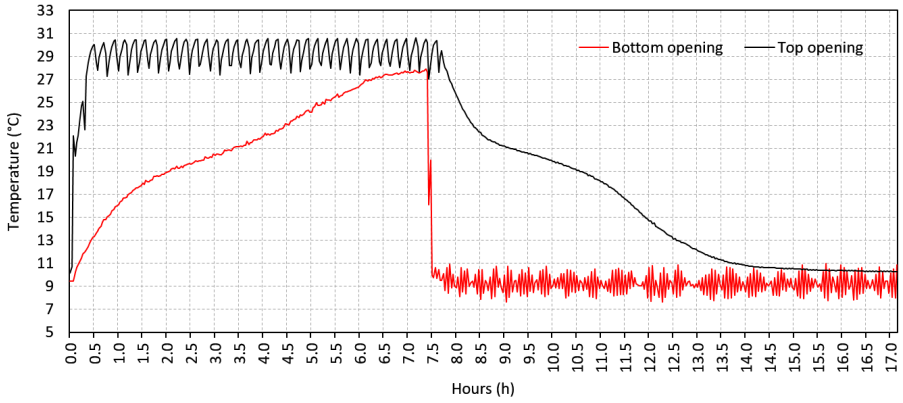

Figure 3-5 The inlet and outlet air temperature of the PCM heat exchanger.

Figure 3-6 shows the PCM temperature at different positions of the PCM plates. For the melting process (0 - 7.5 h), the PCM in the top of the PCM plates melt first, then the lower part of the PCM plates starts melting. For the freezing process (7.5 h - 15 h), the airflow changes the direction. The lower part of the PCM pates melts first. Clear phase transition can be seen in both melting and freezing processes around 20-22 °C.

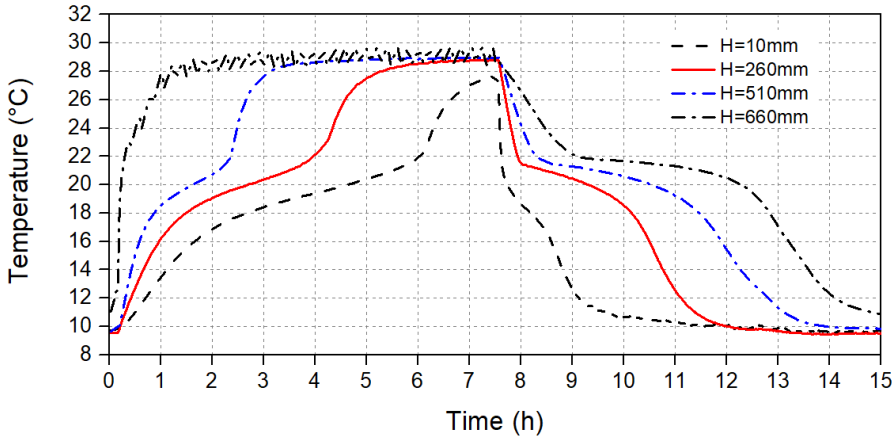

Figure 3-6 The PCM temperature at different positions of the plates (average of all the measured plates).

Figure 3-7 shows the PCM temperature distribution along with the depth of the PCM plates. It is seen that the temperature difference at different depths is not so big. The depth of the PCM plate does not influence the temperature distribution inside the PCM plates, due to the evenly distributed airflow in the gaps between the PCM plates. As a consequence, it is reasonable to simplify the numerical model of the PCM heat exchanger for the night cooling application in 2 dimensional.

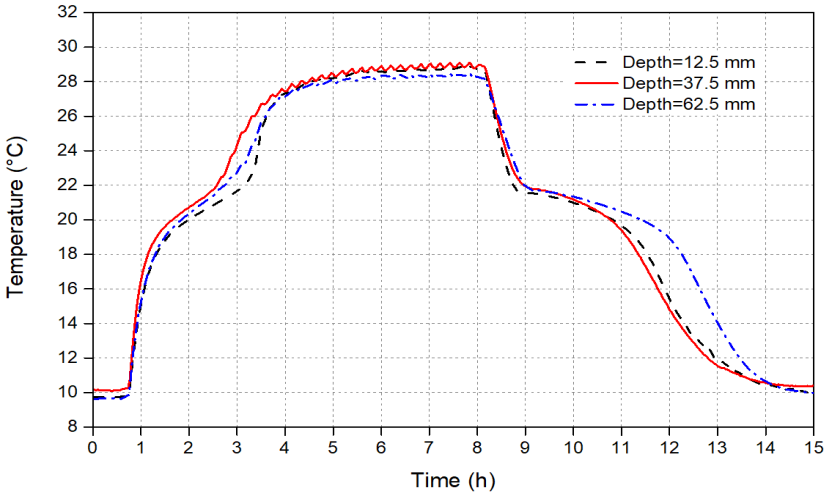

Figure 3-7 The PCM temperature in the heat exchanger with the same height. [66]

3.1.2.2. With artificial sun

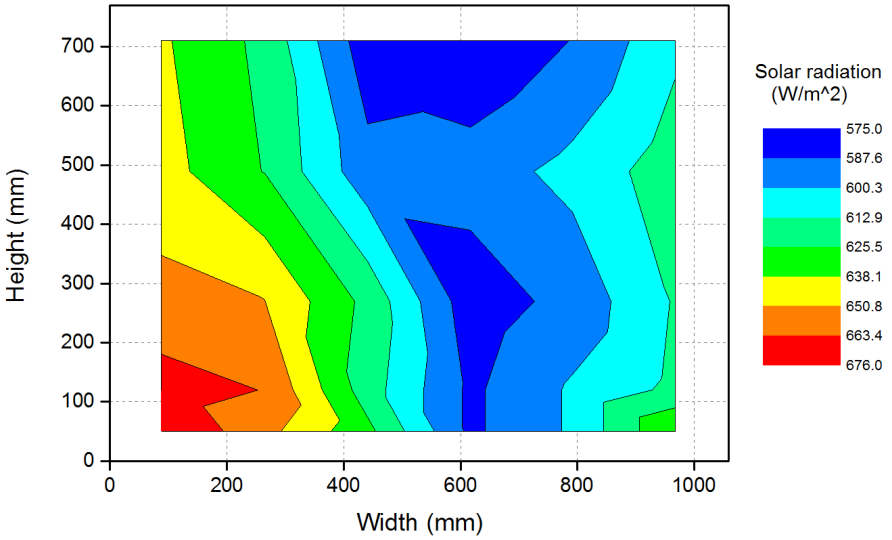

Figure 3-8 Solar radiation distribution on the surface of the PCM unit.

In Figure 3-8 one can see the solar radiation distribution on the out layer of glass surface of the PCM unit. The solar radiation has been measured in 30 different points, mapping the entire surface to assess precisely the total solar gain to the collector. The average solar radiation is 618.2W/m². The distribution of the solar radiation is uneven. The left side has more radiation than the left side, and the middle part has less solar radiation. The deviation of the solar radiation (I_{max} - I_{min}) is 9.35%.

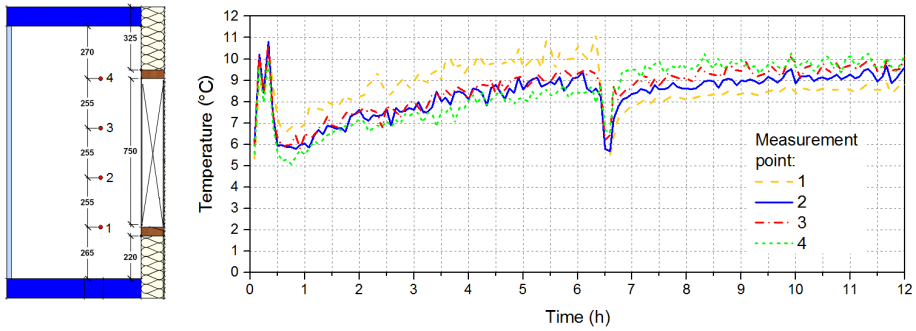

Figure 3-9 The temperature inside the cold box.

Figure 3-9 shows the vertical distribution of the air temperature in the *Cold Box* during the experiment. The artificial sun is activated during the first 6.3 hours and then turned off. The temperature fluctuations in the beginning and in the middle of the test are caused by the sudden change of solar load in the *Cold Box* when the artificial sun is turned on or off. For 0.5 h-6.3 h, measurement point 1 has the highest temperature value. This is probably because the solar radiation at the measurement point 1 is the highest, as seen in Figure 8 (width = 530 mm). In the heat storage mode, the vertical inhomogeneity of the air temperature in the cold box is lower than 3 °C. In the ventilation preheating mode, it is lower than 2 °C.

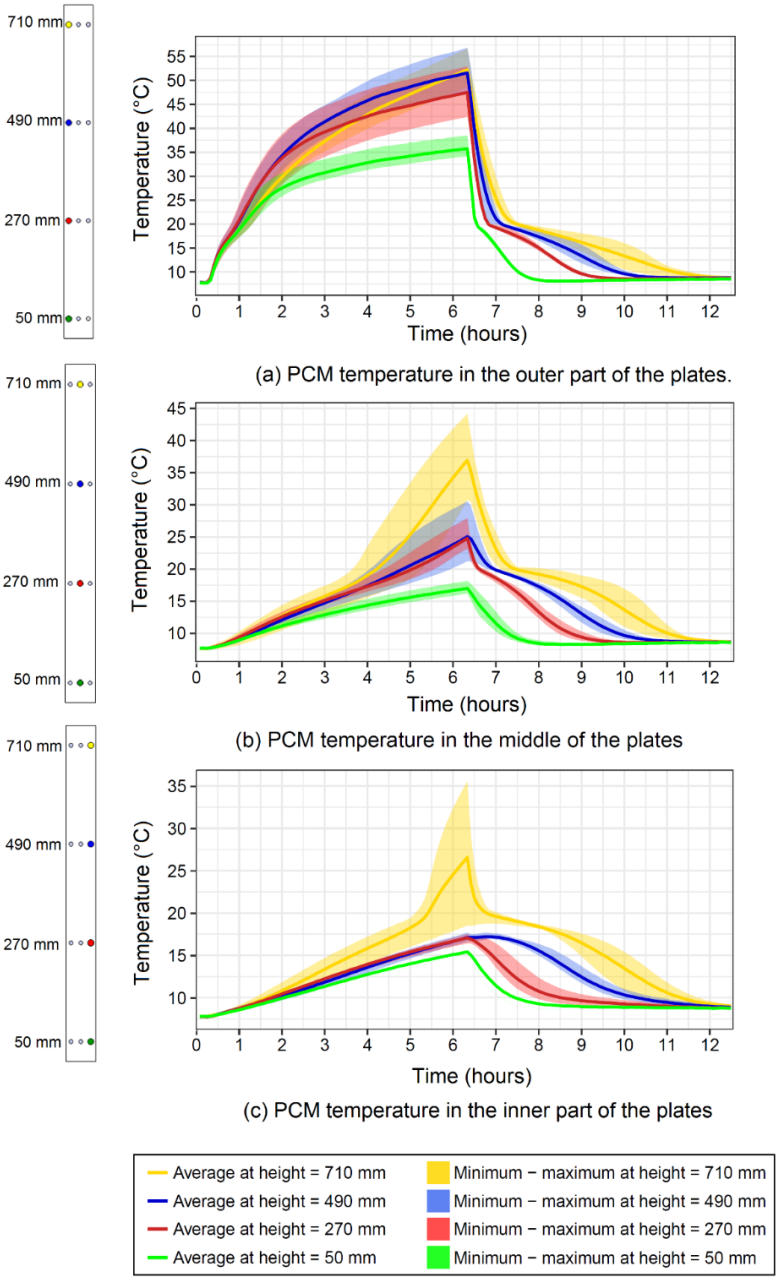

Figure 3-10 PCM temperature measurements at different heights of the heat exchanger plates during the experimental test.

In Figure 3-10 one can see the PCM temperature at different positions within the collector plates at four different heights. At each height, the temperature profiles are established from 4 measurement points along the width of the heat exchanger. The average temperature at different heights are shown as solid curves. The color shades around the solid curves represent the temperature range (minimum and maximum) for all the measurement points. Temperature stratification is visibly clear along with the height of the heat exchanger.

Figure 3-10(a) shows that during the solar energy storage mode, the PCM temperature in the outer part of the plates rises quickly. The phase transition occurs at the same time in the entire height of the collector during 0.7 h - 1.3 h. The temperature gradient between measurement points at 50 mm and the other ones is significant. The reason is that the PCM temperature close to the radiation surface is more influenced by the radiation rather than the convection of hot air inside the air gaps. During the ventilation preheating mode, the phase transition occurs during a longer period (6.5 h - 10.5 h). The PCM at the same height has a similar heating rate and reaches the phase transition temperature at a similar time. The PCM at the lower height solidifies first, because it is closer to the inlet. Similarly, the higher the PCM in the heat exchanger, the later it solidifies.

Figure 3-10(b) shows the PCM temperature in the middle of the collector plates. During the solar energy storage mode, the PCM at the height 710 mm melts first (at around 3 h), then at 490 mm and 270 mm. The PCM at the height of 50 mm does not reach the melting peak of the material during the two modes. The temperature stratification is partly due to solar radiation and partly due to the convection inside the air gaps. During the ventilation preheating mode, the temperature profiles show the same pattern as the PCM temperature in the outer part of the plates and are lower than in the middle of the plates. The phase transition occurs at 6.5 h - 10.5 h. Also, the PCM at the same height has a similar heating rate and reaches the phase transition temperature at a similar time. The PCM at the lower height solidifies first, followed by the PCM at higher heights.

Figure 3-10(c) shows the PCM temperature in the inner part of the plates. During the solar energy storage mode, only the temperature of PCM at the height of 710 mm reaches the melting peak. The phase transition occurs during 4 h - 5.6 h. The stratification of temperature only occurs at the top of the plates. It is more influenced by the convection inside the air gaps than solar radiation. During the ventilation preheating mode, the temperature profiles show the same pattern as the PCM temperature in the outer and middle parts of the plates.

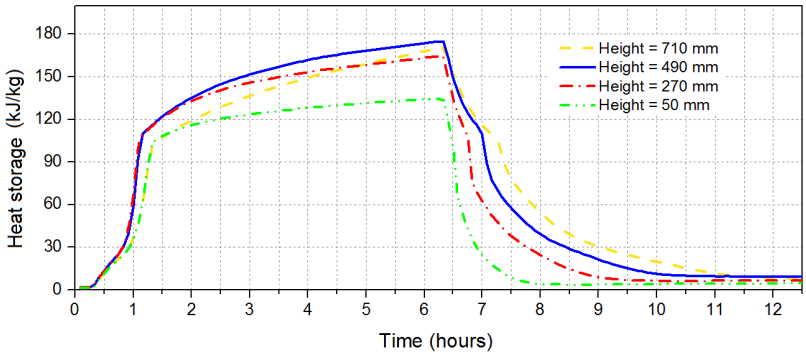

(a) Heat storage in the outer part of the PCM plates

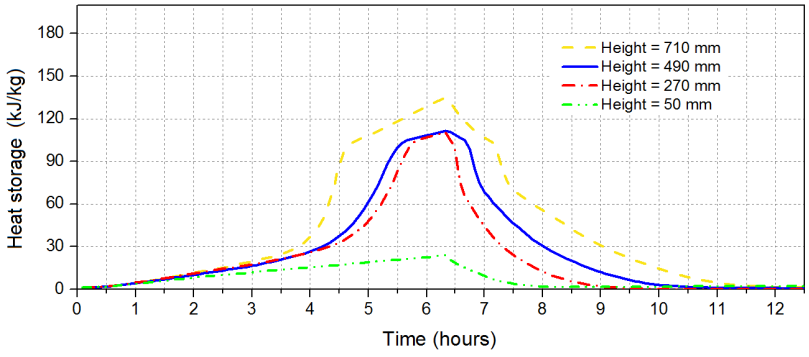

(b) Heat storage in the middle of the PCM plates

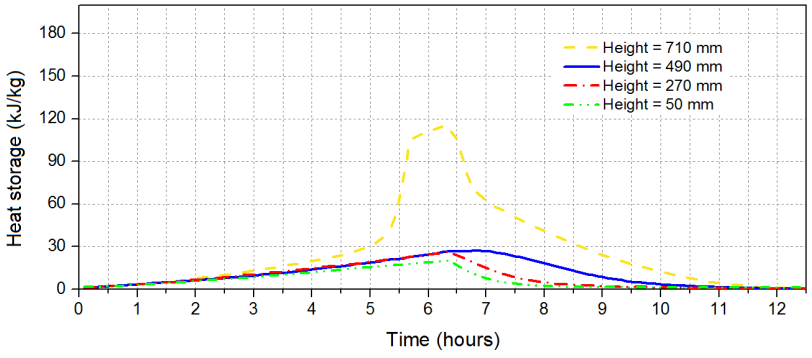

(c) Heat storage in the inner part of the PCM plates

Figure 3-11 Heat storage capacity of PCM in the two experimental modes.

Figure 3-11(a) shows the heat storage capacity of PCM in the outer part of the plates. The heat storage increases rapidly from 0.7 h - 1.3 h, which is due to the latent heat storage of the PCM during the phase transition period. At 6.5 h, the PCM at the height 50 mm starts releasing latent heat. At 10.5 h, the PCM at the height 710 mm finishes latent heat releasing. The heat storage profiles of all the measurement points present a sharp peak. Thus one can deduce that the PCM in the whole outer part of the plates has effective sensible and latent heat storage. Figure 3-11(b) shows the heat storage capacity of PCM in the middle of the plates. In the energy storage mode, the measurement points at all heights have the full latent and sensible heat storage except the height 50 mm. The heat storage ability of the PCM in the inner part of the plates is seen in Figure 3-11(c). Only the PCM at the height 710 mm has the full latent heat storage, which means most of the inner part of the plates is not activated. It emphasizes the necessity of an optimization of the depth of the plates. The total stored energy by all the plates E_{stored} is 5.84 MJ.

The energy storage efficiency is 41.7%, which is calculated based on Equation (3-1).

$$\eta_1 = \frac{E_{recieved}}{E_{stored}} = \frac{\Delta t \cdot I \cdot A}{E_{stored}} \qquad \textbf{3-1}$$

Where

$E_{recieved}$ is the energy received by the PCM during the solar energy storage mode; E_{stored} is the energy stored during the solar energy storage mode; Δt is the entire time of the solar energy storage mode; *I* is the average solar radiation density received by the surface of the heat exchanger; A is the surface area of the heat exchanger exposed to the solar radiation.

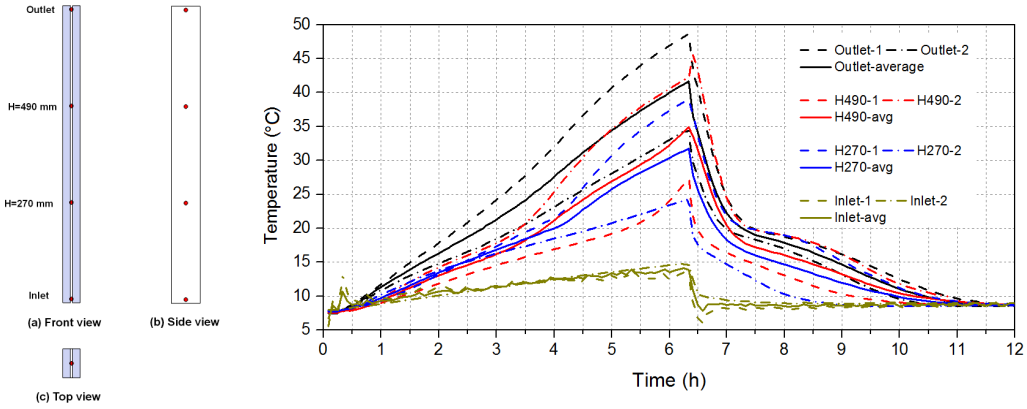

Figure 3-12 The temperature distribution in the air gap

Figure 3-12 shows the temperature distribution at different heights of the air gap and at the inlet and outlet. The air temperatures at 270 mm and 490 mm are similar. For the solar storage mode, the outlet air temperature is influenced by the ambient PCM temperature as well as the frame of the heat exchanger. For the ventilation preheating mode, the inlet air temperature is more influenced by the air temperature inside the *Cold Box*. The energy released from the PCM to the ventilation system during the ventilation preheating mode $E_{released}$ is calculated by Equation (3-2).

$$E_{released} = \int_t q_{air} \rho_{air} Cp_{air} (T_{outlet} - T_{inlet}) \qquad \textbf{3-2}$$

Where q is the airflow rate inside the heat exchanger during the ventilation pre-heating mode; ρ is the density of the air; Cp is the specific heat capacity of the air; T_{outlet} is the outlet air temperature of the heat exchanger; T_{inlet} is the inlet air temperature of the heat exchanger.

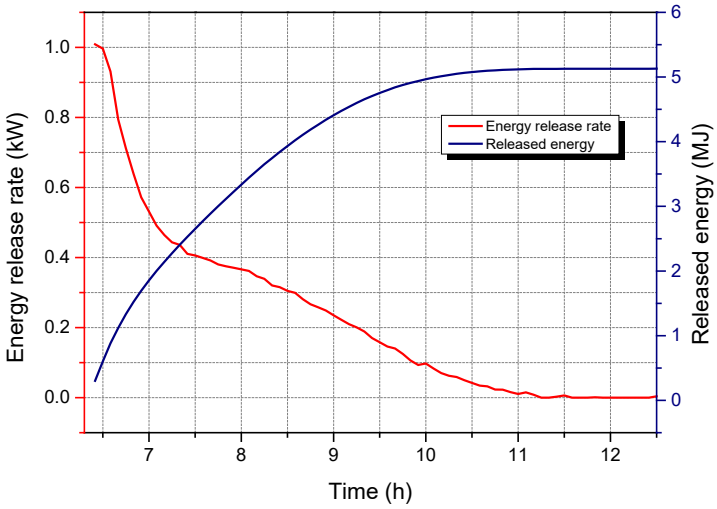

Figure 3-13 The energy release rate and release energy of the heat exchanger during ventilation preheating mode.

Figure 3-13 presents the energy release rate and the released energy of the heat exchanger along with the time during ventilation preheating mode. The energy release rate of the heat exchanger shows a similar trend as the outlet air temperature. The total released energy within the 6.3 h - 12.5 h time period is 5.13 MJ.

The pre-heating efficiency of the heat exchanger is 87.8%, which is calculated by Equation (3-3).

$$\eta_2 = \frac{E_{stored}}{E_{released}} \qquad \textbf{3-3}$$

The overall energy efficiency of the heat exchanger is calculated by Equation (3-4).

$$\eta_3 = \eta_1 \cdot \eta_2 \qquad \textbf{3-4}$$

The overall energy efficiency of the heat exchanger is 36.6%. The limited overall energy efficiency is mainly caused by the low energy storage efficiency of the heat exchanger, which is prevailingly due to the low heat storage capacity in the inner side of the PCM plates. This part of the PCM can be removed or activated by a better configuration design of the heat exchanger.

3.2. NUMERICAL STUDY OF THE PCM HEAT EXCHANGER

3.2.1. THE NIGHT COOLING APPLICATION

Considering a PCM heat exchanger made of parallel PCM plates. The plate thickness and the air gap between plates are 5mm, and the height of the PCM plates is 770 mm, as seen in Figure 3-14.

The model is simplified into 2D with symmetry boundary conditions for heat transfer and laminar flow[66]. The calculation domain is half of the PCM plate and half of the air gap. The descriptions and details of the model is in Appendix A: *"A new ventilated window with PCM heat exchanger – performance analysis and design optimization."*[66]

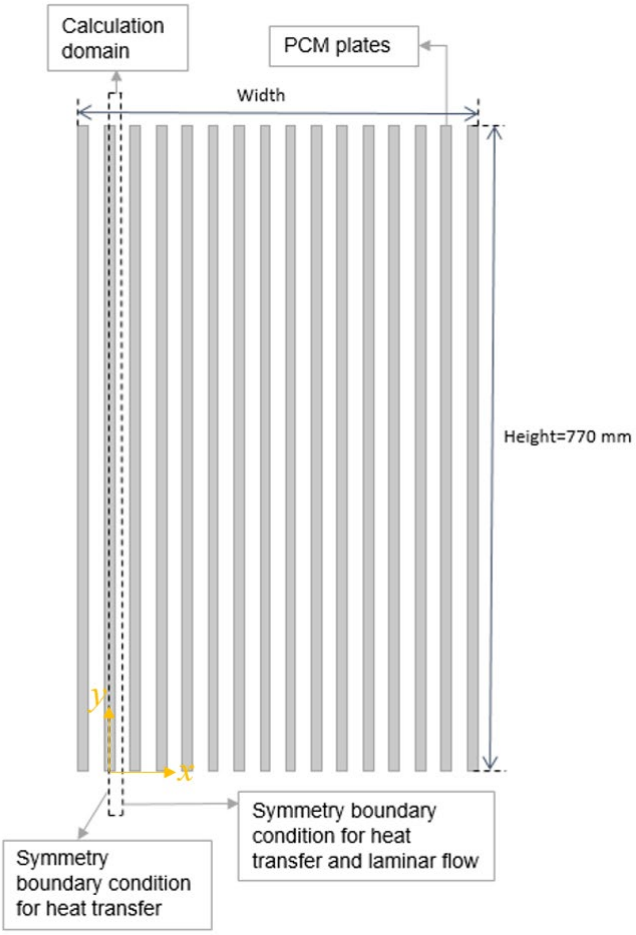

Figure 3-14 The calculation domain of the numerical model.

Due to the big aspect ratio, different meshing methods are applied to the long side and the short side. It is denser on the short side. It is also denser in the boundary layer than in the domain part. The meshing contains 275162 elements. The average meshing quality is 0.86. The mesh quality is calculated by the ratios of the inscribed and circumscribed circles' or spheres' radii for the simplex corresponding to each corner of the element[80]. The mesh element quality measures the regularity of the mesh elements' shapes[81]. The meshing details are in Figure 3-15.

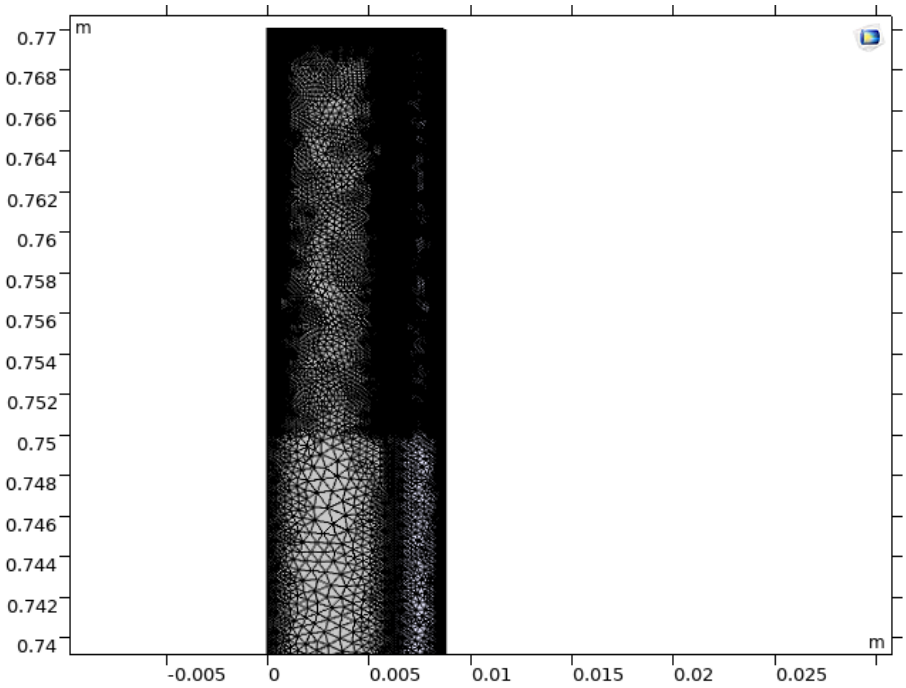

Figure 3-15 The meshing details of the finite element model.

3.2.2. THE SOLAR ENERGY STORAGE APPLICATION

The 3D finite element model is built in COMSOL Multiphysics. The model solves heat transfer and laminar flow multiphysics[79]. The model simulates the parallel PCM plates and the laminar flow between the plates. The buoyancy force is added to the flow. The model is simplified by applying symmetry boundary conditions to save computation time. The simplification is possible because the boundary conditions for each plate and air gap are the same (except the ones close to the frame of the heat exchanger). The symmetry boundaries and the meshing of the model are shown in Figure 3-16. The meshing contains 179192 elements. The average meshing quality is 0.58.

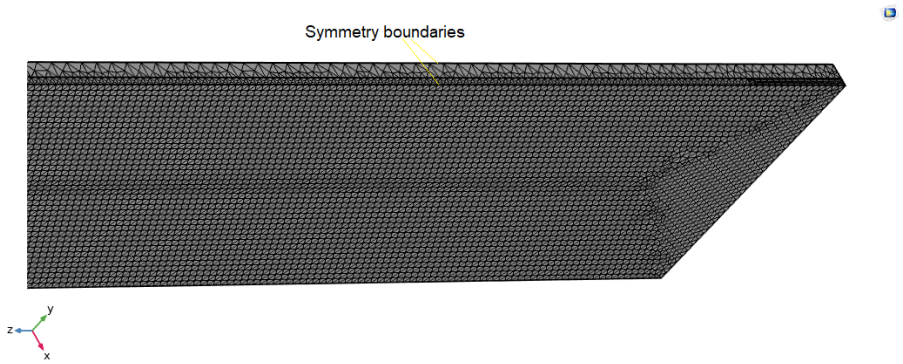

Figure 3-16 The meshing details of the 3D solar energy storage model.

The convection heat transfer in the PCM is neglected because the PCM is encapsulated in shape stable fiberboards. It is verified later in the model validation part. The details of the model are shown in Appendix B: *"Experimental and numerical study of a PCM solar air heat exchanger and its ventilation preheating effectiveness."*[79]

3.2.3. MODEL VALIDATION

The night cooling model is verified by the data from the experiment described in chapter 3.1.2.1. The average error for the freezing process is 2.38%, for the melting process is 4.79%. Please refer to Appendix A[66] for more information about model details and model validation.

The solar energy storage model is verified by the experimental data from the experiment described in chapter 3.1.2.2. The average error is 4.02. For more information about model details and model validation, please refer to Appendix B [79].

3.3. CONFIGURATION OPTIMIZATION OF THE PCM HEAT EXCHANGER

3.3.1. NIGHT COOLING APPLICATION

The climate data of one extreme day in Copenhagen is used as the boundary condition for configuration optimization, as shown in Figure 3-17. The data is from the Design Reference Year measured by DMI[82].

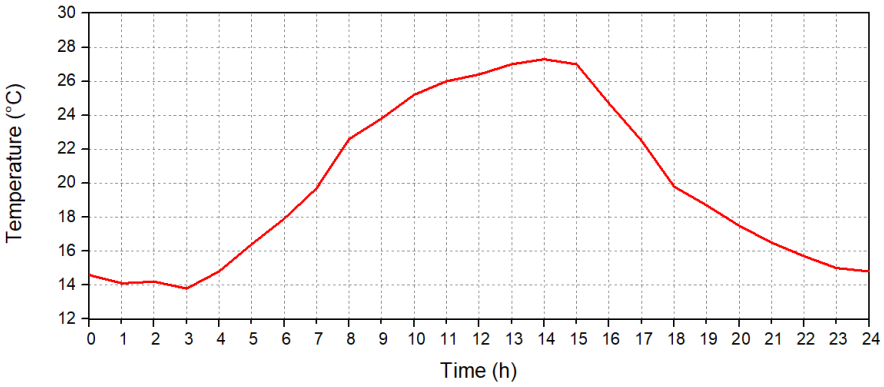

Figure 3-17 The outdoor dry-bulb air temperature of a sever summer day in Copenhagen.[66]

PCM heat exchanger with 4 different plate thicknesses is chosen. The air gap thickness and plate depth are all the same, which is 5 mm. The airflow rate in each PCM heat exchanger is 106 m^3/h. The details of the simulated cases are in Table 3-1.

Table 3-1 The cases for PCM plate thickness optimization.[66]

d (mm)	e (mm)	Air velocity (m/s)	Number of plates in total	Plate depth (mm)	Air flow rate (m^3/h)	Total PCM surface area (m^2)	Total PCM volume (m^3)
5	5	0.74	106	75	106	22.30	0.052
10		1.09	70			15.69	0.069
15		1.48	53			12.62	0.078
20		1.78	42			10.58	0.083

The discharged heat for PCM heat exchangers with different plate thicknesses are shown in Figure 3-18. All the cases have similar discharged heat rate for the first 3 h. PCM heat exchanger with 5 mm plate thickness discharges fastest, while with 20 mm

plate thickness discharges slowest but the discharged heat of which is the highest. For 5.5 h discharging time, the 10 mm plate thickness performs better considering both discharging speed and total discharged heat[66].

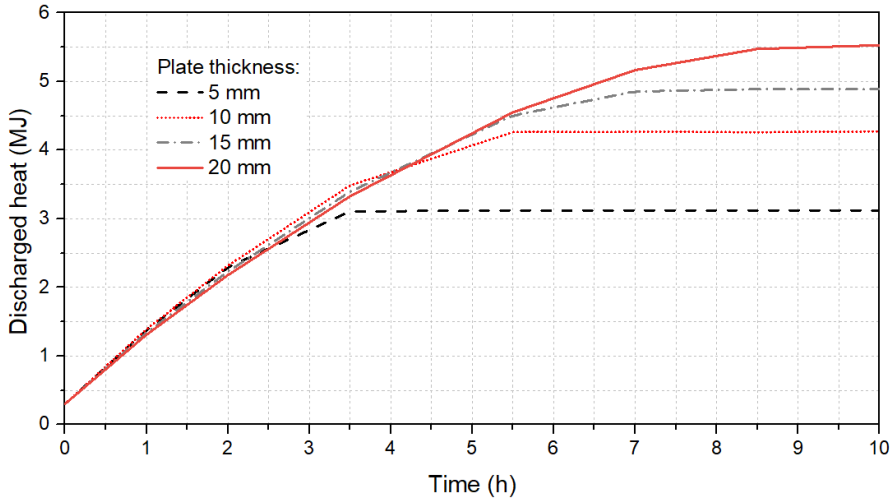

Figure 3-18 The total discharged heat of the PCM for the heat exchanger with different plate thicknesses in the night cooling period.[66]

Figure 3-19 compares the ventilation pre-cooling ability of the PCM heat exchangers using 5 mm plates and 10 mm plates. In the period 11:00-15:00, the PCM heat exchanger with 10 mm plates cools down the ventilation by average 6.5°C for 3.9 h effect hours (with supply air temperature lower than 23°C), while for PCM heat exchanger with 5 mm thickness, the effect hour is 2.8 h[66].

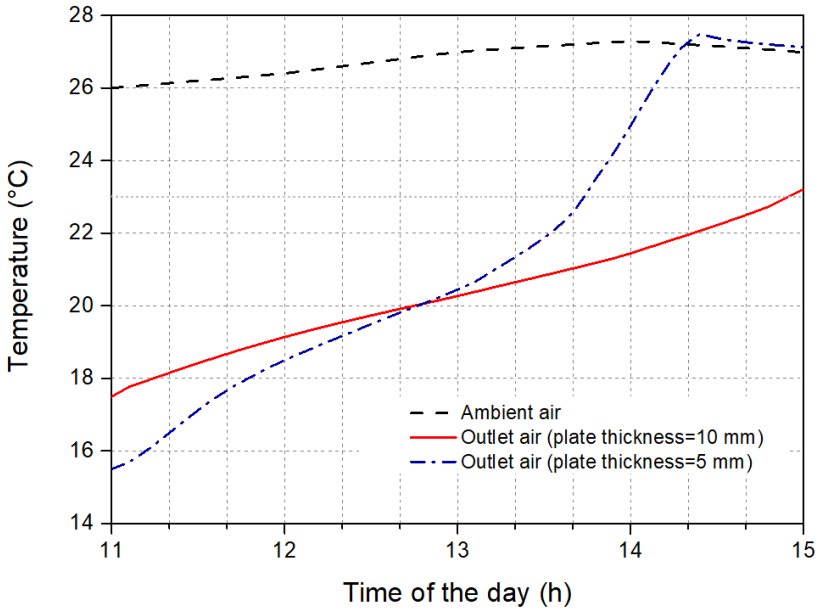

Figure 3-19 The outlet air temperature of the PCM heat exchanger in the daytime ventilation pre-cooling period.[66]

The optimized plate thickness for the PCM heat exchanger is 10 mm for both high charging/discharging speed and high charging/discharging heat amount[66].

3.3.2. SOLAR ENERGY STORAGE APPLICATION

The solar radiation from the sun is a key parameter that influences the effect of the solar energy storage application. When the PCM plates are exposed to sunlight, the PCM in different depths of the PCM plate melts at different times because the heat transfer direction is along with the depth of the PCM plate. Figure 3-20 shows the PCM temperature distribution in the middle panel of PCM plates with different depths after 6 h charging by 550 W artificial sunlight[79]. The heat flux is from the right side. It shows that the PCM plate with a smaller depth has a higher PCM temperature and a higher amount of melted PCM for the whole plate. Figure 3-21 shows that the PCM plate with a smaller depth has a higher melt fraction, and reaches a stable state faster[79]. However, the stored latent heat by the PCM plate with smaller depth is also smaller, seen in Figure 3-22. For the PCM plate with bigger depth (100 mm or 110 mm), the PCM cannot fully melt during the 6 h charge. PCM plate with 90 mm depth is optimized for the charging speed and the stored latent heat[79].

A similar optimization process is done for the air gap thickness between the PCM plates. It is found out that the optimized air gap thickness is 6 mm[79].

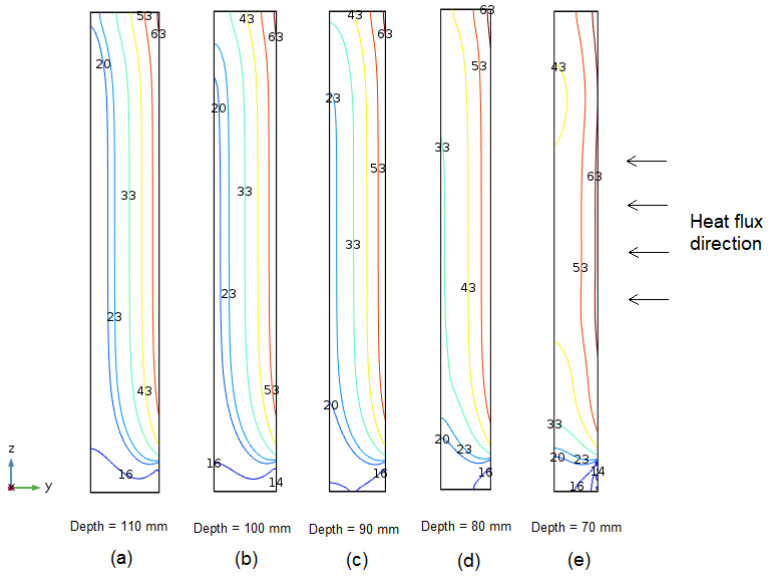

Figure 3-20 The temperature distribution in the PCM plates at 6 h.[79]

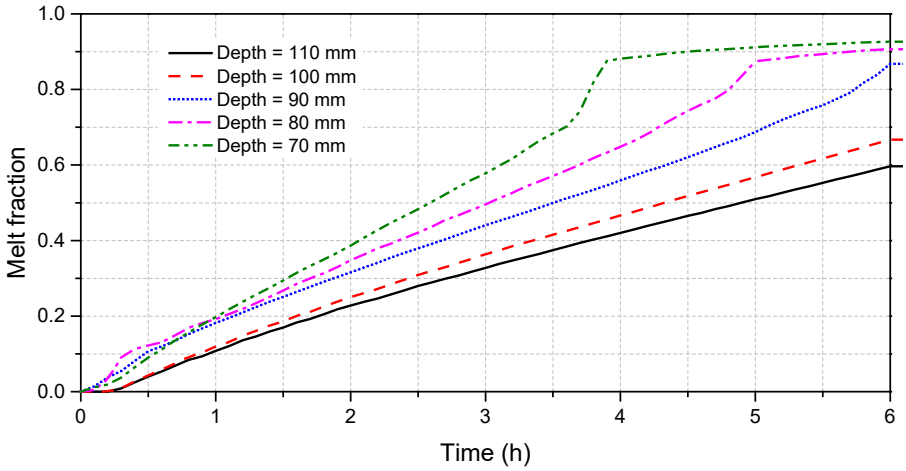

Figure 3-21 The melt fraction of the PCM along with charging time.[79]

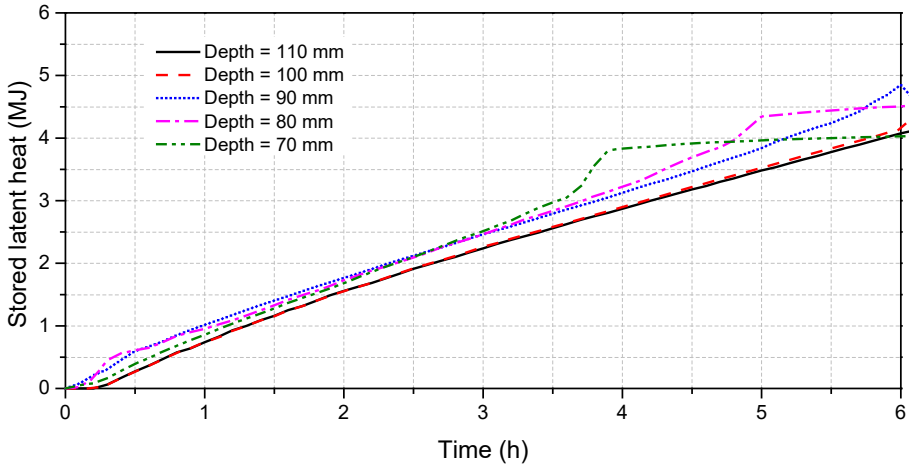

Figure 3-22 The stored latent heat of the PCM along with charging time.[79]

3.4. CONCLUSIONS

The experiment of the night cooling application has the main conclusion that the PCM temperature is equally distributed along with the depth of the PCM plates, which indicates that the numerical model for night cooling application could be simplified into 2 dimensional.

The experiment of the solar energy storage application has the main conclusion that the PCM temperature is not equally distributed along with both the depth and the height of the PCM plates. In addition, considering the buoyancy drive in the PCM cavity, a 3-dimensional numerical model would be more accurate for the application.

The numerical models built for night cooling application and solar energy storage application are both verified by experimental data. The optimized configuration of the PCM heat exchanger for the night cooling application is 10 mm plate thickness. The optimized configuration of the PCM heat exchanger for the solar energy storage application is 6 mm air gap thickness and 90 mm plate depth.

CHAPTER 4. THE EFFECT OF PCM ENHANCED VENTILATED WINDOW ON THE ENERGY PERFORMANCE OF THE SYSTEM

The optimized configuration of the PCM heat exchanger in Chapter 3 is used to enhance a ventilated window for both night cooling purpose and solar energy storage purpose. This chapter firstly presents an experimental study of the PCMVW to study the thermal performance of the PCMVW and the potential ways to improve the system. The Energyplus models of an apartment with 4 PCMVWs are then built and validated by the experimental data. The models are used for control strategy development, including summer night cooling control strategy, winter solar energy storage control strategy and advanced shading control strategy.

4.1. EXPERIMENTAL STUDY OF THE PCM ENHANCED VENTILATED WINDOW

4.1.1. EXPERIMENTAL SETUP

The PCM enhanced ventilated window and normal ventilated window are tested in the façade lab on the top floor of the Department of Civil Engineering. The windows are mounted in the façade facing south. The building is located in an open area with no obstructions from the surroundings on the south[27].

Figure 4-1 shows the tested windows. The PCMVW includes a PCM heat exchanger and a VW, and the Ref is a normal ventilated window. The configuration of the PCM heat exchanger selected here is based on the configuration optimization for both summer and winter applications in chapter 3. The two windows have the same type of vents, to guide the airflow from outdoor to indoor through the windows.

Figure 4-1 The experimental setup of PCMVW and reference VW.[27]

Two fans are used for each window separately, to provide controllable flow in each window. 180 K-type thermocouples are used for the temperature measurement in all the windows. More details about the experimental setup can be found in Appendix C [27].

4.1.2. EXPERIMENTAL RESULTS

4.1.2.1 Night cooling application

The night cooling application of PCMVW for summer and transition seasons is firstly tested. The test includes an external shading for the PCM heat exchanger, to avoid the heat from the sun during the daytime. During the night, the hot PCM is cooled down by ventilating the cold outdoor air to the PCM heat exchanger. During the day, the cold PCM is used to pre-cool the ventilated air before ventilating into the room[27]. In this test, the PCMVW is ventilated through the PCM heat exchanger and ventilated

window all the time. The Ref VW is ventilated through the ventilated window the whole time[27].

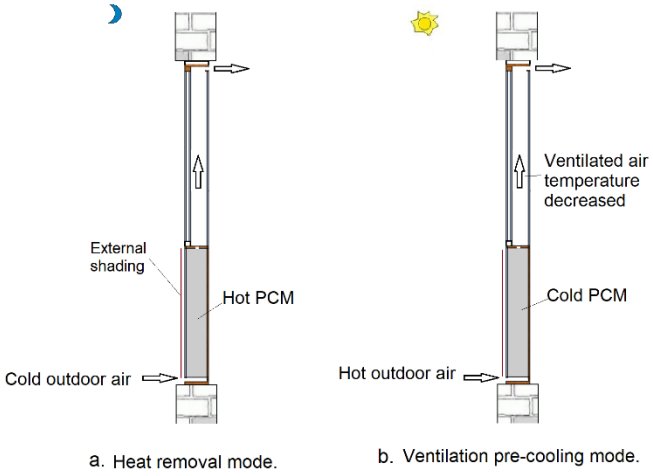

Figure 4-2 The working principle of the night cooling application. [27]

The data of 13 days with different outdoor climate conditions are gathered and analyzed. The PCMVW has 4 thermal and energy performance indicators for summer night cooling application: heat removal amount, ventilation energy-saving, inlet temperature decrease and cooling effect hours[27]. Those indicators are calculated by comparing the room inlet air temperature of a PCMVW and a reference VW.

The linear correlations between outdoor climate parameters and the indicators are shown in Figure 4-3. Strong linear correlations can be found for heat removal amount, ventilation energy-saving and inlet temperature decrease[27]. The cooling effect hours have no strong correlation with the outdoor average temperature difference. The inlet air temperature of the PCMVW is by average 1.4°C lower for 7 hours compared to the conventional VW[27]. The average energy saving is 0.7 MJ/day for the tested days[27].

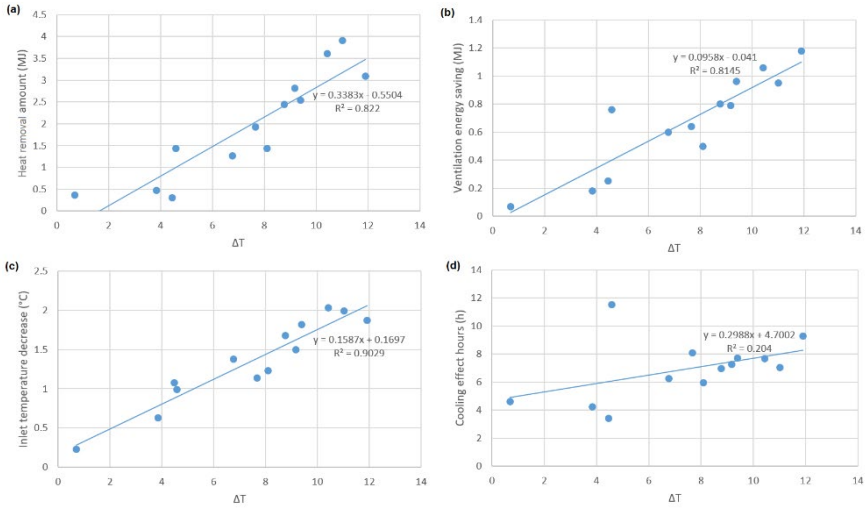

Figure 4-3 The relations of PCMVW indicators to the outdoor climate conditions. [27]

4.1.2.2 Solar energy storage application

The solar energy storage application operates normally in winter or in transition seasons when ventilation pre-heating is needed. The heat storage mode is on during the daytime when the PCM stores the heat from solar radiation. While during the ventilation preheating mode, the ambient air temperature is quite low[27]. The hot PCM is then releasing the heat to the ventilation, to provide heat to the room as well as avoid the cold draft. The PCMVW is ventilated through VW in 8:30-18:30, through PCM and VW in 18:30-next day 8:30, while Ref VW ventilates through VW all day and night[27]. The control strategy of the PCMVW is shown in Figure 4-4.

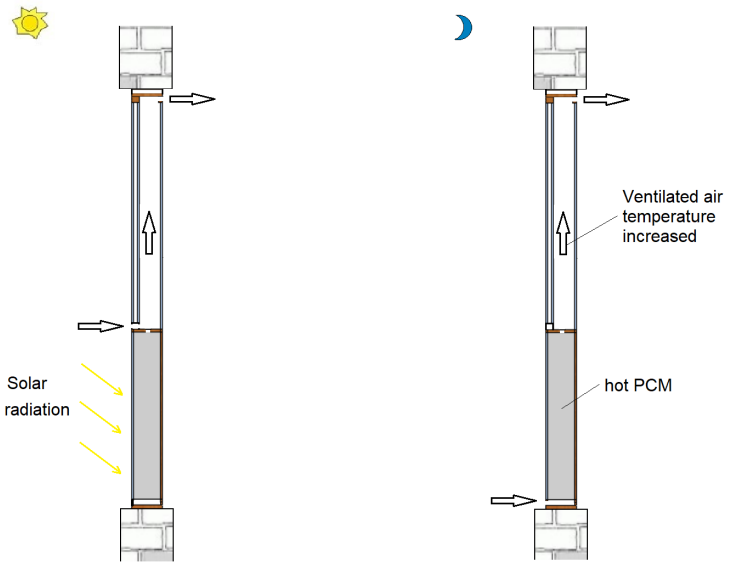

Figure 4-4 The working principle of the solar energy storage application. [27]

Figure 4-5 shows the outdoor weather parameters in relation to the PCMVW performance indicators. The heat storage amount, ventilation energy-saving, inlet air temperature increase have a linear correlation with solar radiation level, while the heating effect hours has a linear correlation with night time average outdoor air temperature[27]. The latter is not so well fitted. One reason may be the low airflow rate through the PCMVW, which makes the heat release process slow. Compared to the conventional VW, the PCMVW can provide by average 2°C higher inlet air temperature to the room for an average of 12 hours[27]. The average energy saving is 1.6 MJ/day[27].

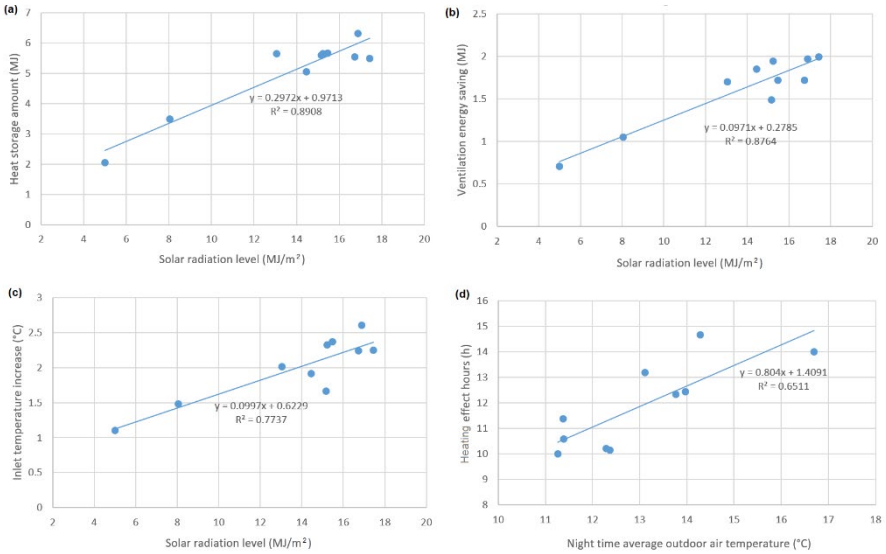

Figure 4-5 The ventilation performance indicators as functions of the climate parameters. [27]

4.1.2.3 Blinds for mechanical ventilation and self-cooling natural ventilation

The between-glass venetian blinds are introduced in the VW. The blinds have two sides: one absorption side and one reflection side. The absorption side is used for winter solar energy storage application, to increase the heat gain from the VW. The reflection side is used in summer night cooling application, to decrease the heat gain from the VW. Moreover, the reflection blinds in the combination of VW self-cooling can decrease the chance of the room from overheating, in transition or winter seasons.

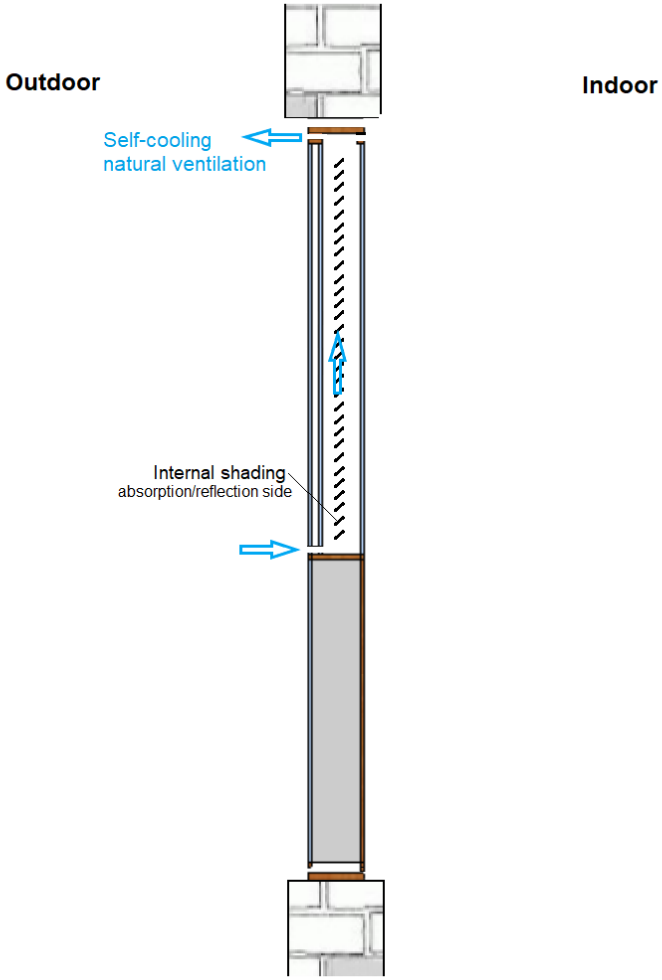

Figure 4-6 The working principle of the VW self-cooling[28].

The self-cooling mode of the VW operates when the indoor air temperature is too high. The VW is ventilated by natural ventilation, to decrease the air temperature in the VW, thus decreasing the room heat gain through the VW. Figure 4-7 shows the window glass surface temperature for VW with and without self-cooling. It indicates that with self-cooling, it can decrease the window inner surface temperature by an average of 0.8 °C. It has to be mentioned that the self-cooling effect highly depends on multiple outdoor weather conditions such as wind pressure, wind speed, and outdoor air temperature. And in this experiment, the blinds are not turned on, which can also influence the self-cooling effect.

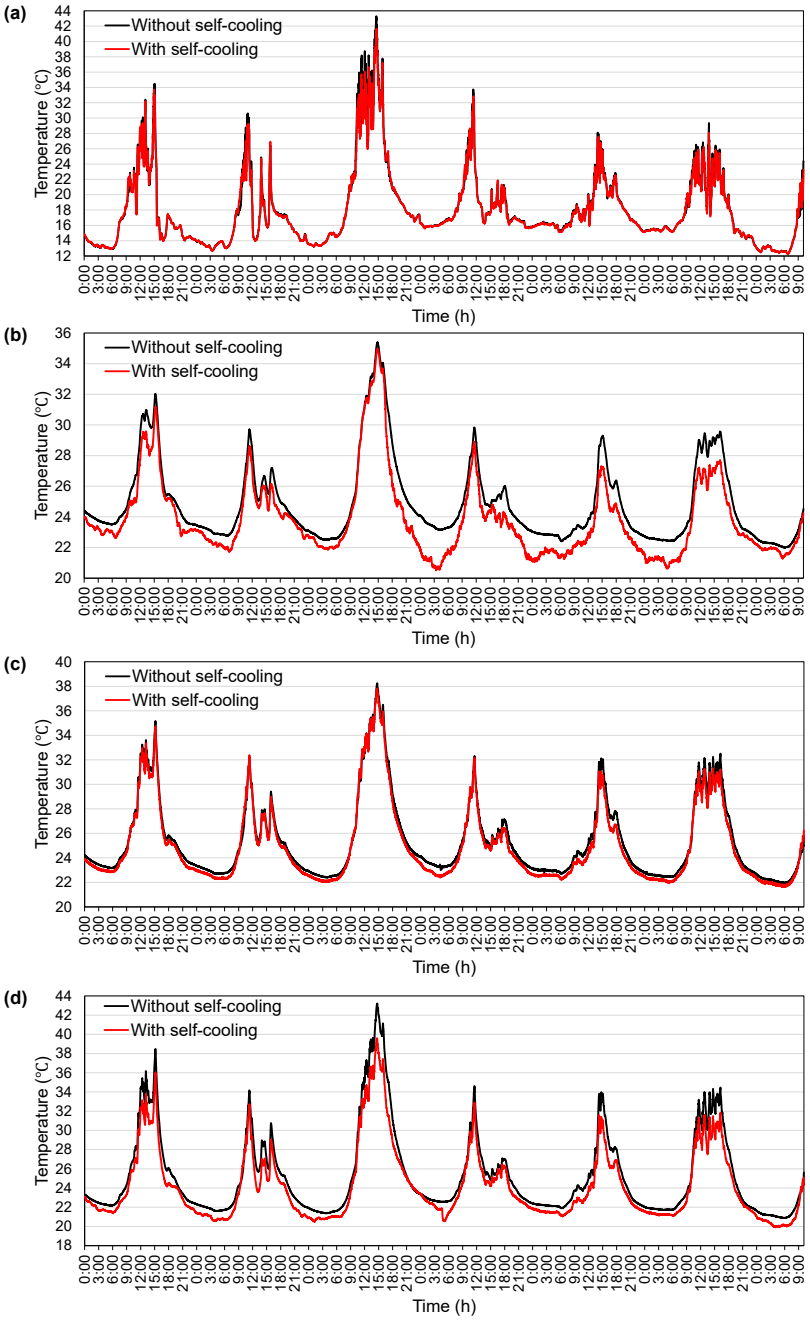

Figure 4-7 The VW inner surface temperature with and without self-cooling. (a) external surface temperature, (b) top of the internal surface temperature, (c) middle of the internal

surface temperature and (d) bottom of the internal surface temperature of the two double windows with and without shading.

Two days are tested for natural ventilation with blinds. The blinds with the reflection side in one of the VWs are used in 14-10-2019, and the blinds with the absorption side on one of the VWs are used in 31-10-2019. The outdoor wind conditions are depicted in Figure 4-8 and Figure 4-10. The wind directions in those two days are mostly from the southwest. The south-facing VWs in the façade lab are under good natural ventilation conditions.

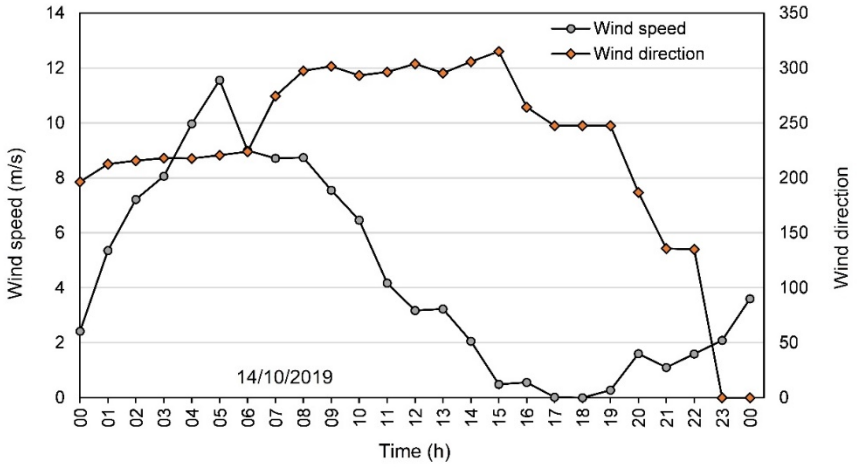

Figure 4-8 The outdoor wind speed and wind direction. [27]

Figure 4-9 and Figure 4-11 show the internal surface temperature of the 2 VWs and the accordingly hourly outdoor air temperature and solar radiation. In Figure 4-9, window 1 is with closed reflection blinds, while window 2 is with open blinds. The internal glass surface temperature of window 1 is higher than window 2, which may due to the high sunlight angle, so that blinds in window 1 actually got more sunlight hit on the absorption side. In Figure 4-11, window 1 is with open blinds, while window 2 is with absorption blinds towards outdoor. The results of the glass surface temperature show that window 2 with absorption blinds can increase its temperature greatly, especially when the solar radiation is high.

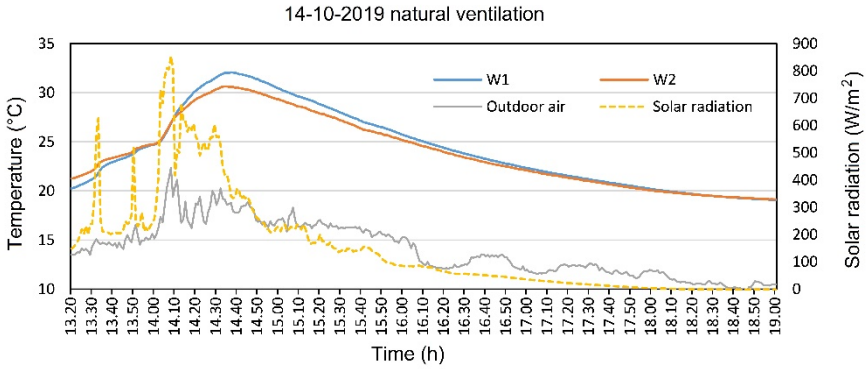

Figure 4-9 The inner glass surface temperature and outdoor climate. The two windows are under natural ventilation. Window 1 blinds close, reflection side towards outdoor; w2 blinds open.

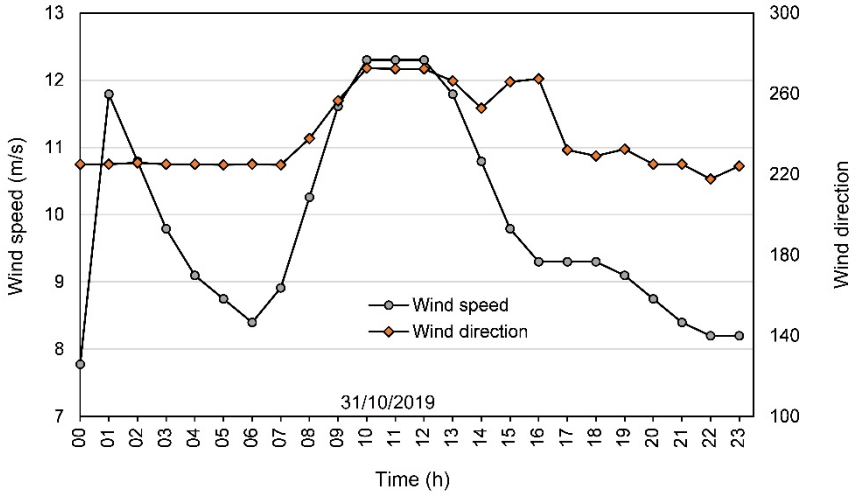

Figure 4-10 The measured outdoor wind speed and wind direction. [27]

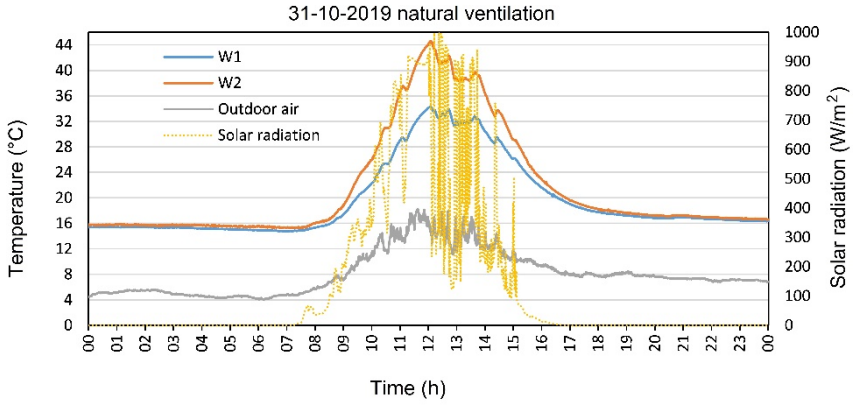

Figure 4-11 The inner glass surface temperature and outdoor climate. The two windows are under natural ventilation. Window 1 blinds open; w2 blinds close, absorption side towards outdoor.

4.2. NUMERICAL STUDY OF THE PCMVW IN AN APARTMENT

4.2.1. MODEL DESCRIPTION

The model is built on a 3-room apartment on the second floor of a 3 floors apartment building[28] as seen in Figure 4-12. The northeast and southwest walls of the apartment are external walls. All the other constructions are set as adiabatic surfaces, because that they are adjacent to the internal air-conditioned rooms. 2 PCMVWs are installed in room 1, 1 PCMVW in room 2 and 1 PCMVW in room 3. The properties of the constructions in the model are in Table 4-1.

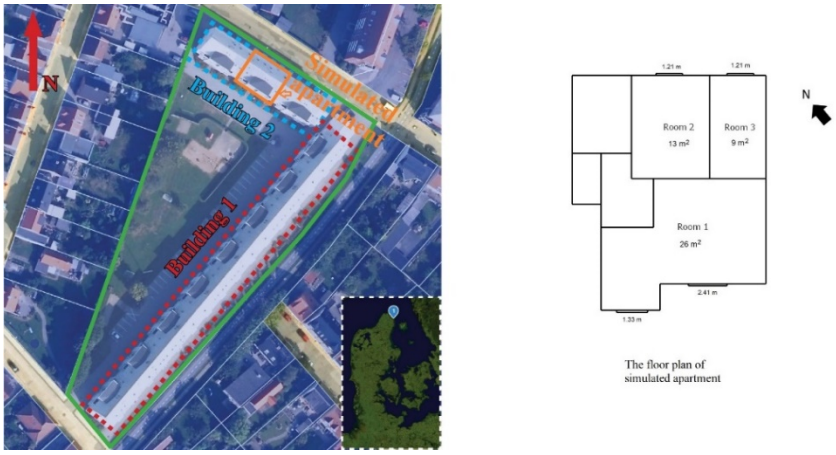

Figure 4-12 The building floor plan for simulation.[28]

Table 4-1 The properties of the constructions. [28]

Material	Thickness [m]	Thermal Conductivity [W/m·K]	Resistance [m²·K/W]
Wood	0.015	0.12	0.125
Insulation	0.245	0.037	6.621622
Brick	0.31	0.77	0.402597

The internal heat gains are from the occupants and equipment. The occupant schedule (Figure 4-13) differs from the days of the week, and the electricity consumption schedule differs from the months of the year (Figure 4-14), according to the report [83]. The number of people and electricity loads of each room refers to a survey form the national building research institute[84].

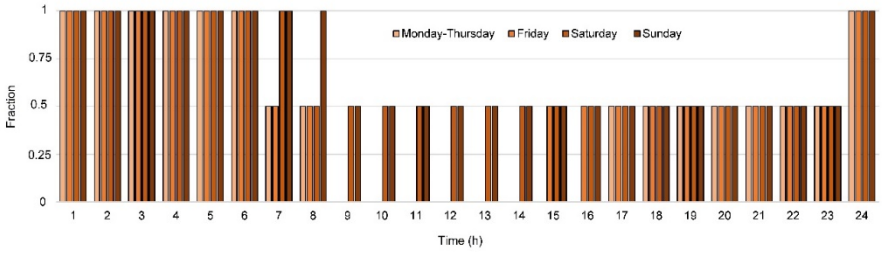

Figure 4-13 The occupant schedule of the apartment. [28]

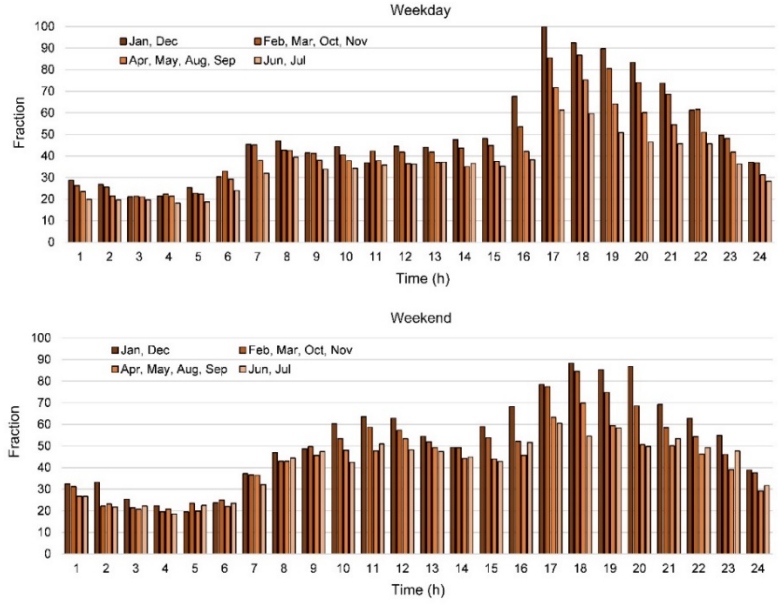

Figure 4-14 The electricity consumption schedule based on a survey in Denmark. [28]

Table 4-2 The people and electricity load of the rooms. [28]

	Room 1	Room 2	Room 3
Number of people	0.941	0.463	0.332
Maximum electricity load(W)	324.05	158.54	109.59

The ventilation flow rate of each room is calculated by the minimum fresh air of the occupants, which is 30 m^3/h/person[85].

The venetian blinds in the VW have two functional sides with different solar transmittance/reflectance coefficients. For summer night cooling application, the reflection side with a high solar reflection coefficient is turned to the outside. For the winter solar energy storage application, the absorption side with a low solar reflection coefficient is turned to the outside[28].

During the summer, the PCM heat exchanger is covered by external shading to avoid heat from the sunlight. During the winter, the external shading is turned off so that the PCM can store solar energy[28].

4.2.2. MODEL VALIDATION

The modeling results of PCM temperature, air temperature in the PCM heat exchanger and air temperature in the VW are compared with experimental results, as shown in Figure 4-15 and Figure 4-16. The modeling average error for summer night cooling application is 5.4%, and for winter solar energy storage is 8.8%[28].

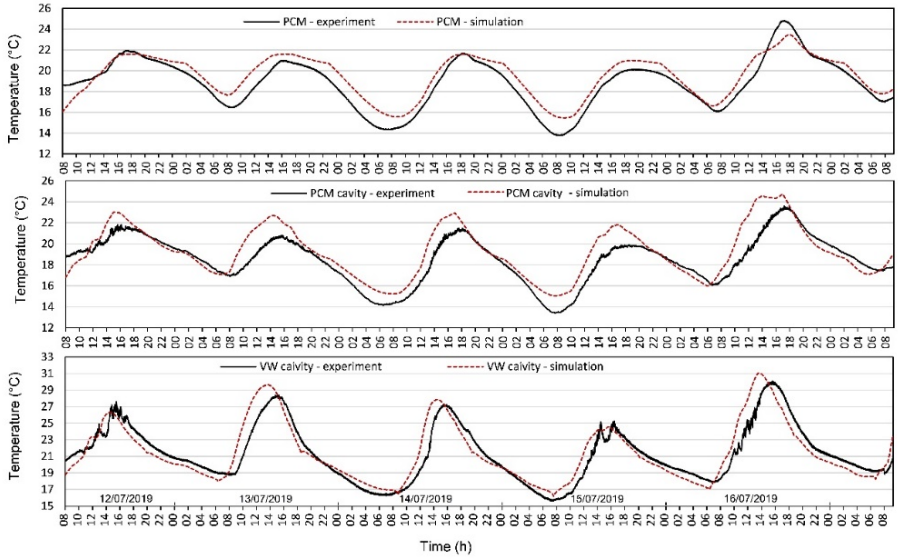

Figure 4-15 The model validation of night cooling application.[28]

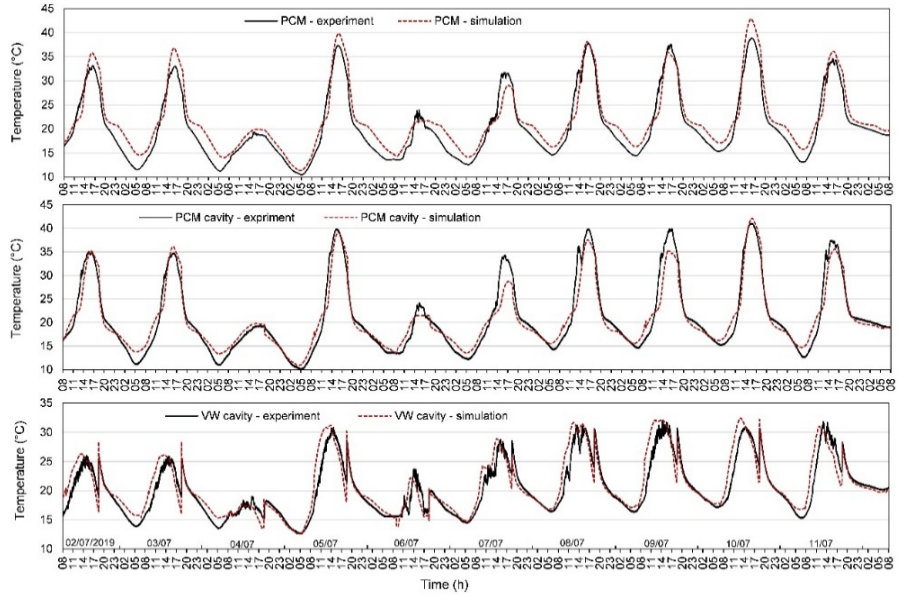

Figure 4-16 The model validation of solar energy storage application. [28]

4.2.3. THE PCMVW PERFORMANCE

The thermal and energy performances of the PCMVW are compared to 2 other ventilation systems: the ventilated window without PCM (VW, no PCM) system and normal window without VW and PCM (no VW, no PCM) system for both night cooling application during summer (May - October) shown in Figure 4-17 and solar energy storage application during winter (November - April) shown in Figure 4-19.

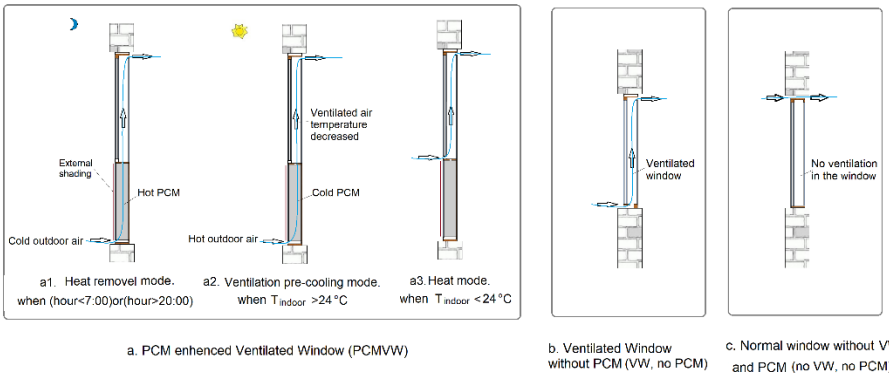

Figure 4-17 The comparison of PCMVW to 2 other ventilation systems for summer night cooling application.[28]

Figure 4-18 shows the energy demand of the 3 ventilation systems during the summer period. It is seen that for both rooms, the PCMVW system has the least energy demand, while the VW, no PCM system has the highest energy demand. Room 3 has a similar external wall and floor area, thus the energy demand per square meter floor area is similar to room 2[28]. In this study, the energy performance of room 3 with PCMVW is not further discussed. For room 1, the cooling energy saving percentage of PCMVW compared to VW, no PCM system and no VW, no PCM system is 46% and 27% respectively[28]. For room 2, the percentage is 51% and 38% respectively[28].

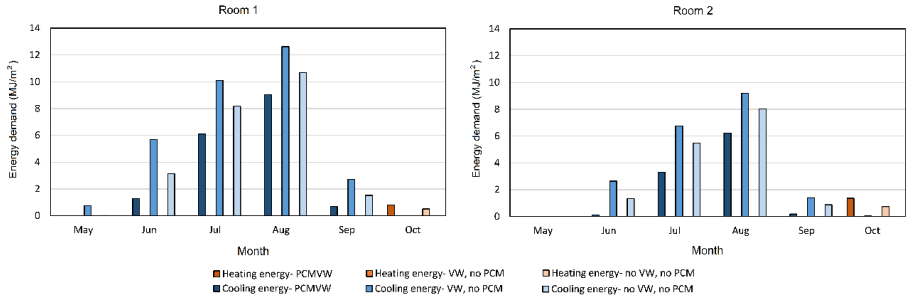

Figure 4-18 The energy demand of the rooms with 3 different ventilation systems during summer.[28]

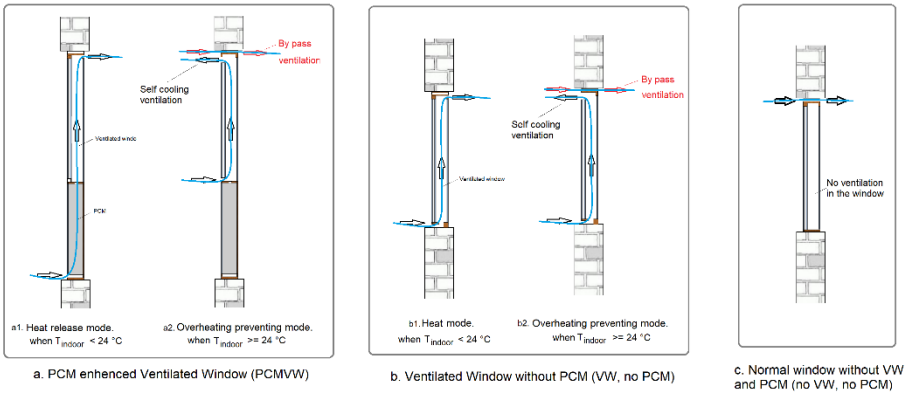

Figure 4-19 The comparison of PCMVW to 2 other ventilation systems for winter energy storage application.[28]

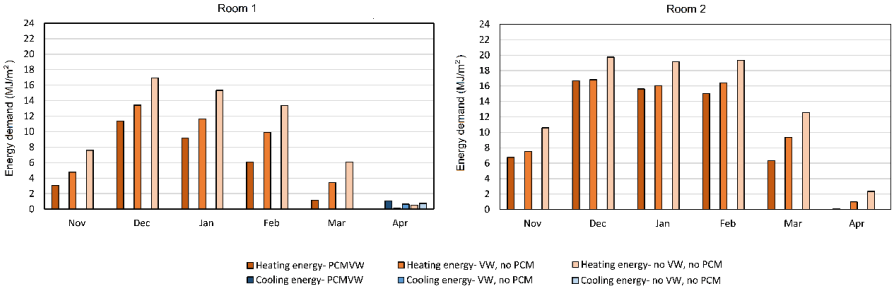

Figure 4-20 The energy demand of the rooms with 3 different ventilation systems during winter.[28]

Figure 4-20 shows the energy demand of the 3 ventilation systems during the winter period. It is seen that for both rooms, the PCMVW has the least energy demand, and the no VW, no PCM system has the highest energy demand. For room 1, the heating energy saving percentage of PCMVW compared to VW, no PCM system and no VW, no PCM system is 29% and 48% respectively[28]. For room 2, the percentage is 10% and 28% respectively[28].

For more details about the thermal and energy performance of the PCMVW in comparison with the 2 other ventilation systems, please refer to Appendix D [28]: *"Performance and control strategy development of a PCM enhanced ventilated window system by a combined experimental and numerical study."*

4.3. CONTROL STRATEGY DEVELOPMENT

4.3.1. SUMMER NIGHT COOLING APPLICATION CONTROL STRATEGY DEVELOPMENT

The primitive control strategy shown in Figure 4-2 has the disadvantage that the VW is not well shaded, which limits the cooling ability of the PCMVW. In addition, the situation when the room is over cooled is not taken into consideration. Some new control strategies are evaluated in this chapter. Control strategy 1 adds the between-glass reflection shading in the VW and adds heat mode when the indoor air temperature is low, as seen in Figure 4-21. In control strategy 2, the high-temperature ambient air is ventilated directly from the PCM heat exchanger to the indoor room in ventilation pre-cooling mode (Figure 4-22). In control strategy 3, the air conditioning temperature setpoint is changed. The pre-cooling mode is operated when the indoor air temperature is above 26°C. Moreover, the bypass ventilation is turned on when the indoor air temperature is between 22 °C and 26 °C[28], as seen in Figure 4-23.

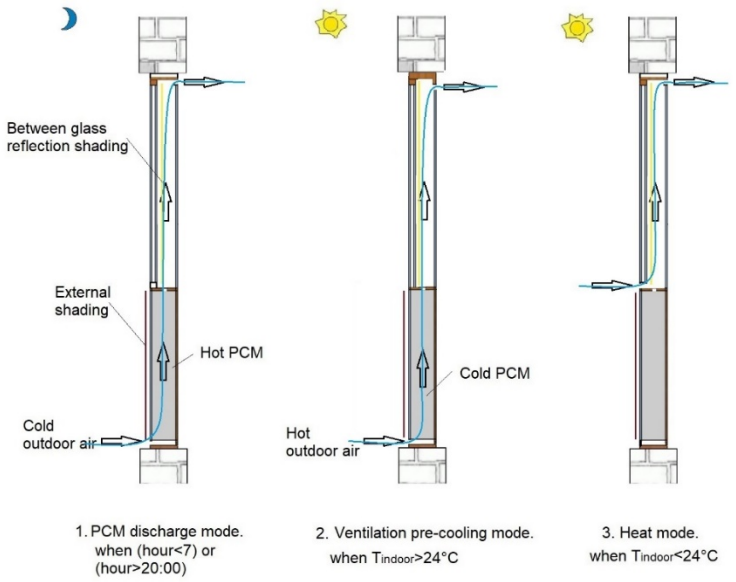

Figure 4-21 The summer night cooling control strategy 1. [28]

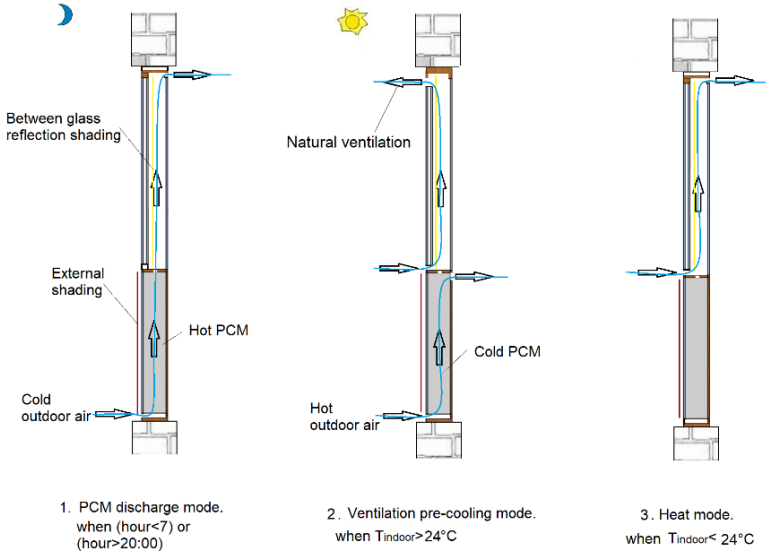

Figure 4-22 The summer night cooling control strategy 2. [28]

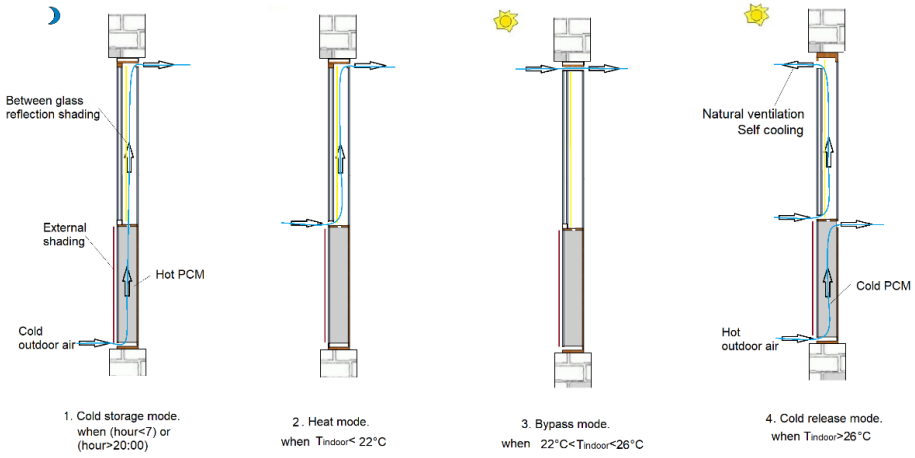

Figure 4-23 The summer night cooling control strategy 3. [28]

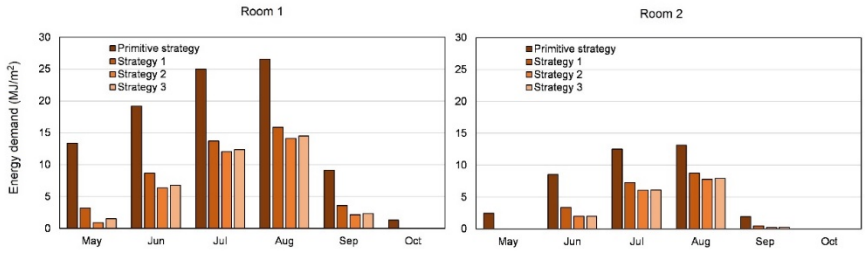

Figure 4-24 The HVAC cooling energy demands of the rooms using PCMVW with different summer control strategies. [28]

The HVAC cooling energy demands of the rooms in different orientations are calculated based on different control strategies. Figure 4-24 shows the results. Compared to the primitive control strategy, all the 3 improving control strategies have much less energy demand. Control strategy 2 saves 62.3% energy for the southwest oriented room, and 58.2% for the northeast oriented room[28].

4.3.2. WINTER SOLAR ENERGY STORAGE APPLICATION CONTROL STRATEGY DEVELOPMENT

The primitive winter solar energy storage application primitive control strategy shown in Figure 4-4 has some disadvantages. It fails to assess the potential of the overheating of the room as well as providing corresponding solutions. Besides that, the ventilated air through the VW may have the potential of high heat loss. For the purpose of improving the energy performance of the PCMVW, 3 more control strategies are simulated by the validated model. The between glass absorption shading is added to the VW, to absorb the solar energy for ventilation preheating. Compared to the primitive control strategy, control strategy 1 added overheating preventing mode (Figure 4-25 (3)), to prevent the indoor air temperature from getting too high. In this mode, the VW self-cooling ventilation is operated, where the outdoor air is ventilated to the VW to cool it down by natural ventilation, and the outdoor air is directly ventilated into the indoor room. Control strategy 2 ventilates directly from the PCM heat exchanger to the indoor room during the heat release mode, in the hope that the heat loss can be decreased, as seen in Figure 4-26. Compared to control strategy 1, control strategy 3 introduces different indoor air temperature setpoint, as shown in Figure 4-27. The heat release mode is operated when the indoor air temperature is below 22 °C. The overheating mode is operated when the indoor air temperature is above 26°C. The ventilation bypass mode is turned on when the indoor air temperature is within the thermal comfort range [22°C-26°C][28].

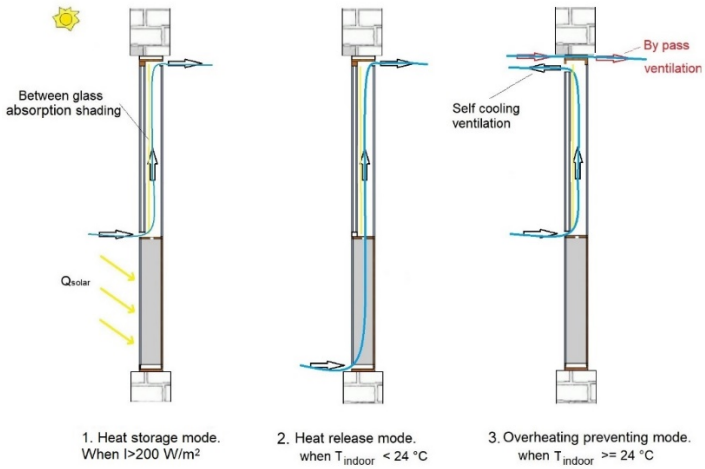

Figure 4-25 Winter solar energy storage control strategy 1. [28]

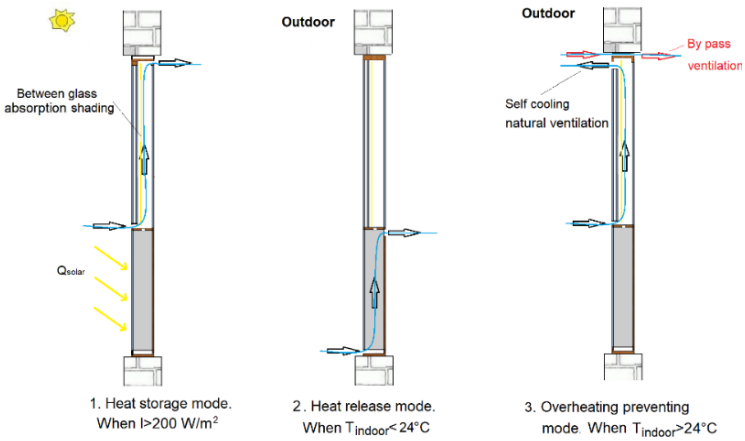

Figure 4-26 Winter solar energy storage control strategy 2. [28]

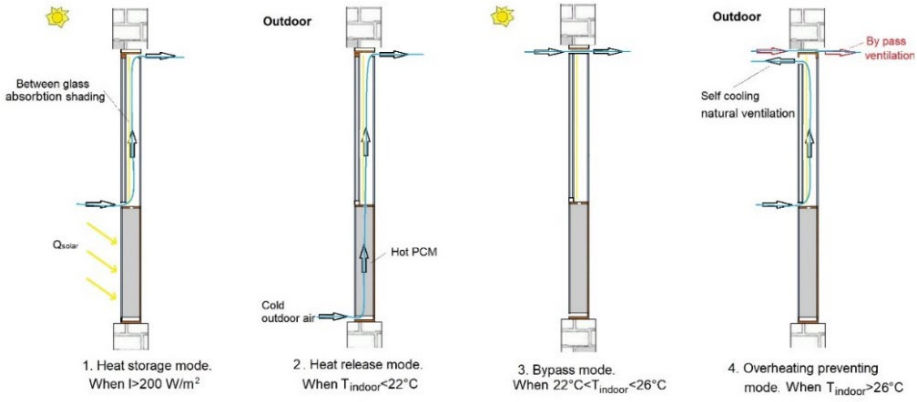

Figure 4-27 Winter solar energy storage control strategy 3. [28]

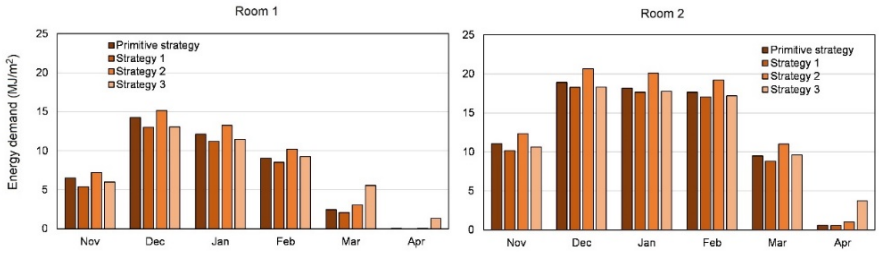

Figure 4-28 The HVAC heating energy demands of the rooms using PCMVW with different winter control strategies. [28]

The HVAC energy consumption of the models using different winter control strategies is shown in Figure 4-28. There are no significant differences among the simulated cases, which means the energy saving of the winter solar energy storage application is robust in terms of control strategies[28]. Overall, control strategy 1 has a simple control strategy but the lowest HVAC energy consumption. Control strategy 2 has the highest energy consumption, which may due to the missing of extra heat supply from the air been heated up by the solar radiation in the VW. In comparison with the primitive control strategy, control strategy 1 has 9.4% energy saving for the room with southwest orientated external windows; this number for the room with northeast orientated external windows is 4.4%[28].

For more information about the model validation and control strategy development, please refer to Appendix D [28]: *"Performance and control strategy development of a PCM enhanced ventilated window system by a combined experimental and numerical study."*

4.4. CONCLUSIONS

The experimental tests of the PCMVW in comparison with the conventional VW has the conclusions that for summer night cooling application, the PCMVW performance indicators such as heat removal amount, ventilation energy-saving and inlet air temperature decrease is more related to the outdoor day/night air temperature difference; for winter solar energy storage application, the PCMVW performance indicators are more related to the solar radiation level.

For summer application, the PCMVW decreases the room inlet air temperature by average 1.4 °C for 7 hours; for winter application, the PCMVW increases the room inlet air temperature by average 2°C for 12 hours compared with a conventional VW.

The VW self-cooling experiment has the conclusion that the self-cooling function can decrease the inner glass surface temperature of the VW, and potentially decreases the heat gain of the room form the window. However, the cooling effect is limited, and

the VW self-cooling function should be operated in combination with some advanced shading control strategies.

The VW advanced shading control experiment is then been carried out, and it has the conclusion that the absorption side of the shading blinds can greatly increase the inner glass temperature and potentially add the heat gain of the VW for winter application. However, the cooling effect of the reflection side of the shading blinds is limited, due to the improper placement of the blinds or some other measurement uncertainties during the experiment.

The experiment is complicated and limited by a lot of features such as time and energy-consuming, high cost of material resources and human resources, weather and location limitation, complicated setup, etc. On the contrary, the simulation is more flexible and less energy consumption. Therefore, the Energyplus model is built and verified by the experimental data. The model is then used to calculate the annual energy consumption of the building with PCMVW, and analyze the influence of different control strategies on energy consumption.

The comparison of the PCMVW to 2 ventilation systems shows that the PCMVW has a big energy-saving potential for both summer night cooling application and winter solar energy storage application. For the room facing southeast, the PCMVW saves 46% and 27% during summer, and 29% and 48% during winter compared to the VW no PCM system and the no VW no PCM system; while for the room facing northwest, the PCMVW saves 51% and 38% during summer, and 10% and 28% during winter compared to the VW no PCM system and the no VW no PCM system.

The conclusions from the Energyplus model for control strategy development are that for summer night cooling application, it is better to ventilate directly from the PCM heat exchanger to the room (instead of ventilating from the PCM heat exchanger to the VW before ventilating to the room)[28]. On the contrary, for winter solar energy storage application, it is better to ventilate from the PCM heat exchanger to the VW before ventilating to the room. The winter application is robust in terms of different control strategies. More attention should be paid for summer application, for example, the shading control and the right air distribution[28].

CHAPTER 5. CONCLUSIONS

The conventional ventilated window (VW) has the disadvantage of low heating/cooling efficiency for ventilation heating/cooling purposes. Due to the high latent heat storage ability, PCM has been selected for the thermal storage to assist the VW for ventilation pretreatment. However, it has been a challenge to apply PCM for both heating and cooling purposes for existing and new buildings.

To solve those problems, the concept of a highly integrated PCM enhanced ventilated window (PCMVW) system is proposed for this PhD study. The objective is to make the PCMVW as a split system designed to be convenient for installation and requiring little building space. The PCMVW includes a VW on top and a PCM heat exchanger on the bottom. The two parts are connected by vents and electronic valves. It works for both ventilation cooling and heating purposes. For cooling purpose, the night ventilation cools down the PCM. The low-temperature PCM is used to pre-cool the ventilation. For heating purpose, the PCM stores the solar energy during the day and releases the heat into the ventilation to heat up the ventilated air.

The literature review of the PCM as thermal energy storage in ventilation systems has resulted in the conclusion that the application of the PCM is limited to its low thermal conductivity and multiphase. Consequently, more attention should be paid to the PCM configuration design. Moreover, the sensitivity analysis of the hysteresis degree and phase transition temperature on the building energy demand shows that the hysteresis degree has a higher influence on the summer and winter energy demand. The modeling of a PCM system should take into account the temperature hysteresis of PCM.

The development of the PCMVW and ventilation control strategy has resulted in the conclusions below:

1. The design and optimization of the PCM heat exchanger are done in three steps: 1) the development and test of a PCM heat exchanger in the climate chamber, 2) the construction of the numerical model and model validation, and 3) the development of the configuration of the PCM heat exchanger.

   The development and test of the PCM heat exchanger show that, for night cooling application, the PCM temperature is evenly distributed along with the depth of the PCM plates during both melting and freezing processes, thus the numerical model for it could be simplified into a 2-dimensional model. However, for solar energy storage application, the PCM temperature is not evenly distributed along with the depth of the PCM plates during the melting process by solar radiation, thus a 3-dimensional model would be more accurate. The numerical models built for night

cooling application and solar energy storage application are both validated by experimental data.

To achieve good thermal storage within the limited total physical volume inside the PCM heat exchanger, the configuration optimization of the PCM heat exchanger for the night cooling application is 10 mm plate thickness. The optimum configurations of the PCM heat exchanger for the solar energy storage application is 6 mm air gap thickness and 90 mm plate depth.

2. The PCM heat exchanger with the optimized configuration is integrated with the VW in the façade lab. The test of a PCMVW in comparison with a conventional VW shows that the PCMVW can significantly improve the energy performance for both heating and cooling purposes compared to the VW. However, the cooling ability of the night cooling application is limited without advanced ventilation design and shading control. Subsequently, with the completion of the self-cooling experiment and shading control experiment, the results show some improvements in the system performance.
3. The numerical model of the PCMVW and its energy consumption prediction is built in EnergyPlus for a 3-room apartment installing four PCMVWs in different orientations. The model is verified by the experimental data for all the applications. The PCMVW has a big energy-saving potential compared to 2 other ventilation systems for both summer and winter applications.
4. The developed control strategies of the PCMVW are that for summer night cooling application, it is better to ventilate directly from the PCM heat exchanger into the room instead of ventilating from the PCM heat exchanger to the VW before ventilating into the room. On the contrary, for winter solar energy storage application, it is better to ventilate from the PCM heat exchanger to the VW before ventilating into the room. The winter application is robust in terms of different control strategies. More attention should be paid for summer application, e.g. the shading control and the right air distribution.

As an engineering approach, the design of the PCMVW for ventilation pretreatment is fulfilled, and the results are solid and practicable to the building ventilation design for both new buildings and existing buildings. The design process is applicable to other similar building components.

CHAPTER 6. FUTURE WORKS

This research study presents the development of the PCM enhanced ventilated window experimentally and numerically and its thermal and energy performance. The optimized control strategies for summer and winter seasons are given respectively. However, some future works are required.

The advantage of the PCMVW system over other building ventilation technology is not clear. The thermal performance and energy-saving potential of the PCMVW system in comparison with other ventilation systems or the same PCMVW system with different PCMs should be conducted.

The control strategy could be further optimized based on the function of the building. Moreover, the development and the test of the PCMVW are only in the lab. It would be necessary to install the PCMVW in the building site and test its thermal and energy performance for the yearly operation.

Future works also include to effectively apply the PCM in some other ventilation application or building components.

LITERATURE LIST

[1] International Energy Agency. Key World Energy Statistics 2018. n.d.

[2] IEA. World Energy Outlook 2018. OECD/IEA 2018. doi:10.1787/20725302.

[3] Kamali S. Review of free cooling system using phase change material for building. Energy and Buildings 2014;80:131–6. doi:10.1016/J.ENBUILD.2014.05.021.

[4] International energy Agency. 2018 Global Status Report Towards a zero-emission, efficient and resilient buildings and construction sector. n.d.

[5] Liu M, Heiselberg P. Energy flexibility of a nearly zero-energy building with weather predictive control on a convective building energy system and evaluated with different metrics. Applied Energy 2019;233–234:764–75. doi:10.1016/J.APENERGY.2018.10.070.

[6] International Energy Agency. EBC Annex 62 Ventilative Cooling Project Summery Report. 2018.

[7] Guo R, Hu Y, Liu M, Heiselberg P. Influence of design parameters on the night ventilation performance in office buildings based on sensitivity analysis. Sustainable Cities and Society 2019;50:101661. doi:10.1016/J.SCS.2019.101661.

[8] Johra H, Heiselberg PK, Le Dréau J, Dréau J Le. Influence of envelope, structural thermal mass and indoor content on the building heating energy flexibility. Energy and Buildings 2018;183:325–39. doi:10.1016/j.enbuild.2018.11.012.

[9] Pomianowski M, Heiselberg P, Zhang Y. Review of thermal energy storage technologies based on PCM application in buildings. Energy and Buildings 2013;67:56–69. doi:10.1016/j.enbuild.2013.08.006.

[10] Johra H, Heiselberg P. Influence of internal thermal mass on the indoor thermal dynamics and integration of phase change materials in furniture for building energy storage: A review. Renewable and Sustainable Energy Reviews 2017;69:19–32. doi:10.1016/J.RSER.2016.11.145.

[11] Wu T, Lei C. A review of research and development on water wall for building applications. Energy and Buildings 2016;112:198–208. doi:10.1016/j.enbuild.2015.12.003.

[12] Najafian A, Haghighat F, Moreau A. Integration of PCM in domestic hot water tanks: Optimization for shifting peak demand. Energy and Buildings 2015;106:59–64. doi:10.1016/j.enbuild.2015.05.036.

[13] Navarro L, de Gracia A, Niall D, Castell A, Browne M, McCormack SJ, et al. Thermal energy storage in building integrated thermal systems: A review. Part 2. Integration as passive system. Renewable Energy 2016;85:1334–56. doi:10.1016/j.renene.2015.06.064.

[14] Iten M, Liu S, Shukla A, Shukla A. A review on the air-PCM-TES application for free cooling and heating in the buildings. vol. 61. 2016. doi:10.1016/j.rser.2016.03.007.

[15] Akeiber H, Nejat P, Majid MZA, Wahid MA, Jomehzadeh F, Zeynali Famileh I, et al. A review on phase change material (PCM) for sustainable passive cooling in building envelopes. Renewable and Sustainable Energy Reviews 2016;60:1470–97. doi:10.1016/j.rser.2016.03.036.

[16] Konuklu Y, Ostry M, Paksoy HO, Charvat P. Review on using microencapsulated phase change materials (PCM) in building applications. Energy and Buildings 2015;106:134–55. doi:10.1016/j.enbuild.2015.07.019.

[17] Pomianowski M, Kvols P, Lund R. Initial development of a combined PCM and TABS solution for heat storage and cooling 2011;1:483–90.

[18] Fang G, Tang F, Cao L. Preparation, thermal properties and applications of shape-stabilized thermal energy storage materials. Renewable and Sustainable Energy Reviews 2014;40:237–59. doi:10.1016/j.rser.2014.07.179.

[19] Heiselberg P, Hicham J. European Commission : CORDIS : Projects and Results : Final ReportSummary - CLIMAWIN (An intelligent window for optimal ventilation and minimum thermal loss). n.d.

[20] Diarce G, Urresti A, García-Romero A, Delgado A, Erkoreka A, Escudero C, et al. Ventilated active façades with PCM. Applied Energy 2013;109:530–7. doi:10.1016/j.apenergy.2013.01.032.

[21] De Gracia A, Navarro L, Castell A, Ruiz-Pardo Á, Álvarez S, Cabeza LF. Thermal analysis of a ventilated facade with PCM for cooling applications. Energy and Buildings 2013;65:508–15. doi:10.1016/j.enbuild.2013.06.032.

[22] Carlos JS, Corvacho H, Silva PD, Castro-Gomes JP. Real climate experimental study of two double window systems with preheating of

ventilation air. Energy and Buildings 2010;42:928–34.

[23] Appelfeld D, Svendsen S. Experimental analysis of energy performance of a ventilated window for heat recovery under controlled conditions. Energy and Buildings 2011;43:3200–7. doi:10.1016/J.ENBUILD.2011.08.018.

[24] Chow T, Lin Z, Fong K, Chan L, He M. Thermal performance of natural airflow window in subtropical and temperate climate zones – A comparative study. Energy Conversion and Management 2009;50:1884–90. doi:10.1016/J.ENCONMAN.2009.04.028.

[25] Liu M, Heiselberg PK, Larsen OK, Mortensen L, Rose J. Investigation of Different Configurations of a Ventilated Window to Optimize Both Energy Efficiency and Thermal Comfort. Energy Procedia 2017;132:478–83. doi:10.1016/j.egypro.2017.09.660.

[26] Heiselberg C, Kvols P, Kalyanova O. CLIMAWIN: Technical Summary Report. 2013.

[27] Hu Y, Heiselberg P, Guo R. Ventilation cooling/heating performance of a PCM enhanced ventilated window - an experimental study. Energy and Buildings 2020;Accepted:109903. doi:10.1016/j.enbuild.2020.109903.

[28] Hu Y, Guo R, Heiselberg P. Performance and control strategy development of a PCM enhanced ventilated window system by a combined experimental and numerical study. Renewable Energy 2020;Accepted.

[29] Cao L, Su D, Tang Y, Fang G, Tang F. Properties evaluation and applications of thermal energystorage materials in buildings. Renewable and Sustainable Energy Reviews 2015;48:500–22. doi:10.1016/j.rser.2015.04.041.

[30] Aroul Raj VA, Velraj R. Review on free cooling of buildings using phase change materials. Renewable and Sustainable Energy Reviews 2010;14:2819–29. doi:10.1016/j.rser.2010.07.004.

[31] Baetens R, Jelle BP, Gustavsen A. Phase change materials for building applications: A state-of-the-art review. Energy and Buildings 2010;42:1361–8. doi:10.1016/j.enbuild.2010.03.026.

[32] Mantilla Gilart P, Yedra Martínez Á, González Barriuso M, Manteca Martínez C, Manteca Martínez C. Development of PCM/carbon-based composite materials. Solar Energy Materials and Solar Cells 2012;107:205–
11. doi:10.1016/j.solmat.2012.06.014.

[33] Alshaer WG, Nada SA, Rady MA, Le Bot C, Palomo Del Barrio E. Numerical investigations of using carbon foam/PCM/Nano carbon tubes composites in thermal management of electronic equipment. Energy Conversion and Management 2015;89:873–84. doi:10.1016/j.enconman.2014.10.045.

[34] Deng Z, Liu X, Zhang C, Huang Y, Chen Y, Chen Y. Melting behaviors of PCM in porous metal foam characterized by fractal geometry. International Journal of Heat and Mass Transfer 2017;113:1031–42. doi:10.1016/j.ijheatmasstransfer.2017.05.126.

[35] Li WQ, Qu ZG, He YL, Tao YB, Tao YB. Experimental study of a passive thermal management system for high-powered lithium ion batteries using porous metal foam saturated with phase change materials. Journal of Power Sources 2014;255:9–15. doi:10.1016/j.jpowsour.2014.01.006.

[36] Mat S, Al-Abidi AA, Sopian K, Sulaiman MY, Mohammad AT, Mohammad AT. Enhance heat transfer for PCM melting in triplex tube with internal–external fins. Energy Conversion and Management 2013;74:223–36. doi:10.1016/j.enconman.2013.05.003.

[37] Ettouney HM, Alatiqi I, Al-Sahali M, Ahmad Al-Ali S, Al-Ali SA. Heat transfer enhancement by metal screens and metal spheres in phase change energy storage systems. Renewable Energy 2004;29:841–60. doi:10.1016/j.renene.2003.11.003.

[38] Ma Z, Lin W, Sohel MI. Nano-enhanced phase change materials for improved building performance. Renewable and Sustainable Energy Reviews 2016;58:1256–68. doi:10.1016/j.rser.2015.12.234.

[39] Khodadadi JM, Fan L, Babaei H. Thermal conductivity enhancement of nanostructure-based colloidal suspensions utilized as phase change materials for thermal energy storage: A review. Renewable and Sustainable Energy Reviews 2013;24:418–44. doi:10.1016/j.rser.2013.03.031.

[40] Zalba B, Marín JM, Cabeza LF, Mehling H. Free-cooling of buildings with phase change materials. International Journal of Refrigeration 2004;27:839–49. doi:10.1016/j.ijrefrig.2004.03.015.

[41] Marín JM, Zalba B, Cabeza LF, Mehling H. Improvement of a thermal energy storage using plates with paraffin-graphite composite. International Journal of Heat and Mass Transfer 2005;48:2561–70. doi:10.1016/j.ijheatmasstransfer.2004.11.027.

[42] Chen X, Zhang Q, Zhai ZJ. Energy saving potential of a ventilation system

with a latent heat thermal energy storage unit under different climatic conditions. Energy and Buildings 2016;118:339–49. doi:10.1016/j.enbuild.2016.02.049.

[43] Xiang Y, Zhou G. Thermal performance of a window-based cooling unit using phase change materials combined with night ventilation. Energy and Buildings 2015;108:267–78. doi:10.1016/j.enbuild.2015.09.030.

[44] Koschenz M, Lehmann B. Development of a thermally activated ceiling panel with PCM for application in lightweight and retrofitted buildings. Energy and Buildings 2004;36:567–78. doi:10.1016/j.enbuild.2004.01.029.

[45] Hu Y, Guo R, Johra H, Heiselberg P. Temperature hysteresis of phase change materials and its impact on building modeling. Building Simulation 2020;Submitted.

[46] Gschwander S, Lazaro A, Cabeza LF, Günther E, Fois M, Chui J. Development of a Test Standard for PCM and TCM Characterization Part 1: Characterization of Phase Change Materials Compact Thermal Energy Storage: Material Development for System Integration 2011.

[47] Lázaro A, Günther E, Mehling H, Hiebler S, Marín JM, Zalba B. Verification of a T-history installation to measure enthalpy versus temperature curves of phase change materials. Measurement Science and Technology 2006;17:2168–74. doi:10.1088/0957-0233/17/8/016.

[48] Diaconu BM, Varga S, Oliveira AC. Experimental assessment of heat storage properties and heat transfer characteristics of a phase change material slurry for air conditioning applications. Applied Energy 87:620–8. doi:10.1016/j.apenergy.2009.05.002.

[49] HE B, MARTIN V, SETTERWALL F. Phase transition temperature ranges and storage density of paraffin wax phase change materials. Energy 2004;29:1785–804. doi:10.1016/j.energy.2004.03.002.

[50] Kuznik F, Virgone J. Experimental investigation of wallboard containing phase change material: Data for validation of numerical modeling. Energy and Buildings 2009;41:561–70. doi:10.1016/J.ENBUILD.2008.11.022.

[51] Arkar C, Medved S. Influence of accuracy of thermal property data of a phase change material on the result of a numerical model of a packed bed latent heat storage with spheres. Thermochimica Acta 2005;438:192–201. doi:10.1016/j.tca.2005.08.032.

[52] Iten M, Liu S, Shukla A, Silva PD. Investigating the impact of Cp-T values determined by DSC on the PCM-CFD model. Applied Thermal Engineering 2017;117:65–75. doi:10.1016/J.APPLTHERMALENG.2017.02.021.

[53] Yinping Z, Yi J, Yi J. A simple method, the -history method, of determining the heat of fusion, specific heat and thermal conductivity of phase-change materials. Measurement Science and Technology 1999;10:201–5. doi:10.1088/0957-0233/10/3/015.

[54] Tabares-Velasco PC, Christensen C, Bianchi M. Verification and validation of EnergyPlus phase change material model for opaque wall assemblies. Building and Environment 2012;54:186–96. doi:10.1016/J.BUILDENV.2012.02.019.

[55] Evola G, Marletta L, Sicurella F. Simulation of a ventilated cavity to enhance the effectiveness of PCM wallboards for summer thermal comfort in buildings. Energy and Buildings 2014;70:480–9. doi:10.1016/j.enbuild.2013.11.089.

[56] Tabares-Velasco PC, Griffith B. Diagnostic test cases for verifying surface heat transfer algorithms and boundary conditions in building energy simulation programs. Journal of Building Performance Simulation 2012;5:329–46. doi:10.1080/19401493.2011.595501.

[57] Saffari M, de Gracia A, Ushak S, Cabeza LF. Economic impact of integrating PCM as passive system in buildings using Fanger comfort model. Energy and Buildings 2016;112:159–72. doi:10.1016/j.enbuild.2015.12.006.

[58] Chernousov AA, Chan BYB. Numerical simulation of thermal mass enhanced envelopes for office buildings in subtropical climate zones. Energy and Buildings 2016;118:214–25. doi:10.1016/j.enbuild.2016.02.054.

[59] Ramakrishnan S, Wang X, Alam M, Sanjayan J, Wilson J. Parametric analysis for performance enhancement of phase change materials in naturally ventilated buildings. Energy and Buildings 2016;124:35–45. doi:10.1016/j.enbuild.2016.04.065.

[60] Ahmad M, Bontemps A, Sallée H, Quenard D. Thermal testing and numerical simulation of a prototype cell using light wallboards coupling vacuum isolation panels and phase change material. Energy and Buildings 2006;38:673–81.

[61] Dentel A, Stephan W. Phase change materials in passive and active wall constructions Model description and implementing into TRNSYS 2013.

[62] Heim D, Clarke JA. Numerical modelling and thermal simulation of PCM–gypsum composites with ESP-r. Energy and Buildings 2004;36:795–805. doi:10.1016/J.ENBUILD.2004.01.004.

[63] Kośny J, Fallahi A, Shukla N, Kossecka E, Ahbari R. Thermal load mitigation and passive cooling in residential attics containing PCM-enhanced insulations. Solar Energy 2014;108:164–77. doi:10.1016/J.SOLENER.2014.05.007.

[64] Heim D. Isothermal storage of solar energy in building construction. Renewable Energy 2010;35:788–96. doi:10.1016/J.RENENE.2009.09.005.

[65] Susman G, Dehouche Z, Cheechern T, Craig S. Tests of prototype PCM "sails" for office cooling. Applied Thermal Engineering 2011;31:717–26. doi:10.1016/J.APPLTHERMALENG.2010.10.008.

[66] Hu Y, Heiselberg PK. A new ventilated window with PCM heat exchanger—Performance analysis and design optimization. Energy and Buildings 2018;169:185–94. doi:10.1016/j.enbuild.2018.03.060.

[67] Virgone J, Trabelsi A. 2D Conduction Simulation of a PCM Storage Coupled with a Heat Pump in a Ventilation System. Applied Sciences 2016;6:193. doi:http://dx.doi.org/10.3390/app6070193.

[68] American Society of Heating R and A-CE. 2013 ASHRAE handbook : fundamentals. n.d.

[69] Barreneche C, Navarro H, Serrano S, Cabeza LF, Inés Fernández A. New database on phase change materials for thermal energy storage in buildings to help PCM selection. Energy Procedia 2014;57:2408–15. doi:10.1016/j.egypro.2014.10.249.

[70] Castell A, Solé C, Solé C. An overview on design methodologies for liquid–solid PCM storage systems. Renewable and Sustainable Energy Reviews 2015;52:289–307. doi:10.1016/j.rser.2015.07.119.

[71] Hoes P, Hensen JLM. The potential of lightweight low-energy houses with hybrid adaptable thermal storage: Comparing the performance of promising concepts. Energy and Buildings 2016;110:79–93. doi:10.1016/j.enbuild.2015.10.036.

[72] Turnpenny JR, Etheridge DW, Reay DA. Novel ventilation cooling system for reducing air conditioning in buildings. Part I: testing and theoretical modelling. Applied Thermal Engineering 2000;20:1019–37.

doi:10.1016/S1359-4311(99)00068-X.

[73] Turnpenny JR, Etheridge DW, Reay DA. Novel ventilation system for reducing air conditioning in buildings. Part II: testing of prototype. Applied Thermal Engineering 2001;21:1203–17. doi:10.1016/S1359-4311(01)00003-5.

[74] Peippo K, Kauranen P, Lund PD. A multicomponent PCM wall optimized for passive solar heating. Energy and Buildings 1991;17:259–70. doi:10.1016/0378-7788(91)90009-R.

[75] Tyagi VV, Buddhi D. PCM thermal storage in buildings: A state of art. Renewable and Sustainable Energy Reviews 2007;11:1146–66. doi:10.1016/j.rser.2005.10.002.

[76] Agyenim F, Hewitt N, Eames P, Smyth M. A review of materials, heat transfer and phase change problem formulation for latent heat thermal energy storage systems (LHTESS). Renewable and Sustainable Energy Reviews 2010;14:615–28. doi:10.1016/j.rser.2009.10.015.

[77] Pasupathy A, Velraj R. Effect of double layer phase change material in building roof for year round thermal management. Energy and Buildings 2008;40:193–203.

[78] Jin X, Zhang X. Thermal analysis of a double layer phase change material floor. Applied Thermal Engineering 2011;31:1576–81. doi:10.1016/j.applthermaleng.2011.01.023.

[79] Hu Y, Heiselberg P, Johra H, Guo R. Experimental and numerical study of a PCM solar air heat exchanger and its ventilation preheating effectiveness. Renewable Energy 2019;145:106–15. doi:10.1016/J.RENENE.2019.05.115.

[80] Expression for mesh quality parameter n.d. https://www.comsol.dk/forum/thread/77231/expression-for-mesh-quality-parameter (accessed February 25, 2020).

[81] COMSOL Multiphysics Reference Manual. n.d.

[82] BSim - Climate data n.d. http://sbi.dk/bsim/Pages/Klimadata.aspx#TRY (accessed November 16, 2017).

[83] Jensen R, Nørgaard J, Daniels O, Justesen R. Person- og forbrugsprofiler: bygningsintegreret energiforsyning. 2011.

[84] Wittchen, Kim Bjarne. Vurdering af potentialet for varmebesparelser i eksisterende boliger. 2004.

[85] EN 15251: Indoor environmental input parameters for design and assessment of energy performance of buildings – addressing indoor air quality, thermal environment, lighting and acoustics. vol. 3. 2007. doi:10.1520/E2019-03R13.Copyright.

PUBLICATIONS FOR THE THESIS

Thesis Title: PCM enhanced ventilated window- configuration and control strategy development

Name of Ph.D. Student: Yue Hu

Name of Supervisor: Professor Per K. Heiselberg

List of Publications:

1) Y. Hu, P.K. Heiselberg, A new ventilated window with PCM heat exchanger – performance analysis and design optimization, Energy and Buildings.(2018). doi:10.1016/J.ENBUILD.2018.03.060.
2) Y. Hu, P.K. Heiselberg, H. Johra, R. Guo, Experimental and numerical study of a PCM solar air heat exchanger and its ventilation preheating effectiveness, Renewable Energy. 145 (2020) 106–115. doi:10.1016/J.RENENE.2019.05.115.
3) Y. Hu, P. Heiselberg, R. Guo, Ventilation cooling/heating performance of a PCM enhanced ventilated window - an experimental study, Energy and Buildings 2020. doi: 10.1016/j.enbuild.2020.109903.
4) Y. Hu, R. Guo, P. Heiselberg, Performance and control strategy development of a PCM enhanced ventilated window system by a combined experimental and numerical study. Renew Energy 2020. Accepted.
5) Y. Hu, R. Guo, H. Johra, P. Heiselberg, Temperature hysteresis of phase change materials and its impact on building modeling. Building simulation: an international journal; Submitted.

Other publications:

1) Y. Hu, P. Heiselberg, Thermal performance of ventilated solar collector with energy storage containing phase change material, in: 38th AIVC Conf. "Ventilating Heal. Low-Energy Build., Nottingham, UK, 2017. pp 603-612.
2) Y. Hu, P. Heiselberg, R. Guo, Experimental analysis of PCM heat exchanger in ventilated window system, in: 39th AIVC, 2018: pp. 484–490.
3) Y. Hu, P. Heiselberg, R. Guo, PCM solar air collector with ventilated window system and its ventilation pre-heating effectiveness, in: Building Simulation, Rome, 2019.
4) R. Guo, Y. Hu, M. Liu, & P. Heiselberg, Optimal night mechanical ventilation control strategy in office buildings. X IAQVEC Conference (2019). In IOP Conference Series: Materials Science and Engineering (Vol. 609, No. 3, p. 032013).
5) R. Guo, Y. Hu, P. Heiselberg, A review of the performance indicators of night-time ventilation. 39th AIVC Conference (2018).

6) R. Guo, Y. Hu, M. Liu, P. Heiselberg, Influence of design parameters on the night ventilation performance in office buildings based on sensitivity analysis. Sustainable Cities and Society (2019), 101661. https://doi.org/10.1016/j.scs.2019.101661

This thesis has been submitted for assessment in partial fulfilment of the Ph.D. degree. The thesis is based on the submitted or published scientific papers which are listed above. Parts of the papers are used directly or indirectly in the extended summary of the thesis. As part of the assessment, co-author statements have been made available to the assessment committee and are also available at the Faculty.

APPENDICES

Appendix A. Paper 1 98
Appendix B. Paper 2 109
Appendix C. Paper 3 120
Appendix D. Paper 4 133
Appendix E. Paper 5 179

Appendix A. Paper 1

Y. Hu, P.K. Heiselberg, A new ventilated window with PCM heat exchanger – performance analysis and design optimization, Energy and Buildings. (2018). doi:10.1016/J.ENBUILD.2018.03.060.

Energy & Buildings 169 (2018) 185–194

Contents lists available at ScienceDirect

Energy & Buildings

journal homepage: www.elsevier.com/locate/enbuild

A new ventilated window with PCM heat exchanger—Performance analysis and design optimization

Yue Hu*, Per Kvols Heiselberg

Department of Civil Engineering, Aalborg University, Thomas Manns Vej 23, Aalborg 9220, Denmark

ARTICLE INFO

Article history:
Received 23 January 2018
Revised 21 March 2018
Accepted 22 March 2018
Available online 29 March 2018

Keywords:
Phase change material
Ventilated window
Ventilation pretreatment
PCM modeling

ABSTRACT

This paper proposes a ventilated window with a phase change material (PCM) heat exchanger as a new window application. In summer, night ventilation mode is operated to discharge energy stored in PCM by the ambient cold air, which can be reloaded again, when ventilation pre-cooled air is provided.

Numerical model is built and verified by full-scale experiment to evaluate the PCM ventilation system. The nonlinear properties and hysteresis of PCM are set in the model. The conclusion is that the configuration optimization should be based on different climates. In the case study in Copenhagen, the heat exchanger with 10 mm plate thickness is optimized. It can cool down the ventilated air 6.5 °C on average in 3.9 h pre-cooling effective time with 3.19 MJ/day energy saving. The material cost saving is 16.87% compared to 20 mm plate thickness which has similar discharged heat amount. Nevertheless, the heat exchanger with 5 mm plate thickness has a faster thermal response and a higher cost saving ability, which is good for the climate when the period of outdoor air temperature suitable for night ventilation in a day is short.

1. Introduction

Renewable energy has been used in low energy buildings and other building applications to cut down the building energy consumption for a sustainable building environment. This kind of energy is mostly intermittent and highly depends on the outdoor climate, such as solar energy. A thermal energy storage (TES) system is a promising way to improve the efficiency of solar energy applications. Phase change material (PCM) is a good candidate for TES because of its thermal properties, such as high latent heat and isothermal heat transfer process. Moreover, the physical properties of PCM make it easy to integrate into building elements. Therefore, it has gained a large interest in research and building market recently [1].

PCM is different from other materials in the way that it can absorb or release a large amount of latent heat when changing phase [2]. The energy density of the material is relatively high so that the volume of the system could be smaller in comparison with other TES. In addition, the temperature of PCM will stay almost constant in the phase change period, which means the surface temperature of building envelope will not be too high, thus avoiding a high heat transfer [3]. Organic PCMs are drawing much attention because they have high latent heat capacity and stable physical and chemical properties [4]. Moreover, for some of them, the transition temperature is in the thermal comfort range of human body, which makes them good candidates to combine with air conditioning systems, ventilation systems as well as building envelopes [5].

PCM has been used in many building applications for thermal storage and thermal control. One of the applications is mixing PCM with building material for building constructions, such as gypsum board, plaster, concrete or other wall boards. It can also be a component like blind and layer for ceiling and wall. Michal et al. [6] mixed PCM with concrete and built a hollow concrete deck. The thermal properties of the new concrete construction were numerically and experimentally studied and compared with other materials. The results showed that there is an energy-saving potential for mixing PCM in concrete constructions. Active PCM applications include applying PCM in air conditioning system, ventilation façade, etc. Diarce et al. [7] studied the thermal properties of an actively ventilated façade with PCM board in the outer layer. The study compared the thermal behavior of the system with traditional constructions by modeling in Design Builder. The results showed that the thermal storage increases greatly in the phase change process of PCM, which decreased the chance of overheating for the envelope. Alvaro et al. [8] studied the thermal performance of a ventilated façade with macro encapsulated PCM in its air cavity. The results showed that with night ventilation, the system could greatly reduce the cooling load. Hicham et al. [9,10] built and tested a double-layer window with PCM shading device in the

* Corresponding author.
E-mail address: hy@civil.aau.dk (Y. Hu).

https://doi.org/10.1016/j.enbuild.2018.03.060
0378-7788/

middle of glazing layers. The results showed that the PCM shading device decreases the U value of the window.

The main drawback of PCM is its low thermal conductivity [11]. The heat is absorbed by the surface layer of PCM but is blocked due to the low thermal conductivity, which results in a long time for the melting procedure. Consequently, the thickness of PCM implementations should be within a certain limited range. Another drawback of PCM is its thermal expansion. The volume expansion of paraffin wax is in the order of 10% volume change [12,13], which is similar to the inorganic PCM, but smaller forces as paraffin wax is softer [13]. In this paper the PCM used is paraffin wax 22, which has a phase change temperature at 22 °C. The PCM is absorbed by fiber board (50% PCM and 50% fiber). The soft texture and air voids in the fiber board make the expansion possible. Moreover, the temperature change range of PCM in night ventilation application is smaller than the ones tested in the above literature, so the expansion of PCM is less considered in this work.

An accurate numerical model for PCM applications is necessary in order to give guidance for the engineering optimization and architectural design. However, the nonlinear properties of PCM make it difficult for the modeling [14]. For example, the heat capacity, enthalpy, viscosity and thermal conductivity could be dependent on temperature, and the heat capacity as a function of temperature is different in the freezing and melting processes because of the hysteresis effect. For organic PCM, there is also the problem of purification of the material, which makes the properties more complicated. For nonorganic PCM, there are problems such as supercooling effect, phase segregation, unstable thermal and chemical composition [15]. Those phenomena were considered in some experimental works [16–18], but the ideal or average heat capacity was used and the hysteresis was ignored in most of the modeling and numerical works [19–23].

Some other software such as COMSOL Multiphysics or FEMLAB (the predecessor of COMSOL) have been used to solve the numerical problems in relation to PCM. COMSOL Multiphysics is good at solving multi-physics problems and modeling complicated and irregular components with non-linear properties. A conduction heat transfer model in COMSOL using the DSC measured non-linear heat capacity was verified by data from experiment [18]. The temperature in the center of the PCM plate from the experiment was compared to the numerical model. The result showed a good consistency. Another study was about modeling of an innovative honeycomb wallboard in COMSOL using fictive heat capacity from DSC measurement [24]. The model showed good agreement with the experimental results. A similar model for a PCM storage facility was built in COMSOL Multiphysics using two different approximation methods for heat capacity. The results showed that both the effective heat capacity method and the enthalpy method are good at estimating the heat transfer process [25].

This paper proposes a new ventilated window with a PCM heat exchanger and analyzes the system performance in summer. A finite model considering nonlinear properties and hysteresis of PCM is built in COMSOL Multiphysics to simulate the heat transfer in the heat exchanger, and is verified by full-scale laboratory experiment. The model is used to study the thermal behavior of the system in night ventilation mode and ventilation air pre-cooling mode, as well as to estimate the energy saving potential when precooling the ventilated air in cases in Copenhagen.

2. System performance analysis

Fig. 1 illustrates a normal room with a ventilated window. A heat exchanger made of PCM plates is integrated with the ventilated window to precool the ventilated air, the overview of the PCM heat exchanger and plates can be seen in Fig. 7. The ventilated window is mounted into the building envelope as a conventional window, in which way the building structures do not need special designs for new buildings or reconstructions for existing buildings. The inlet is at the bottom of the window, which is powered by fans to guarantee air circulation. Air from ambient goes through the heat exchanger and ventilated cavity to the indoor or outdoor zone, depending on whether room ventilation is needed or not.

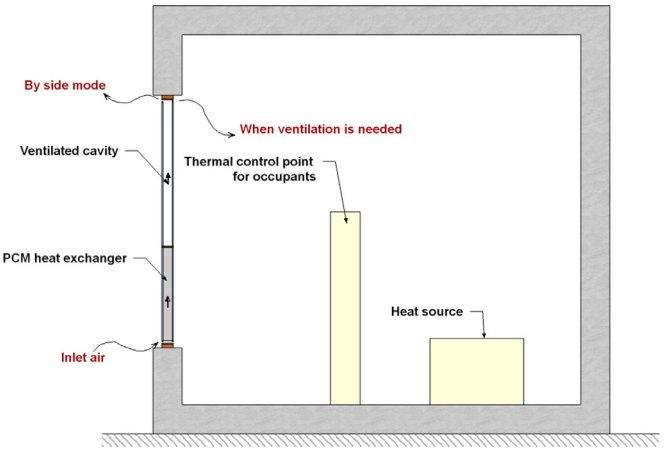

Fig. 1. Ventilation widow with PCM heat exchanger.

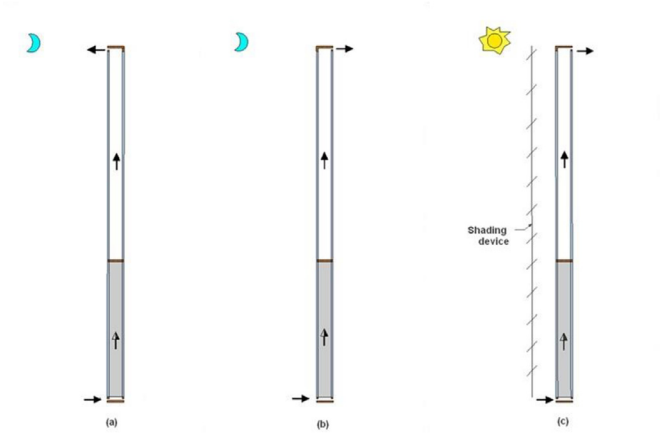

Fig. 2. The operation strategies of the PCM ventilation system in summer: (a) night ventilation mode; (b) night free cooling mode; (c) daytime ventilation pre-cooling mode.

Fig. 2 describes the operation strategies of the system. In summer, night ventilation is part of the control strategies. Heat is released from the PCM heat exchanger by cold ambient air during the night. The PCM is reloaded again during daytime by precooling of the outdoor air when ventilation is needed. In the daytime, a shading device is used to prevent the overheating of the system.

Fig. 3 shows the structure of ventilated window. It consists of a ventilated cavity in the upper part and heat exchanger in the lower part. The ventilated cavity is similar to a double glazing window with ventilation in the air gap. The heat exchanger is made of PCM plates located at the same distance from each other to form small air gaps for ventilation. The thickness of the air gap is chosen as 5 mm according to former work [26] in order to guarantee large total PCM volume in the heat exchanger, which is related to large heat storage/release possibility. However, the low thermal conductivity of PCM limits the thickness of PCM plates. As a result, the total amount of PCM is limited and should be optimized.

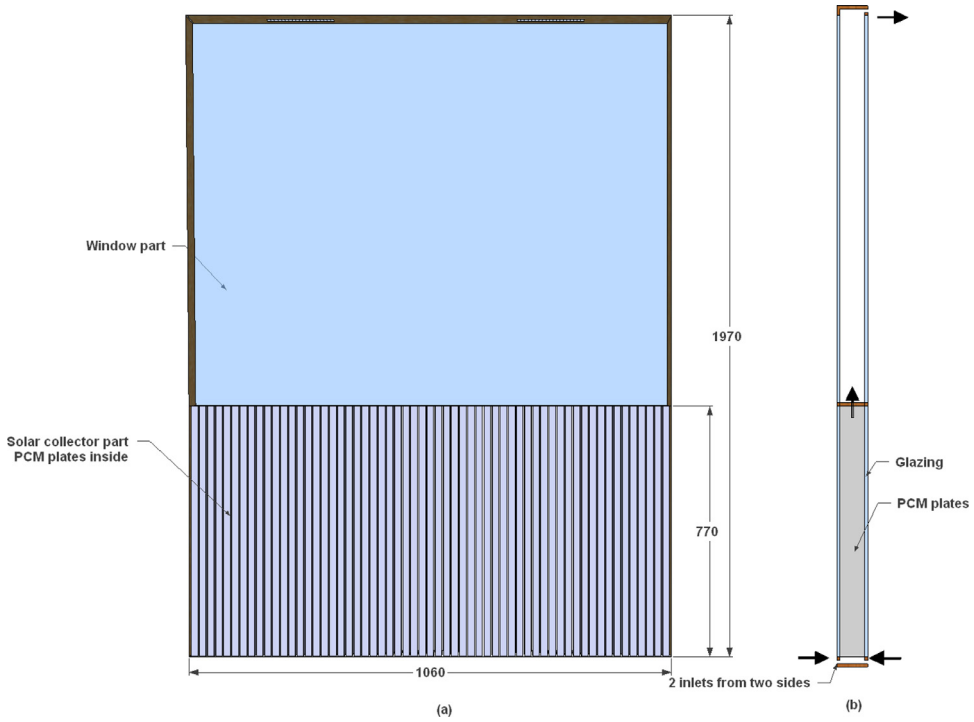

Fig. 3. Description of the ventilated window with PCM heat exchanger (a) front view; (b) side view.

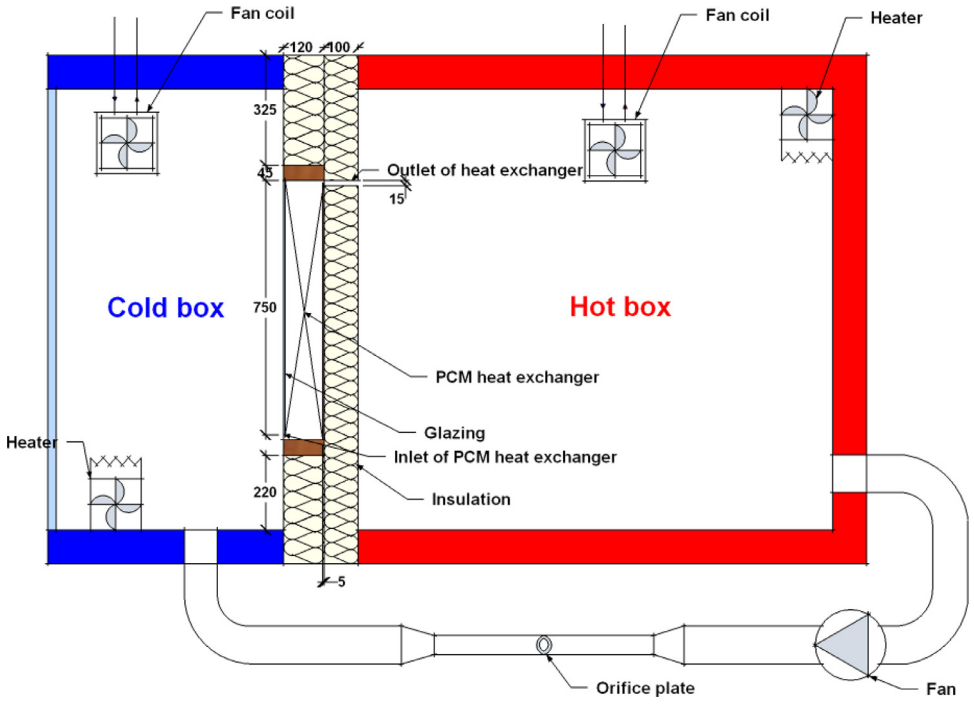

Fig. 4. Setup of hot box and cold box for testing the heat exchanger.

3. Experimental setup

The heat transfer process of the PCM heat exchanger is studied by full-scale experiments in a hot box and cold box, as seen in Figs. 4 and 5. Both of them are equipped with a water cooling system and an electric heating coil. A proportional–integral–derivative (PID) controller is used to getting the accurate temperature in the two boxes. Moreover, a fancoil provides recirculating airflow at a speed of approximately 0.2 m/s to keep the homogeneous of air temperature in each of the hot box and the cold box. A fan provides an airflow inside the heat exchanger, which creates circulation between the hot box and cold box. The flow rate is measured by an orifice plate with an uncertainty of ±7.5%.

The heat exchanger is mounted in between the two boxes, as shown in Fig. 4. It is supported by insulation boards. It is made of a wooden frame, a glazing cover, and many parallel vertical PCM boards. The distance between any two boards is 5 mm. The details of the PCM plate inside the heat exchanger are shown in

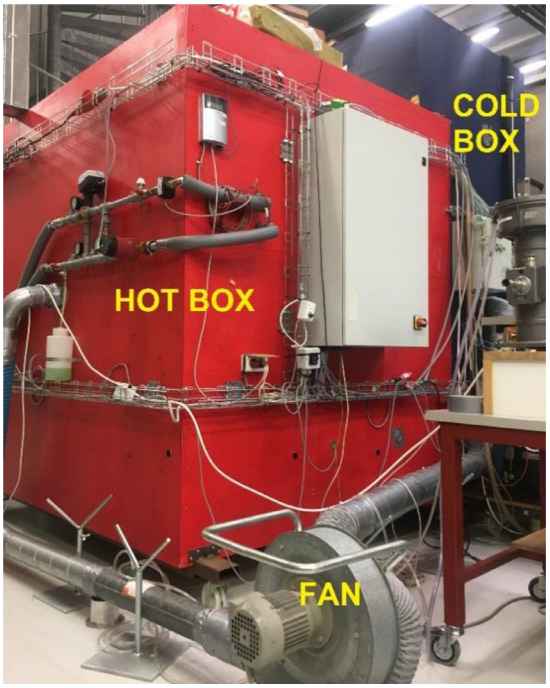

Fig. 5. Ventilation system between hot box and cold box.

Table 1
Thermal properties of paraffin wax 22.

Property	Manufacture data (Pure paraffin wax)	DSC measurement (Fiber absorbed PCM)
Phase change temperature (°C)	22	15–23
Density (kg/m^3)	820	–
Specific heat (kJ/kg/K)	2.85	2.3
Thermal conductivity (W/m/K)	0.18	–
Latent heat (kJ/kg)	216	117
Max operation temperature (°C)	400	–

Fig. 6. 56K-type thermocouples are used for monitoring the air and PCM temperature, as shown in Fig. 7. The calibration accuracy is ± 0.15 K. The logging time step is 300 s.

The thickness of PCM boards tested in this study is 12.5 mm. The air temperature inside the hot box is kept at 29 ± 1 °C and the cold box is kept at 9 ± 1 °C by PID controller. The flow rate of the fan (same as the flow rate inside the heat exchanger) is 106 m^3/h. Firstly, the fan provides airflow from the hot box to the cold box, thus the cold air goes into the inlet of the heat exchanger (in the bottom of the heat exchanger) to cool down the material. After the freezing process is done, the fan direction is changed, resulting in the hot air going into the outlet of the heat exchanger (in the top of the heat exchanger) to melt the material.

The PCM used in the system is paraffin wax with a melting temperature of 22 °C. The PCM is absorbed in a natural fiberboard to form a shape steady plate. The properties of the plate are measured by differential scanning calorimetry (DSC) technology with a heat rate of 0.5 °C/min for freezing and melting processes. Table 1 lists the properties of PCM based on the manufacturer and the DSC measurement.

Fig. 8 shows the heat capacity of the PCM plate in melting and freezing processes from DSC measurement. The total latent heat capacity for the freezing process is 118.8 kJ/kg and for the melting process is 115.2 kJ/kg in the temperature range of [10 °C–30 °C]. The measurement difference is 3.13% between melting and freezing.

Two additional samples are tested in heat rate 0.5 °C/min. The difference for enthalpy in the freezing process is 1.03% and in melting process is 0.16%. The difference of hysteresis between melting and freezing is 0.5 °C–1 °C. This is because the results depend highly on the measurement method.

In this paper, the thermal charge and discharge time is defined as the time period starting from initial condition to the time where the thermal charge or discharge rate is not lower than the fan power. In this work, the fan power is 30 W when the airflow rate is 106 m^3/h.

4. Methodology

4.1. Numerical model

The finite element model is built in COMSOL Multiphysics. The interface of Conjugate Heat Transfer and Laminar Flow multiphysics is used to simulate the coupling between heat transfer and fluid flow. The Laminar Flow interface solves for the conservation of energy, mass, and momentum in fluids, as shown in Eqs. (1)–(3). The flow is assumed incompressible.

$$\rho\frac{\partial \mathrm{u}}{\partial t}+\rho(\mathrm{u}\cdot\nabla)\mathrm{u}=-\nabla p+\mu\nabla^2\mathrm{u}+\rho g\beta\Delta T \tag{1}$$

$$\nabla\cdot\mathrm{u}=0 \tag{2}$$

$$\frac{\partial T}{\partial t}+u\cdot\nabla T=\frac{\lambda}{\rho Cp}\nabla^2 T \tag{3}$$

Where ρ is the density (kg/m^3), u is the velocity of air (m/s), t is the time(s), p is the pressure (Pa), μ is the dynamic viscosity (kg/m/s), g is the acceleration of gravity (m/s^2), β is coefficient of thermal expansion, T is the temperature(°C), λ is the heat conductivity (W/m/ °C), and Cp is the specific heat (kJ/kg).

The Heat Transfer in Solids interface provides features for modeling heat transfer by conduction. The convection is 0 in the fiberboard-based shape steady PCM. The fictive heat capacity based on DSC measurement is used to solve the equation. The energy equation is given in Eq. (4).

$$\frac{\partial T}{\partial t}=\frac{\lambda}{\rho Cp(T)}\nabla^2 T \tag{4}$$

In this work, a 2D model is built for summer case. Half of the PCM plate and half of the air cavity are chosen as the calculation domain, as shown in Fig. 9.

Some hypotheses are necessary to simplify the calculation process. The flow in between the two plates is considered as a 2-dimensional flow to simplify the calculation. The boundary conditions could be simplified as symmetry because of the periodic arrange of PCM plates and air gaps between the plates. Moreover, the thickness of thermal and velocity boundary layers are both considered less than half of the distance between two plates.

Symmetry boundary conditions are considered at x = 0 and x = $(d+e)/2$, as seen in Eqs. (5) and (6).

$$-n\cdot q=0,\ \mathrm{x}=0 \text{ and } \mathrm{x}=(d+e)/2 \tag{5}$$

$$u\cdot n=0,\ \mathrm{x}=(d+e)/2 \tag{6}$$

Thermal insulation boundary conditions are chosen at the top and bottom of the plates, as shown in Eq. (7).

$$-n\cdot q=0, 0<x<d/2, y=0 \text{ and } y=770 \tag{7}$$

The initial boundary conditions are as in Eqs. (8)–(10).

$$T(x,y,0)=T_0 \tag{8}$$

$$T(x,0,t)=T_{inlet}, d/2<x<(d+e)/2 \tag{9}$$

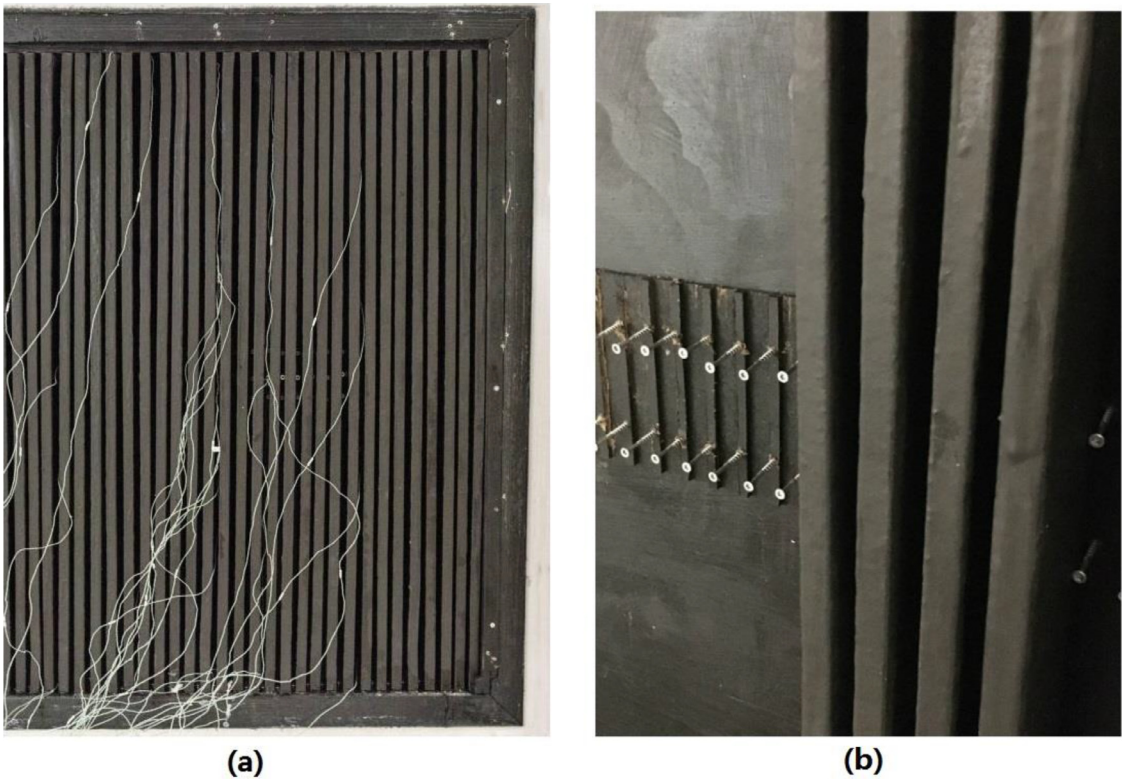

Fig. 6. PCM plates inside the wood frame (a) overview; (b) details in installation.

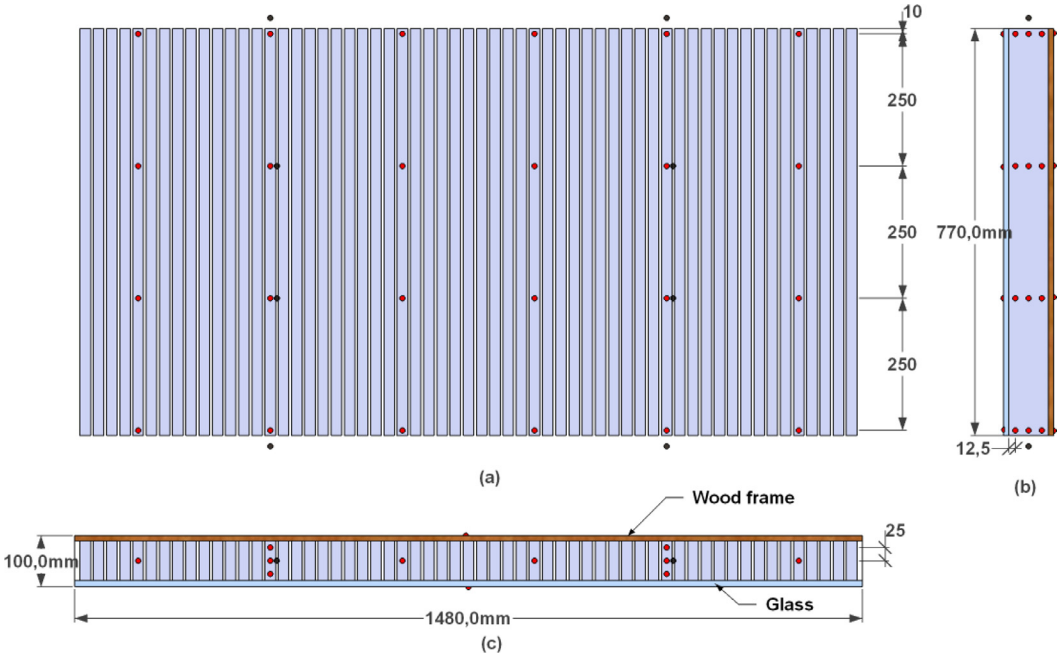

Fig. 7. Temperature measurement of the PCM heat exchanger. Red ones represent the PCM temperature measurement points and the black ones are the air temperature measurement points. (a) front view; (b) side view; (c) top view.

$$Q(x, y, t) = 106\mathrm{m}^3/\mathrm{h} \tag{10}$$

The solidification capability of PCM is a key energy performance factor for PCM components in buildings [27]. In this work, a severe summer day in Copenhagen is chosen as the input of the model. Night ventilation mode is analyzed firstly to optimize the PCM plate thickness in the discharging process. Afterwards, the charging process in order to cool down the ventilated air is simulated and the energy saving potential of the heat exchanger is analyzed.

4.2. Model validation

Fig. 10 shows the average temperature curves of the PCM plate with different heights in the freezing process. The results from simulation show good consistency with the experimental data. The

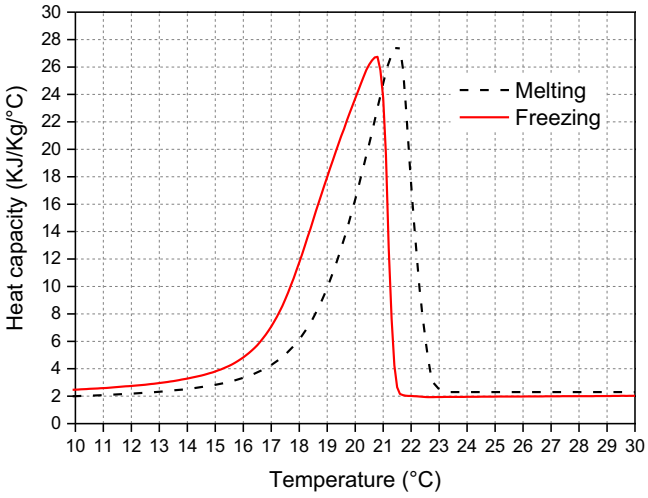

Fig. 8. DSC measured heat capacity of the PCM plate in freezing and melting processes.

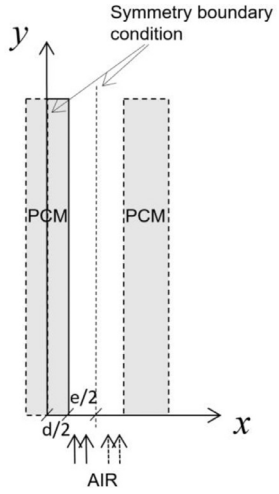

Fig. 9. Calculated domain for numerical model.

average error (ε) is 2.38%, which is defined in Eq. (11). The temperature curves at heights 260 mm and 510 mm show better accuracy than in 10 mm and 760 mm. One possible explanation is that the air distribution near the inlet and outlet is complicated in a real situation. For the experiment, the inlet air temperature fluctuates at 8–10 °C because of the limitation of PID controller, which also influences the accuracy of the experiment. As a result, the final value around 7.5 h from the experiment is not convergent at 10 °C. The variations in density between melt and solid can also affect the results.

$$\varepsilon = \left| \frac{\text{Experimental value} - \text{Simulation value}}{\text{Experimental value}} \right| \times 100\% \qquad (11)$$

The phase change start temperature in both simulation results and experimental data is clear. But the end temperature is not. The heat capacity of the material determines the temperature change process. As seen in Fig. 8, the heat capacity used in the model changed sharply around 21.5 °C in the freezing process, but smoothly at the lower temperature. However, the phase change start temperature in the experimental data is higher than the simulation results (except in 10 mm). It is due to the limitation of accuracy in DSC measurement for heat capacity. The uncertainty in the experiment also affects the error between experimental data and simulation results. Nevertheless, the total error is within a reasonable range.

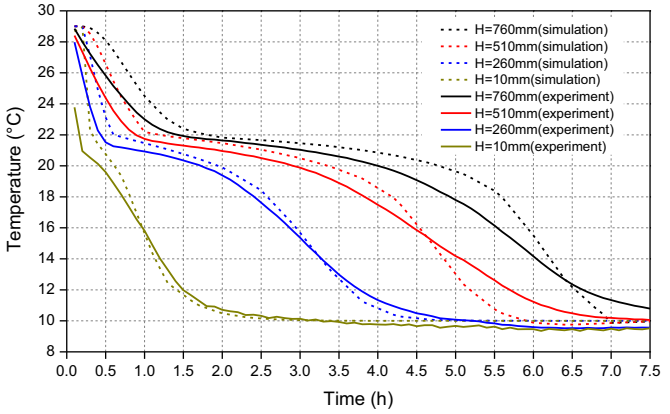

Fig. 10. Temperature in the middle of the PCM plate with different heights in the freezing process.

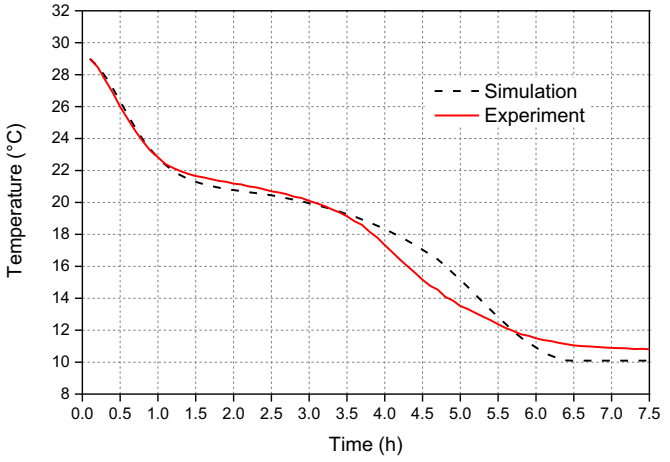

Fig. 11. Outlet air temperature in the freezing process.

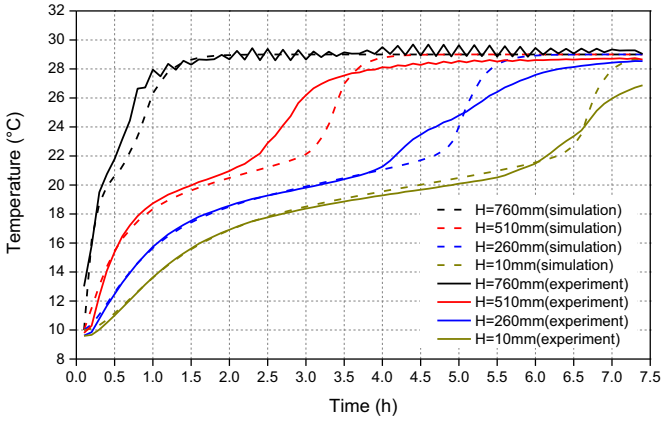

Fig. 12. Temperature in the middle of the PCM plate with different heights in the melting process.

Fig. 11 shows the outlet air temperature curves in the freezing process. The error between experimental data and simulation result is 4.41%. The error is higher than the error of PCM temperature, because the air temperature measurement is influenced by more elements such as variability of inlet temperature (8–10 °C) and variability of air flow rate.

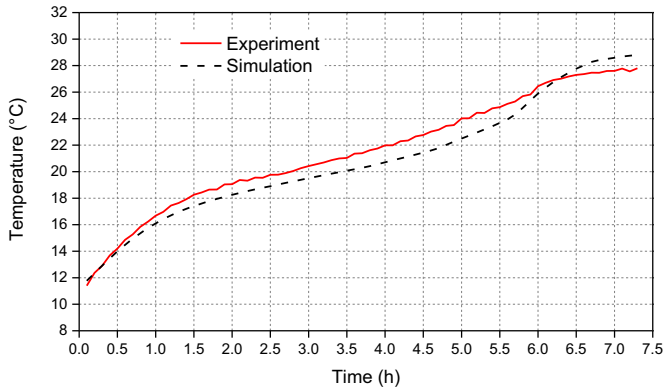

Fig. 13. Outlet air temperature in the melting process.

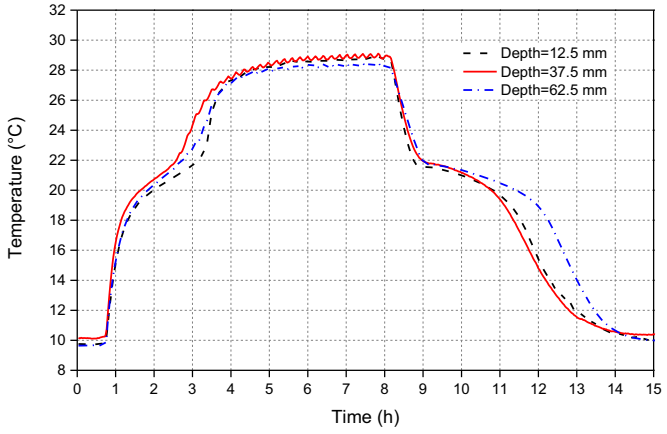

Fig. 14. The temperature homogeneity along the length of the PCM plate from experiment.

Fig. 12 shows the average temperature curves of the PCM plate with different heights in the melting process. The results from simulation show good consistency with experimental data. The average error is 4.79%. Similar to Fig. 9, the end temperature of phase change in both simulation results and experimental data is clear. But the start temperature is not. As seen in Fig. 7, the heat capacity used in the model changed sharply around 23 °C in the melting process, but smoothly at the lower temperature. However, the phase change end temperature in experimental data is lower than the simulation results, which means that the hysteresis of melting and freezing processes should be smaller than the DSC measurement results. Nevertheless, the total error is within a reasonable range.

Similarly, Fig. 13 shows the outlet air temperature curves in the melting process. The error between experimental data and simulation results is 3.96%, which is within a reasonable range.

The model output results show good agreement with the experimental data in freezing and melting processes, for both PCM temperature and outlet air temperature. The numerical model is reliable to simulate the heat transfer inside the heat exchanger.

The temperature change along the length of the PCM plate is shown in Fig. 14. The average temperature deviation to the middle point is 2.6% when the depth is 12.5 mm, and 4.2% when the depth is 62.5 mm, which are all in the reasonable range. It is feasible that the numerical model of PCM plates is simplified as 2D.

4.3. Climate analysis

Fig. 15 shows the summer outdoor air temperature in Copenhagen. The weather data is obtained from the Design Reference Year based on measurements conducted by DMI to get a typical summer condition [28]. There are 27 days where the maximum outdoor air temperature is above 23 °C. There are 194 h in which the outdoor air temperature is above 23 °C in those 27 days, which are necessary for applying ventilation pre-cooling. Among the days when ventilation pre-cooling is necessary, the minimum temperature is all below 18.1 °C, and 11 days of them the minimum temperature during the night are below 14 °C, which are suitable for the application of night ventilation.

A severe summer day in Copenhagen is chosen as the model input. As shown in Fig. 16, the average air temperature from 0:00 to 4:00 is around 14 °C, which is suitable for night ventilation. The air temperature from 11:00 to 15:00 is higher than 26 °C and air conditioning is needed to remove the cooling load from the ventilated fresh air. The control strategy is designed accordingly. The fan is turned on from 0:00 to 4:00, and the system is in night ventilation mode. It is turned on again from 11:00 to 15:00 in the daytime ventilation pre-cooling mode.

5. Results

5.1. Summer night ventilation mode

Night ventilation for PCM solidification is analyzed based on some assumptions. The ventilation starts from a point where the PCM system is fully charged with heat. The system needs to be discharged by the low-temperature ambient air. The cold air is ventilated from the bottom of the heat exchanger and into the air gaps between the PCM plates. The ventilation is stopped when the PCM is fully cooled down or the ambient air temperature is too high to remove heat from the PCM. The inlet air temperature is set as 14 °C as the average temperature during the midnight observed in Copenhagen is around 14 °C.

The thickness of PCM plates inside the heat exchanger should be chosen in a way that both the heat transfer amount and response time are optimized. The PCM utilization rate is also an important element to decide the right design of PCM heat exchanger and save material cost.

4 models with different plate thicknesses are calculated and compared. Table 2 shows the differences between the models.

Fig. 17 shows the outlet air temperature of the heat exchanger in the night ventilation mode. For the first two hours, the difference of outlet air temperature for different plate thicknesses is not so big. It is the sensible heat being released from the PCM to the ventilated air, and it is quite small in comparison with latent heat. A slower temperature change for all the cases is observed from around 21 °C until 14 °C, during which period the PCM in the heat exchanger is going through a phase change process and the released energy density is relatively high. Moreover, the system response time for the 5 mm plate thickness is relatively short and for 20 mm is relatively long.

Fig. 18 illustrates the heat release from the heat exchanger with different plate thicknesses. For 0–5 h discharge time, the cold storage amounts are similar for 10, 15, and 20 mm plate thickness. A big difference is shown for 5 mm plate thickness after around 3.6 h. For a specific summer case, the discharge time is limited by the outdoor climate as well as fan energy consumption. A PCM heat exchanger with 10 mm plate thickness is recommended, and the discharge time is recommended as 4–5 h to maximize the cold storage to the system volume. For 10 mm plate thickness, the cold storage ability is similar to 20 mm plate thickness within the recommended discharge time. However, the cost of material in the heat exchanger decreased by 16.87%. For the cases in which the efficient discharge time is shorter (0–3.6 h) because of the climate limitation, the recommended plate thickness is 5 mm. The cost of

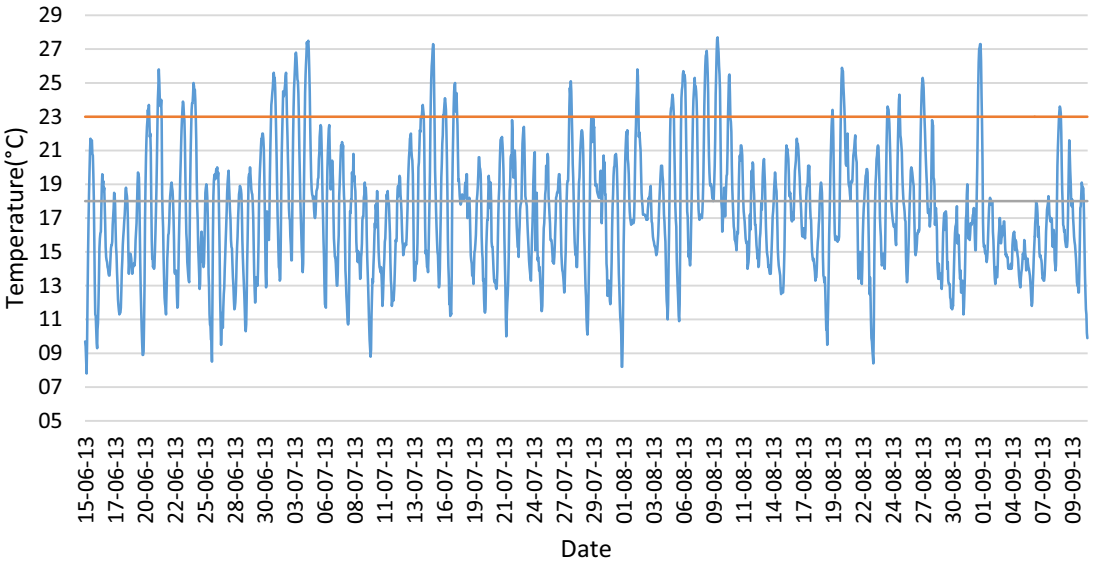

Fig. 15. Summer outdoor air temperature in Copenhagen from the Design Reference Year.

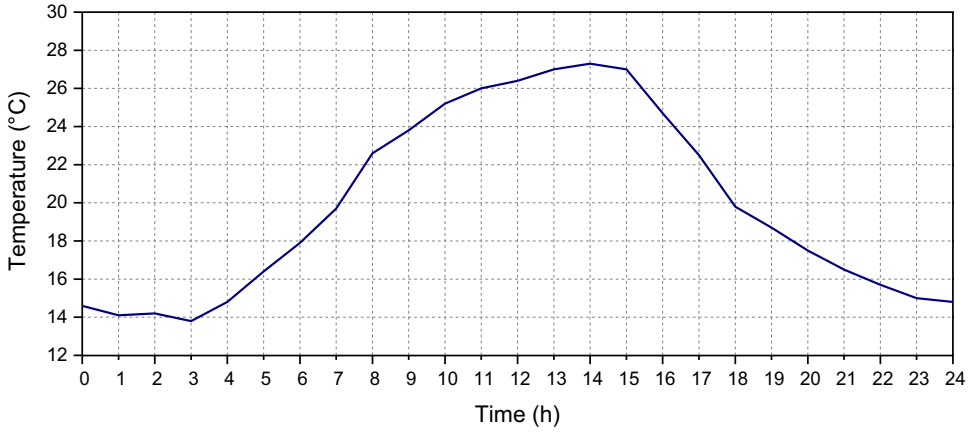

Fig. 16. Outdoor air temperature (07.15) for a severe summer day in Copenhagen.

Table 2
Models of heat exchanger with different PCM plate thicknesses.

d (mm)	e (mm)	Air velocity (m/s)	Number of plates in total	Plate depth (mm)	Air flow rate (m^3/h)	Total PCM surface area (m^2)	Total PCM volume (m^3)
5	5	0.74	106	75	106	22.30	0.052
10		1.09	70			15.69	0.069
15		1.48	53			12.62	0.078
20		1.78	42			10.58	0.083

material in the heat exchanger decreased by 37.35% compared to 20 mm plate thickness.

5.2. Pre-cooling potential

The whole heat transfer process for discharge and charge together is complicated because of the hysteresis between the melting and freezing processes. The temperature change may not be consecutive if the PCM does not go through the full phase change process. For the modeling of the charging process, the difficulty lies in the definition of the initial values from the former process.

Fig. 19 describes the enthalpy transfer when the PCM cools down first and then goes through the melting process. The enthalpy curves for melting and freezing are based on the DSC measurement. Process 2 is the enthalpy transition between freezing and melting. It is not horizontal because of the change of the sensible heat. It is parallel to the beginning of the freezing process. The recharged heat and the initial temperature of melting process could be confirmed in this way. Once the initial temperature of melting process is confirmed, the corresponding Cp in melting process could be determined, as shown in Fig. 20.

The enthalpy and heat capacity transitions are set in the numerical model. Two models are calculated, with a plate thickness of 5 mm and 10 mm respectively. The outdoor air temperature in the severe summer day in Copenhagen is used as model input. The time for night ventilation mode is 00:00–04:00. The time for ventilation pre-cooling mode is 11:00–15:00.

Fig. 21 shows the cooling ability of the heat exchanger in ventilation pre-cooling mode. The average temperature difference between the ambient air and outlet air is 6.5 °C from 11:00 to 15:00 when the plate thickness is 10 mm. The average temperature differ-

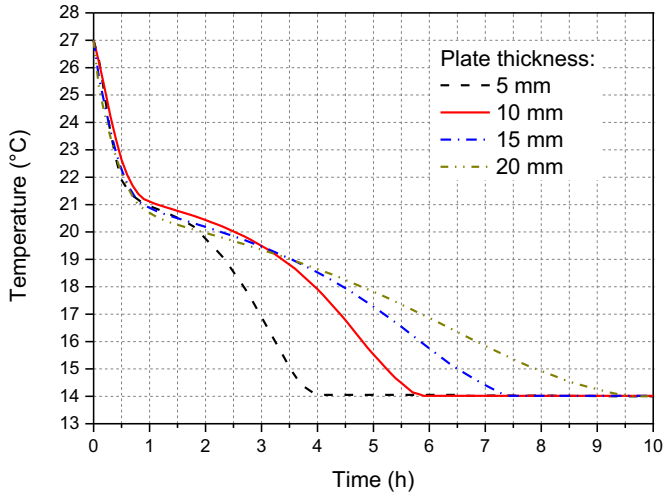

Fig. 17. Outlet air temperature of the heat exchanger with different plate thicknesses.

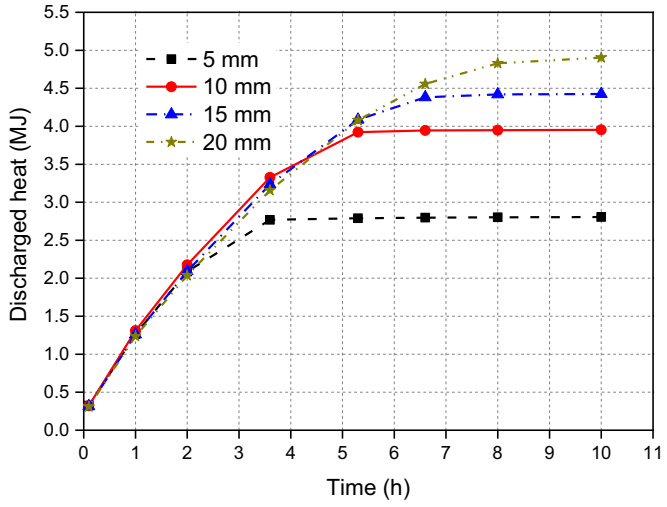

Fig. 18. Discharged heat from the heat exchanger with different plate thicknesses.

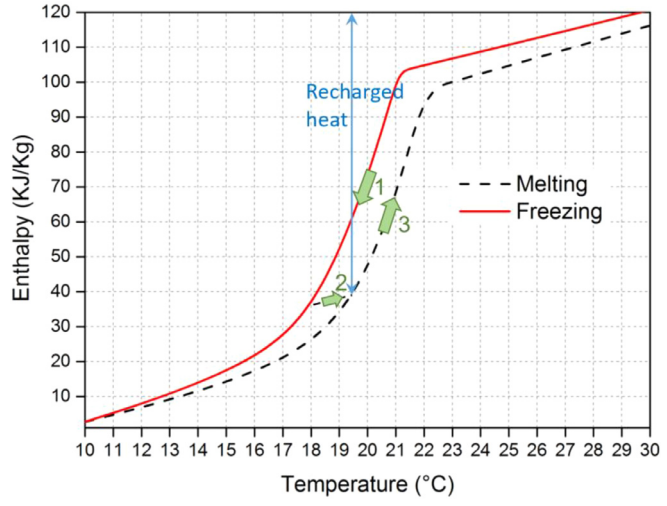

Fig. 19. Enthalpy in relation to temperature transition.

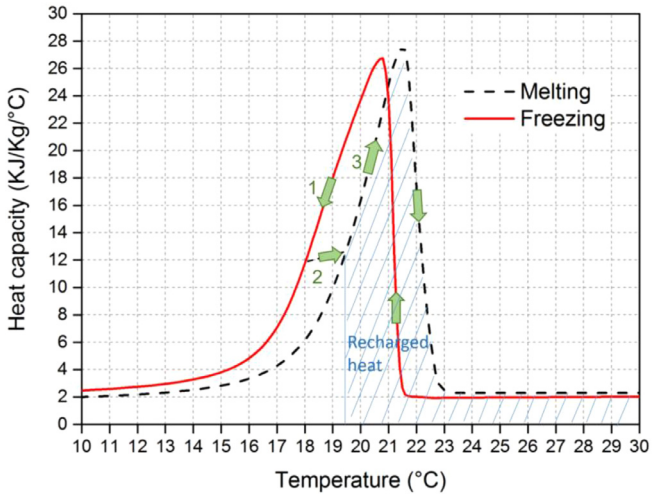

Fig. 20. Heat capacity in relation to temperature transition.

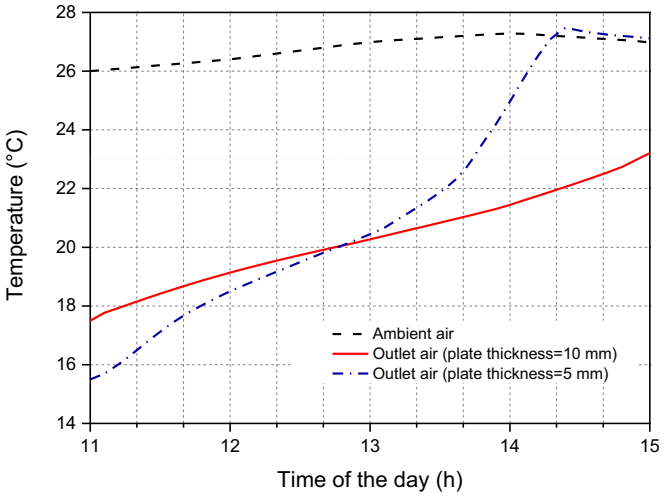

Fig. 21. Cooling ability of the heat exchanger in ventilation pre-cooling mode.

ence between the ambient air and outlet air is 7.11 °C from 11:00 to 13:48 when the plate thickness is 5 mm.

The discharge efficiency (ζ) is calculated by the ratio between the heat storage in pre-cooling mode and the heat release in the night ventilation mode, which is in Eq. (12).

$$\zeta = \frac{\rho_{air} q C p_{air} \int_{t_m}^{t_n} |T_{ambient} - T_{inlet}| dt}{\rho_{air} q C p_{air} \int_{t_i}^{t_j} |T_{outlet} - T_{inlet}| dt} \quad (12)$$

Where $t_m = 0$ h, $t_n = 4$ h, $t_i = 11$ h, $t_j = 15$ h.

When the plate thickness is 10 mm, the discharged heat in night ventilation mode is 3.55 MJ in this work. The charged heat for air pre-cooling mode is 3.19 MJ. The discharge efficiency of the heat exchanger is 89.85%. The effect time (the outlet air temperature lower than 23 °C) is 3.9 h. When the plate thickness is 5 mm, the discharged heat in night ventilation mode is 2.79 MJ. The charged heat for air pre-cooling mode is 2.52 MJ. The discharge efficiency of the heat exchanger is 90.32%. The effect time is 2.7 h.

In comparison, a heat exchanger with 5 mm plate thickness has a shorter discharge time and shorter charge time. It can be cooled down faster and recharged faster, which is good for the climate when the outdoor air temperature suitable for night ventilation is short, such as hot summer climate (but such climate always has long hours in which cooling is needed during daytime). A heat exchanger with 10 mm plate thickness has longer discharge time and

charge time. There is more stability of outlet air temperature in the ventilation pre-cooling mode as well.

6. Conclusions

This paper presents a new window application for pre-cooling of ventilation air using a PCM heat exchanger. In summer, the PCM heat exchanger is discharged by night ventilation, and recharged by high-temperature ambient air in pre-cooling mode.

The design and optimization processes of the heat exchanger are conducted by means of numerical modeling, which is verified by full-scale experiments. The nonlinear properties and hysteresis of PCM are set in the model. The hysteresis of PCM used in the model is slightly overvalued by DSC measurement, but the deviation from the experiment lies within a reasonable range.

The numerical works are conducted based on a severe summer day in Copenhagen. Results show that in night ventilation mode, the increase in PCM plate thickness does not have a big influence on the outlet air temperature and discharged heat in the first hours of the discharge process. 10 mm plate thickness for the heat exchanger is recommended when 4–5 h discharge time available during the night, which saves 16.87% material cost with similar discharged heat (compared with the heat exchanger with 20 mm plate thickness). 5 mm plate thickness for the heat exchanger is recommended when there is only 0–3.6 h discharge time available during the night, which saves 37.35% material cost with similar discharged heat.

In ventilation pre-cooling mode, the saved energy from the heat exchanger with 10 mm plate thickness is 3.19 MJ/day. The discharge efficiency of the heat exchanger is 89.85%.The effect pre-cooling time is 3.9 h. The saved energy from the heat exchanger with 5 mm plate thickness is 2.52 MJ/day. The discharge efficiency of the heat exchanger is 90.32%. The effect pre-cooling time is 2.7 h.

In the case study in Copenhagen, the heat exchanger with 10 mm plate thickness has more stable pre-cooled air temperature in longer effective pre-cooling time with a higher energy saving amount than 5 mm, and the discharge can be fulfilled during the night in this climate. Nevertheless, the heat exchanger with 5 mm plate thickness has a fast thermal response, which is good for the climate where the duration of outdoor air temperature suitable for night ventilation is short.

New methods to get more accurate PCM heat capacity is essential for future works. It is also necessary to conduct more climate analyses to verify the optimized results. In the next stage, the studies will include the feasibility of applying the PCM heat exchanger for solar energy storage in winter and its air pre-heating effect.

Acknowledgment

This work is carried out within the EU Horizon 2020 research and innovation programme under grant agreement NO. 768576 (ReCO2ST). Moreover, the first author gratefully acknowledge the financial support from the Chinese Scholarship Council (CSC No. 201606050118).

References

[1] M. Iten, S. Liu, A. Shukla, A. Shukla, A review on the air-PCM-TES application for free cooling and heating in the buildings, Renew. Sustain, Energy Rev. 61 (2016) 175–186, doi:10.1016/j.rser.2016.03.007.
[2] H. Akeiber, P. Nejat, M.Z.A. Majid, M.A. Wahid, F. Jomehzadeh, I. Zeynali Famileh, J.K. Calautit, B.R. Hughes, S.A. Zaki, A review on phase change material (PCM) for sustainable passive cooling in building envelopes, Renewable Sustainable Energy Rev. 60 (2016) 1470–1497, doi:10.1016/j.rser.2016.03.036.
[3] E. Osterman, V.V.V. Tyagi, V. Butala, N.A.A. Rahim, U. Stritih, Review of PCM based cooling technologies for buildings, Energy Build. 49 (2012) 37–49, doi:10.1016/j.enbuild.2012.03.022.
[4] H. Johra, P. Heiselberg, Influence of internal thermal mass on the indoor thermal dynamics and integration of phase change materials in furniture for building energy storage: a review, Renewable Sustainable Energy Rev. 69 (2017) 19–32, doi:10.1016/J.RSER.2016.11.145.
[5] V.A. Aroul Raj, R. Velraj, Review on free cooling of buildings using phase change materials, Renewable Sustainable Energy Rev. 14 (2010) 2819–2829, doi:10.1016/j.rser.2010.07.004.
[6] M. Pomianowski, P. Heiselberg, R. Lund Jensen, Dynamic heat storage and cooling capacity of a concrete deck with PCM and thermally activated building system, Energy Build. 53 (2012) 96–107, doi:10.1016/j.enbuild.2012.07.007.
[7] G. Diarce, A. Urresti, A. García-Romero, A. Delgado, A. Erkoreka, C. Escudero, Á. Campos-Celador, Ventilated active façades with PCM, Appl. Energy 109 (2013) 530–537, doi:10.1016/j.apenergy.2013.01.032.
[8] A. De Gracia, L. Navarro, A. Castell, Á. Ruiz-Pardo, S. Álvarez, L.F. Cabeza, Thermal analysis of a ventilated facade with PCM for cooling applications, Energy Build. 65 (2013) 508–515, doi:10.1016/j.enbuild.2013.06.032.
[9] L. Karlsen, P. Heiselberg, I. Bryn, H. Johra, Solar shading control strategy for office buildings in cold climate, Energy Build. 118 (2016) 316–328, doi:10.1016/j.enbuild.2016.03.014.
[10] P. Heiselberg, O. Kalyanova, CLIMAWIN: Technical Summary Report, vol. 160, 2013, p. 92 http://vbn.aau.dk/files/203815355/CLIMAWIN_Technical_Summary_Report.pdf.
[11] L. Fan, J.M. Khodadadi, Thermal conductivity enhancement of phase change materials for thermal energy storage: a review, Renewable Sustainable Energy Rev. 15 (2011) 24–46, doi:10.1016/J.RSER.2010.08.007.
[12] W.M. Huang, Y. Zhao, C.C. Wang, Z. Ding, H. Purnawali, C. Tang, J.L. Zhang, Thermo/chemo-responsive shape memory effect in polymers: a sketch of working mechanisms, fundamentals and optimization, J. Polym. Res. 19 (2012) 9952, doi:10.1007/s10965-012-9952-z.
[13] Heat and cold storage with PCM, Springer Berlin Heidelberg, Berlin, Heidelberg, 2008, doi:10.1007/978-3-540-68557-9.
[14] Modeling phase change materials behavior in building applications: comments on material characterization and model validation, Renewable Energy 61 (2014) 132–135, doi:10.1016/J.RENENE.2012.10.027.
[15] R. Baetens, B.P. Jelle, A. Gustavsen, Phase change materials for building applications: a state-of-the-art review, Energy Build. 42 (2010) 1361–1368, doi:10.1016/j.enbuild.2010.03.026.
[16] F. Kuznik, J. Virgone, Experimental investigation of wallboard containing phase change material: Data for validation of numerical modeling, Energy Build. 41 (2009) 561–570, doi:10.1016/J.ENBUILD.2008.11.022.
[17] A. Buonomano, G. De Luca, U. Montanaro, A. Palombo, Innovative technologies for NZEBs: an energy and economic analysis tool and a case study of a non-residential building for the mediterranean climate, Energy Build. 121 (2016) 318–343, doi:10.1016/j.enbuild.2015.08.037.
[18] J. Virgone, A. Trabelsi, 2D Conduction Simulation of a PCM Storage Coupled with a Heat Pump in a Ventilation System, Appl. Sci. 6 (2016) 193. http://dx.doi.org/10.3390/app6070193.
[19] Verification and validation of EnergyPlus phase change material model for opaque wall assemblies, Build. Environ. 54 (2012) 186–196, doi:10.1016/J.BUILDENV.2012.02.019.
[20] Establishment and experimental verification of PCM room's TRNSYS heat transfer model based on latent heat utilization ratio, Energy Build. 84 (2014) 287–298, doi:10.1016/J.ENBUILD.2014.07.082.
[21] Numerical modelling and thermal simulation of PCM–gypsum composites with ESP-r, Energy Build. 36 (2004) 795–805, doi:10.1016/J.ENBUILD.2004.01.004.
[22] K. Biswas, J. Lu, P. Soroushian, S. Shrestha, S. Shrestha, Combined experimental and numerical evaluation of a prototype nano-PCM enhanced wallboard, Appl. Energy. 131 (2014) 517–529, doi:10.1016/j.apenergy.2014.02.047.
[23] M. Liu, W. Saman, F. Bruno, Validation of a mathematical model for encapsulated phase change material flat slabs for cooling applications, Appl. Therm. Eng. 31 (2011) 2340–2347, doi:10.1016/j.applthermaleng.2011.03.034.
[24] C. Hasse, M. Grenet, A. Bontemps, R. Dendievel, H. Sallée, Realization, test and modelling of honeycomb wallboards containing a Phase Change Material, Energy Build. 43 (2010) 232–238, doi:10.1016/j.enbuild.2010.09.017.
[25] P. Lamberg, R. Lehtiniemi, A.-M. Henell, Numerical and experimental investigation of melting and freezing processes in phase change material storage, Int. J. Therm. Sci. 43 (2004) 277–287, doi:10.1016/j.ijthermalsci.2003.07.001.
[26] H. Yue, H. Per, Thermal performance of ventilated solar collector with energy storage containing phase change material, 38th AIVC Conf. "Ventilating Heal. Low-Energy Build, 2017 http://www.aivc.org/resource/thermal-performance-ventilated-solar-collector-energy-storage-containing-phase-change?volume=37270 (accessed November 30, 2017).
[27] J. Kośny, PCM-Enhanced Building Components, Springer International Publishing, Cham, 2015, doi:10.1007/978-3-319-14286-9.
[28] BSim - Climate data, (n.d.). http://sbi.dk/bsim/Pages/Klimadata.aspx#TRY (accessed November 16, 2017).

Appendix B. Paper 2

Y. Hu, P.K. Heiselberg, H. Johra, R. Guo, Experimental and numerical study of a PCM solar air heat exchanger and its ventilation preheating effectiveness, Renewable Energy. 145 (2020) 106–115. doi:10.1016/J.RENENE.2019.05.115.

Renewable Energy 145 (2020) 106–115

Contents lists available at ScienceDirect

Renewable Energy

journal homepage: www.elsevier.com/locate/renene

Experimental and numerical study of a PCM solar air heat exchanger and its ventilation preheating effectiveness

Yue Hu*, Per Kvols Heiselberg, Hicham Johra, Rui Guo

Aalborg University, Division of Architectural Engineering, Department of Civil Engineering, Thomas Manns Vej 23, DK-9220 Aalborg Øst, Denmark

ARTICLE INFO

Article history:
Received 15 January 2019
Received in revised form
8 May 2019
Accepted 28 May 2019
Available online 31 May 2019

Keywords:
Renewable energy
Phase change material
Latent heat storage
Building energy conservation
Solar air heat exchanger

ABSTRACT

This article presents a PCM solar air heat exchanger integrated into ventilated window developed to maximize the use of the solar energy to pre-heat the ventilated air. The system is designed to improve the indoor air quality and thermal comfort by continuous pre-heated air supply at a reduced energy use through the capturing and storing of solar energy. This study examines the thermodynamic behavior of the system both experimentally and numerically. This entails a full-scale experiment in climate boxes to study the thermal storage and heat release ability of the facility. Accordingly, a numerical model combining heat transfer and buoyancy derived laminar flow and nonlinear thermal properties of the PCM is built and validated with the experimental data. The model is then used for configuration optimization of the PCM solar air heat exchanger to maximize the solar energy storage and the ventilation pre-heating effectiveness. The results show that for a 6-h solar charging period, the optimum PCM plate depth is 90 mm and the optimum air gap thickness is 6 mm. The same configuration can be used for both summer night cooling and winter solar energy storage applications. The total stored/released latent heat after one charging period is 93.31 MJ/m^3.

1. Introduction

Building energy use for ventilation and HVAC systems amount to more than one-third of the total energy use in industrial countries [1] and about 40% of the total energy use in Europe [2], and it shows growing trends as a result of increased thermal comfort requirements and climate changes. It has become a burden to the environment and the fossil fuel resources. To diminish the fuel consumption and carbon dioxide emission caused by building energy use, it is necessary to implement innovative technical solutions and renewable energy resources in the built environment. Many researchers have studied renewable energy such as solar energy applied in building energy systems to reduce the traditional building energy use. Excess renewable energy is often stored in thermal energy storage (TES) facilities with the advantages of grid peak shifting, building energy conservation, and the building thermal mass level improvement.

Phase change material (PCM) applied in TES is one of the most promising solutions for renewable energy storage and has recently drawn much attention within the scientific community [3]. Unlike the materials with only sensible energy storage, PCM releases/absorbs large amounts of latent heat during its phase transition in a small temperature range. The heat capacity of PCM during the phase transition period is much higher than the conventional building materials. The high energy density of the PCM offers a large heat storage ability with a relatively small storage volume, which makes it a good candidate for TES [4]. With adequate design and choices, the phase transition of the material occurs within the range of indoor thermal comfort, which allows direct applications of PCM in the building environment [5–7].

Ventilative heating or cooling systems integrating PCM for thermal storage is a common building application, which several research groups have tested and studied. For example, ventilation night cooling during a warm summer discharges PCM units at nighttime (cold storage) and then utilize these units during daytime to cool down the hot outdoor air used as ventilation inlet air [8–11]. Some other strategies focus more on power load peak shaving and demand shifting. For instance, Labat et al. [12] designed a PCM-to-air heat exchanger storage for heating, ventilation, air conditioning (HVAC) systems to shift the cooling demand from high to low electricity price periods. The PCM is discharged (cooled down) by the HVAC systems during low electricity price

* Corresponding author.
E-mail address: hy@civil.aau.dk (Y. Hu).

https://doi.org/10.1016/j.renene.2019.05.115

Nomenclature

Symbols

ρ	density of material [kg/m^3]
Cp	specific heat capacity [J/(kg K)]
T	temperature [°C]
t	time [s]
k	thermal conductivity [W/(m K)]
Q	heat source [W/m^3]
q	heat flux [W/m^2]
q_1	solar radiation [W/m^2]
q_2	natural convection heat flux [W/m^2]
$\overline{h}$	average heat transfer coefficient [W/(m^2·K)]
T_{ext}	temperature in cold box [°C]
$\overline{Nu}_L$	average Nussle number [dimensionless]
L	vertical length of PCM plates [m]
Ra_L	local Rayleigh number [dimensionless]
Pr	Prandtl number [dimensionless]
Gr_L	local Grashof number [dimensionless]
g	gravity acceleration [m/s^2]
α	thermal expansion coefficient [1/K]
μ	dynamic viscosity [Pa s]
u	velocity [m/s]
p	absolute pressure [Pa]
F	buoyancy force [N/m^3]
M	molar mass [kg/mol]
R	universal gas constant [J/(mol K)]

periods. The discharged PCM is then used during high price periods to decrease the energy demand for cooling. In winter time, PCM can be used directly [13–15] or indirectly [16–18] with solar energy systems or as TES integrated with other heating systems such as heat pump [19], floor heating [20], and ceiling heating [21]. Studies have shown that the integration of PCM in the building environment can significantly increase the building heat storage capacity and, thereby, improve the indoor space heating energy flexibility and ease the building demand-side management [22,23]. De Gracia et al. tested a ventilated double skin facade with PCM in the air cavity for both cooling [24] and heating [25] purposes. They found out that such PCM ventilation system can effectively prevent overheating in summer and reduce the electrical consumption of the HVAC system in winter.

Solar collectors can be used for providing pre-heated air to ventilation systems. The traditional solar air collector consists of an absorber and a transparent glass, and it facilities airflow inside the collector. Applications for solar collectors can be found in drying systems for agriculture [26] and marine [27] products, packed bed thermal storage unit [28], as well as space heating systems [29–31]. Nevertheless, a large heat transfer area and high flow rates are required for good performances because of the low thermal capacity and thermal conductivity of the air and the low convection coefficient on the surface of the absorber [32]. Applying PCM to the solar-air collector system has the advantage of more thermal energy storage, longer thermal release time [33], and more stable preheated air temperature [34]. However, the conventional method to apply PCM into a solar collector system is to use the material as the heat storage medium in the storage tank. The heat transfer fluid between the solar collector and the PCM heat storage tank is usually water. The PCM in this system always has a relatively high phase change temperature (around 40–60 °C) [35].

This paper proposes a different solution to apply PCM into the building energy system. It includes a double glazing ventilated window and a PCM heat exchanger. The system is designed to improve the indoor air quality and thermal comfort by continuous pre-heated air supply at a reduced energy use through the capturing and storing of solar energy. The double glazing window works as a trombe wall during the daytime when solar radiation is available. The PCM solar air heat exchanger directly stores the heat from the solar radiation and releases the heat later when solar radiation is less available to pre-heat the ventilated air. It has a smaller volume compare to the conventional PCM tank. The PCM in the solar-air heat exchanger has a phase change temperature around room temperature, which is good for the indoor thermal comfort. The relatively thin PCM plates compensate for the low thermal conductivity of the PCM and make the heat store and release processes faster.

This paper will experimentally and numerically study the thermal behavior of the PCM solar air heat exchanger and optimize its configuration to achieve the highest energy efficiency of the system. For that purpose, a full-scale laboratory experiment for testing the PCM solar air heat exchanger is conducted. Later on, the paper presents a numerical model accounting for the heat transfer and buoyancy effects in the solar air heat exchanger. The model is validated by the experimental data. Finally, the verified model is used to optimize the configuration of the PCM heat exchanger, including the depth of the PCM plates and the air gap thickness between PCM plates.

2. System description

Fig. 1 presents the configuration of the ventilated window with the PCM solar air heat exchanger. The ventilated window is a double glazing window with an air cavity between the two glazing layers, which allows ventilated air to go through. The solar air heat exchanger is made of parallel PCM plates separated by thin air gaps. The PCM plates are mounted in a wood frame with a glass on the front surface. There are openings on the top and bottom of the PCM heat exchanger frame and on the top of the ventilated window, to enable the ventilation of air through the system.

The system is designed to improve the indoor air quality and thermal comfort by continuous pre-heated air supply at a reduced energy use through the capturing and storing of solar energy. Fig. 2 illustrates the operation strategy of the ventilated window system in winter or transition seasons. In the daytime, the system is in solar energy storage mode (see Fig. 2(a)). The solar radiation charges the PCM in the solar air heat exchanger when solar energy is available. The ventilation air only passes the ventilated window and is heated up by the solar radiation, before it enters the indoor room. The ventilation pre-heating mode is on when the solar radiation is less than 200 W/m^2, as seen in Fig. 2(b). The cold ambient air passes the solar air heat exchanger from the bottom, and the stored heat heats it up. Then the pre-heated air passes through the double glazing window into the indoor space. The ventilation bypass mode is on when there is a cooling need in the space, and the inlet air temperature from the window system should be close to the outdoor air temperature, and at a maximum the airflow rate, as seen in Fig. 2(c).

With the new solar air heat exchanger ventilation system, solar energy and the PCM solar storage preheat the ventilation air to make the most use of the solar energy and to increase the inlet air temperature and thermal comfort in winter. It can benefit both the buildings under renovation and the new buildings. In building

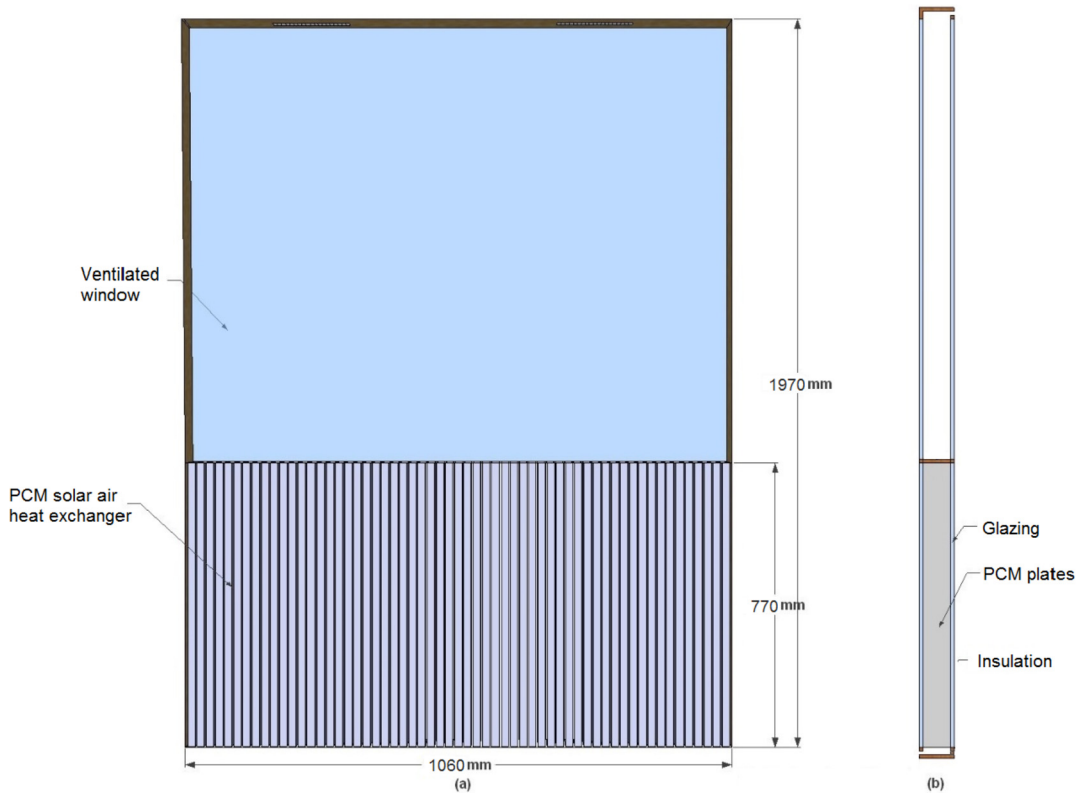

Fig. 1. Description of the ventilated window with PCM heat exchanger [36]. (a) Front view; (b) Side view.

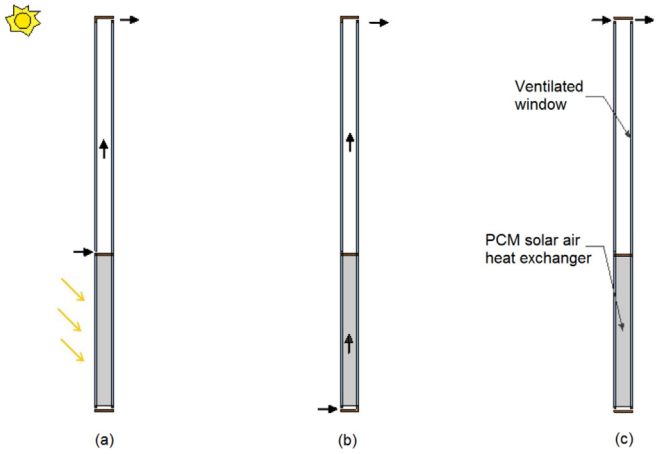

Fig. 2. System operation strategy (a) solar energy storage mode; (b) ventilation pre-heating mode; (c) ventilation bypass mode.

renovation, the install an efficient ventilation system with heat recovery is a challenging work. The application of the presented system can be an alternative method to ensure an energy efficient ventilation solution in these buildings. Moreover, the installation of the application only requires some façade envelope reconstruct. The easy installation of the system makes it good for the building renovation projects. For new buildings with decentralized ventilation solutions, the system can contribute to improve the energy efficiency of the buildings by better capture and utilization of the solar energy. The solar energy added into the building energy system is used to cover the heat demand of the buildings. As a result, the building energy consumption is reduced.

3. Experimental setup

The heat storage and heat release processes of the solar air heat exchanger are tested with a full-scale experiment in a *Hot Box* and *Cold Box* setup in the laboratory, as shown in Fig. 3. Both of the boxes are equipped with cooling coil and electric heater. The air temperature in the cold box is controlled by proportional integral derivative (PID) controllers at $8 \pm 1\,^{\circ}C$. A ventilation system connects the two boxes and creates an under-pressure in the hot box compared to the cold box by operation of a fan in the ventilation duct. It induces an air flow from the cold box to the hot box through the solar heat exchanger. The air flow rate during the ventilation pre-heating mode is kept constant at 106 m^3/h, which is measured by the orifice plate.

An artificial sun is used to provide solar radiation. It is an assembly of 56 OSRAM Ultra-Vitalux lamps mounted on a metal frame (see Fig. 4). The lamps are in an 8×7 matrix to create an even radiant distribution to the surface of the heat exchanger. Each lamp has a power of 300 W. The radiation spectrum of the lamps is similar to the natural alpine sunlight [37]. The distance from the artificial sun to the cold box is 0.95 m.

A pyranometer, Kipp & Zonen CMP 22, is used to measure the solar radiation on the surface of the solar air heat exchanger. The measurement uncertainty is $\pm$ 2%. The temperature and radiation measurement data is collected by a Fluke Helios Plus 2287A data logger every 10 s. The average solar radiation measured on the surface of the PCM solar radiator is 550 W based on 30 evenly distributed measurement points. A slight distribution inhomogeneity can be observed between the right, left, and center parts of the solar collector. The radiation on the left side is higher than the rest of the area. The deviation between the lowest and highest radiation is 9.35%.

The air flow rate is measured by an orifice plate EHBA Ø 125 mm

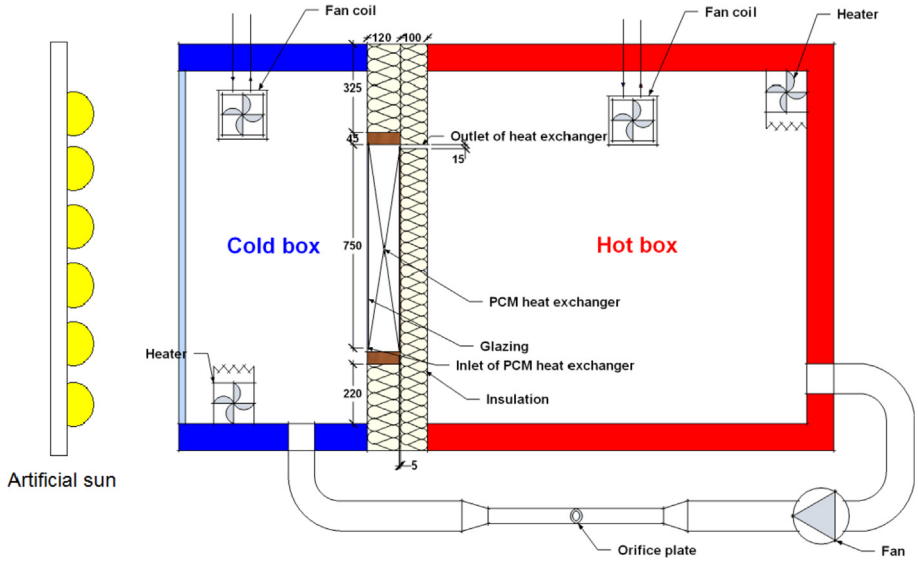

Fig. 3. Experimental setup of the solar air heat exchanger test.

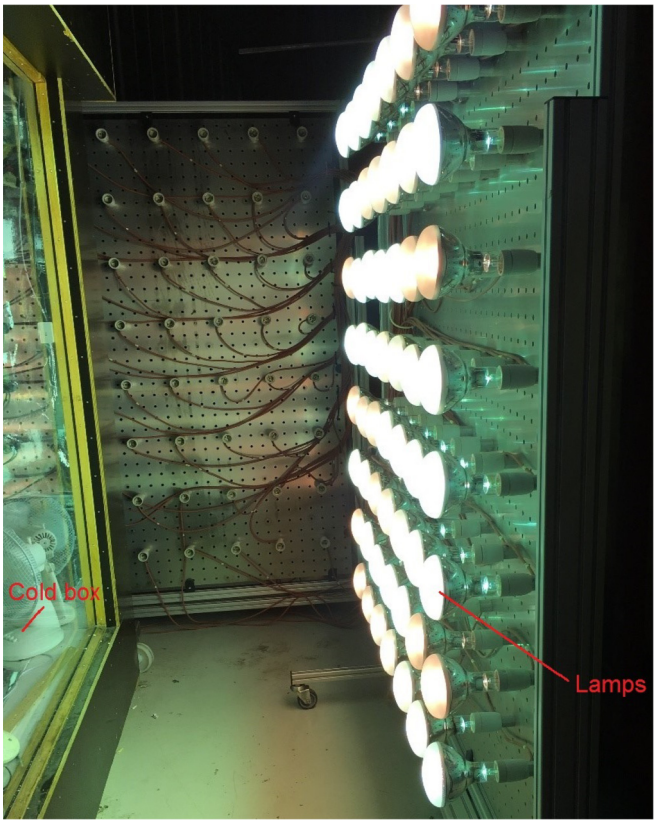

Fig. 4. The artificial sun.

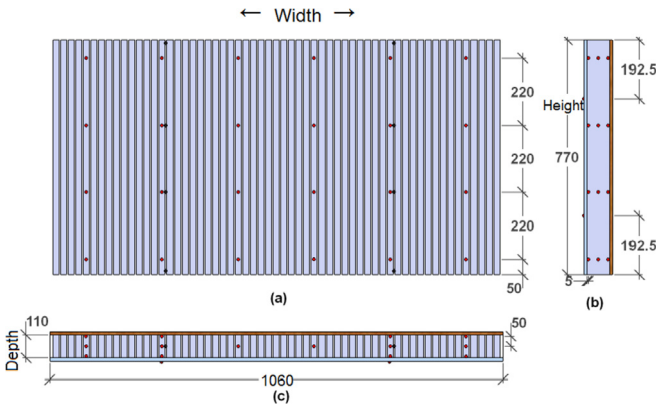

Fig. 5. Temperature measurement points in the solar air heat exchanger.

with an uncertainty of ± 7.5%. 72 calibrated type K thermocouples are used for monitoring the air and PCM temperature, as shown in Fig. 5. The temperature uncertainty is ± 0.15 K. 6 PCM plates are chosen to measure the material temperature at different heights and depths in the heat exchanger. Four of them are with 12 measurement points each, and two are with 4 measurement points each. For the air temperature measurements, the thermocouples are protected from solar radiation by mechanically ventilated silver-coated tubes (see Fig. 6).

The PCM used in the solar air heat exchanger is 50% paraffin wax impregnated fiberboard. It is a shape-stable PCM compound. The properties of the PCM compound are measured by Differential Scanning Calorimetry (DSC). The heating/cooling rate during the measurement is 0.5 °C/min for freezing and melting processes. The results show that the PCM has a melting range of 16 °C–23 °C and a freezing range of 14 °C–21.5 °C. The melting peak is at 20.7 °C, and the freezing peak is at 21.5 °C. Based on the results 0.8 °C temperature hysteresis is observed. The total heat capacity of the PCM plates is 117 kJ/kg (for a 10 °C–30 °C temperature range). More details about the measured PCM properties are available in Ref. [36]. The thickness of the PCM plates is 12.5 mm, the depth of the PCM plates is 110 mm, and the thickness of the air gaps is 6 mm in the experimental setup.

4. Numerical methods

This chapter describes the numerical methods for the heat transfer in the PCM solar air heat exchanger. Chapter 4.1 introduces the numerical model. Chapter 4.2 is the validation of the model with experimental data.

Fig. 6. Measurement of air temperature in the cold box.

4.1. Model description

A 3D model is built in COMSOL Multiphysics. Symmetry boundary conditions are used to save computational time, with half of the PCM plate and half of the air cavity. The PCM plate is modeled with a heat transfer module. The fluid in the air cavity inside the heat exchanger is modeled by heat transfer conjunct laminar flow module.

Heat transfer in the PCM is considered as conduction heat transfer. The PCM is encapsulated in the cellular structure of the fiber board. It is therefore assumed that no convection takes place within the shape steady micro-encapsulated PCM plates. The governing heat equation for the thermal energy transferred by conduction is as follows:

$$\rho Cp\frac{\partial T}{\partial t}=\nabla\cdot(k\nabla T)+Q \tag{1}$$

The heat flux between the outdoor environment and the solar air heat exchanger (q) consists of the solar radiation (q_1) and the natural convection (q_2) components.

$$q=q_1+q_2 \tag{2}$$

The solar radiation q_1 is depending on the height of the measurement points on the surface of the window. It is evaluated based on the average horizontal solar radiation measured along the width of the glass surface. The solar radiation transmittance rate of the glass is 90%. The reflection and absorption of the glass are not simulated.

The convection heat flux q_2 is calculated based on Equations (3)–(7) [38].

$$q_2=\overline{h}(T_{ext}-T) \tag{3}$$

The average heat transfer coefficient $\overline{h}$ is solved base on Equation (4).

$$\overline{Nu}_L=\frac{\overline{h}L}{k}=\begin{cases}0.68+\dfrac{0.67Ra_L^{1/4}}{\left(1+(0.492/Pr)^{9/16}\right)^{4/9}} & Ra_L\le 10^9\\ \left(0.825+\dfrac{0.387Ra_L^{1/6}}{\left(1+(0.492/Pr)^{9/16}\right)^{8/27}}\right)^2 & Ra_L\ge 10^9\end{cases} \tag{4}$$

Where the local Rayleigh number Ra_L is defined by Equation (5).

$$Ra_L=Gr_LPr \tag{5}$$

Where

$$Gr_L=\frac{\rho^2 g\alpha Cp}{\mu k}\Delta TL^3 \tag{6}$$

$$Pr=\frac{Cp\mu}{k} \tag{7}$$

For the fluid flow, the Navier-Stokes equations govern the motion of the fluid in the air cavities between the PCM plates [39]. For weakly compressible Newtonian fluids such as air, the momentum equation is as follows:

$$\rho\left(\frac{\partial u}{\partial t}+u\cdot\nabla u\right)=-\nabla p+\nabla\cdot\left(\mu\left(\nabla u+(\nabla u)^T\right)-\frac{2}{3}\mu(\nabla\cdot u)\right)+F \tag{8}$$

F is the buoyancy force, which is defined as:

$$F=-g\rho(T) \tag{9}$$

The continuity equation is written as:

$$\frac{\partial\rho}{\partial t}+\nabla\cdot(\rho u)=0 \tag{10}$$

$$\frac{\partial\rho}{\partial t}=\frac{\partial p}{\partial t}\frac{M}{RT}-\frac{\partial T}{\partial t}\frac{pM}{RT^2} \tag{11}$$

For the weakly compressible flow, the pressure change is neglected. The continuity equation can be written as:

$$\frac{\partial T}{\partial t}\frac{pM}{RT^2}+\nabla\cdot(\rho u)=0 \tag{12}$$

The numerical model used for the ventilation pre-heating mode is a 2D heat transfer conjunct laminar flow model which was proposed and verified in previous work [36]. The simple 2D model has a good agreement with the heat transfer process in the heat exchanger with fewer meshes and smaller computational time but a higher mesh density than a 3D model.

4.2. Model validation

Fig. 7 shows the temperature curves of PCM at different positions on the PCM plates. Each curve is an average of the measured temperatures in the same position on different PCM plates. The simulation results show good agreement with the experimental data. The average error for the PCM temperature at the outer part, middle part, and inner part of the plates is 5.95%, 1.82%, and 4.28% respectively. The error is defined in Eq. (13).

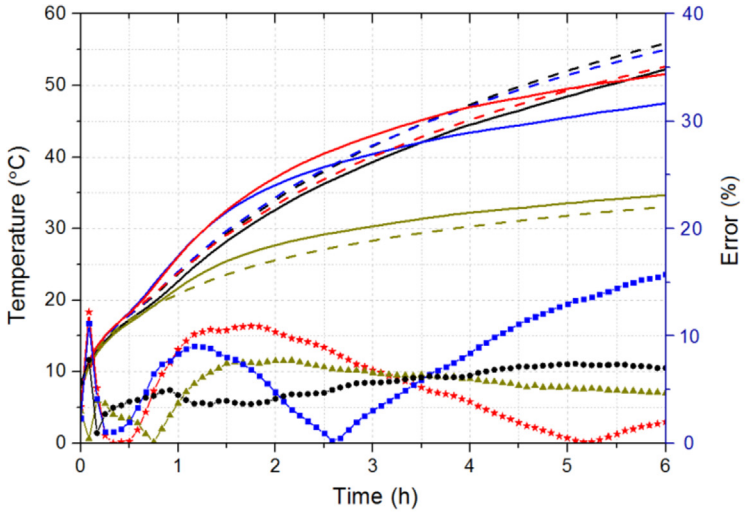

(a) PCM temperature in the outer part of the plates.

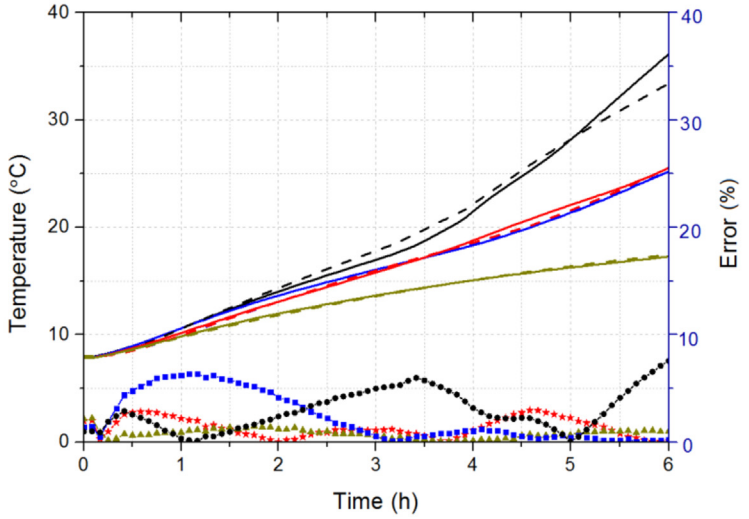

(b) PCM temperature in the middle part of the plates.

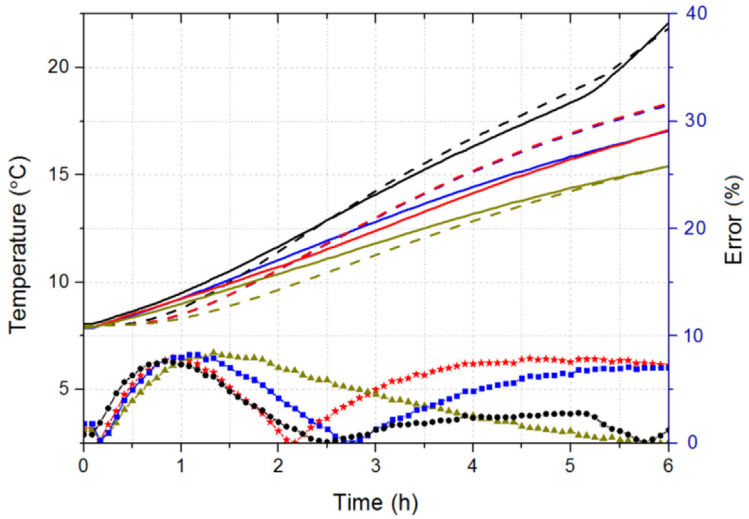

(c) PCM temperature in the inner part of the plates.

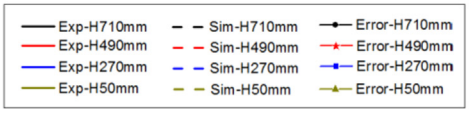

Fig. 7. Model validation with experimental data.

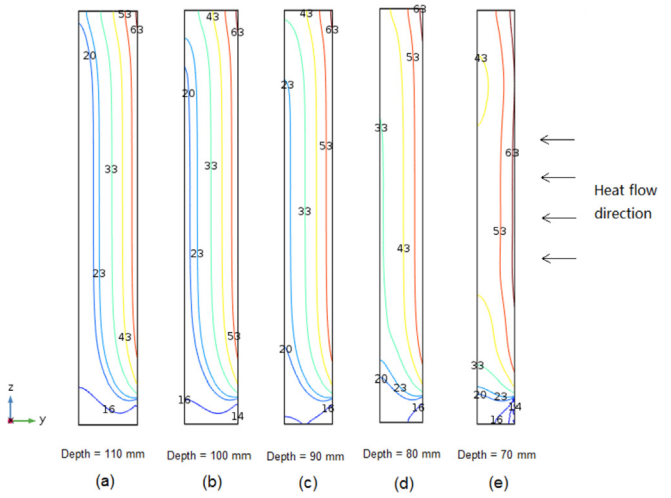

Fig. 8. Vertical PCM temperature profile in the middle of the plates after 6 h charging for different plate depths.

$$error = \left| \frac{\text{Experiment value} - \text{Simulation value}}{\text{Experiment value}} \right| \times 100\% \qquad (13)$$

5. Results and discussion

In this section, the optimized results of the depth of the PCM plates and the thickness of the air gap are presented. All the cases have an air flow rate set at 106 m^3/h. 5 cases with different plate depths are studied first. The air gap thickness is kept at 6 mm, the same as in the experimental setup. The aim of using the PCM solar air heat exchanger for ventilation preheating is to save heating energy use mainly in winter and transition seasons. The optimization is based on the energy saving potential of the PCM heat exchanger exposed to 550 W solar charging for 6 h, which is equal to the average daily radiation received in April in Denmark.

Fig. 8 shows the temperature at the vertical section in the middle of the PCM plates at time 6 h. A 550 W evenly distributed heat flow is applied to each of the PCM plates from the right side. From the temperature contours shown in Fig. 8, it can be observed that the PCM melt in the top right side of the PCM plate. The right side of the PCM starts melting first. The heat is transferred into the left side of the plate by the conduction in the PCM plates and the convection in the air gaps between the PCM plates. The area of the PCM plate with a temperature lower than 23 °C decreases with the decrease of plate depth, which indicates a higher melting fraction for a smaller PCM plate depth. However, the total volume of the PCM is decreasing with the decreasing of the PCM plate depth. Therefore, there exits an optimum PCM plate depth to maximum both the PCM melt fraction and the PCM volume in the system. The PCM at the bottom of the plate has a lower temperature because of the shelter of the inlet of the PCM heat exchanger, which prevented sunlight to reach this part. The PCM temperature is highest in the upper right corner, because of the heat flow direction and convection in the air gap between the PCM plates.

The PCM is considered fully melted (maximum latent heat storage) when its temperature rises above 23 °C base on the feature of the PCM heat capacity curve. Figs. 9 and 10 show the fraction of melted PCM and the stored latent heat for the cases with different PCM plate depths.

The PCM melt fraction is nearly maximized when the plate depth is 90 mm, and the stored latent heat is the highest for 6 h charging with 90 mm plate depth, as shown in Figs. 9 and 10. For the time period 0.5 h–5.7 h, the slopes of the curves for both melt fraction and stored latent heat are lower than for the periods 0 h–0.5 h and 5.7 h–6 h, due to the occurrence of the phase transition. The same phenomenon is observed for all the other cases. For the 70 mm and 80 mm plate depths, the PCM melt fraction reaches a constant value, meaning that the PCM in the plates is melted completely. The maximum melt fraction cannot reach 1, because the opaque insulation in the inlet of the heat exchanger in the solar energy storage mode shades the PCM plates from solar radiation at the bottom. The total PCM volume in the heat exchanger is growing with the increase of the plate depth, which increases the total thermal storage capacity. However, the charging time of the PCM increases, and the plates may not be fully melted at the end of the charging period due to the relatively low thermal conductivity of the PCM. Therefore, the melted fraction at 6 h for 100 mm and 110 mm plate depths is only 59.5% and 69.8% respectively. As a result, the stored latent heat for both depths are not the highest among all the five cases. The optimized plate depth is 90 mm with a 90.2% melt fraction for 6 h heat charging period. However, the optimized result may be different with a different heat radiation rate or charging time, which is not studied in this work.

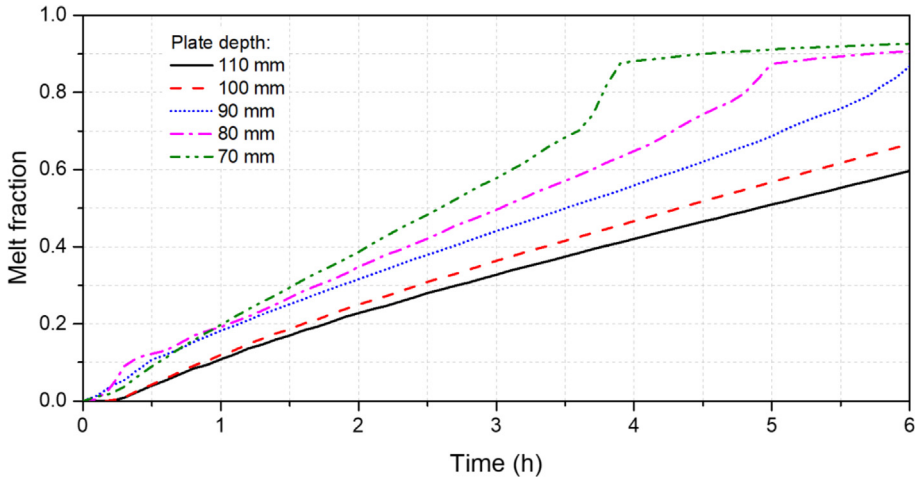

Fig. 9. The PCM melt fraction as function of time for cases with different PCM plate depths.

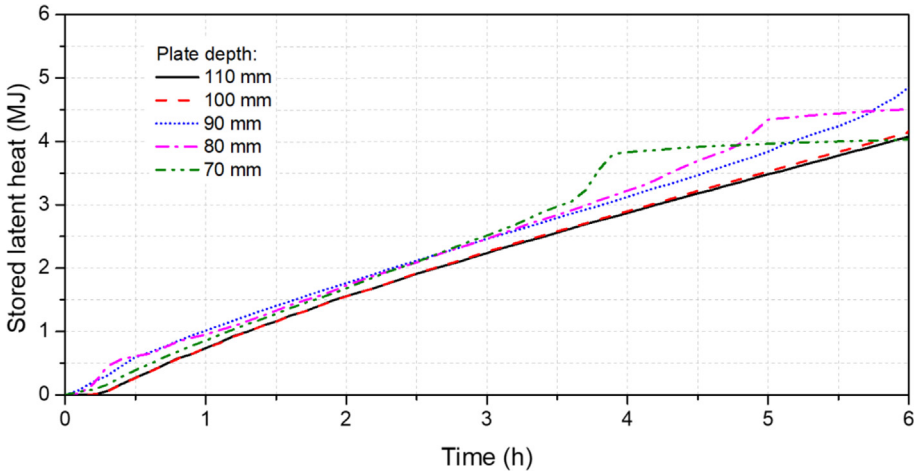

Fig. 10. The stored latent heat as function of time for cases with different PCM plate depths.

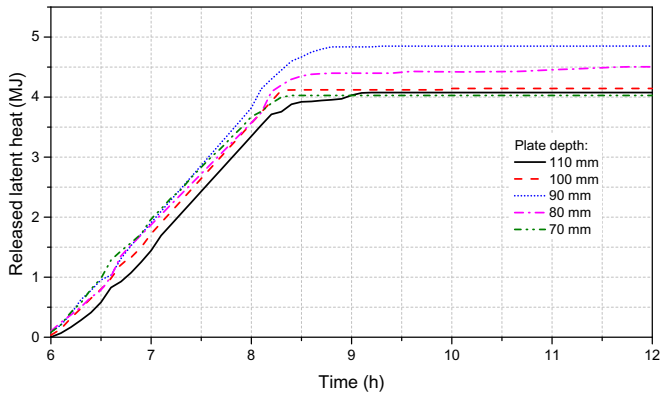

Fig. 11. The released latent heat from the PCM heat exchanger in ventilation pre-heating mode.

Fig. 11 shows the released latent heat from the PCM heat exchanger to the ventilated air when the system is in ventilation pre-heating mode. The discharge time for the energy stored are similar for all the studied cases, in the range of 2 h–3 h. It indicates that the depth of PCM plates has less influence on the discharge time. For 90 mm plate thickness, the released latent heat from the PCM to the ventilation is the highest, which is 4.85 MJ, equaling to 93.31 MJ per cube meter PCM.

The optimization of the air gap thickness in the PCM solar air heat exchanger is then investigated. 6 cases with different air gap thicknesses are compared. Fig. 12 and Fig. 13 show the results about the melt fraction and the stored latent heat of the PCM heat exchanger respectively. The total PCM volume in the solar air heat exchanger decreases with the increase of the air gap thickness, because of the fixed configuration of the PCM solar air heat exchanger available, but the PCM melting speed and charging time are improved with the increase of the air gap thickness.

As shown in Fig. 13, the stored latent heat after 6 h charging for models with 3, 4, 5, and 6 mm air gap thicknesses are similar. However, the PCM melt fraction is lower for 3, 4, and 5 mm air gap thicknesses. The optimized air gap thickness is 6 mm, which is similar to the optimum configuration for summer night ventilation (5 mm air gap thickness) with similar stored and released latent heat [36]. It indicates that the same configuration can be used for both summer night cooling and winter solar energy storage applications.

Fig. 14 shows the released latent heat from the PCM heat exchanger in ventilation pre-heating mode. The discharge rate decreases with the increase of the air gap thickness. However, the discharged time for all the cases are all in the level of 3.5 h–4 h and

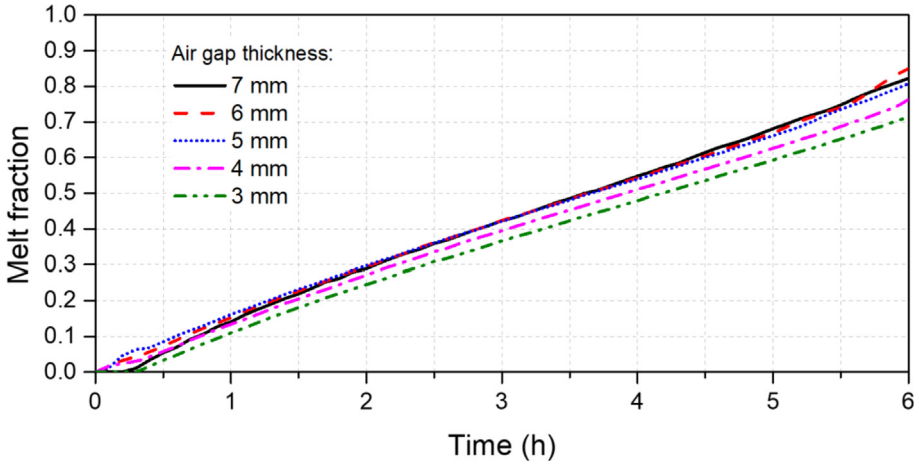

Fig. 12. The PCM melt fraction as function of time for models with different air gap thicknesses.

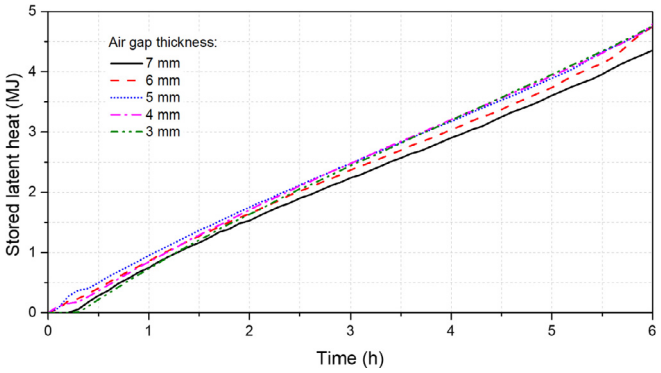

Fig. 13. The stored latent heat along with time for models with different air gap thicknesses.

numerical model with conjunct heat transfer and buoyancy driven laminar flow is built. The simulation results are in good agreement with the experimental data. Configuration optimization is conducted with different plate depths and different air gap thicknesses for a PCM heat exchanger in both the solar energy storage and the ventilation pre-heating modes. For a 6-h solar charging period, the optimum PCM plate depth is 90 mm and the optimum air gap thickness is 6 mm. The same configuration can be used for both summer night cooling and winter solar energy storage applications. The total stored and released latent heat during one charge is 93.31 MJ/m^3.

The airflow rate in the experiment and the model is higher than the required fresh air for a typical residential room. Further research should include the analysis of the air flow rate effect on the PCM discharge time. It should also include analysis in different

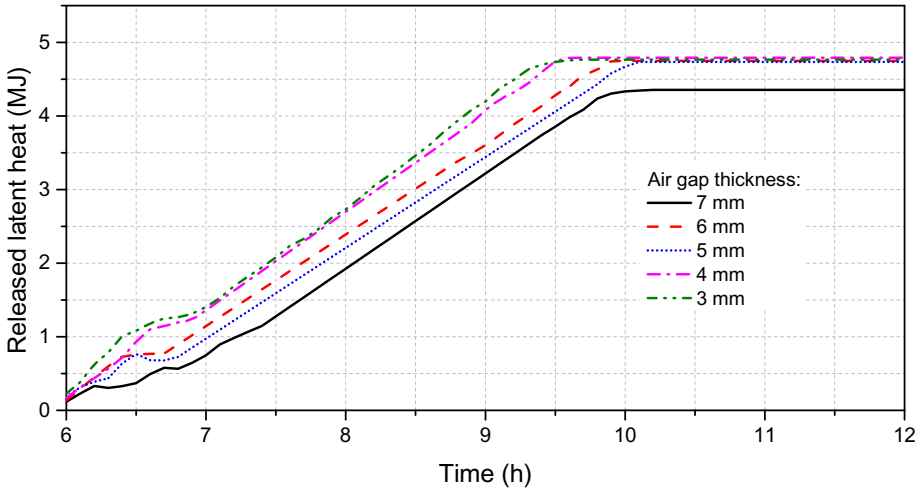

Fig. 14. The released latent heat from the PCM heat exchanger in ventilation pre-heating mode.

have no big differentials. The released energy is more related to the latent heat storage in the solar energy storage mode than to the air gap thickness.

6. Conclusions

This article presents the application of PCM into a solar air heat exchanger in a ventilated window system. Firstly, the paper introduced the configuration and working principle of the system. When solar energy is available, solar radiation charges the PCM solar air collector. The ventilation air only passes through the ventilated window to be pre-heated by solar radiation. When the solar radiation is lower than 200 W/m^2, the ventilation air passes through the PCM solar collector, where the PCM heat storage preheats it, and then the air is supplied to the room to make the most use of the captured solar energy to increase the air inlet temperature and thermal comfort in winter. In building renovation, it can be challenging to install an efficient ventilation system with heat recovery and the application of the presented system can be an alternative method to ensure an energy efficient ventilation solution in these buildings. Also, for new buildings with decentralized ventilation solutions, the system can contribute to improve the energy efficiency of the buildings by better capture and utilization of the solar energy.

This study presents a full-scale experimental test to evaluate the thermal behavior of the solar air heat exchanger. Accordingly, a climate zones to verify the optimization, and estimate the annually building energy saving potential of the system.

Acknowledgment

The EU Horizon 2020 research and innovation program under grant agreement NO. 768576(ReCO2ST) and the Chinese Scholarship Council (CSC No. 201606050118) supported this work.

References

[1] P. Heiselberg, H. Brohus, A. Hesselholt, H. Rasmussen, E. Seinre, S. Thomas, Application of sensitivity analysis in design of sustainable buildings, Renew. Energy 34 (2009) 2030–2036, https://doi.org/10.1016/J.RENENE.2009.02.016.
[2] H. Johra, P. Heiselberg, Influence of internal thermal mass on the indoor thermal dynamics and integration of phase change materials in furniture for building energy storage: a review, Renew. Sustain. Energy Rev. 69 (2017) 19–32, https://doi.org/10.1016/J.RSER.2016.11.145.
[3] M. Pomianowski, P. Heiselberg, Y. Zhang, Review of thermal energy storage technologies based on PCM application in buildings, Energy Build. 67 (2013) 56–69, https://doi.org/10.1016/j.enbuild.2013.08.006.
[4] M. Pomianowski, P. Heiselberg, R.L. Jensen, Full-scale investigation of the dynamic heat storage of concrete decks with PCM and enhanced heat transfer surface area, Energy Build. 59 (2013) 287–300, https://doi.org/10.1016/j.enbuild.2012.12.013.
[5] F. Kuznik, J. Virgone, Experimental investigation of wallboard containing phase change material: data for validation of numerical modeling, Energy Build. 41 (2009) 561–570, https://doi.org/10.1016/J.ENBUILD.2008.11.022.
[6] M. Pomianowski, P. Heiselberg, R.L. Jensen, R. Cheng, Y. Zhang, A new experimental method to determine specific heat capacity of inhomogeneous concrete material with incorporated microencapsulated-PCM, Cement Concr.

Res. 55 (2014) 22–34, https://doi.org/10.1016/J.CEMCONRES.2013.09.012.
[7] H. Johra, P. Heiselberg, Influence of internal thermal mass on the indoor thermal dynamics and integration of phase change materials in furniture for building energy storage: a review, Renew. Sustain. Energy Rev. 69 (2017) 19–32, https://doi.org/10.1016/J.RSER.2016.11.145.
[8] J. Borderon, J. Virgone, R. Cantin, Modeling and simulation of a phase change material system for improving summer comfort in domestic residence, Appl. Energy 140 (2015) 288–296. https://doi.org/10.1016/j.apenergy.2014.11.062.
[9] G. Hed, R. Bellander, Mathematical modelling of PCM air heat exchanger, Energy Build. 38 (2006) 82–89, https://doi.org/10.1016/J.ENBUILD.2005.04.002.
[10] G. Diarce, Á. Campos-Celador, K. Martin, A. Urresti, A. García-Romero, J.M. Sala, A comparative study of the CFD modeling of a ventilated active faÃ§ade including phase change materials, Appl. Energy 126 (2014) 307–317, https://doi.org/10.1016/j.apenergy.2014.03.080.
[11] M. Pomianowski, P. Heiselberg, R. Lund Jensen, Dynamic heat storage and cooling capacity of a concrete deck with PCM and thermally activated building system, Energy Build. 53 (2012) 96–107, https://doi.org/10.1016/j.enbuild.2012.07.007.
[12] M. Labat, J. Virgone, D. David, F. Kuznik, Experimental assessment of a PCM to air heat exchanger storage system for building ventilation application, Appl. Therm. Eng. 66 (2014) 375–382, https://doi.org/10.1016/j.applthermaleng.2014.02.025.
[13] S. Liu, Y. Li, Heating performance of a solar chimney combined PCM: a numerical case study, Energy Build. 99 (2015) 117–130, https://doi.org/10.1016/J.ENBUILD.2015.04.020.
[14] G. Fraisse, K. Johannes, V. Trillat-Berdal, G. Achard, The Use of a Heavy Internal Wall with a Ventilated Air Gap to Store Solar Energy and Improve Summer Comfort in Timber Frame Houses, Energy Build. 38 (2006) 293–302.
[15] F. Goia, M. Perino, V. Serra, Experimental analysis of the energy performance of a full-scale PCM glazing prototype, Sol. Energy 100 (2014) 217–233, https://doi.org/10.1016/j.solener.2013.12.002.
[16] J.F. Belmonte, M.A. Izquierdo-Barrientos, A.E. Molina, J.A. Almendros-Ibáñez, Air-based solar systems for building heating with PCM fluidized bed energy storage, Energy Build. 130 (2016) 150–165, https://doi.org/10.1016/J.ENBUILD.2016.08.041.
[17] U. Stritih, P. Charvat, R. Koželj, L. Klimes, E. Osterman, M. Ostry, V. Butala, PCM thermal energy storage in solar heating of ventilation air—experimental and numerical investigations, Sustain. Cities Soc. 37 (2018) 104–115, https://doi.org/10.1016/j.scs.2017.10.018.
[18] G. Serale, E. Fabrizio, M. Perino, Design of a low-temperature solar heating system based on a slurry Phase Change Material (PCS), Energy Build. 106 (2015) 44–58, https://doi.org/10.1016/j.enbuild.2015.06.063.
[19] J. Mazo, M. Delgado, J.M. Marin, B. Zalba, Modeling a radiant floor system with Phase Change Material (PCM) integrated into a building simulation tool: analysis of a case study of a floor heating system coupled to a heat pump, Energy Build. 47 (2011) 458–466, https://doi.org/10.1016/j.enbuild.2011.12.022.
[20] P. Devaux, M.M. Farid, Benefits of PCM underfloor heating with PCM wallboards for space heating in winter, Appl. Energy 191 (2017) 593–602, https://doi.org/10.1016/j.apenergy.2017.01.060.
[21] M. Koschenz, B. Lehmann, Development of a thermally activated ceiling panel with PCM for application in lightweight and retrofitted buildings, Energy Build. 36 (2004) 567–578, https://doi.org/10.1016/j.enbuild.2004.01.029.
[22] J.L.D. H. Johra, P. Heiselberg, Numerical analysis of the impact of thermal inertia from the furniture/indoor content and phase change materials on the building energy flexibility, in: Proc. 15th IBPSA Conf. Int. Build. Perform. Simul. Assoc. San Fr. CA, USA., n.d.
[23] H. Johra, Integration of a Magnetocaloric Heat Pump in Energy Flexible Buildings, Aalborg University, 2018. http://vbn.aau.dk/files/281673345/PHD_Hicham_Johra_E_pdf.pdf. (Accessed 4 July 2018).
[24] A. De Gracia, L. Navarro, A. Castell, Á. Ruiz-Pardo, S. Álvarez, L.F. Cabeza, Thermal analysis of a ventilated facade with PCM for cooling applications, Energy Build. 65 (2013) 508–515, https://doi.org/10.1016/j.enbuild.2013.06.032.
[25] A. De Gracia, L. Navarro, A. Castell, Á. Ruiz-Pardo, S. Alvárez, L.F. Cabeza, Experimental study of a ventilated facade with PCM during winter period, Energy Build. 58 (2013) 324–332, https://doi.org/10.1016/j.enbuild.2012.10.026.
[26] T. Koyuncu, Performance of various design of solar air heaters for crop drying applications, Renew. Energy 31 (2006) 1073–1088, https://doi.org/10.1016/J.RENENE.2005.05.017.
[27] A. Fudholi, K. Sopian, M.H. Ruslan, M.A. Alghoul, M.Y. Sulaiman, Review of solar dryers for agricultural and marine products, Renew. Sustain. Energy Rev. 14 (2010) 1–30, https://doi.org/10.1016/j.rser.2009.07.032.
[28] S. Bouadila, M. Lazaar, S. Skouri, S. Kooli, A. Farhat, Energy and exergy analysis of a new solar air heater with latent storage energy, Int. J. Hydrogen Energy 39 (2014) 15266–15274, https://doi.org/10.1016/J.IJHYDENE.2014.04.074.
[29] M.J. Huang, P.C. Eames, S. Mccormack, P. Griffiths, N.J. Hewitt, Micro-encapsulated phase change slurries for thermal energy storage in a residential solar energy system, Renew. Energy 36 (2011) 2932–2939, https://doi.org/10.1016/j.renene.2011.04.004.
[30] E. Bilgen, B.J.D. Bakeka, Solar collector systems to provide hot air in rural applications, Renew. Energy 33 (2008) 1461–1468, https://doi.org/10.1016/J.RENENE.2007.09.018.
[31] B.L. Evans, S.A. Klein, J.A. Duffie, A design method for active-passive hybrid space heating systems, Sol. Energy 35 (1985) 189–197, https://doi.org/10.1016/0038-092X(85)90010-6.
[32] A. Saxena, Varun, A.A. El-Sebaii, A thermodynamic review of solar air heaters, Renew. Sustain. Energy Rev. 43 (2015) 863–890, https://doi.org/10.1016/J.RSER.2014.11.059.
[33] A. El Khadraoui, S. Bouadila, S. Kooli, A. Farhat, A. Guizani, Thermal behavior of indirect solar dryer: nocturnal usage of solar air collector with PCM, J. Clean. Prod. 148 (2017) 37–48, https://doi.org/10.1016/J.JCLEPRO.2017.01.149.
[34] A. Reyes, L. Henríquez-Vargas, R. Aravena, F. Sepúlveda, Experimental analysis, modeling and simulation of a solar energy accumulator with paraffin wax as PCM, Energy Convers. Manag. 105 (2015) 189–196, https://doi.org/10.1016/J.ENCONMAN.2015.07.068.
[35] Heat and Cold Storage with PCM, Springer Berlin Heidelberg, Berlin, Heidelberg, 2008, https://doi.org/10.1007/978-3-540-68557-9.
[36] Y. Hu, P.K. Heiselberg, A new ventilated window with PCM heat exchanger—performance analysis and design optimization, Energy Build. 169 (2018) 185–194, https://doi.org/10.1016/j.enbuild.2018.03.060.
[37] C. Heiselberg, P. Kvols, O. Kalyanova, CLIMAWIN: Technical Summary Report, 2013. http://vbn.aau.dk/files/203815355/CLIMAWIN_Technical_Summary_Report.pdf. (Accessed 30 March 2018).
[38] F.P. Incropera, D.P. DeWitt, Fundamentals of Heat and Mass Transfer, J. Wiley, 2002.
[39] User's guide comsol multiphysics ®. www.comsol.com/support/knowledgebase. (Accessed 6 May 2019).

Appendix C. Paper 3

Y. Hu, P. Heiselberg, R. Guo, Ventilation cooling/heating performance of a PCM enhanced ventilated window - an experimental study, Energy and Buildings 2020. Accepted. Reprinted by the permission of the Editor of the Journal.

Energy & Buildings 214 (2020) 109903

Contents lists available at ScienceDirect

Energy & Buildings

journal homepage: www.elsevier.com/locate/enbuild

Ventilation cooling/heating performance of a PCM enhanced ventilated window - an experimental study

Yue Hu*, Per Kvols Heiselberg, Rui Guo

Aalborg University, Division of Architectural Engineering, Department of Civil Engineering, Thomas Manns Vej 23, DK-9220 Aalborg Øst, Denmark

ARTICLE INFO

Article history:
Received 25 September 2019
Revised 12 February 2020
Accepted 24 February 2020
Available online 25 February 2020

Keywords:
Phase change material
Ventilated window
Night cooling application
Solar energy storage
Ventilation pre-cooling
Ventilation pre-heating

ABSTRACT

This paper presents a phase change material enhanced ventilated window (PCMVW) for both ventilation pre-cooling and pre-heating purposes. The PCM heat exchanger is used as a heat sink in the ventilation pre-cooling application and thermal energy storage in the ventilation pre-heating application. The paper presents a night cooling experiment and a solar energy storage experiment in order to investigate the thermal and energy performance of the PCMVW, and a ventilated window (VW) self-cooling experiment for overheating protection. Two VWs were tested in the façade lab in Aalborg (Denmark), and one of them is with PCM heat exchanger. The two windows were equipped with the same outdoor conditions and ventilation airflow. The experimental results show that for ventilation pre-cooling application with the PCM heat exchanger, the room inlet air temperature is by average 1.4 °C lower for 7 h during the daytime compared to the normal VW. The average energy saving is 0.7 MJ/day compared to a normal VW. The PCMVW cooling capacity is limited without advanced blinds control and system operation control. In ventilation pre-heating application, the PCM increases the inlet air temperature of the VW by 2.0 °C for 12 h. The average energy saving is 1.6 MJ/day compared to a normal VW. Buildings in a climate with high outdoor air temperature differences can benefit more from the PCMVW in ventilation pre-cooling application, but the pre-cooling ability is limited. While in ventilation pre-heating application the buildings in the climate with higher solar radiation levels has a higher energy performance. Moreover, the VW self-cooling application is more effective to decrease the overheating of the room than VW without self-cooling.

1. Introduction

Building energy for heating, cooling, and ventilation accounts for one-third of the total primary energy consumption in industrial countries and is becoming a major pollutant to the environment [1]. To sufficiently reduce the CO_2 emission, it is necessary to apply some innovative technologies and solutions, such as renewable energy applications. Among them, thermal energy storage (TES) is a promising way to store intermittent renewable energy for building energy supply. The TES can be sorted by sensible heat storage and latent heat storage. Phase change material (PCM) as TES has the advantage of high latent heat capacity and high energy storage density, due to a large amount of heat released/absorbed during the phase transition period. Some of the PCMs have the melting/freezing temperature near the thermal comfort temperature, which is good for building applications.

Researchers and engineers have done a lot of work for applying PCM in building systems, including passive applications and active applications. In passive applications, the PCM increases the thermal mass level and thermal inertia of the building or the building components. It is heated up or cooled down without any mechanical heating or cooling additions [2].

Passive applications include mixing PCM in constructions such as concrete [3,4], wall board [5], roof [6], floor [7], and so on. It has been proved to be effective with regards to achieving a better indoor climate and saving building energy. However, the PCM facilities for building applications are mostly limited to volume due to its low thermal conductivity. Caixia et al. [8] experimentally studied the application of moveable PCM thermal energy storage to disaster-relief prefabricated temporary houses during summer time. The results show that mobile PCM storage can decrease indoor air temperature by 3.2–3.6 °C. Later on, they built a

* Corresponding author.
E-mail address: hy@civil.aau.dk (Y. Hu).

https://doi.org/10.1016/j.enbuild.2020.109903

Nomenclature

Symbols

Cp_{air}	Specific heat capacity of the air [J/(kg•K)]
T	Temperature [°C]
t	Ventilation time [s]
q	Flowrate[m^3/h]
ρ_{air}	Air density [kg/m^3]
T_{inlet}	Inlet air temperature of the PCM heat exchanger [°C]
T_{outlet}	Outlet air temperature of the PCM heat exchanger [°C]
Q_1	Ventilation energy saving in night cooling application [MJ]
Q_2	Ventilation energy saving in solar energy storage application [MJ]
$T_{ref\ inlet}$	Inlet air temperature to the room from the reference window [°C]
$T_{PCMVW\ inlet}$	Inlet air temperature to the room from the PCMVW [°C]
r	Correlation coefficient
$\overline{T}_{night}$	Night time average outdoor air temperature [°C]
$\overline{T}_{day}$	Day time average outdoor air temperature [°C]
DT	Daytime and nighttime outdoor air temperature difference [°C]
U	Thermal transmittance
g	Total solar energy transmittance

HVAC	Heating, ventilation and air condition system
PCM	Phase change material
TES	Thermal energy storage
VW	Ventilated window
PCMVW	PCM enhanced ventilated window
Ref	Reference window(ventilated window)

numerical model to optimize the position and thickness of the PCM [9]. They discovered that the best design is to move the PCM to the outdoor during the night time for night cooling and bring it to the indoor room during the daytime, in order to decrease the indoor air temperature. The optimized PCM thickness of the PCM thermal storage is 20 mm. Memon et al. [10] tested a small-scaled concrete wall container with macro encapsulated PCM. The tests show that the PCM can reduce the indoor air temperature by 2.9 °C. Amir et al. [11] examined the performance of PCM in a residential building to improve its resiliency to extreme outdoor conditions in case of power outages. They determined that, for some climates, PCM can be beneficial for both energy saving and resiliency (24 h maximum temperature drop with respect to baseline building). The thickness of the PCM for the wall envelope in this application is 10 mm.

In active applications, the PCM is usually totally or partly heated up or cooled down by mechanically forced fluids such as air and water. An active application could be PCM in HVAC system [12], ventilated ceiling [13,14,15], double-skin façade [16], and other ventilation systems. The performance of active PCM applications is mostly higher than that of passive PCM applications. Mossafa et al. [17] studied a PCM-TES free cooling system for the ventilation pre-cooling purpose in summer. They conclude that the coefficient of performance (COP) of this facility can be as high as 7.63. Gonzalo et al. [18] evaluated a ventilation façade with PCM in the outer layer experimentally and numerically. The comparisons to the other conventional envelope show that the PCM increases the thermal inertia of the envelope and provides better thermal response. The authors suggested the necessity of optimization of the airflow rate design. Furthermore, they studied the thermal performance of the ventilated façade during severe winter conditions [19] and found that it increased the indoor temperature from 9 °C to 18 °C.

The ventilated window (VW) is originally designed for better thermal and energy performances of the ventilation system. The VW utilizes the hot air accumulated in the window cavity from transmission heat loss and solar radiation for heating purpose, and self-cooling by outdoor air for cooling purpose [20]. Several studies have investigated this matter numerically and experimentally. Jorge et al. [21] experimentally studied the pre-heating performance of the VW and found that it can increase the inlet air temperature by 6–12 °C. David et al. [22] studied the energy performance of the VW in a controlled climate and found the VW can decrease 10% of the heating demand. Tin-tai et al. [23] numerically studied the cooling and heating abilities of the VW in summer and winter respectively. They found that it is quite effective for both decreasing the cooling load and increasing the space heat gain in Hong Kong and Beijing.

In this study, the PCM adds additional thermal storage to the VW for cooling/heating purposes respectively. In ventilation pre-heating application, the PCM is cooled down from the ambient air by nighttime ventilation, and the cold PCM pre-cools the ventilated air during the daytime. In ventilation pre-heating application, the PCM stores solar energy during the daytime. It supplies pre-heated air to the VW when heating is demanded.

The PCM has the disadvantage of low thermal conductivity. In this study, the PCM heat exchanger is made by thin PCM plates (thickness = 0.0125 m), to compensate for this disadvantage. The distance between two PCM plates is set as 0.006 m; it is an optimized value for both the heat discharge/charge rate and the total thermal storage capacity of the PCM heat exchanger in both ventilation pre-cooling [24] and ventilation pre-heating [25] cases.

This paper experimentally studied the thermal and energy performances of the PCMVW for ventilation pre-heating and pre-cooling respectively. The study chose some main parameters that influence the thermal and energy performances of the PCMVW. Moreover, the annual energy-saving potential of this system with different control strategies in a building in different climate zones should be examined in modeling simulations, and this paper provided useful experimental data for model validation.

2. Experimental setup

Two windows are set up in the south wall of the façade lab. The lab is located on the top floor of the building and is in an open area with no obstructions from the surroundings. The PCM enhanced ventilated window (PCMVW) system is made by two parts: the PCM heat exchanger part and the VW part, see Fig. 1. The PCM heat exchanger is made by 62 parallel PCM plates (12.5 mm × 110 mm × 670 mm) in a wooden frame. The distance between the two plates is 6 mm. The PCM used in this experiment is paraffin wax (50%) absorbed in fiberboards. The total heat capacity of the PCM is 117 kJ/kg (10 °C - 30 °C), including the latent heat and sensible heat. The melting and freezing peaks are 21.5 °C and 20.7 °C respectively, as shown in Fig. 2. The specific heat of the PCM is 2.3 KJ/kg/ °C, the density of the PCM is 820 kg/m^3, and the thermal conductivity of the material is 0.18 W/m/ °C.

The outside of the heat exchanger is covered by a glass surface facing outdoor. The inner side of the heat exchanger is insulated by 30 mm wood fiber from the indoor room. The VW is made by a double panel glass (U = 1.1 W/m^2, g = 0.63) in the exterior and a single panel glass (U = 5.7 W/m^2, g = 0.79) in the interior. A 120 mm air cavity between the two glass panels is the path for the ventilated air. The reference window (Ref window) is with the same configuration as the VW in PCMVW system. The

Fig. 1. Experimental setup. The PCMVW in the left and the Reference window in the right.

PCM cooling performance is measured by comparing the temperature difference between the PCMVW system and the conventional VW (Ref window). In ventilation pre-cooling application, the PCM works as a heat sink during the night time. The relatively hot PCM is cooled down by the low-temperature outdoor air in the heat removal mode, as shown in Fig. 3(a). In the ventilation pre-cooling mode, which is mostly during the daytime, the hot outdoor air is ventilated through the cold PCM before ventilating into the room. In this way, the PCM provides pre-cooled air to the indoor HVAC systems, as shown in Fig. 3(b). During the test, the glass surface of the PCM heat exchanger is shaded by a 5 mm wooden board. For the PCMVW system, the ventilated air goes through both the PCM heat exchanger and the VW for the whole day and night, with 50 m^3/h ventilation flow rate. For the Ref window, the VW is ventilated for the whole day and night with the same airflow rate. The ventilation goes from the bottom of the VW, through the ventilated cavity to the indoor room. The flow rate chosen here is based on the ventilation rates for the residences category I recommended by EN 15251 [26] for a 1–2 persons' room.

In ventilation pre-heating application, the PCM works as thermal energy storage. In heat storage mode (Fig. 4(a)), the PCM stores solar energy during the daytime when solar radiation is available. The ventilation only goes through the VW. The air in the VW is heated up mainly by solar radiation. The ventilation of the window brings the hot air to the room so as to decrease the heat supply from the HVAC system and to decrease the heat loss from the window as well. In the ventilation pre-heating mode (Fig. 4(b)), the ventilation goes through both the PCM heat exchanger and the VW. The cold ambient air is heated up by the relatively hot PCM before supply to the indoor room. In this way, the PCM is providing pre-heated air to the indoor HVAC system. In this experiment, the PCM starts to provide heat to the ventilation at 18:30. Before 18:30, only the VW part of PCMVW system is used. The Ref window is ventilated through the VW part the whole day and night.

The VW self-cooling mode is operated when the indoor air temperature is too high for both ventilation pre-cooling and pre-heating cases. In this mode, the vents at the top and bottom of the VW are opened towards the outdoor in order to let the air

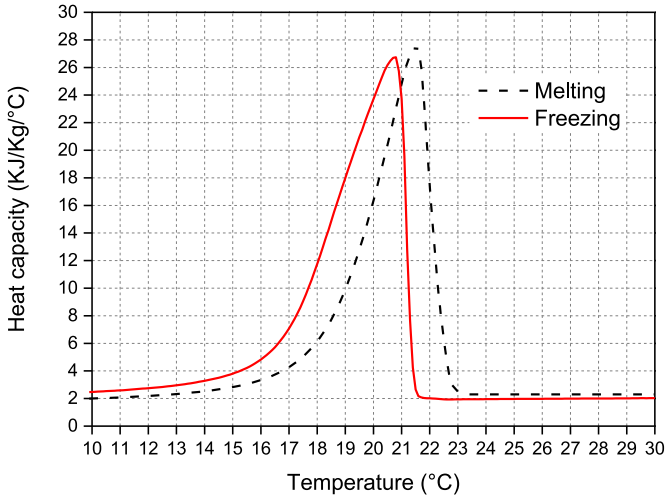

Fig. 2. Heat capacity of the PCM by DSC measurement under heating/cooling rate: 0.5 °C/min [24].

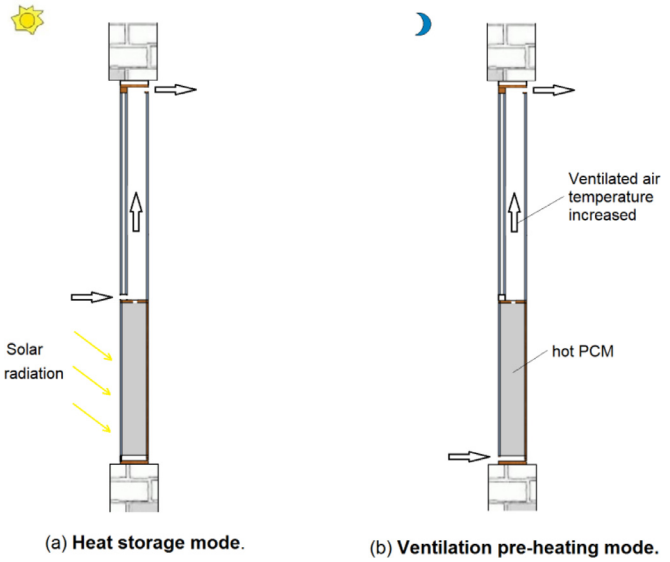

Fig. 4. Working principle of the PCMVW system in ventilation pre-heating application.

driven by natural ventilation and convection pass through the double window, see Fig. 5. It prevents overheating of the window by decreasing the temperature in the VW; thus it decreases the heat gain of the indoor environment from the window.

The ventilation of the two windows is provided by two fans for separate flow rate control, see Fig. 6. The total power of the fans is 93 W. The flow rate of the fans is measured and controlled by Lindab UltraLink FTCU.

The PCMVW system has three sets of valves in three different positions: at the bottom and the top of the PCM heat exchanger, and at the top of the VW, see Fig. 7. Each valve is controlled by a small motor with a specific ID that can be controlled by a computer, see Fig. 8. The power of each motor is 1.2 W. The valves control where the source air comes from. The Ref window has two sets of valves at the bottom and the top of the VW. The valves and motors are the same as in the PCMVW system.

180 type K thermocouples are used for temperature measurement. Fig. 7 shows a part of them. The measured temperature uncertainty is ± 0.15 °C. Three PCM plates and three air cavities between PCM plates are chosen for the temperature measurement in the PCM heat exchanger. A Kipp & Zonen CMP 22 pyranometer with ± 2% measurement uncertainty is used for outdoor solar radiation measurement. The temperature and radiation measurement data are collected by two Fluke Helios Plus 2287A data loggers. The log frequency is 10 s.

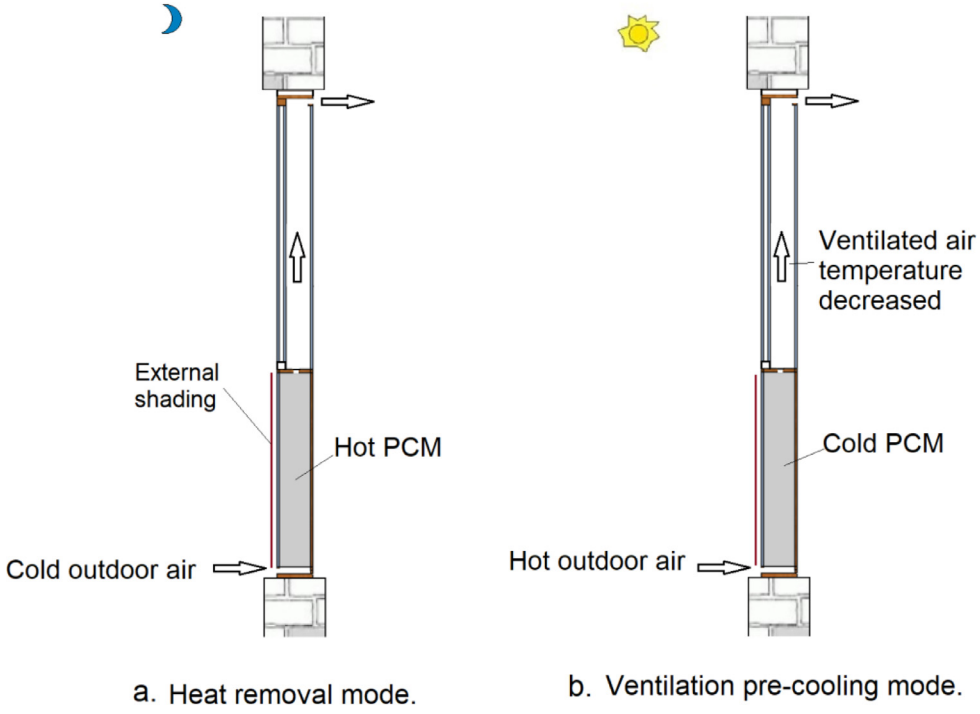

Fig. 3. Working principle of the PCMVW system in ventilation pre-cooling application.

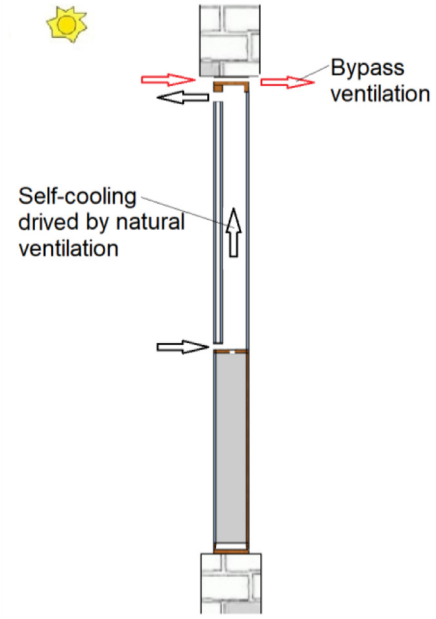

Fig. 5. Working principle of the VW self-cooling.

3. Results

3.1. Ventilation pre-cooling application

The experiment for ventilation pre-cooling application was operated from June 26–30 and July 12– 22, 2019, with 50 m^3/h airflow rate for both windows. The PCMVW system is ventilated through both the PCM heat exchanger and VW, while the Ref window is ventilated only through the VW. The purpose of this test is to determine the main parameters that influence the PCM thermal and energy performance, by analyzing the system as well as comparing it with the results from the Ref window. Figs. 9–11 show some of the measured results.

The PCM temperature has a periodic variation along with the fluctuation of the outdoor air temperature, as seen in Fig. 9. The PCM has a temperature drop during the night period and a temperature rise during the daytime. The $\overline{T}_{night}$ is defined as the average outdoor air temperature during the PCM heat removal mode. The$\overline{T}_{day}$ is defined as the average outdoor air temperature during the PCM ventilation pre-cooling mode. The DT is defined as $\overline{T}_{day}$ - $\overline{T}_{night}$. The outdoor air temperature difference varies from [1–12 °C].

Four indexes are defined to represent the PCM thermal and energy performances in ventilation pre-cooling application. These indexes are Heat removal amount, Ventilation energy saving amount, Inlet temperate decrease, and Cooling effect hours. The four indexes are chosen to compare the performance of the PCMVW to the reference VW in 3 aspects: the PCM thermal behavior, thermal and energy effect of the air system, and the system effective time. There are more indexes in literature, but they are all in the category of the aforementioned 3 aspects.

In the ventilation pre-cooling mode of the PCMVW system, the PCM cools down the ventilated air in the PCM unit. The air in the PCM unit has a temperature stratification, see Fig. 10. In this period, the inlet air temperature is the highest, and is close to the outdoor air temperature. The heat removal amount is calculated by the amount of heat removed from the ventilated air by the PCM, which can be calculated by the temperature drop of the ventilated air.

$$\text{Heat removal amount} = \int_{t} q\rho_{air} Cp_{air}(T_{inlet} - T_{outlet})dt \quad (1)$$

Where t is the time period when PCM cools down the ventilated air in Fig. 10.

The ventilation inlet air temperature to the room is illustrated in Fig. 11. During the PCM ventilation pre-cooling mode, the inlet of the PCMVW system is lower than the Ref window. The PCM effective time is defined as the hours when the inlet air temperature of the PCMVW window is 0.5 °C lower than the Ref window, namely $T_{\text{ref inlet}}$- $T_{\text{PCMVW inlet}}$ > 0.5 °C. The inlet temperature decrease is the average value of $T_{\text{ref inlet}}$- $T_{\text{PCMVW inlet}}$ during the effective hours. The ventilation energy saving in ventilation pre-heating application is calculated by Eq. (2).

$$Q_1 = \int_{t'} q\rho_{air} Cp_{air}(T_{\text{refinlet}} - T_{\text{PCMVWinlet}})dt \quad (2)$$

Fig. 6. The exhaust fans for the ventilation system.

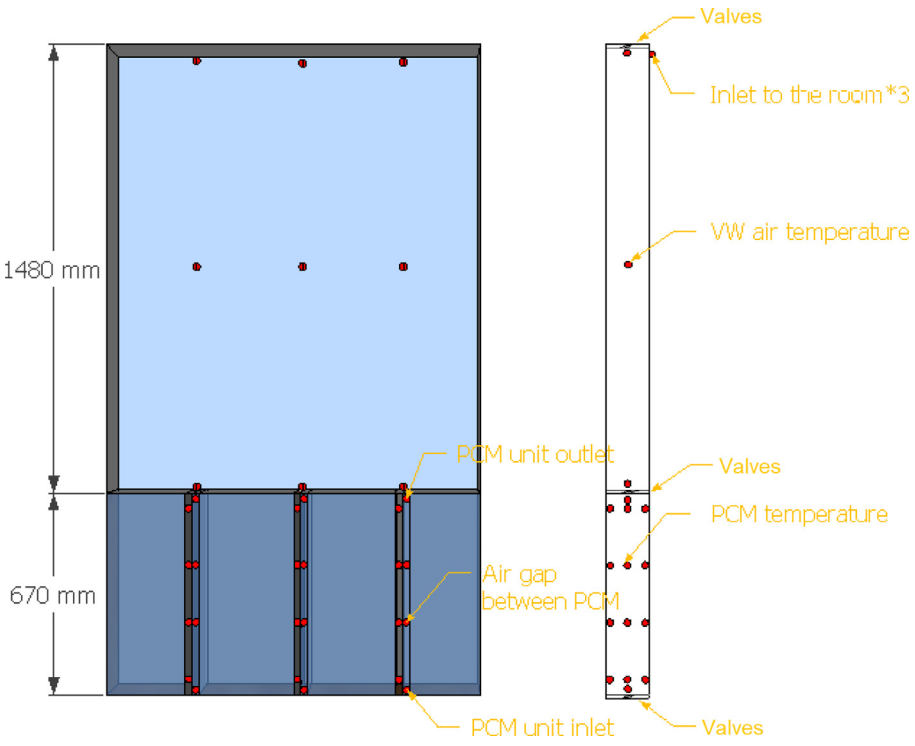

Fig. 7. Temperature measurement in the PCMVW system.

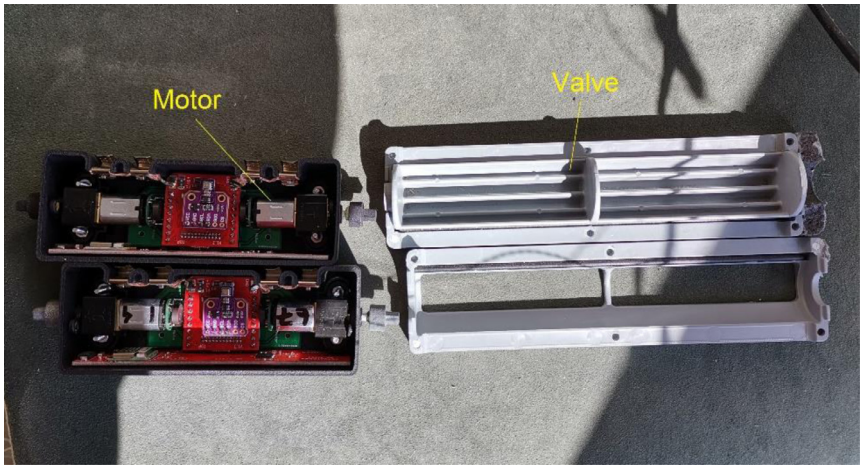

Fig. 8. Valves and motors for airflow direction control.

Where t' is the PCM effective time.

The correlation coefficient r between two variables x and y measure their linear association. Given a pair of variables $\{(x_1,y_1), \bullet\bullet\bullet(x_i,y_i), \bullet\bullet\bullet(x_n,y_n)\}$,

$$r = \frac{\sum_{i=1}^{n}(x_i-\bar{x})(y_i-\bar{y})}{\sqrt{\sum_{i=1}^{n}(x_i-\bar{x})^2}\sqrt{\sum_{i=1}^{n}(y_i-\bar{y})^2}} \tag{3}$$

Where n is the sample size, and

$$\bar{x} = \frac{1}{n}\sum_{i=1}^{n} x_i$$
$$\bar{y} = \frac{1}{n}\sum_{i=1}^{n} y_i \tag{4}$$

$-1 \le r \le 1$. $r = 0$ indicates there is no linear correlation between x and y. $r = 1$ is total positive linear correlation and $r = -1$ is total negative correlation.

Table 1 shows the correlation coefficient between the outdoor environment and the PCM thermal and energy performance when $q = 50$ m^3/h. The DT has the strongest correlation with all four indexes. It indicates that the day and night temperature difference has the highest influence on PCM thermal and energy performance.$\overline{T}_{night}$ has a negative correlation with the four indexes. While$\overline{T}_{day}$ has a positive correlation with the four indexes.

The Heat removal amount, Ventilation energy saving amount, and Inlet temperate decrease are in positive linear relation with DT, see Fig. 12. Compare Fig. 12(a) and (b), the heat removal amount, and ventilation energy saving are both increasing along with the increase of the DT. The ventilation energy saving is much smaller than the PCM heat removal amount, due to the heat gain

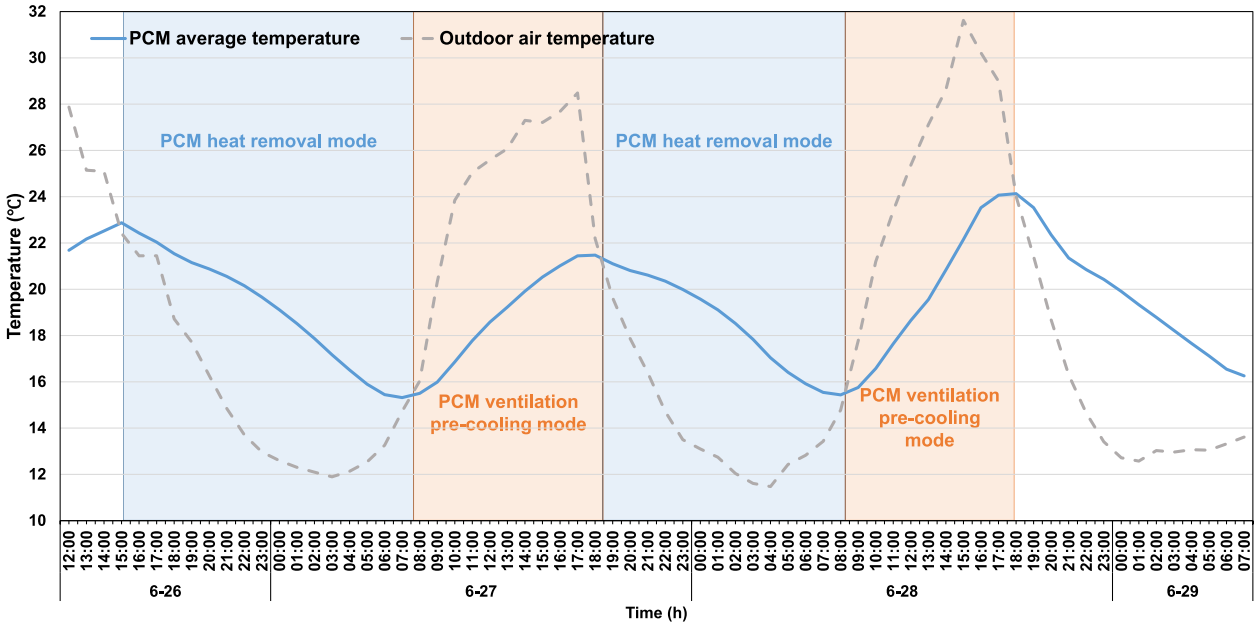

Fig. 9. The average PCM temperature in function with outdoor air temperature.

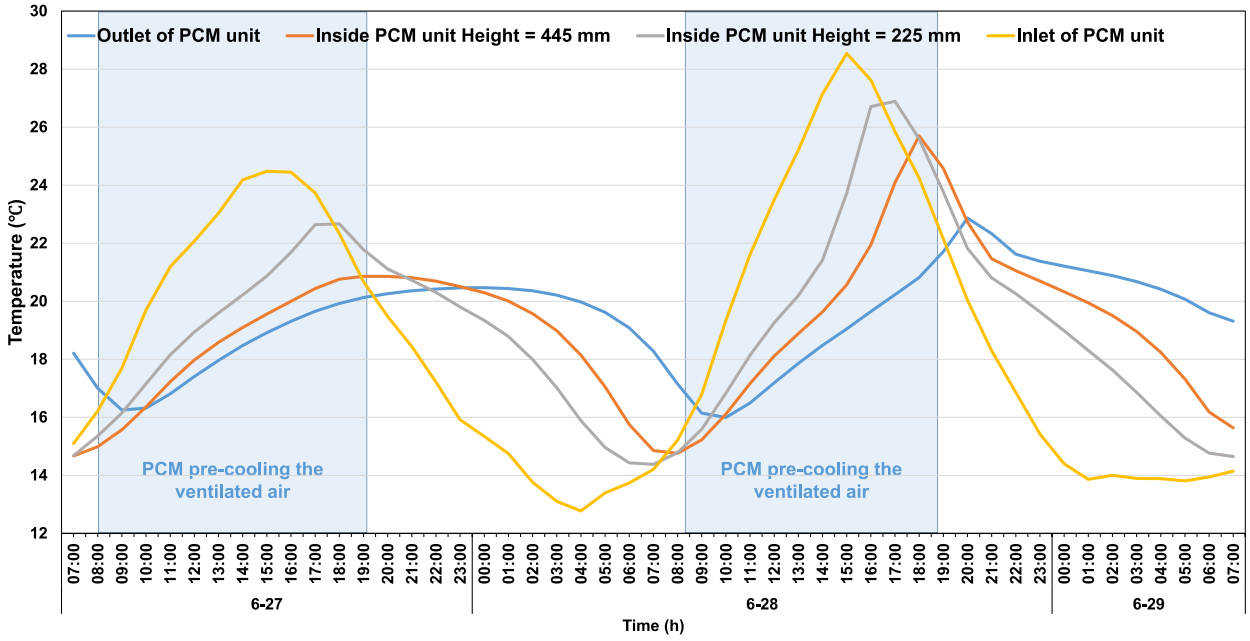

Fig. 10. Air temperature in the PCM unit.

Table 1
Correlation coefficient between the outdoor climate and the PCM thermal and energy performance in ventilation pre-cooling application.

Correlation coefficient (r)	Heat removal amount	Ventilation energy saving	Inlet temperate decrease	Cooling effect hours
$\overline{T}_{night}$ -$\overline{T}_{day}$ (DT)	0.91	0.92	0.95	0.55
$\overline{T}_{night}$	−0.58	−0.48	−0.47	−0.33
$\overline{T}_{day}$	0.51	0.61	0.65	0.32

from the VW part. The average heat removal amount is 2.0 MJ per day and the average ventilation energy saving compared to normal VW is 0.7 MJ per day. Fig. 12(c) shows the linear fit of room average inlet temperature decrease in relation to DT. It has the best linear fit. The PCM is effective to provide an inlet temperature decrease for all the tested days. The average inlet temperature decrease is 1.4 °C. Fig. 12(d) shows the correlation between the cooling effect hours and DT. The linear correlation is not strong in this case. For all the measured days, the deviation of the cooling effect hours is not big. The average cooling effect hours is 7.0 h. The PCM is effective in providing pre-cooled air for a long time during the daytime.

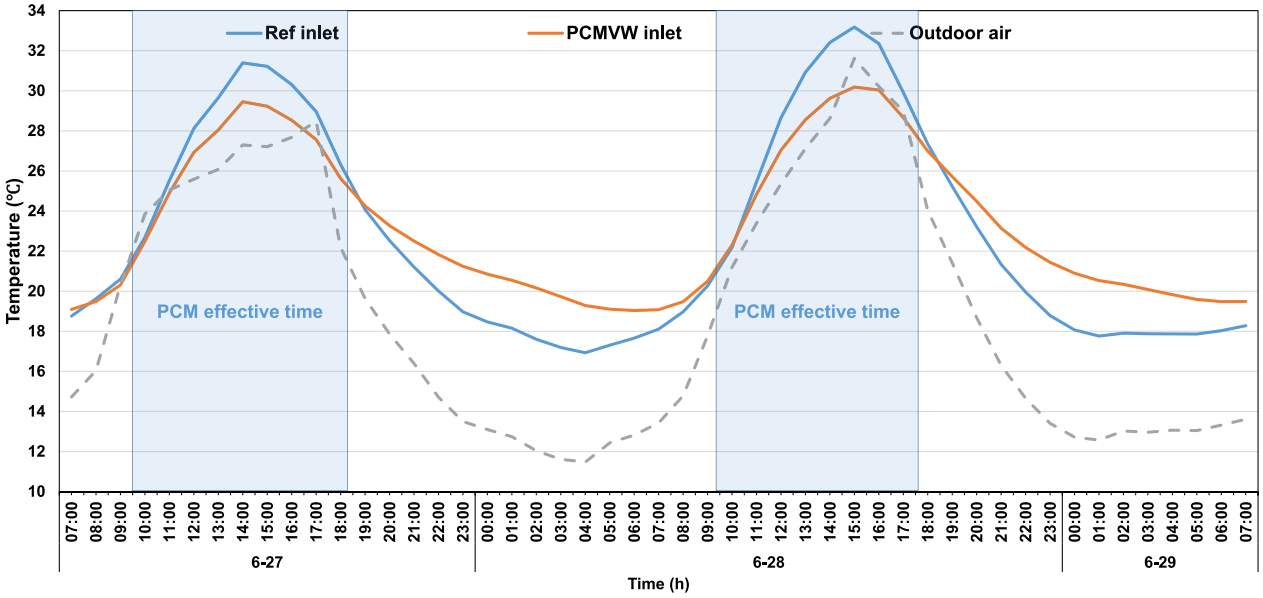

Fig. 11. The room inlet air temperature for both windows.

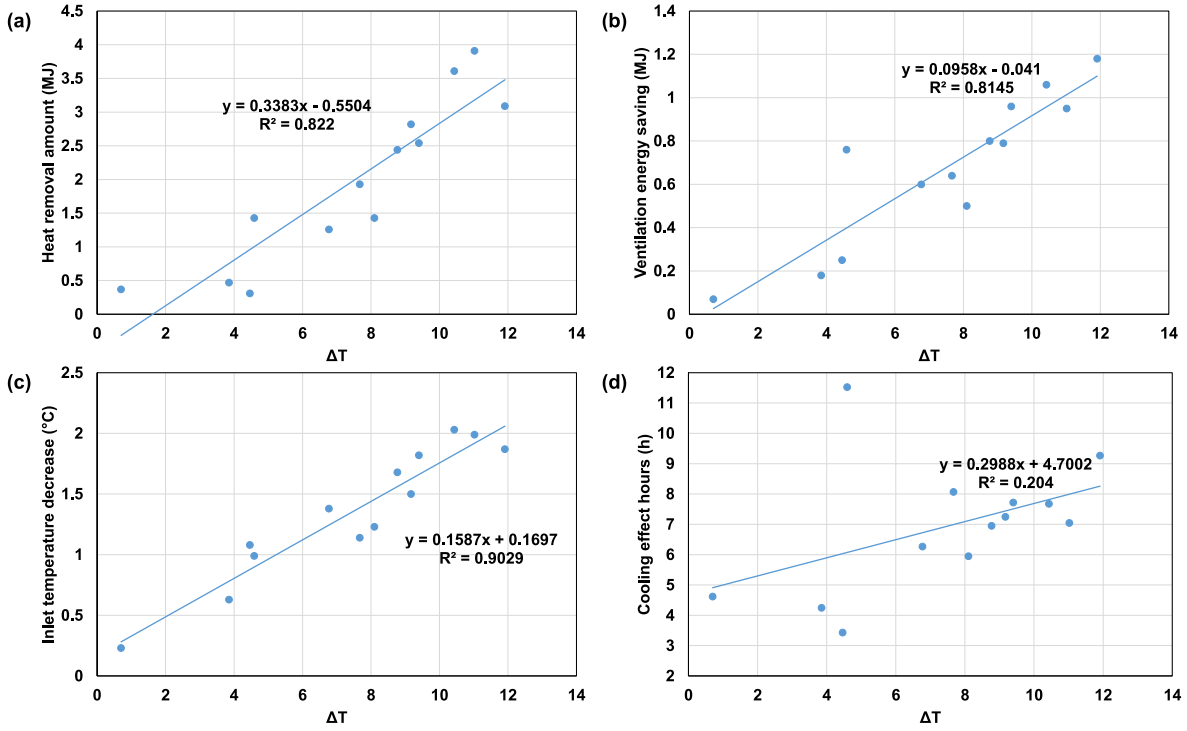

Fig. 12. The daily PCM thermal and energy performance as functions of DT: (a) heat removal amount as a function of DT, (b) ventilation energy saving as a function of DT, (c) inlet temperature decrease as a function of DT and (d) cooling effect hours as a function of DT. R^2 is the variation of the measured date from the prediction functions.

The cooling performance of the PCMVW system is based on a comparison with a normal VW. For both systems, the performance is limited by the solar heat gain in the VW. Consequently, the inlet air temperature presented in Fig. 11 is similar or even higher than the outdoor air temperature.

3.2. Solar energy storage application

The solar energy storage experiment was done on July 2–July 12, 2019. The time of the heat storage mode is set as 8:30–18:30, when both windows are ventilated only through the VW. The time of ventilation pre-heating mode is set as 18:30–8:30 the next day, when the PCMVW system ventilates through both PCM heat exchanger and VW, while the Ref window ventilates through VW. Fig. 13 shows the measured outdoor weather condition and the PCM temperature. The solar radiation level is the total solar radiation (both direct and diffuse) received by the south wall. It is calculated by the daily integration of the solar radiation per square meter surface. The solar radiation level is within the range [3–18 W/m^2] and the nighttime outdoor air temperature within the range [11–17 °C]. The daily outdoor air temperature varies from [12.5–20.5 °C].

Similar to the ventilation pre-cooling application, four indexes are defined to represent the PCM thermal and energy performance for ventilation pre-heating application. These indexes are Heat storage amount, Ventilation energy saving amount, Inlet

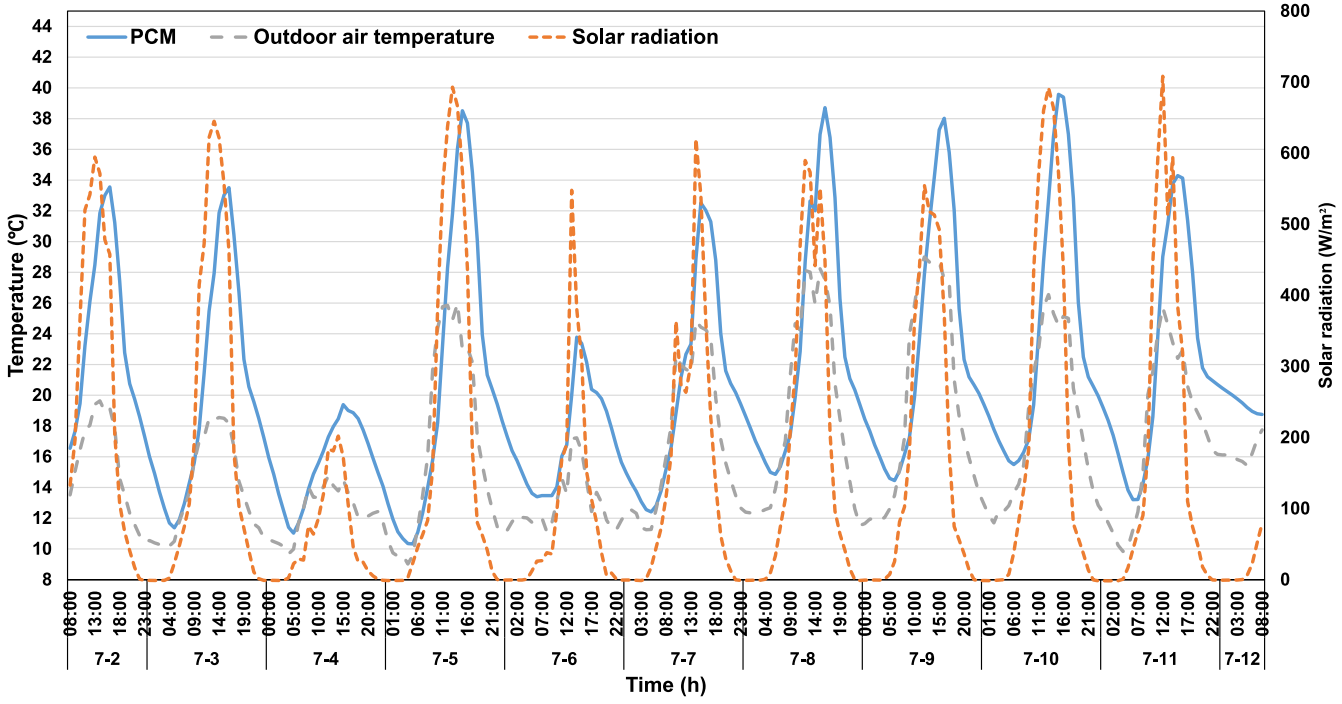

Fig. 13. The measured weather condition and PCM average temperature.

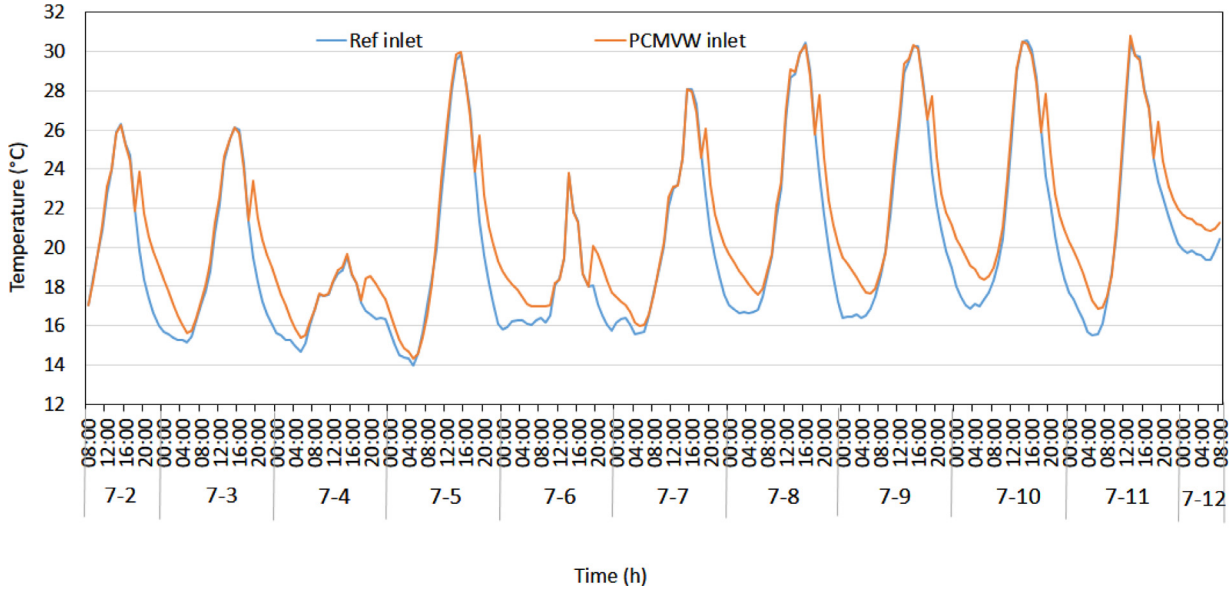

Fig. 14. Room ventilation inlet air temperature.

temperature increase, and Heating effect hours. The PCM heat storage amount is defined by the PCM temperature rise until 18:30. This section will later on investigate the correlations with the solar radiation and outdoor air temperature.

Fig. 14 shows the room ventilation inlet air temperature. The inlet air temperature of the PCMVW window is higher than the Ref window for most of the time during the ventilation pre-heating mode. The ventilation energy saving amount in ventilation pre-heating application is defined as:

$$Q_2 = \int_{t''} q\rho_{air} Cp_{air}(T_{\mathrm{PCMVWinlet}} - T_{\mathrm{refinlet}})dt \quad (5)$$

t''- Ventilation pre-heating time.

$q = 50\ \mathrm{m^3/h}$.

The inlet temperature increase is the average of$(T_{\mathrm{PCMVWinlet}} - T_{\mathrm{refinlet}})$in ventilation pre-heating mode. The heating effect hours are the hours when $T_{\mathrm{PCMVW\ inlet}}$ - $T_{\mathrm{ref\ inlet}} > 0.5\ ^{\circ}\mathrm{C}$.

Table 2 shows the correlation coefficient between the outdoor climate and the PCM thermal and energy performance in ventilation pre-heating application. Solar radiation has the strongest correlation with ventilation energy saving, PCM heat storage amount, and room inlet temperature increase, while nighttime outdoor air average temperature has the strongest correlation with Heating effect hours.

Fig. 15 shows the daily PCM thermal and energy performance as functions of solar radiation and nighttime average outdoor air temperature. Fig. 15(a) shows the linear correlation between the PCM

Table 2
Correlation coefficient between the outdoor climate and the PCM thermal and energy performance in ventilation pre-cooling application.

Correlation coefficient (r)	Ventilation energy saving	PCM heat storage amount	Inlet temperature increase	Heating effect hours
Solar radiation	0.94	0.94	0.88	0.43
$\overline{T}_{day}$	0.81	0.69	0.54	0.74
$\overline{T}_{night}$	0.25	0.35	−0.07	0.81
DT	0.88	0.68	0.70	0.54

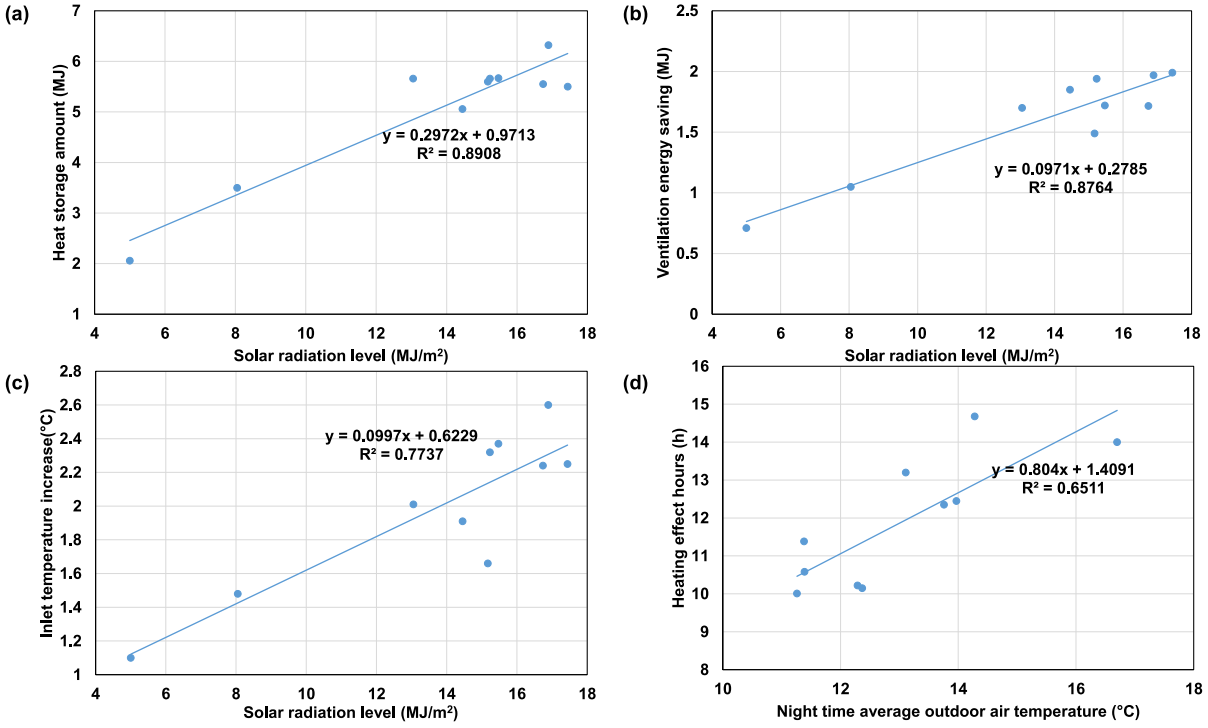

Fig. 15. The daily PCM thermal and energy performance as functions of solar radiation and nighttime average outdoor air temperature: (a) heat removal amount as function of solar radiation level, (b) ventilation energy saving as function of solar radiation level, (c) inlet temperature increase as function of solar radiation level and (d) heating effect hours as function of nighttime average outdoor air temperature.

heat storage amount and the solar radiation level. The higher the received solar radiation, the larger the heat storage amount. The average heat storage amount is 5.1 MJ per day. Fig. 15(b) shows the linear correlation between ventilation energy saving and the solar radiation level. It has a similar trend as the PCM heat storage amount, except for the fact that ventilation energy saving is much smaller than the heat storage amount. The average ventilation energy saving is 1.6 MJ per day. Fig. 15(c) indicates the daily average inlet temperature increase in relation to solar radiation level. It shows the same positive linear correlation. The PCM is effective in providing an inlet temperature increase for all the tested cases. The lowest inlet temperature increase is 1.1 °C for the worst tested scenario. The average inlet temperature increase is 2.0 °C. The best linear fit for heating effect hours is with the night time average outdoor air temperature, see Fig. 15(d). The cooling effect hours for all the tested days are high. The average cooling effect hours is 11.9 h per day. The PCM is effective in providing pre-heated air in long enough period during the night, even in the days when the solar radiation level is relatively low.

3.3. Ventilated window self-cooling application

The VW self-cooling mode and its thermal performance to reduce heat gain through the widow are tested, in conditions without shading. Two double windows, one with self-cooling, one without self-cooling are tested. For the one with self-cooling, the vents in the bottom and top of the VW are open towards the outdoor environment. All vents are turned off for the double window without self-cooling. It works as a double-skin façade. The convection air force pushes out the hot air inside the double window. Natural ventilation also occurs when there is wind pressure on the exterior surface. The self-cooling performance is evaluated by measuring the surface temperature of the double window in the period 7th August- 13th August. This section provides the main results.

Fig. 16 shows the surface temperature of the two double windows without shading. The external surface temperature in Fig. 16(a) shows a small difference for both double windows with and without self-cooling. The internal surface temperature for the two double windows are showing different levels of discrepancies, see Fig. 16(b)–(d). The bottom of the internal surface temperature of the window with self-cooling is on average 1.1 °C lower without self-cooling. The top of the internal surface has an average 0.8 °C temperature difference between the two windows. The middle of the internal surface shows the lowest discrepancy, which is 0.4 °C. It indicates that natural ventilation, which is driven by wind pressure, dominates the air ventilation in the double window. In average, the window with self-cooling control can reduce the glass surface temperature by 0.8 °C.

The effect of VW self-cooling application is very limited in the presented experiment. In fact, it is more related to outdoor weather conditions, such as wind direction and wind speed. It is not stable due to the unstable outdoor weather conditions. The VW self-cooling application has to be operated in combination with

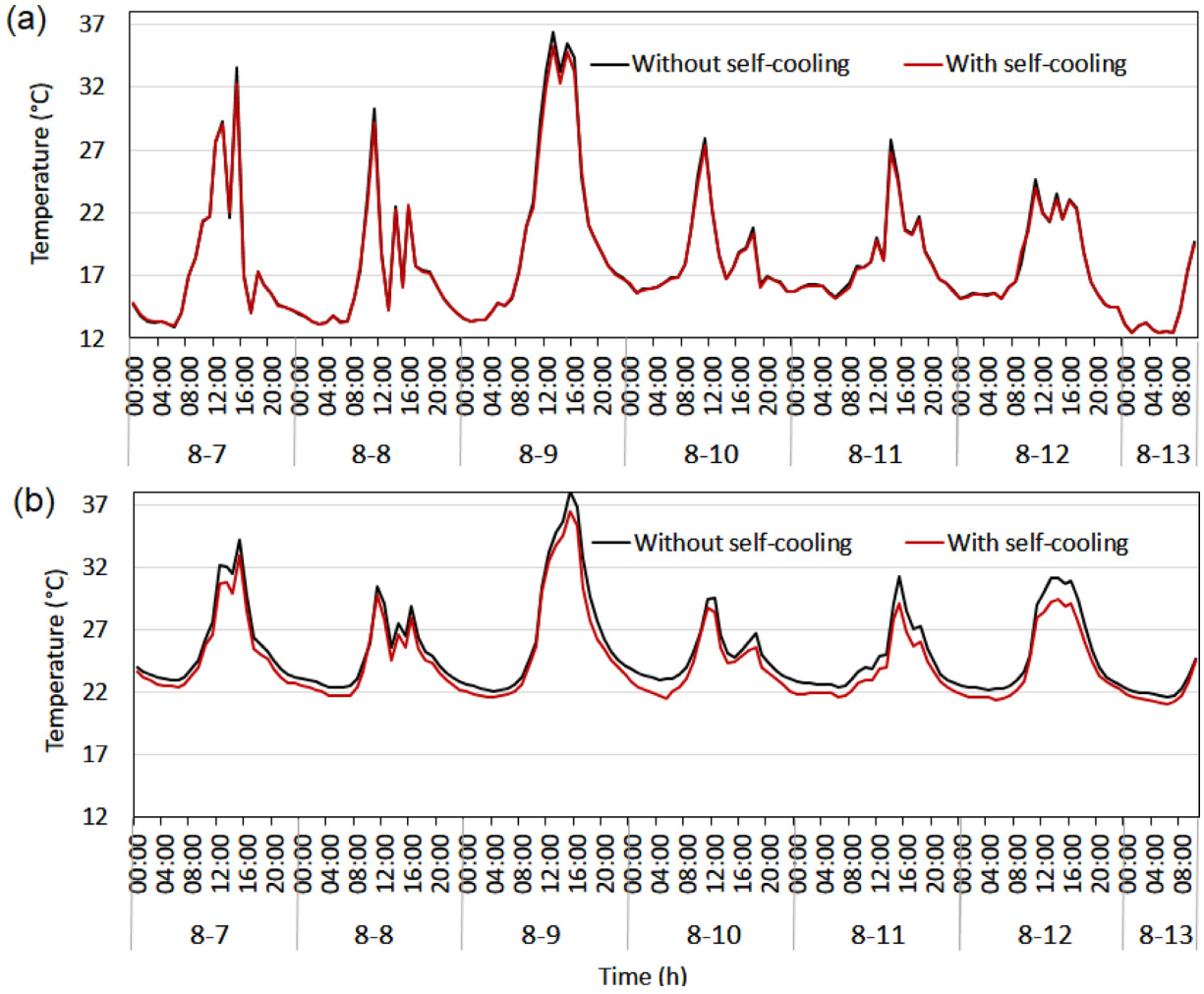

Fig. 16. (a) external surface temperature, (b) internal surface temperature of the two double windows with and without shading.

other PCMVW control strategies to potentially decrease the indoor heat load.

4. Conclusions

This paper experimentally studied a phase change material enhanced ventilated window (PCMVW) and its thermal and energy performance in both ventilation pre-cooling application and ventilation pre-heating application. In ventilation pre-cooling application, the PCM works as a heat sink. The material is cooled down by night ventilation. The cold PCM cools down the ventilation during the daytime. In ventilation pre-heating application, the PCM works as thermal energy storage for solar energy during the daytime and releases the heat for ventilation pre-heating during night time or when ventilation pre-heating is needed. The PCM adds additional thermal energy to the VW. The VW has a self-cooling mode so as to reduce the heat gain through the window when the indoor air temperature is too high. The PCM thermal and energy performance is valued by heat removal/heat storage amount, ventilation energy saving amount, inlet temperature decrease/increase and cooling/heating effect hours.

The experimental setup includes the PCMVW and a Ref window. The Ref window is a VW that has the same configuration as the PCMVW system. The PCM thermal and energy performances are calculated by analyzing the PCM condition as well as comparing the ventilated air conditions with the Ref window. This work presents three different experiments for night cooling, solar energy storage, and double window self-cooling effect.

The night cooling experiment results show that with the PCM heat exchanger, the room inlet air temperature is by average 1.4 °C lower in 7.0 h than the normal VW. The average ventilation energy saving compared to a normal VW is 0.7 MJ/day for the tested period. It is also found that the daily outdoor air temperature difference has the highest influence on the thermal and energy performance. Buildings in a climate with high daily outdoor air temperature differences can benefit more from the PCMVW system in ventilation pre-cooling application. However, the pre-cooling effect of the PCMVW is limited.

The conclusion of the solar energy storage experiment results is that the PCM heat exchanger can increase the inlet air temperature of the VW by 2.0 °C for 12.0 h. The average ventilation energy saving is 1.6 MJ/day compared with a normal VW. The solar radiation level affects the heat storage amount, ventilation energy saving amount, and the inlet air temperature the most. The heating effect hours are more influenced by nighttime outdoor air temperatures, but the overall heating effect hours are quite high even with the lowest night time average outdoor air temperature. Buildings in a climate with higher solar radiation levels can benefit more from the PCMVW system in ventilation pre-heating application. The VW self-cooling experiment demonstrated that the self-cooling mode of the VW can reduce the glass surface temperature by an average of 0.8 °C.

For both ventilation pre-cooling and ventilation pre-heating applications, the PCM heat removal/storage amounts are much higher than the ventilation energy saving. This is because the ventilation goes through the double window part before it is supplied to the indoor room, and the heat loss/gain from the double window is quite high. Even in such cases, the PCM still provides pre-cooled/pre-heated air with long effect time to the room. The thermal and energy performance of PCMVW system can be further improved by two methods: 1. Develop some new control strategies that the ventilation goes from the PCM unit directly to the indoor room. 2. Add solar reflect/absorb curtain in the VW. Those can be done by numerical modeling in future works.

Different ventilation airflow rates can affect thermal and energy performances. However, it is less applicable in experiments than in models to achieve exactly the same boundary conditions. The examination of different control strategies to combine PCM unit ventilation, double window self-cooling, and reflect/absorb curtain is more complicated to fulfill in experiments. The control strategies in building level can be more complicated by involving the indoor environment. Different control strategies should be developed considering both PCM condition and indoor air temperature setpoint.

Declaration of Competing Interest

None.

CRediT authorship contribution statement

Yue Hu: Conceptualization, Data curation, Investigation, Methodology, Writing - original draft, Writing - review & editing. **Per Kvols Heiselberg:** Conceptualization, Funding acquisition, Supervision, Writing - review & editing. **Rui Guo:** Visualization, Writing - review & editing.

Acknowledgements

The authors gratefully acknowledge the EU Horizon 2020 research and innovation program under grant agreement NO. 768576 (ReCO2ST) and the Chinese Scholarship Council(CSC No. 201606050118).

Reference

[1] P. Heiselberg, H. Brohus, A. Hesselholt, H. Rasmussen, E. Seinre, S Thomas, Application of sensitivity analysis in design of sustainable buildings, Renew. Energy 34 (2009) 2030–2036, doi:10.1016/J.RENENE.2009.02.016.
[2] M. Pomianowski, P. Heiselberg, Y Zhang, Review of thermal energy storage technologies based on PCM application in buildings, Energy Build. 67 (2013) 56–69, doi:10.1016/j.enbuild.2013.08.006.
[3] M. Pomianowski, P. Heiselberg, R.L. Jensen, R Lund Jensen, Dynamic heat storage and cooling capacity of a concrete deck with PCM and thermally activated building system, Energy Build. 53 (2012) 96–107, doi:10.1016/j.enbuild.2012.07.007.
[4] M. Pomianowski, P. Heiselberg, R.L Jensen, Full-scale investigation of the dynamic heat storage of concrete decks with PCM and enhanced heat transfer surface area, Energy Build. 59 (2013) 287–300, doi:10.1016/j.enbuild.2012.12.013.
[5] F. Kuznik, J. Virgone, Experimental investigation of wallboard containing phase change material: data for validation of numerical modeling, Energy Build. 41 (2009) 561–570, doi:10.1016/J.ENBUILD.2008.11.022.
[6] A. De Gracia, L. Navarro, A. Castell, L.F. Cabeza, L.F Cabeza, Numerical study on the thermal performance of a ventilated facade with PCM, Appl. Therm. Eng. 61 (2013) 372–380, doi:10.1016/j.applthermaleng.2013.07.035.
[7] X. Jin, X. Zhang, Thermal analysis of a double layer phase change material floor, Appl. Therm. Eng. 31 (2011) 1576–1581, doi:10.1016/j.applthermaleng.2011.01.023.
[8] C. Wang, X. Huang, S. Deng, E. Long, J Niu, An experimental study on applying PCMs to disaster-relief prefabricated temporary houses for improving internal thermal environment in summer, Energy Build. 179 (2018) 301–310, doi:10.1016/J.ENBUILD.2018.09.028.
[9] C. Wang, S. Deng, J. Niu, E Long, A numerical study on optimizing the designs of applying PCMs to a disaster-relief prefabricated temporary-house (PTH) to improve its summer daytime indoor thermal environment, Energy 181 (2019) 239–249, doi:10.1016/J.ENERGY.2019.05.165.
[10] S.A. Memon, H.Z. Cui, H. Zhang, F Xing, Utilization of macro encapsulated phase change materials for the development of thermal energy storage and structural lightweight aggregate concrete, Appl. Energy 139 (2015) 43–55, doi:10.1016/J.APENERGY.2014.11.022.
[11] A. Baniassadi, D.J. Sailor, H.J Bryan, Effectiveness of phase change materials for improving the resiliency of residential buildings to extreme thermal conditions, Sol. Energy 188 (2019) 190–199, doi:10.1016/J.SOLENER.2019.06.011.
[12] M. Yamaha, S. Misaki, The evaluation of peak shaving by a thermal storage system using phase-change materials in air distribution systems, HVAC&R Res. 12 (2006) 861–869, doi:10.1080/10789669.2006.10391213.
[13] K. Yanbing, J. Yi, Z Yinping, Modeling and experimental study on an innovative passive cooling system—NVP system, Energy Build. 35 (2003) 417–425, doi:10.1016/S0378-7788(02)00141-X.
[14] X. Wang, J. Niu, Performance of cooled-ceiling operating with MPCM slurry, Energy Convers. Manage. 50 (2009) 583–591, doi:10.1016/J.ENCONMAN.2008.10.021.
[15] T. Kondo, S. Iwamoto, Research on thermal storage using rock wool PCM ceiling board, ASHRAE Trans. (2006) 526–531.
[16] A. De Gracia, L. Navarro, A. Castell, L.F Cabeza, Energy performance of a ventilated double skin facade with PCM under different climates, Energy Build. 91 (2015) 37–42, doi:10.1016/j.enbuild.2015.01.011.
[17] A.H. Mosaffa, C.A. Infante Ferreira, M.A. Rosen, F Talati, Thermal performance optimization of free cooling systems using enhanced latent heat thermal storage unit, Appl. Therm. Eng. 59 (2013) 473–479, doi:10.1016/J.APPLTHERMALENG.2013.06.011.
[18] G. Diarce, A. Urresti, A. García-Romero, A. Delgado, A. Erkoreka, C. Escudero, et al., Ventilated active façades with PCM, Appl. Energy 109 (2013) 530–537, doi:10.1016/j.apenergy.2013.01.032.
[19] A. De Gracia, L. Navarro, A. Castell, Ruiz-Pardo Á, S. Alvárez, L.F Cabeza, Experimental study of a ventilated facade with PCM during winter period, Energy Build. 58 (2013) 324–332, doi:10.1016/j.enbuild.2012.10.026.
[20] M. Liu, P.K. Heiselberg, O.K. Larsen, L. Mortensen, J Rose, Investigation of different configurations of a ventilated window to optimize both energy efficiency and thermal comfort, Energy Procedia 132 (2017) 478–483, doi:10.1016/j.egypro.2017.09.660.
[21] J.S. Carlos, H. Corvacho, P.D. Silva, J.P Castro-Gomes, Real climate experimental study of two double window systems with preheating of ventilation air, Energy Build. 42 (2010) 928–934.
[22] D. Appelfeld, S. Svendsen, Experimental analysis of energy performance of a ventilated window for heat recovery under controlled conditions, Energy Build. 43 (2011) 3200–3207, doi:10.1016/J.ENBUILD.2011.08.018.
[23] T. Chow, Z. Lin, K. Fong, L. Chan, M He, Thermal performance of natural airflow window in subtropical and temperate climate zones – a comparative study, Energy Convers. Manage. 50 (2009) 1884–1890, doi:10.1016/J.ENCONMAN.2009.04.028.
[24] Y. Hu, P.K. Heiselberg, A new ventilated window with PCM heat exchanger – performance analysis and design optimization, Energy Build. (2018), doi:10.1016/J.ENBUILD.2018.03.060.
[25] Y. Hu, P.K. Heiselberg, H. Johra, R Guo, Experimental and numerical study of a PCM solar air heat exchanger and its ventilation preheating effectiveness, Renew. Energy (2019) 145 Under review, doi:10.1016/J.RENENE.2019.05.115.
[26] E.N. 15251, Indoor environmental input parameters for design and assessment of energy performance of buildings – addressing indoor air quality, thermal environment, lighting and acoustics, Eur. Comm. Stand. 3 (2007) 1–52, doi:10.1520/E2019-03R13.Copyright.

Appendix D. Paper 4

Y. Hu, R. Guo, P. Heiselberg, Performance and control strategy development of a PCM enhanced ventilated window system by a combined experimental and numerical study. Renew Energy 2020. Under review. Reprinted by the permission of the Editor of the Journal.

Renewable Energy

(Accepted 23 March 2020)

Performance and control strategy development of a PCM enhanced ventilated window system by a combined experimental and numerical study

Yue Hu*, Rui Guo, Per Kvols Heiselberg

Aalborg University, Division of Architectural Engineering, Department of Civil Engineering, Thomas Manns Vej 23, DK-9220 Aalborg Øst, Denmark

* Corresponding author. Tel.: +45 5282 7174

Abstract

This study proposes a PCM enhanced ventilated window (PCMVW) system for ventilation preheating/precooling purposes for building energy conservation. It is designed into a summer night cooling application and a winter solar energy storage application using different control strategies. An EnergyPlus model of the PCMVW is built to investigate the control strategies. Next, A full-scale experiment is conducted to study the working principle of the PCMVW and to validate the model. With the validated model, the thermal and energy performance of the PCMVW is compared to 2 other ventilation systems and shows that the PCMVW can greatly decrease the cooling/heating energy demand for both summer and winter applications. Finally, the paper proposes control strategies for residential applications under Danish climate conditions. The developed control strategy for summer night cooling application is to use between-glass reflection shading, ventilate directly from PCM heat exchanger to the room while applying VW self-cooling for ventilation pre-cooling mode, and heat the room with air from VW to prevent overcooling of the room. The developed control strategy for winter solar energy storage application is to use between-glass absorption blind, make use of the hot air in VW, and to cool the VW by self-cooling and bypass ventilation to prevent overheating of the room. With the developed control strategies, the building energy saving is up to 62.3% and 9.4% compared to the primitive summer and winter control strategies respectively.

Keywords: Phase change material, ventilated window, ventilation preheating/precooling, control strategy, building energy efficiency

1. Introduction

Many researchers and engineers have successfully applied phase change material (PCM) in building components as latent heat thermal energy storage (LHTES) systems [1]. Compared to sensible heat storage systems that change the storage material temperature, LHTES systems need a much smaller volume of material to store the same amount of energy. The latent heat storage systems, especially PCMs, have recently drawn much attention in the research area and the market, due to their high heat storage ability [2].

The application of PCM in buildings can be divided into passive and active systems. The passive systems with PCMs for building applications include PCMs in the wallboard [3–7], roof[8], concrete system [9–11], glazing [12][13], shading [14], and furniture [15][16]. Those passive systems have a slow response to the heating and cooling needs and are usually used as auxiliaries for the building environment. The active systems with PCMs involve water, air, or other media to accelerate the heat charge and discharge processes of PCMs. These systems have a shorter response time and contribute to a better heat transfer coefficient by replacing the free convection by forced convection. Active PCM systems include PCMs in the ceiling [17], floor [18][19], double-skin façade [20], ventilated window [21], domestic hot water systems[22], and HVAC system[23]. The systems are used for building heating or cooling proposes, usually operating in combination with ventilation or water system.

Building energy systems can benefit from the PCM application when adopting renewable energy as heat or cold sources. The stored energy can be used to create a good indoor environmental quality and save the building energy. One of the most common renewable energies for TES is solar energy. Solar energy has to be stored as it is highly dependent on the outdoor climate conditions during the daytime. PCM has been used as the storage medium in most of the cases, due to its high energy storage ability. The conventional PCM solar energy system includes a PCM tank, a solar collector,

and some heat transfer fluid between the solar collector and the PCM tank [24][25]. PCM can be used as the heat transfer fluid as well[26].

Windows account for a large part of the total building heating and cooling load, regardless of adopting coatings, sealed glazing, and tight gaskets [27]. The basic concept of the ventilated window (VW) is to control the outdoor airflow passing through the cavity of the double window. The aim of the VW is to decrease solar heat gain through the window in summer and minimize the room heating load and improve thermal comfort by utilizing the solar radiation to preheat the ventilation air in winter [28]. Several experimental and numerical research have investigated the VW performance [29–35]. It is found out that the VW can decrease cooling and/or heating demand and improve indoor thermal comfort. However, the pretreated supply air temperature could not reach the room air temperature [35]. Therefore, the supply air temperature needs to be further heated or cooled by additional means. PCM can be a good candidate to provide additional thermal storage in the VW to form an active system for better performance of the VW. In the summer night the PCM is cooled down by night ventilation. It cools the ventilation air in the daytime to decrease the room's cooling load. While in winter, it stores the solar energy in the daytime and heats up the air when heating demand is present.

Few studies have investigated the combination of the VW and PCM. In previous works, the authors demonstrated that a PCM heat exchanger can cool down the ventilated air 6.5 °C average and save 3.19 MJ energy per day based on a night ventilation experiment in summer. The depth of PCM plates was also optimized based on the numerical model, which can reduce the material cost by 16.9% in Copenhagen, Denmark [21]. The authors also investigated the ability of PCMVW pre-cooling in summer and pre-heating in winter through full-scale experiments in Aalborg, Denmark[36]. However, whether the ventilation control strategy of PCMVW adopted in previous work is the best remains to be answered. Moreover, the cooling potential of the PCMVW in previous works was not high enough, which may need extra elements to be added for improvement.

In this paper, the performance of the PCMVW is examined by comparing it with two other ventilation systems. In addition, the control strategies for summer and winter applications are developed respectively with the adding of blinds control to further enhance the energy-saving potential of the PCMVW.

Therefore, this paper investigates the ventilation control strategy of the PCMVW through an EnergyPlus model for a 3-rooms apartment with PCMVWs under Danish climate conditions. Later on, the paper introduces a full-scale experiment in the façade lab of Aalborg University to investigate the thermal properties of the PCMVW. The experiment is done in 3 parts: night cooling application, solar energy storage application and blinds for advanced VW control. The simulation results are compared with the experimental data. In addition, the PCMVW is compared to 2 other ventilation systems in regards to the thermal and energy performance. Lastly, the model is used for control strategy development for summer night cooling application and winter solar energy storage application respectively.

2. Model description

The apartment investigated is a part of a nearly zero-energy residential building with high air tightness and low U value for the constructions. It is a 3-rooms apartment on the second floor of a 3-floor residential building. Figure 1 shows the plan view of the Danish demonstration site and the floor plan of the apartment; rooms are simulated as separate thermal zones, including four windows in total. Only the southwest and northeast walls are set as external walls. Other walls are internal walls adjacent to internal thermal zones. Table 1 shows the properties of the external walls. The infiltration rate is set as 0.1 h^{-1}. The heating set point of the room is 22 °C, and the cooling set point is 26 °C, by the ideal load HVAC system. An exhaust fan with 300 Pa pressure rise and total efficiency of 0.7 drives and controls the outdoor air into the indoor room through the heat exchanger and double glazing window. The specific fan power of the fan fulfills the recommended “good-practice” from the technical note AIVC 65[37]. The daytime ventilation airflow rate should be

larger than the minimum requirement of the fresh air per person or per floor area but should be within the thermal comfort range so it does not cause draft to the indoor environment. The ventilation flow rate is 30 m^3/h/person for all the three models.

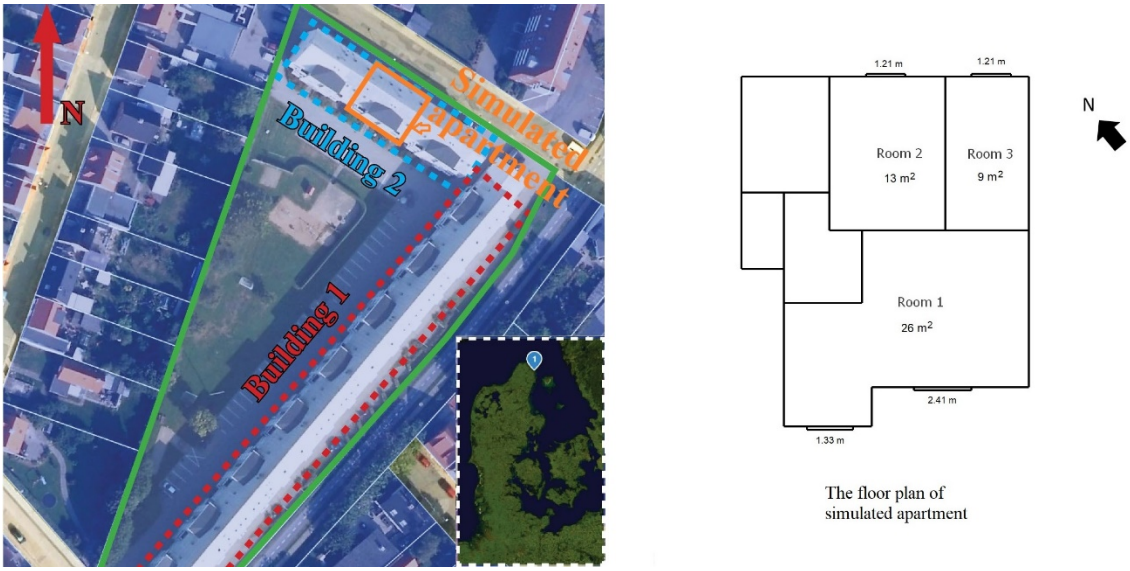

Figure 1 Plan view of the Danish demonstration site and the apartment used for the investigation.

Table 1 The properties of the external wall.

Material	Thickness [m]	Thermal Conductivity [W/m·K]	Resistance [m²·K/W]
Wood	0.02	0.12	0.13
Insulation	0.25	0.04	6.62
Brick	0.31	0.77	0.40

The PCMVW model is separated into three thermal zones: the room, the ventilated window (VW), and the PCM heat exchanger, as seen in Figure 2. The VW is made by a double-glazing panel on the outer surface, a single glazing panel on the inner side, and a ventilated cavity in between them. The glass for both the double-glazing and single glazing is 6 mm. A 13 mm air gap is in the double glazing panel. Parallel PCM plates compose the PCM heat exchanger. The thickness of the plates

is 12.5 mm and the air gap between two plates is 5 mm, which is based on the configuration optimization in[21][38]. The thin PCM plates and relatively large surface area make it faster to activate the PCM heat exchanger. The inlet of the PCM heat exchanger is at the bottom of it. The outlet of the PCM heat exchanger is connected to the ventilated window. The outlet of the ventilated window is either to the indoor room or to the outside environment. The between-glass internal shading is made by venetian blinds with absorption coating (solar reflectance coefficient= 0.15) on one surface and reflection coating (solar reflectance coefficient= 0.6) on the other side. The absorption side is turned on towards outdoor for winter solar storage application, while the reflection side is turned on towards outdoor for summer cooling application.

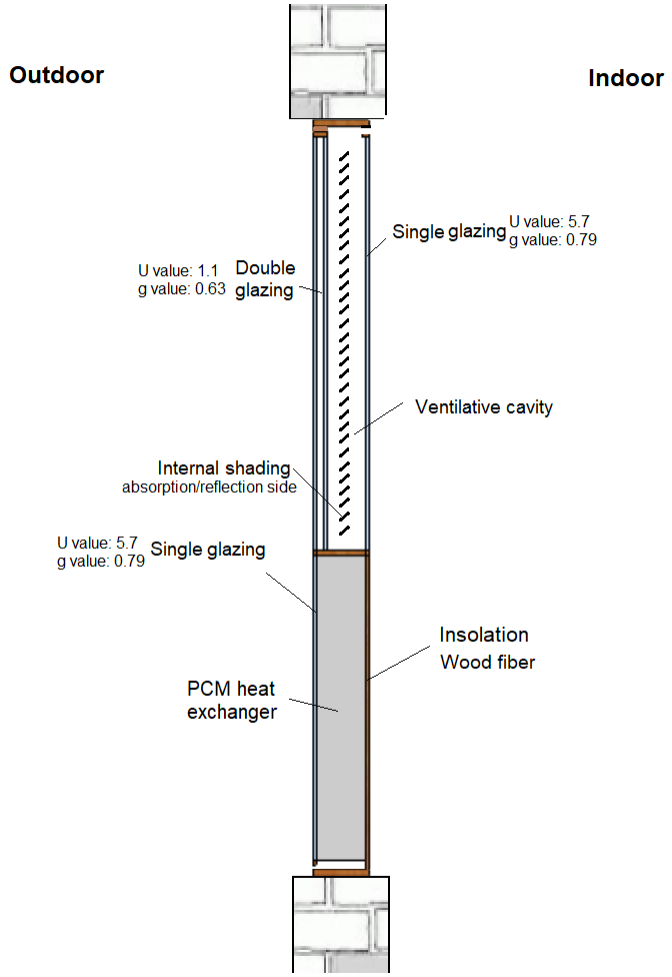

Figure 2 The overview of the VW+PCM model.

The Conduction Finite Difference (CondFD) heat balance algorithm is used in EnergyPlus. It complements the conduction transfer function (CTF) algorithm when simulating the phase change material or materials with changeable thermal conductivities. The zone time step using the CondFD algorithm can be much shorter than CTF. The algorithm uses a fully implicit scheme to solve the heat transfer equations. The enthalpy as a function of the temperature of the PCM is set as the input of the model. The heat capacity of the PCM is calculated based on Equation (1).

$$Cp(T) = \frac{H_i^j - H_i^{j-1}}{T_i^j - T_i^{j-1}} \quad (1)$$

For PCM with hysteresis, the heat capacity depends not only on the current state but also on the previous state. It presents the hysteresis effect between the freezing process and the melting process.

$$Cp(T) = f(T_i^j, T_i^{prev}, PhaseState_j, PhaseState_{prev}) \quad (2)$$

The PCM in the heat exchanger part is a mixture of fiber (50%) and paraffin wax (50%). The heat capacity of the compound was measured by differential scanning calorimetry (DSC) technology in previous work[21]. Figure 3 shows the inputs of the PCM heat capacity in EnergyPlus.

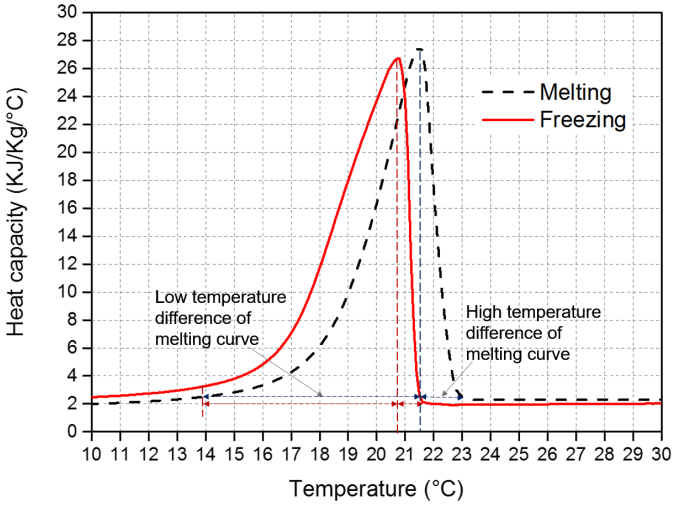

Figure 3 The heat capacity of the PCM measured by DSC[21].

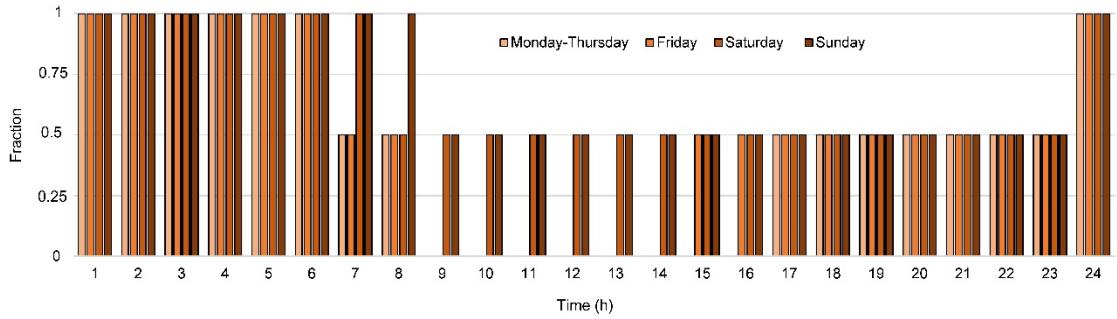

Figure 4 The occupant fraction in functions of time.

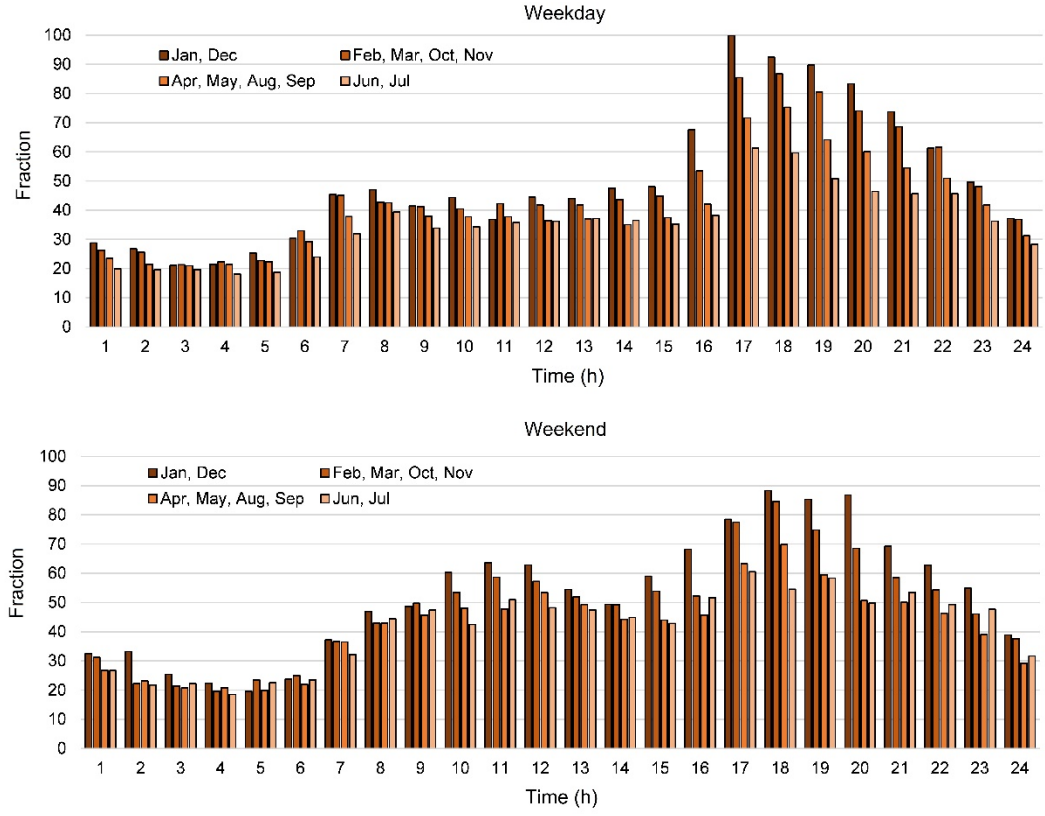

Figure 5 The electricity fraction in functions of time.

Table 2 The distribution of internal heat gains.

	Room 1	Room 2	Room 3

Number of people	0.941	0.463	0.332
Maximum electricity load(W)	324.05	158.54	109.59

The internal loads include the people load and the electricity load. The number of the person for the whole apartment is 1.72 and the people load is 90 W/person, which is based on the surveys for apartments in Denmark in [39]. The occupant schedule and the electricity schedule are shown in Figure 4 and Figure 5 based on the survey in the report [40]. The people load is more in the evenings and differs between weekdays and weekends. The electricity load is also diverse between weekdays and weekends and differs among the months. The electricity load at a full percentage (100%) is 592.18 W. The people load and the electricity load are evenly distributed in each room based on the room area, see Table 2. The people and electricity load at each hour are calculated as the number of people × occupant fraction, maximum electricity load × electricity fraction respectively.

The zone ventilation function is used for single-zone ventilation. The zone mixing function calculates the air change and thermal change between zones. The natural ventilation airflow rate is calculated by the wind speed and thermal stack effect. The airflow by wind speed effect is calculated by Equation (3).

$$Q_w = C_w A f_{schedule} v \quad (3)$$

Where Q_w is the airflow rate driven by wind (m^3/s), C_w is the opening effectiveness, A is the opening area (m^2), $f_{schedule}$ is the schedule of opening fraction, v is the local wind speed (m/s).

The opening effectiveness is calculated by the angle between the effective angle and real-time wind direction for each simulated time step, as shown in Equation (4).

$$C_w = 0.55 - \frac{|EffectiveAngle - WindDirection|}{180} \times 0.25 \quad (4)$$

The airflow rate driven by thermal stack effect Q_s is shown in Equation (5).

$$Q_s = C_s A f_{schedule} \sqrt{2g\Delta h(|T_i - T_o| / T_i)} \quad (5)$$

Where Δh is the height from midpoint of lower opening to the neutral pressure level (m); Ti is the zone air temperature (°C); To is the outdoor air temperature (°C); C_s is the discharge coefficient for opening, which is defined by Equation (6).

$$C_s = 0.4 + 0.0045|T_i - T_o| \quad (6)$$

The total airflow rate is calculated by Equation (7).

$$Q = \sqrt{Q_s^2 + Q_w^2} \quad (7)$$

3. Full-scale experimental test and model validation

The PCMWV is tested in the south surface of the façade lab at Aalborg University. The window is equipped with a ventilation system (including the ducts and valves) to create stable airflow in the window. The experiments include 3 parts: testing the pre-cooling ability of the PCMVW for night cooling application, measuring the pre-heating ability of the PCMVW for solar energy storage application, and testing the reflection/absorption blinds and self-cooling mode of the VW. The PCM temperature, air temperature in the PCM heat exchanger and VW cavity are measured. The measurement points are shown in Figure 6. Temperature sensors and pyranometers are set on the external surface to measure the outdoor air temperature and the solar radiation the façade receives. A weather station on the roof of the building is measuring the weather conditions, include the wind speed and wind direction.

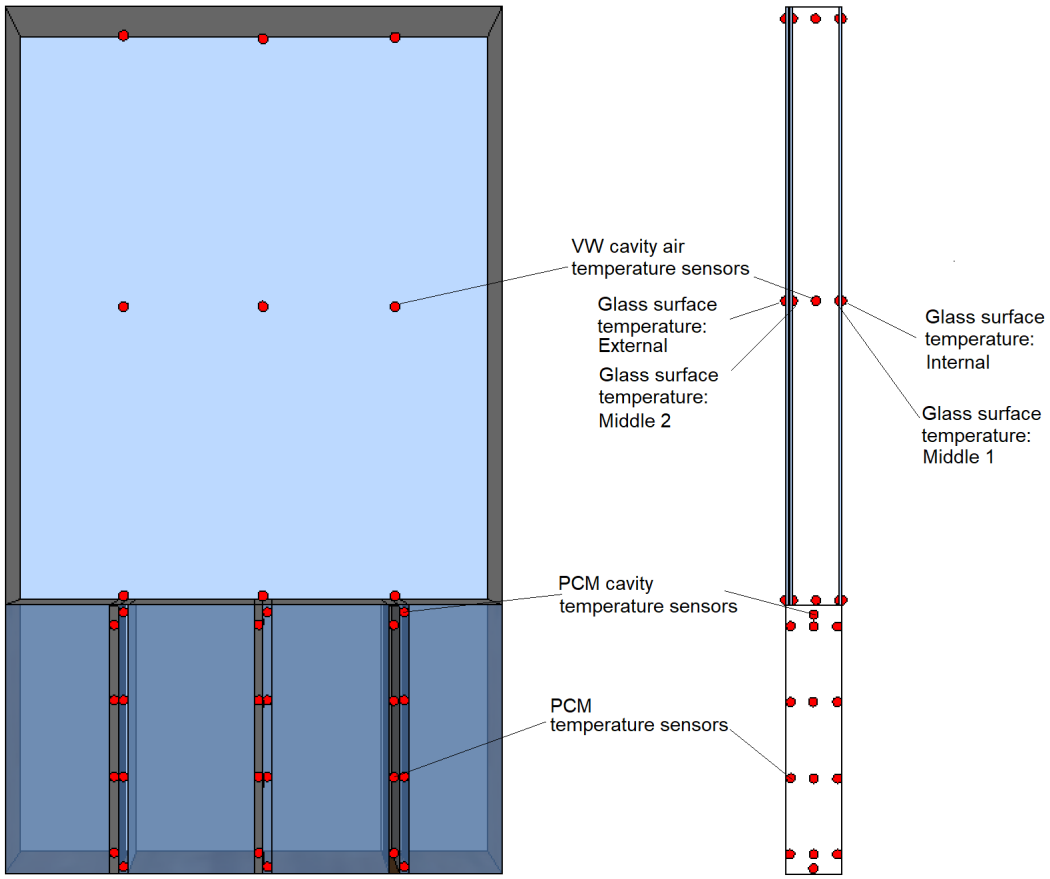

Figure 6 The temperature sensors in the PCMVW.

The aim of the experiment is to validate the numerical model. The experiment thus simplified some of the control strategies. For the summer night cooling application, in the experiment the PCMVW is constantly ventilated. The same ventilation is set in the numerical model, as well as the same outdoor weather conditions and external shading for PCM. For the winter solar energy storage application, the ventilation and outdoor weather conditions are set for the experiment and numerical model of the PCMVW are set as the same as well. For the blinds control, only the VW part with the absorption/reflection blinds is ventilated and tested in the experiment. The corresponding blinds are added and the ventilation is only set in the VW in the numerical model.

3.1 Part 1: Night cooling application

The night cooling application experiment is done to measure the pre-cooling ability of the PCMVW during hot weather conditions. The PCM heat exchanger is shaded with external shading to avoid temperature rise by the sunlight. The ventilated window is not shaded during this experiment, see Figure 7. The PCM is ventilated during the nighttime, to be cooled down by the cold outdoor air. It is then ventilated during the daytime, to pre-cool the ventilated high-temperature outdoor air. The test is done from 12th July-16th July 2017. Figure 8 shows the measured outdoor weather conditions. The minimum outdoor air temperature for all the measured days are below the PCM freezing temperature (20.7°C), which is required for effective night cooling application.

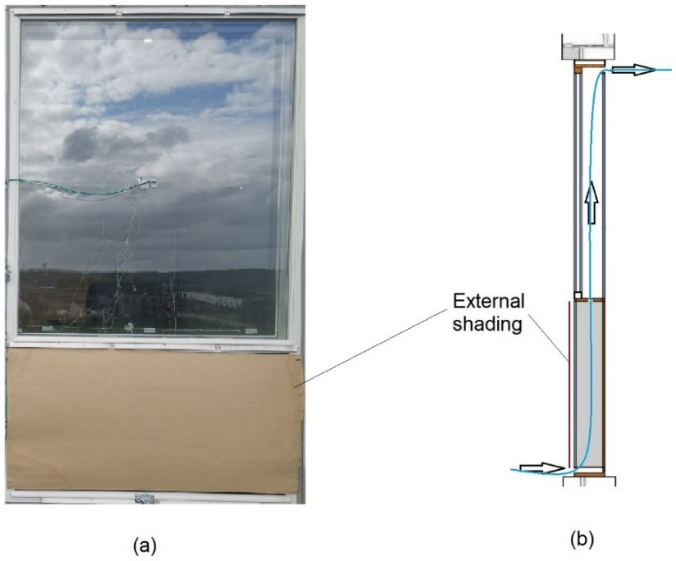

Figure 7 The tested case for summer night cooling application. (a) Experimental setup; (b) sketch of the PCMVW with external shading.

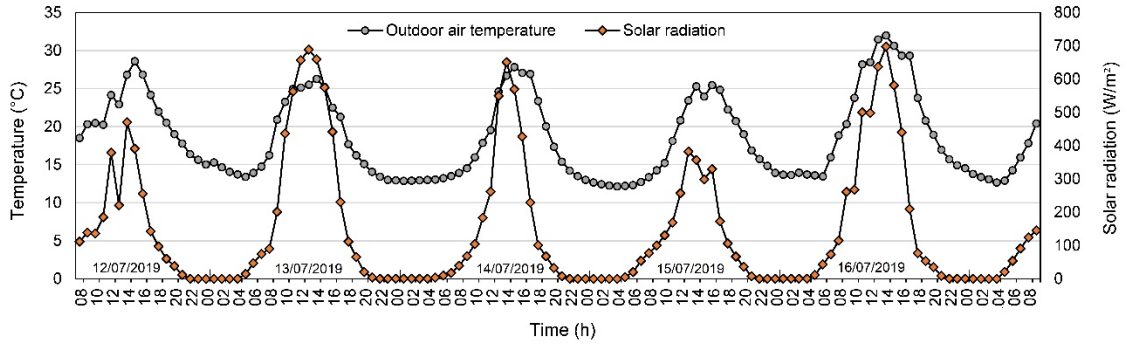

Figure 8 Measured outdoor weather data for summer night cooling application.

Figure 9 shows the PCM temperature, air temperature in the PCM cavity, air temperature in the VW cavity from both experiment and simulation results for night cooling application. It shows good agreements between the experiment and simulation results. The modeling average error for PCM temperature, PCM cavity, VW cavity is 5.0%, 5.7% and 5.4% respectively, which is calculated based on Equation (8). The modeling root mean square error (RMSE) for PCM temperature, PCM cavity, VW cavity is 1.0, 1.3 and 1.5 respectively, which is calculated based on Equation (9). The weather input for the simulation is hourly data, which may cause a part of the discrepancy.

$$error = \left| \frac{\text{Experimental value} - \text{Simulation value}}{\text{Experimental value}} \right| \times 100\% \qquad (8)$$

$$RMSE = \sqrt{\frac{\sum_{i=1}^{N} (\text{Experimental value}_i - \text{Simulation value}_i)^2}{N}} \qquad (9)$$

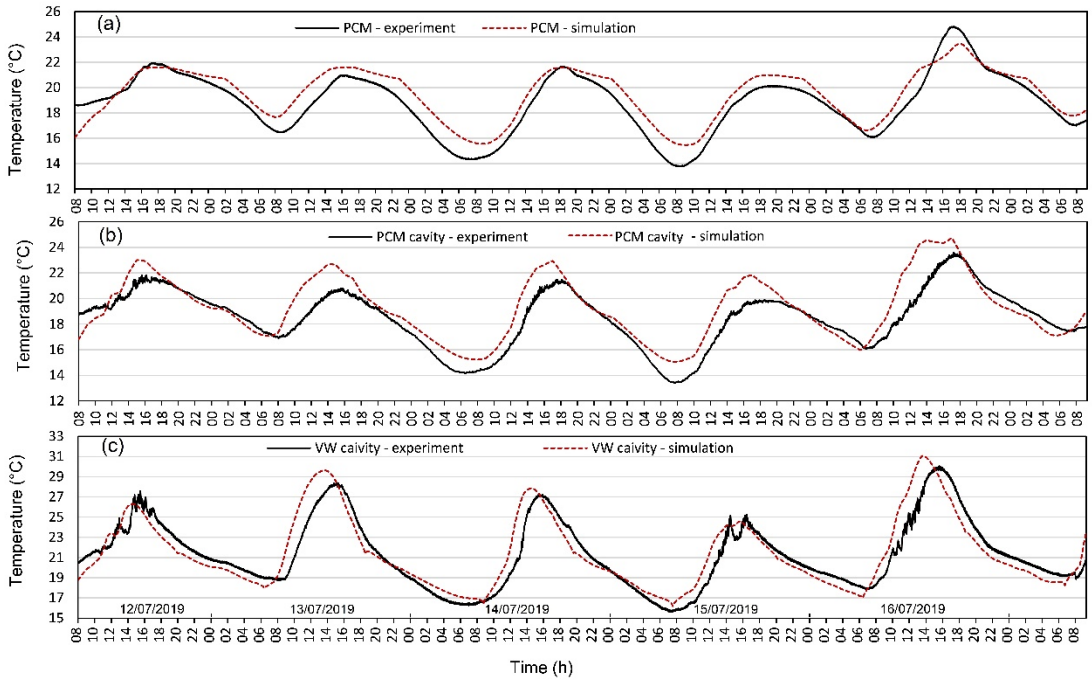

Figure 9 Model validation of summer night cooling application. (a)PCM temperature; (b) air temperature in the PCM cavity; (c) air temperature in the VW cavity.

3.2 Part 2: Solar energy storage application

The solar energy storage application aims at using the stored solar energy to pre-heat the low-temperature ventilation, typically during winter. The test is done from 02-07-2019 to 12-07-2019. In this test, the PCM stores the solar energy during the daytime (8:30-18:30), and releases the energy to pre-heat the ventilation during the night time (18:30-8:30), as illustrated in Figure 10. The measured outdoor weather condition in Figure 11 shows that the solar radiation levels of the measured days are all different. For some days there is high solar radiation, for some other days the solar radiation is low.

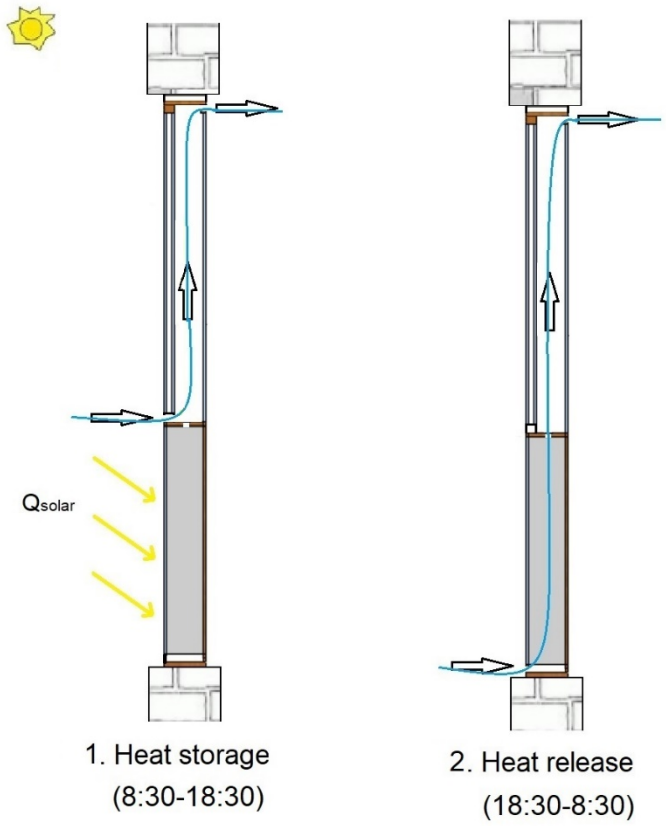

Figure 10 The tested cases for winter solar energy storage application.

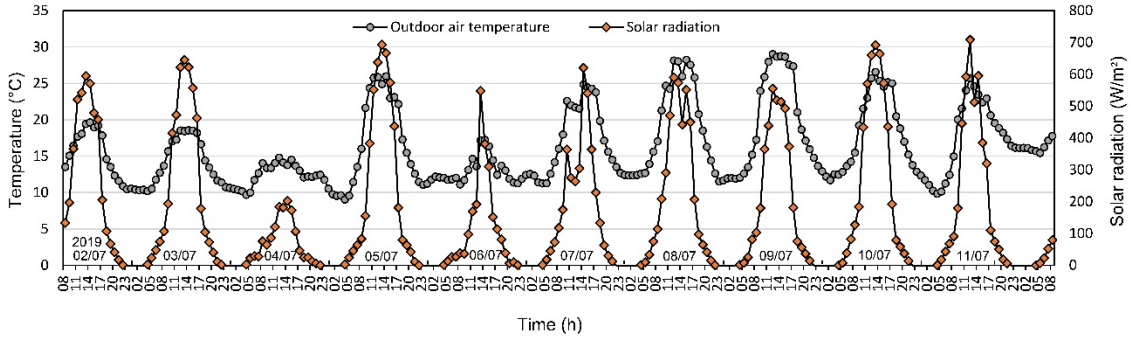

Figure 11 Measured outdoor weather data for winter solar energy usage application.

Figure 12 shows the PCM temperature, air temperature in the PCM cavity, air temperature in the VW cavity from both experiment and simulation results for solar energy storage application. Good agreements can be found between the experiment and simulation results. The modeling average

error for PCM temperature, PCM cavity, VW cavity is 12.5%, 7.1% and 6.8% respectively. The RMSE for PCM temperature, PCM cavity, VW cavity is 2.4, 1.7 and 1.7 respectively.

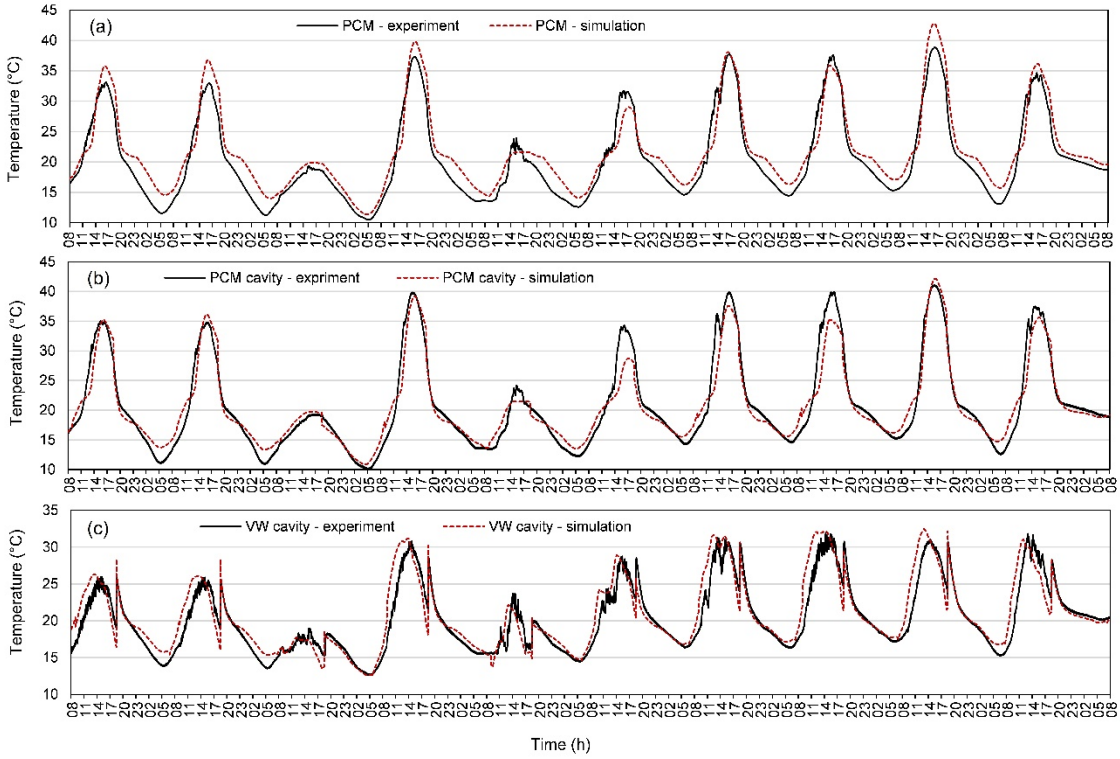

Figure 12 Model validation of winter solar energy usage application. (a) PCM temperature; (b) air temperature in the PCM cavity; (c) air temperature in the VW cavity.

3.3 Part 3: Adding blinds for advanced VW control

A blind with two different functional sides is developed to improve the energy performance of the PCMVW. One side of the blind is painted with a high reflection coating, while the other side is painted with a high absorption coating. Figure 13 shows the occasions when the reflection/absorption side is applicable. For summer cooling application, using reflection shading can decrease the solar heat gain from the VW to the room, as well as decrease the inlet air temperature for room ventilation. For the winter solar energy storage application, using absorption blind can add heat to the VW, thus increases the ventilation preheating effect. For the cases when the indoor air temperature is too high, using shading in cooperation with self-cooling natural

ventilation can effectively decrease the temperature of the VW, thus decreases the heat gain through the window. The blinds not only regulates the air temperature in the VW, but also act as an effective way of the daylight control of the room, to avoid the direct sunlight exposure of the occupants from a low hanging winter sun.

In this experiment, only the VW with reflection/absorption blinds are tested and compared with the numerical model. The PCM is not ventilated or tested.

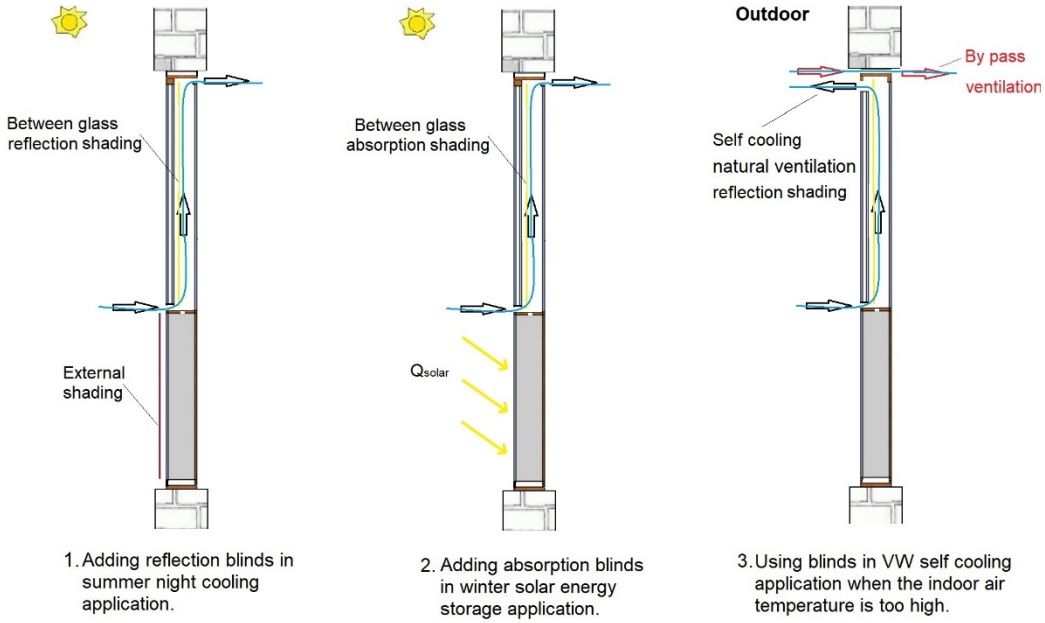

Figure 13 The advanced strategy control with blinds.

The experiment tests the VW with reflection/absorption blind under natural/mechanical ventilation respectively. The VW with reflection blind under natural ventilation is tested in 14-10-2019. The experiment is not done in continuous days because there are no continuous sunny days during the tested period. Figure 14 shows the outdoor wind speed and wind direction. Figure 15 shows the outdoor air temperature, solar radiation on the vertical surface and temperature of the different glass surfaces. The positions of the temperature sensors are in Figure 2. There are good agreements between the measured glass surface temperature and simulated results. The modeling error for

internal, middle 1, middle 2, external sensors is 9.8%, 9.4%, 13.1% and 8.2% respectively. The RMSE for internal, middle 1, middle 2, external sensors is 2.1, 2.0, 2.7 and 1.4 respectively.

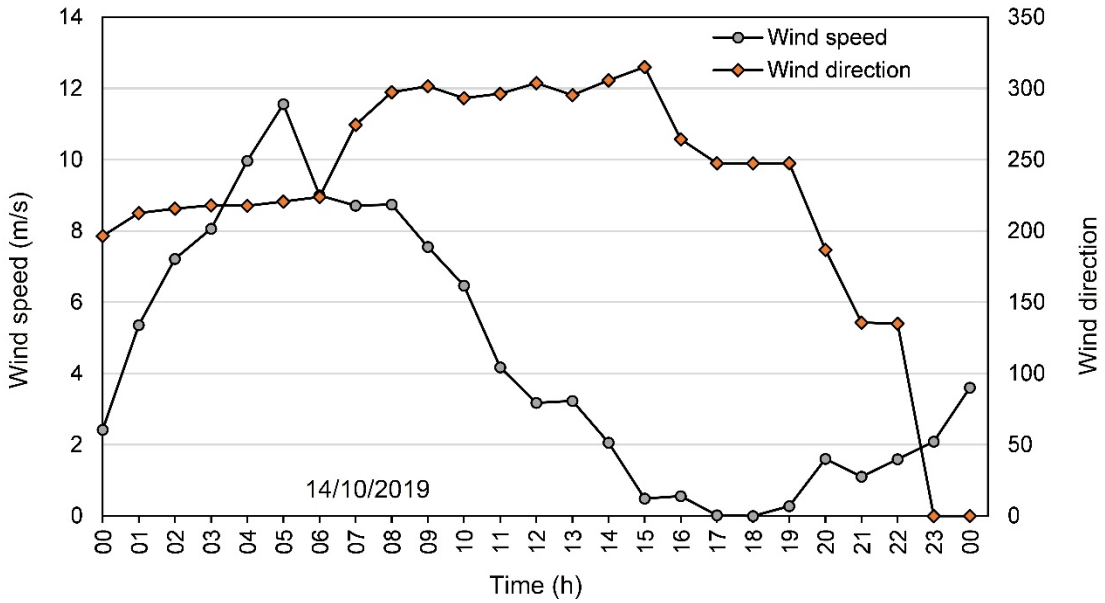

Figure 14 The outdoor wind condition of the tested day for natural ventilation with reflection blind.

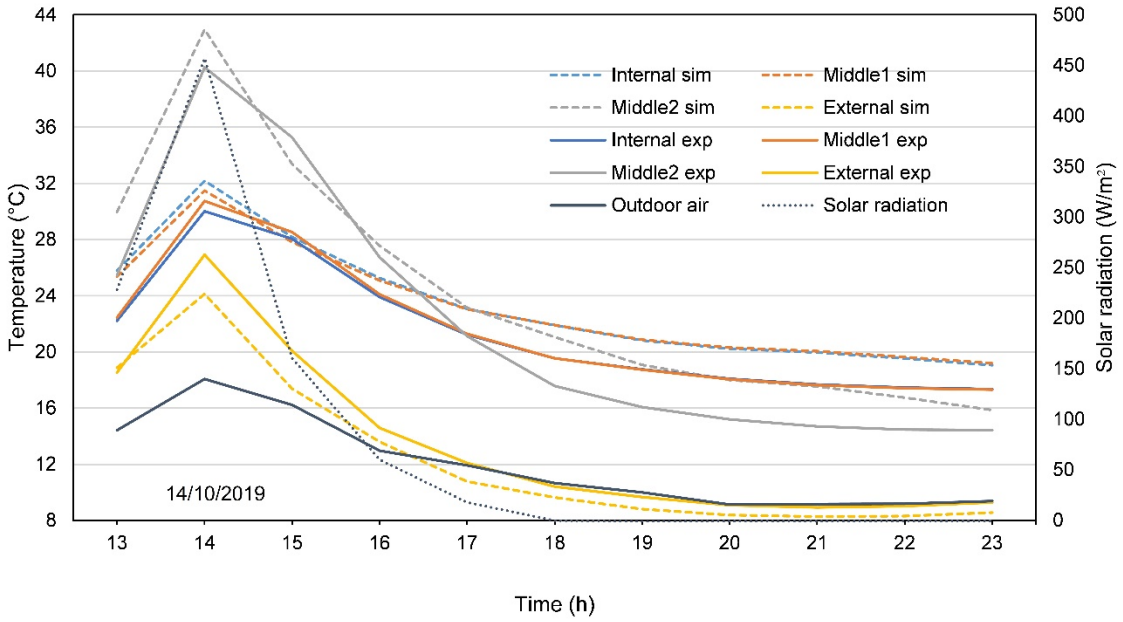

Figure 15 The model validation of double window natural ventilation: with reflection blind for the between-glass blind.

The VW with absorption blind under natural ventilation is tested on 31-10-2019. Figure 16 shows the outdoor wind condition. Figure 17 shows the outdoor air temperature, solar radiation on the vertical surface and temperature of the different glass surfaces. The same trends can be found with the experimental data and simulation results. The modeling error for internal, middle 1, middle 2, external sensors is 8.1%, 9.9%, 8.8% and 11.2% respectively. The RMSE for internal, middle 1, middle 2, external sensors is 2.1, 2.9, 2.8 and 1.6 respectively.

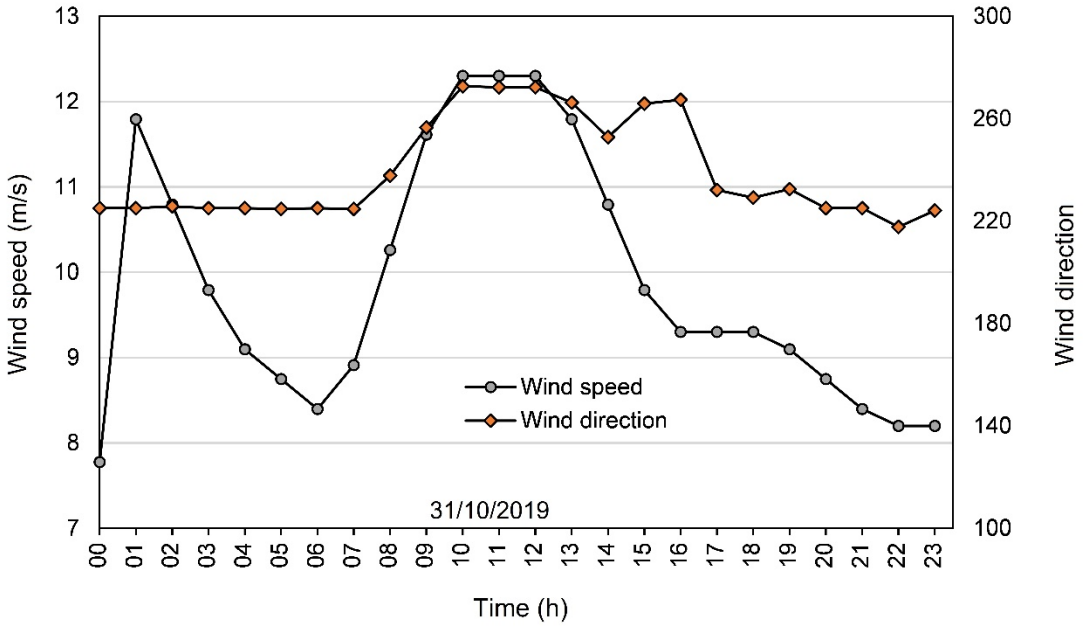

Figure 16 The outdoor wind condition of the tested day for natural ventilation with absorption blind.

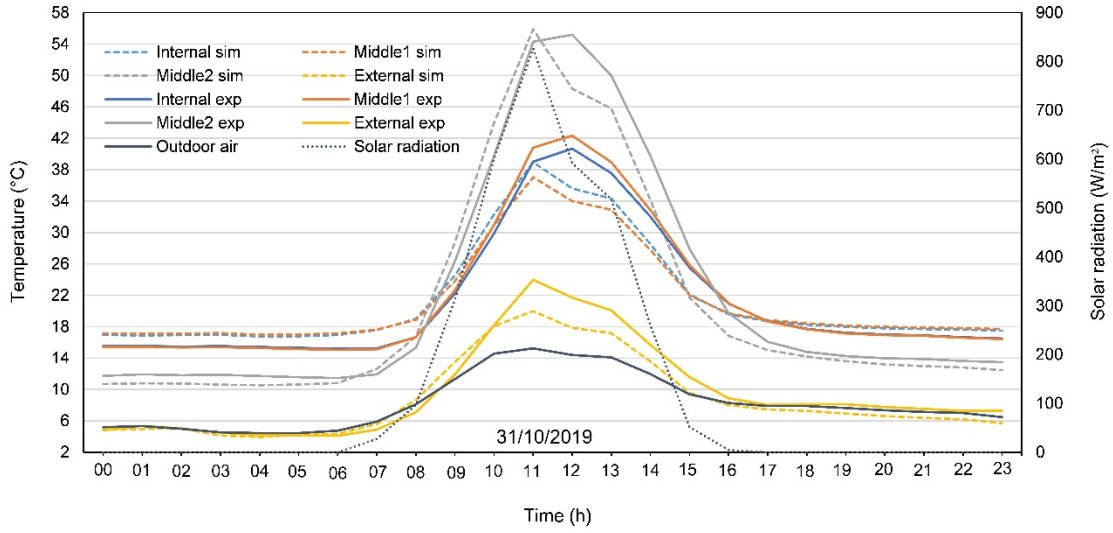

Figure 17 The model validation of double window natural ventilation: with absorption blind for the between-glass blind.

Comparing the 3 experiments, it is seen that the model for night cooling application has the best fit with the experimental results. One possible reason is that the model is less influenced by solar radiation, while the other 2 models are more influenced by solar radiation, especially for blinds testing. The errors come from the measurement uncertainty, uncertainties of material properties provided by the manufacturer, and the unavoidable personal error (for example, the blind is not possible to close at 100% close position to avoid sunlight go through the gaps). Moreover, the hourly average values of outdoor weather conditions are used in the model, which can be a big contribution to the model uncertainty.

4. PCM ventilation performance

The PCMVW and its numerical model are developed and tested. However, the cooling/heating ability of the PCMVW comparing to other ventilation systems remains to be examined. In this chapter, the building with PCMVW is compared with the same building with other 2 ventilation systems: ventilated window without PCM (VW, no PCM) and normal window without both ventilated window and PCM (no VW, no PCM). The heating and cooling energy demands of the

building are compared for summer night cooling and winter solar energy storage applications respectively.

4.1 Summer night cooling effectiveness

The night cooling application is active during May-October. 3 ventilation systems and their ventilation cooling abilities are compared. The windows in the 3 systems have the same configuration and material constitutes. Figure 18 shows the system compositions and operation strategies of the 3 systems. The PCMVW (Figure 18(a)) has 3 operation modes: the heat removel mode during the night time, where the cold outdoor air ventilate through the PCM to cool it down; the ventilation pre-cooling mode, where the PCM cools down the ventilation where the indoor air temperature is too high; the heat mode, where the ventilation only goes through the double window (which is heated up by solar radiation) when the indoor air is overcooled and heating is needed. As references, the VW, no PCM (Figure 18(b)) and no VW, no PCM (Figure 18(c)) systems are ventilated with the same time schedule and airflow rate.

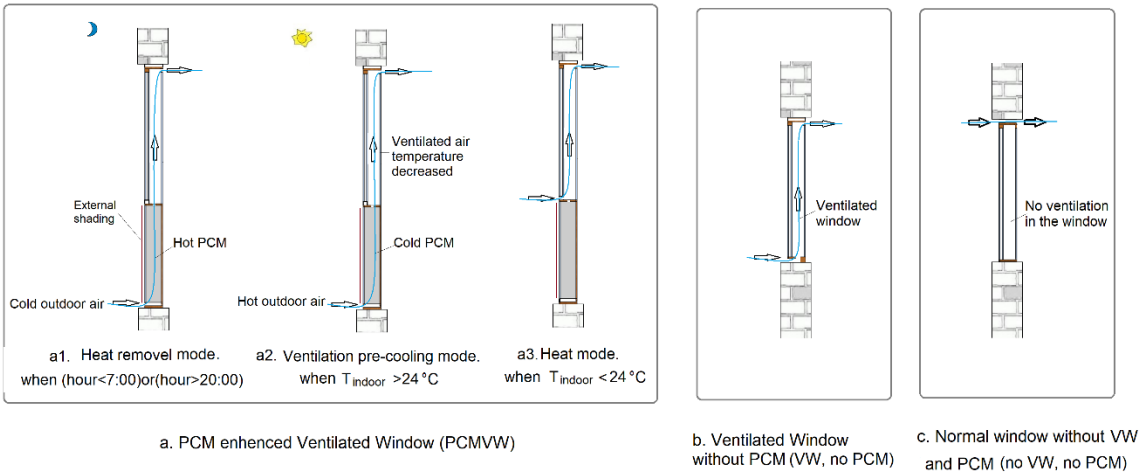

Figure 18 Compare of PCMVW with 2 other ventilation systems for summer night cooling application.

Figure 19 shows the room ventilation inlet air temperature from 1st August- 7th August. For room 1 (southwest room), the no VW, no PCM system has the lowest inlet air temperature (which is

close to the outdoor air temperature), and the VW, no PCM system has the highest inlet air temperature. For room 2 (northeast room), the inlet air temperatures of the 3 systems show the same trends, and are much lower than room 1 with the same ventilation system (except for no VW, no PCM system, which has the same inlet air temperature for the 2 rooms). It is because the windows facing southwest have more heat gains than the windows facing northeast.

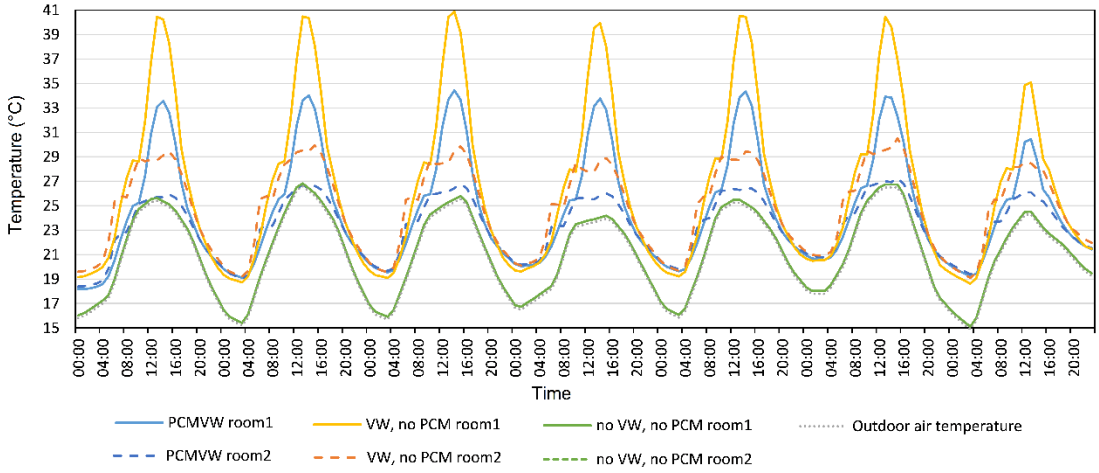

Figure 19 The room ventilation inlet air temperature of the 3 ventilation systems from 1st August- 7th August for summer night cooling application.

Figure 20 shows the inner glass surface temperature of the 3 systems from 1st August- 7th August. The higher the inner glass surface temperature, the higher the amount of heat gain the room gets from the window. For both rooms, the no VW, no PCM system has the highest glass surface temperature, and the PCMVW system has the lowest inner glass surface temperature. The no VW, no PCM system has no ventilation in the window cavity, thus the heat is gathered in the air inside the cavity, which increases the glass surface temperature. While for the PCMVW, the PCM cools down the ventilation, and the relatively low-temperature air potentially cools down the glass surface temperature.

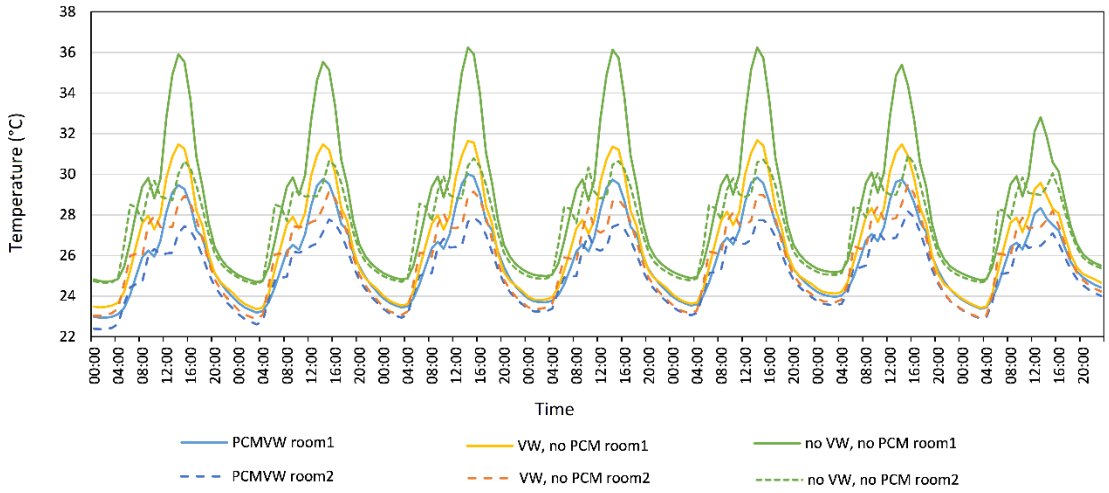

Figure 20 The inner glass surface temperature of the 3 ventilation systems from 1st August- 7th August for summer night cooling application.

The ventilation inlet air temperature and the inner glass surface temperature are not showing the same trend. This indicates that none of them can be used as an indicator to compare the ventilation performance. The energy demands of the building with the 3 systems for the whole summer period are calculated and shown in Figure 21. For both rooms, the VW, no PCM system provides the highest cooling energy demand for all the simulated months, which indicates a poor cooling ability of the VW. The PCMVW provides the lowest cooling energy demand. The heating energy demand is quite low and is present in October. For room 1, the PCMVW reduction in cooling energy demand is 46% compared to VW, no PCM system, and the reduction is 27% compared to the no VW, no PCM system. For room 2, the PCMVW reduction in cooling energy demand is 51% and 38% compared to the other two systems respectively. Room 3 has the same orientation of the external wall as room 2, and the sizes of the two rooms are similar. As a result, the energy demand per square meter floor area is similar, therefore it is not discussed here.

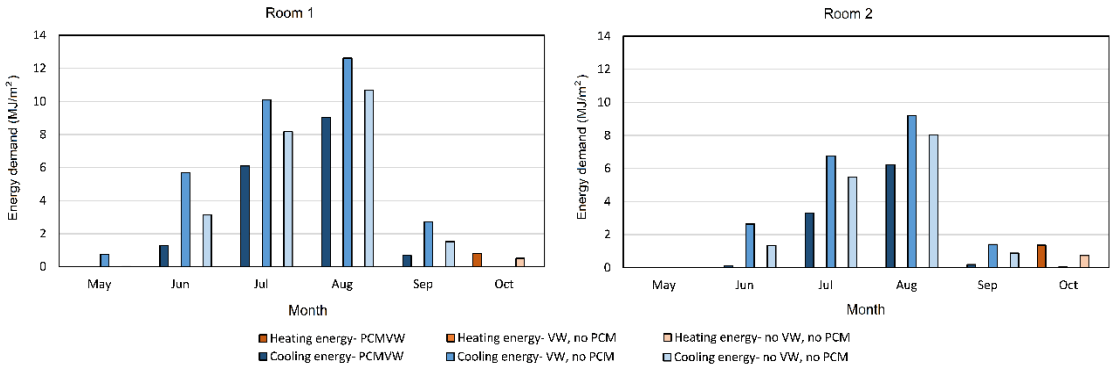

Figure 21 The building energy demand with the 3 different ventilation systems for summer night cooling application.

4.2 Winter solar energy storage effectiveness

The solar energy storage application is active from November- April. The similar 3 systems and their ventilation heating abilities are compared. Figure 22 shows the system compositions and operation strategies of the 3 systems. The PCMVW (Figure 22(a)) has 2 operation modes: the heat release mode, where the ventilation pre-heating is operated when the room is in low temperature; the overheating preventing mode, where the bypass and self-cooling ventilation is operated when the indoor air temperature is too high; meanwhile, the PCM stores the solar energy when the sunlight is available. The VW, no PCM system (Figure 22(b)) has the same ventilation schedule as the PCMVW except there is no PCM heat exchanger. The no VW, no PCM system (Figure 22(c)) is only ventilated with bypass ventilation.

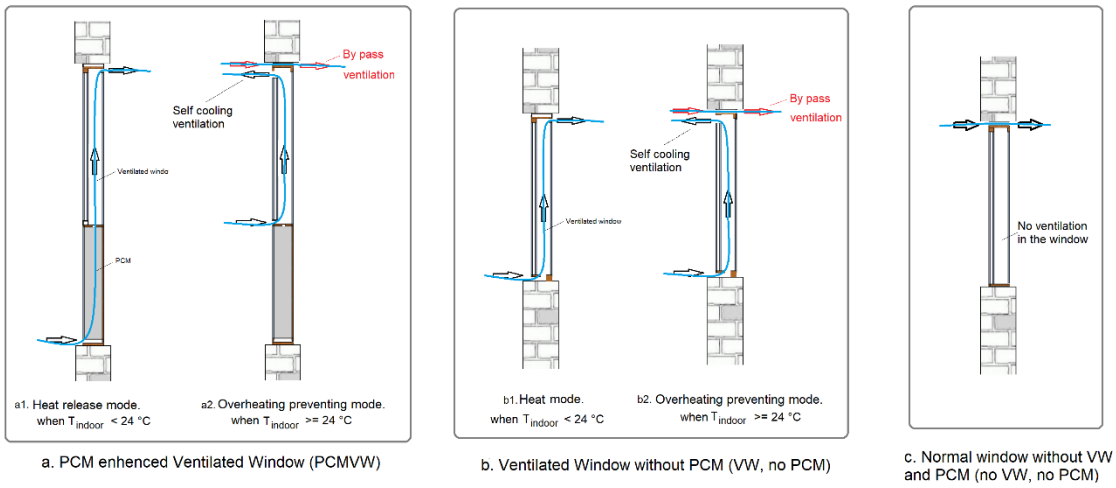

Figure 22 Compare of PCMVW with 2 other ventilation systems for winter solar energy storage application.

Figure 23 shows the room ventilation inlet air temperature during the period 5th February- 23rd February. For both rooms, the PCMVW has the highest inlet air temperature. The no VW, no PCM system has the lowest inlet air temperature. With the same ventilation system, the inlet air temperature of room 1 is much higher than room 2 (except for no VW, no PCM system, which has the same inlet air temperature for the 2 rooms). The windows in southwest façade have more solar heat gains than in northeast façade.

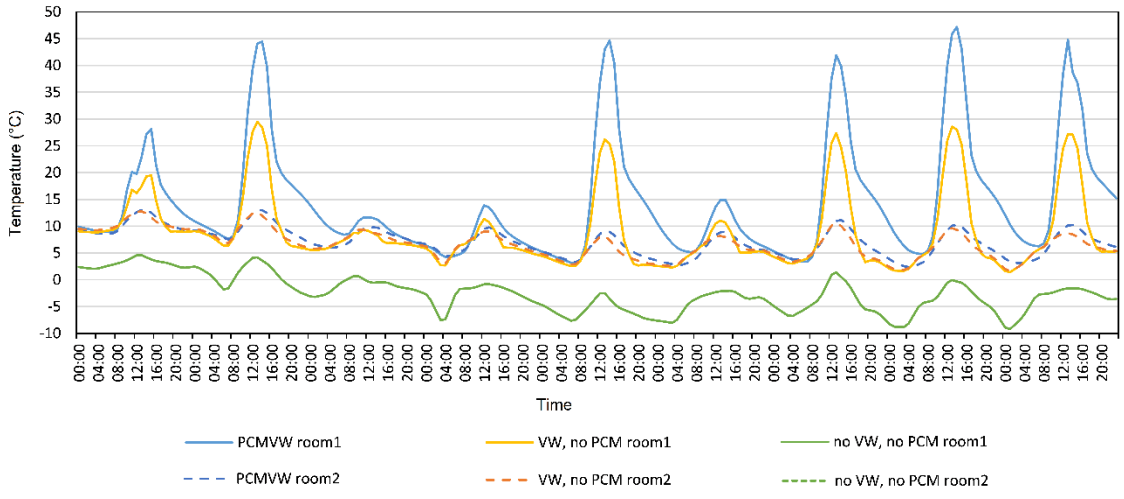

Figure 23 The room ventilation inlet air temperature of the 3 ventilation systems from 5th February- 23rd February for winter solar energy storage application.

Figure 24 shows the inner glass surface temperature of the 3 ventilation systems during the period 5th February- 13th February. For room 1 (southwest room), the no VW, no PCM system has the highest inner glass surface temperature, and the VW, no PCM system has the lowest inner glass surface temperature. However, for room 2 (northeast room), the no VW, no PCM system has the highest inner glass surface temperature, while the PCMVW and the no VW, no PCM systems have a similar inner glass surface temperature for most of the time.

For room 2 (northeast room), when comparing the PCMVW system with the VW, no PCM system, both the ventilation inlet air temperature and the inner glass surface temperature are similar. The PCM does not have a high ventilation heating potential for windows in northeast façade for some winter days, due to the low solar radiation received. However, the situation will be changed during March and May, when the received solar radiation level on the northeast façade increases. This is shown in the energy demand comparison, which can be seen in Figure 25.

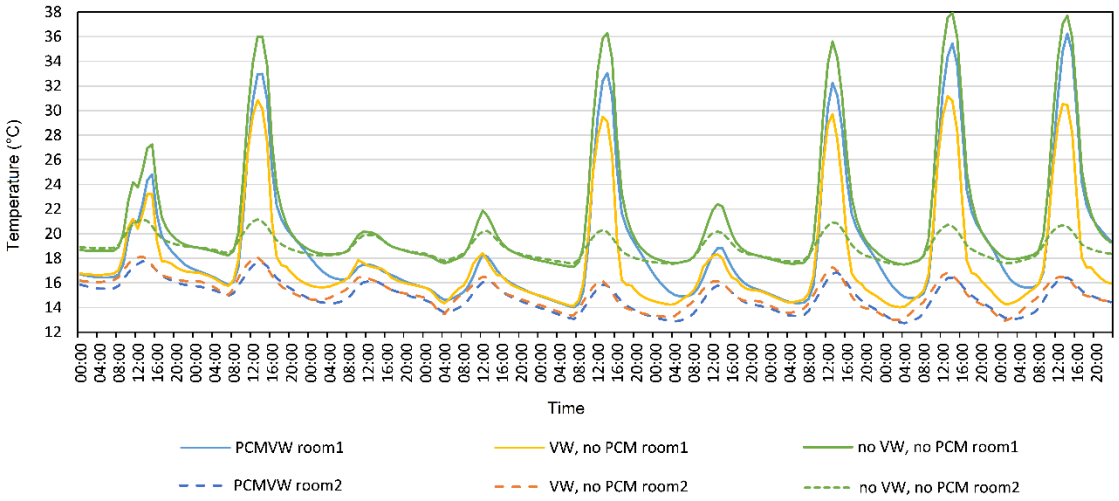

Figure 24 The inner glass surface temperature of the 3 ventilation systems from 5th February- 23rd February for winter solar energy storage application.

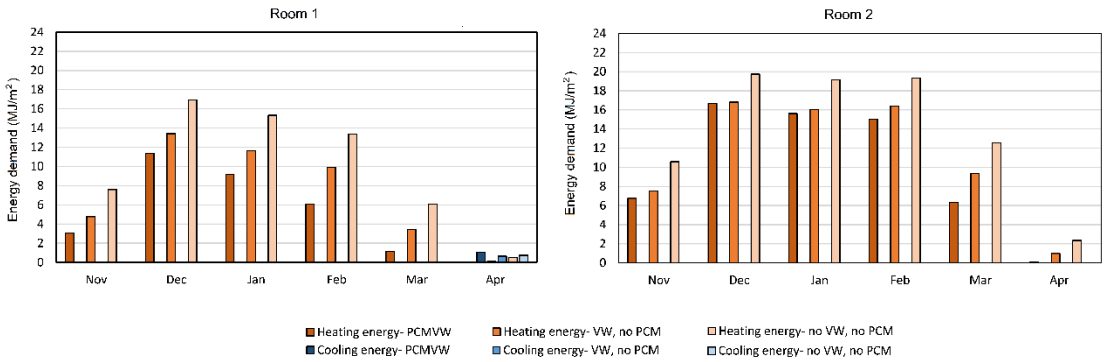

Figure 25 The building energy demand with the 3 different ventilation systems for winter energy storage application.

The energy demands of the building with 3 different systems are calculated separately, as shown in Figure 25. For both rooms, the PCMVW provides the lowest energy demand, and the no VW, no PCM system the highest energy demand. For room 2, the energy demand of the PCMVW and the VW, no PCM systems are similar in December and January. Compared to the no VW, no PCM system and the VW, no PCM system, for room 1, the PCMVW system reduces the heating energy demand by 29% and 48% respectively; for room 2, the PCMVW system reduces the heating energy demand by 10% and 28% respectively.

5. Control strategy development

The primitive control strategies of the PCMVW shown in Figure 7 and Figure 10 can risk the room with overheating, due to the direct solar heat gain through the window, or the excessive heat gain from the ventilation. The control strategy shown in Figure 18(a) has too high room ventilation inlet air temperature during summer, which can be improved by adding shading control. This section develops control strategies to improve the pre-cooling efficiency of the PCMVW. The thermal and energy performance of the PCMVW with different control strategies are analyzed by the numerical model proposed in Section 2.

5.1 Summer night cooling control strategies

Three control strategies are developed for summer night cooling application. Strategy 1 increases between glass reflection shading for the VW, to avoid high solar heat gain from the VW to the room, as seen in Figure . The heat mode is added as a part of the control strategy, in case the room is overcooled and room heating is needed. Based on strategy 1, strategy 2 improves the cold release mode by ventilating directly from the PCM heat exchanger to the room. The VW is self-cooled with natural ventilation, to further avoid its temperature rise by solar radiation, as shown in Figure . Based on strategy 2, strategy 3 differentiates the heating/cooling setpoint, and adds a bypass mode when the indoor air temperature is in the comfortable range, see Figure .

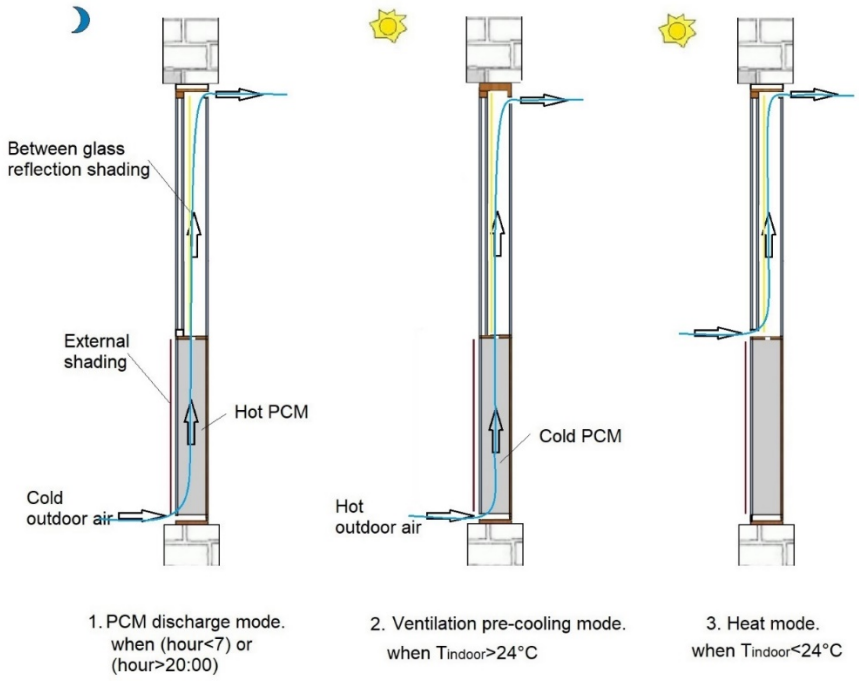

Figure 26 The summer night cooling application control strategy 1.

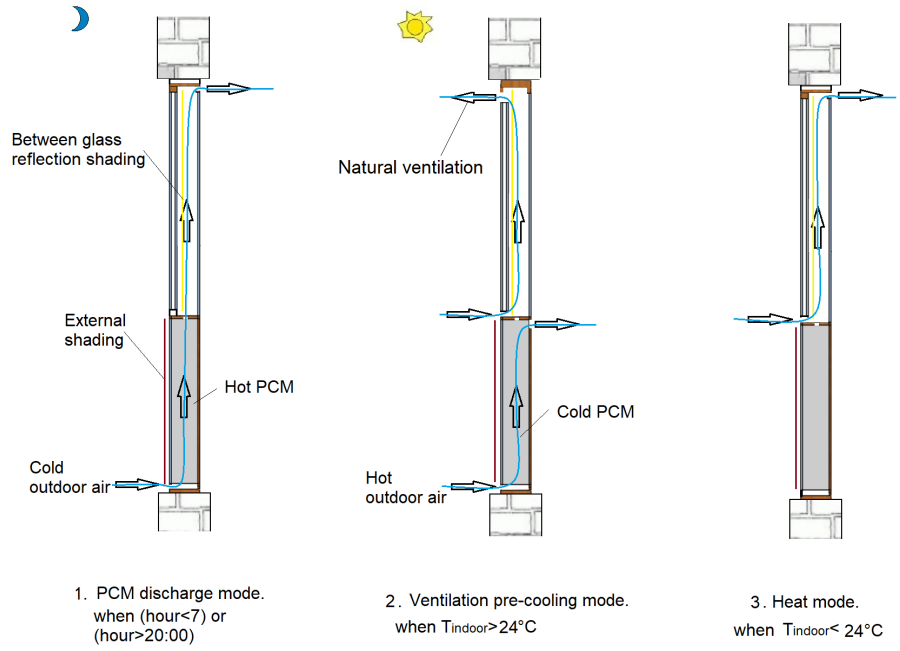

Figure 27 The summer night cooling application control strategy 2.

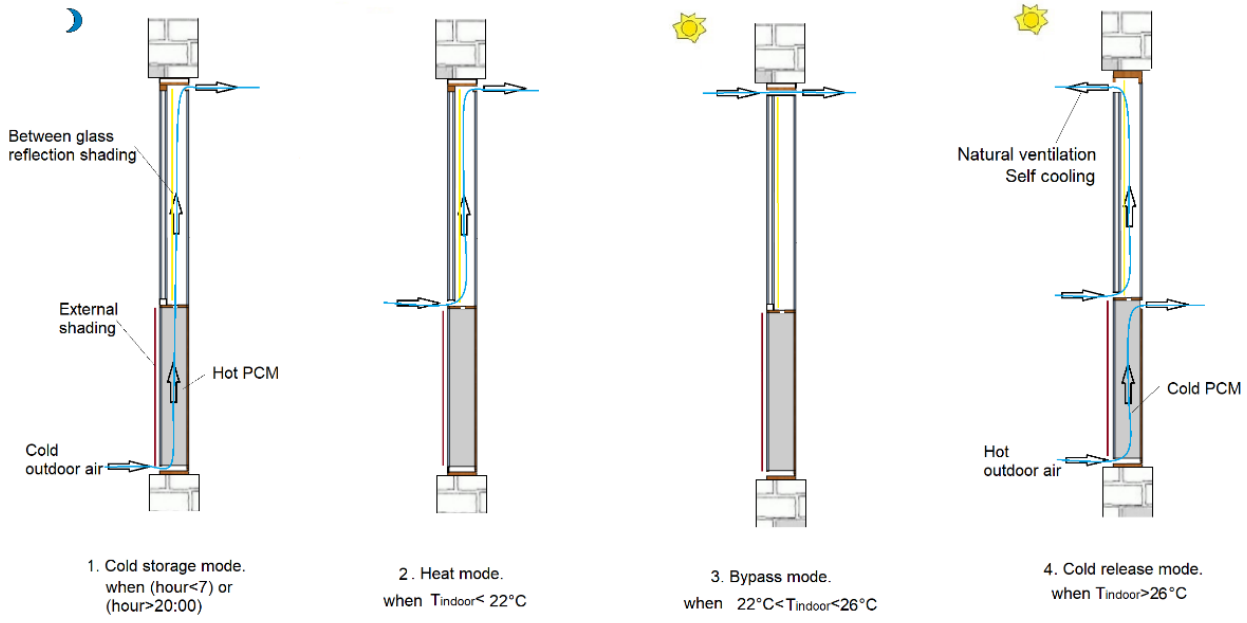

Figure 28 The summer night cooling application control strategy 3.

Figure 29 shows temperature of the primitive strategy > strategy 2 > strategy 1 > strategy 3. The PCM temperature of strategy 3 is the lowest, for the reason that during the daytime, the ventilation time through PCM is the shortest compared to other control strategies. For 5th August – 7th August, the PCM temperature of the 4 strategies are similar. The probable reason is that the night time outdoor air temperature is too high to cool the PCM the PCM temperature of the PCMVW under different control strategies. For both rooms, the PCM down below 21 °C.

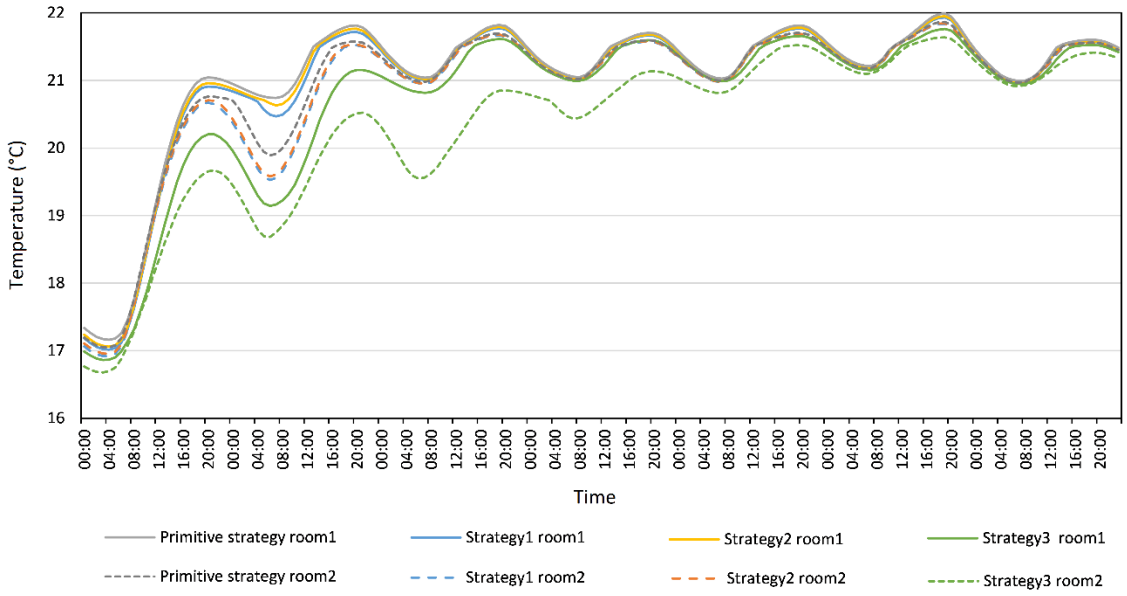

Figure 29. The PCM temperature in the PCMVW using different control strategies from 1st August- 7th August.

The ventilation inlet air temperature of the 4 control strategies are quite different, even though for some days the PCM temperature are similar. For both rooms, the inlet air temperature of primitive strategy > strategy 1 > strategy 3 > strategy 2. For both the primitive strategy and strategy 1, the inlet air temperature of room 1 is much higher than room 2, due to the higher heat gain in the cavity of the ventilated window in room 1. For strategy 2, the ventilation inlet air temperature of the 2 rooms are similar, except 2nd August. Similarly, for strategy 3, the ventilation inlet air temperature of the 2 rooms are similar, except 3rd August, when the PCM temperature of the 2 rooms show a bigger difference.

In comparison, strategy 3 has the lowest PCM temperature for both rooms. However, strategy 2 has the lowest ventilation inlet air temperature. The possible reason is that strategy 2 utilized the cooling ability of the PCM more than strategy 3. Consequently, strategy 2 has the least room energy demand, as seen in Figure 31.

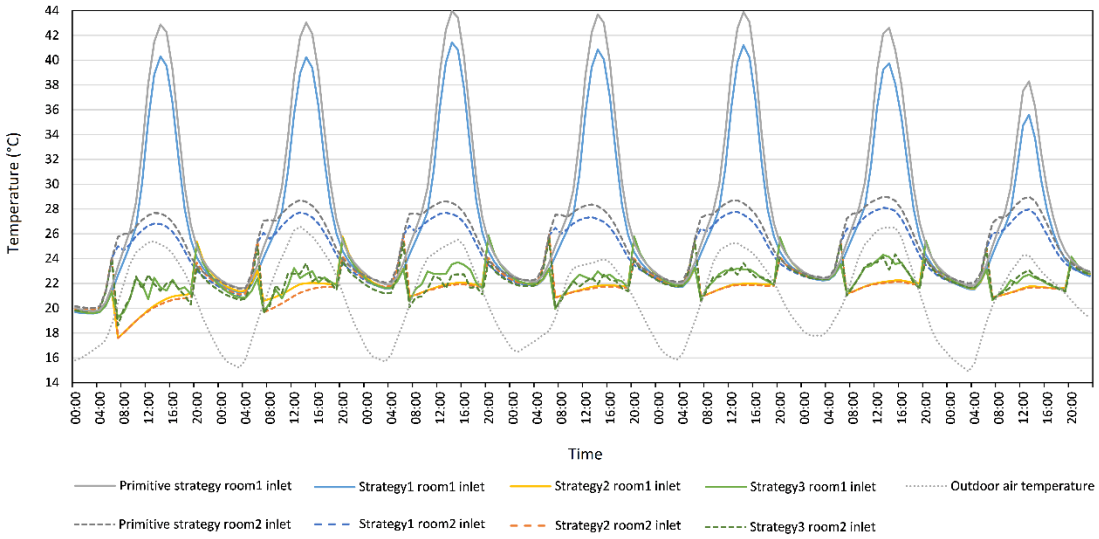

Figure 30. The ventilation inlet air temperature of the PCMVW using different control strategies from 1st August- 7th August.

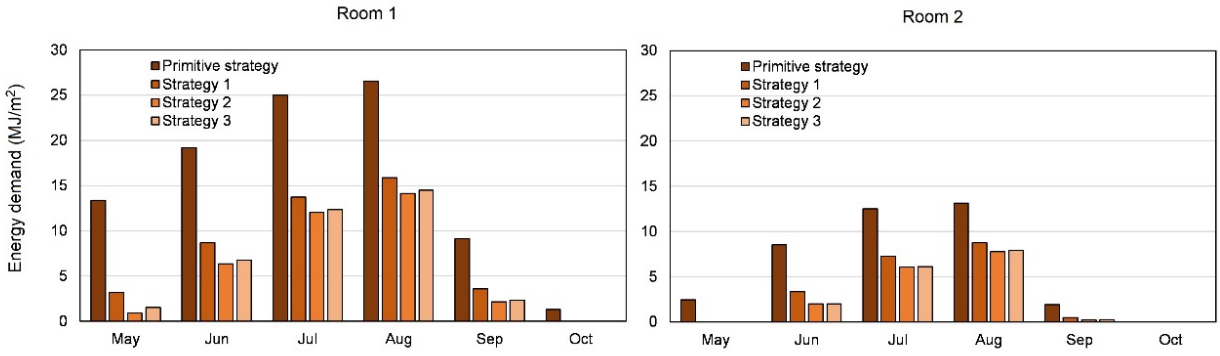

Figure 18 The energy demand using different control strategies for summer night cooling application.

Figure 18 shows the monthly energy demand using the 3 different control strategies for summer night cooling application. In general, room 1 has a higher energy demand than room 2, due to its orientation (southwest). Control strategies 1, 2 and 3 have less energy demand than the primitive

strategy for all the simulated months. Control strategy 3 has slightly higher energy demand than strategy 2, due to the extra energy needed to handle the outdoor air temperature to the thermal comfort temperature during bypass mode. However, the difference between the two control strategies is quite small. The application is robust for temperature setpoint. From the overall energy demand of the system, the conclusion can be drawn that the optimized control strategy is strategy 2. Compared to the primitive strategy, the developed control strategy (strategy 2) saves 62.3% of the energy for the room with windows facing southwest, and 58.2% of the energy for the room with windows facing northeast.

5.2 Winter solar energy usage strategies

For further improvement, 3 more control strategies are developed for the winter control strategy. Strategy 1 (in Figure 19) adds between glass absorption shading to increase the heat gain from the VW. The VW ventilation is operating in heat storage mode, to make use of the hot air in the VW for room ventilation. Moreover, to avoid room overheating, the overheating preventing mode is added by introducing double window self-cooling and bypass ventilation. Based on strategy 1, strategy 2 (in Figure 20) changes the heat release mode by ventilating directly from the PCM heat exchanger to the indoor room. Similarly, strategy 3 has a different heating/cooling setpoint, and adds a bypass mode when the indoor air temperature is in the comfortable range, see Figure 21.

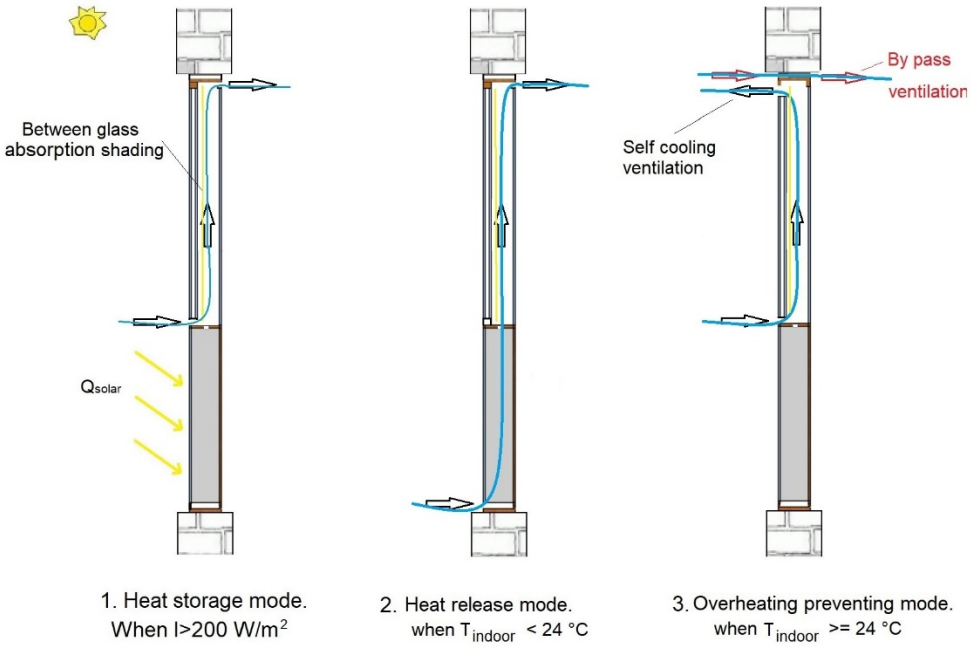

Figure 19 The winter solar energy storage application control strategy 1.

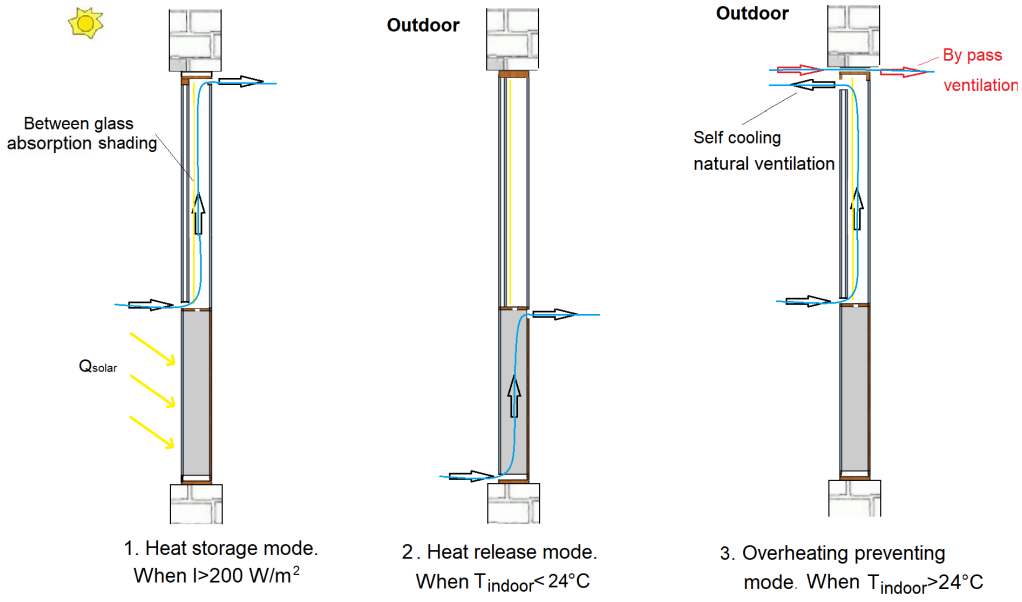

Figure 20 The winter solar energy storage application control strategy 2.

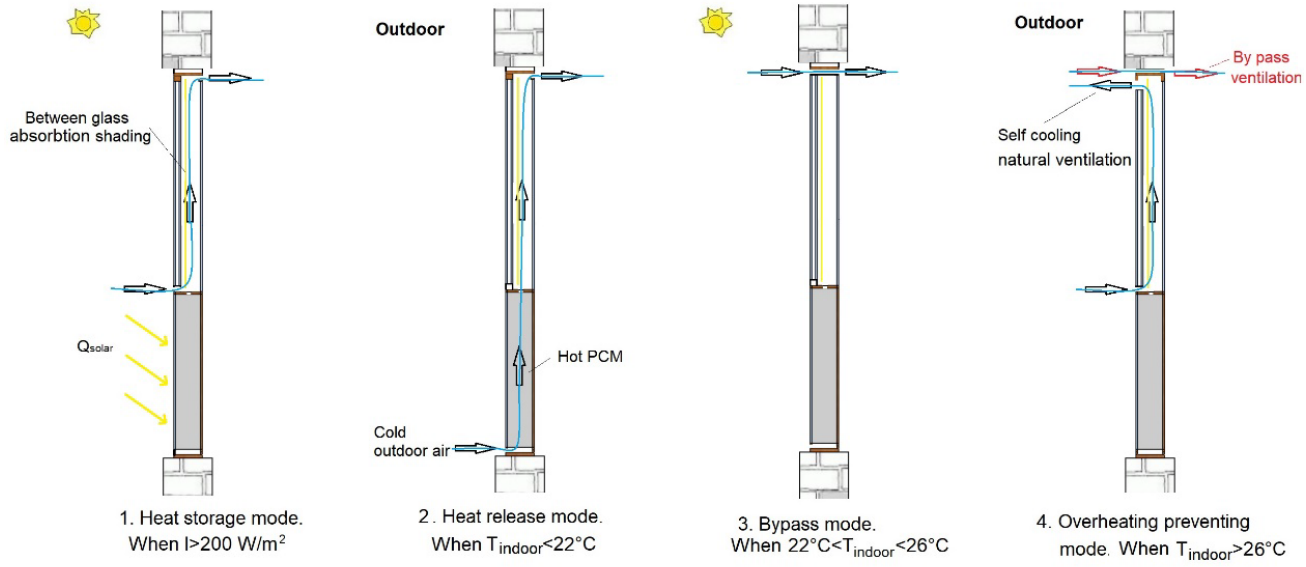

Figure 21 The winter solar energy storage application control strategy 3.

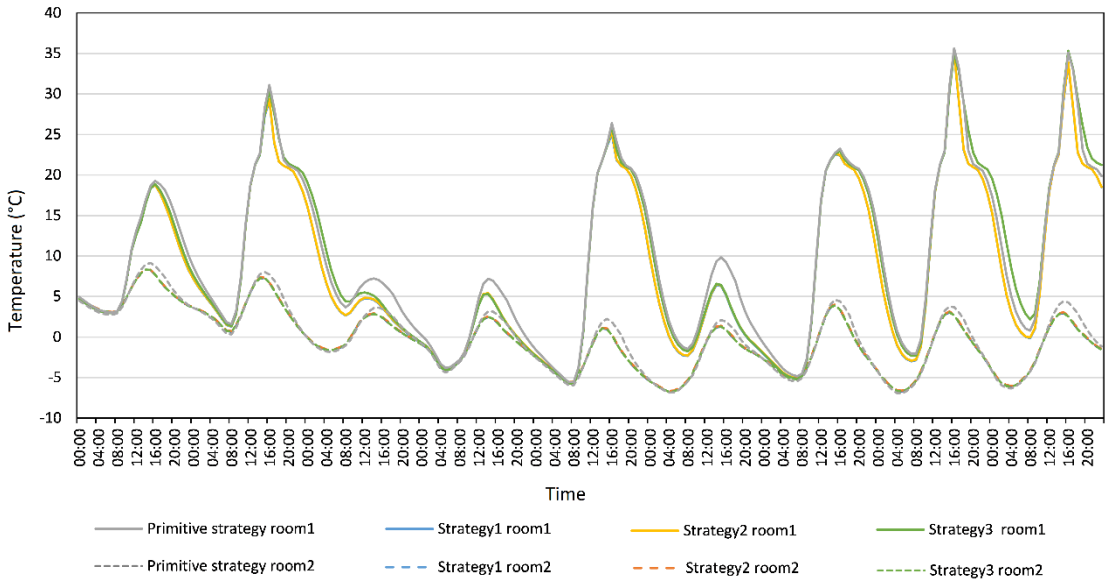

Figure 35. The PCM temperature in the PCMVW using different control strategies from 5th February- 13th February.

The PCM temperature in the PCMVW under different control strategies from 5th February- 13th February are similar for each of the 2 rooms, except for some days the primitive strategy has the highest PCM temperature, which is shown in Figure 35. In addition, room 1 has a much higher

PCM temperature than room 2. It indicates that the PCM temperature is more related to solar radiation and is robust against the control strategies.

The ventilation inlet air temperature, on the contrary, has some differences among the 4 control strategies. For room 1, the primitive strategy has the highest inlet air temperature, strategy 1 and 3 have similar inlet air temperature, except during the afternoon, strategy 3 has a lower inlet air temperature, due to the bypass mode. Strategy 2 has the lowest inlet air temperature in most of the days, especially for the days when the PCM temperature is low. It is due to the heat in the double window is not added to the ventilation during the heat release mode. For room 2, the ventilation inlet air temperature of primitive strategy > strategy 1 = strategy 3 > strategy 2 for most of the time.

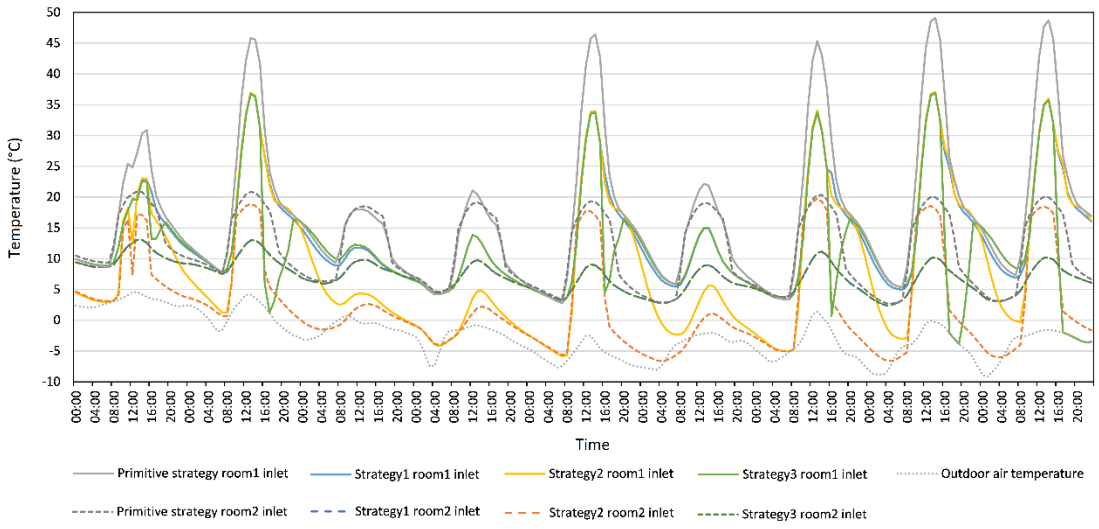

Figure 36. The ventilation inlet air temperature of the PCMVW using different control strategies during 5th February-13th February.

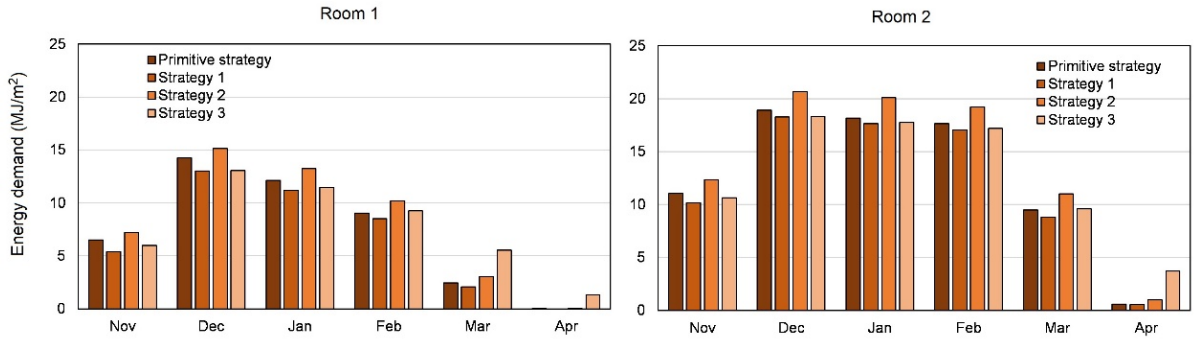

Figure 37 The energy demand using different control strategies for winter solar energy storage application.

Figure 37 shows the monthly energy demand of models using different control strategies for winter solar energy storage application. It shows that compared to the primitive strategy, strategy 1 has the least energy demand for all the simulated months. The primitive control strategy has the highest inlet air temperature. However, it is lacking in the overheating preventing mode, which potentially increased the cooling energy demand. Strategy 2 has the highest energy demand for all the simulated months. The reason is that for both rooms, strategy 2 has the lowest ventilation inlet air temperature, due to the heat in the window cavity is not added into the ventilation. Compared to the primitive strategy, the developed control strategy (strategy 1) saves 9.4% of the energy for the room with windows facing southwest, and 4.4% of the energy for the room with windows facing northeast.

The control strategy development of summer night cooling application has more improvement in energy efficiency than winter solar energy storage application. The potential reason may be that the amount of heat from the solar radiation is limited during winter, so that the PCM is not heated up at very high temperatures in most of the days. However, the air from the PCM heat exchanger is still much higher than the outdoor air temperature. Overall, the winter application is more robust regardless of what control strategy is used.

5. Conclusions

This paper proposed a PCM enhanced ventilated window (PCMVW) system for ventilation pre-treatment purposes. The system works in both summer and winter with different control strategies. In the summer night cooling application, the PCM decreases its temperature by night ventilation, and later it is used for ventilation pre-cooling purpose, by cooling down the high temperature ventilated air during the daytime. In winter solar energy storage application, the PCM stores solar energy during a sunny day, and it is later used for ventilation preheating, by heating up the low temperature ventilated air (mostly during the night time). This paper aims to study the working principle of the PCMVW and to provide sufficient control strategies for Danish buildings using the PCMVW ventilation system.

The numerical model built in EnergyPlus is validated by a full-scale experiment conducted in 3 parts: Summer night cooling application, winter solar energy storage application and blinds with advanced VW control including natural ventilation for self-cooling and mechanical ventilation. The comparisons of the experiment results and simulation data show that the models fit with the experimental data in all aspects. The summer night cooling model has higher accuracy than the winter energy storage model and models with absorption/reflection blinds.

Some conclusions are drawn when comparing the PCMVW with 2 other ventilation systems to test its thermal and energy performance. Compared to the no VW, no PCM system and the VW, no PCM system, the PCMVW for summer night cooling application reduces the cooling energy demand by 46% and 27% respectively for room 1, and 51% and 38% respectively for room 2; for winter solar energy storage application, the PCMVW reduces the heating energy demand by 29% and 48% respectively for room 1, and 10% and 28% respectively for room 2.

The conclusions for control strategy development under Danish weather conditions are:

The developed control strategy for summer night cooling application is to use between-glass reflection shading, ventilate directly from PCM heat exchanger to the room while applying VW self-cooling for ventilation pre-cooling mode, and heat the room with air from VW to prevent overcooling of the room. The model chose different modes based on the indoor temperature sensor. Compared to the primitive strategy, the developed control strategy saves 62.3% of the energy for the room with windows facing southwest, and 58.2% of the energy for the room with windows facing northeast.

The developed control strategy for winter solar energy storage application is to use between-glass absorption blind, make use of the hot air in VW, and to cool the VW by self-cooling and bypass ventilation to prevent the overheating of the room. Compared to the primitive strategy, the developed control strategy saves 9.4% of the energy for the room with windows facing southwest, and 4.4% of the energy for the room with windows facing northeast.

The orientations of the windows have no influence on the results of the developed control strategy. However, it has a big influence on the room's energy demand. The room with southwest facing windows has higher energy savings compared to the room with northeast facing windows. Moreover, the control strategy development of summer night cooling application has more improvement in energy efficiency than winter solar energy storage application. However, the energy demands among different control strategies have no significant differences except for the primitive control strategy for summer night cooling application. In general, the energy saving potential of PCMVW is robust regardless of the control strategies, especially for winter solar energy storage application.

Acknowledgment

The EU Horizon 2020 research and innovation program under grant agreement NO. 768576(ReCO2ST) supported this work.

Reference

[1] N. Soares, J.J.J. Costa, A.R.R. Gaspar, P. Santos, Review of passive PCM latent heat thermal energy storage systems towards buildings' energy efficiency, Elsevier, 2013. doi:10.1016/j.enbuild.2012.12.042.

[2] M. Pomianowski, P. Heiselberg, Y. Zhang, Review of thermal energy storage technologies based on PCM application in buildings, Energy and Buildings. 67 (2013) 56–69. doi:10.1016/j.enbuild.2013.08.006.

[3] F. Kuznik, J. Virgone, K. Johannes, In-situ study of thermal comfort enhancement in a renovated building equipped with phase change material wallboard, Renewable Energy. 36 (2011) 1458–1462. doi:10.1016/j.renene.2010.11.008.

[4] Y. Zhang, K. Lin, Y. Jiang, G. Zhou, Thermal storage and nonlinear heat-transfer characteristics of PCM wallboard, Energy and Buildings. 40 (2008) 1771–1779. doi:10.1016/j.enbuild.2008.03.005.

[5] H. Liu, H.B. Awbi, Performance of phase change material boards under natural convection, Building and Environment. 44 (2009) 1788–1793. doi:10.1016/j.buildenv.2008.12.002.

[6] P.K.S. Rathore, S.K. Shukla, An experimental evaluation of thermal behavior of the building envelope using macroencapsulated PCM for energy savings, Renewable Energy. 149 (2020) 1300–1313. doi:10.1016/J.RENENE.2019.10.130.

[7] H. Wang, W. Lu, Z. Wu, G. Zhang, Parametric analysis of applying PCM wallboards for energy saving in high-rise lightweight buildings in Shanghai, Renewable Energy. 145 (2020) 52–64. doi:10.1016/J.RENENE.2019.05.124.

[8] J. Yu, Q. Yang, H. Ye, Y. Luo, J. Huang, X. Xu, W. Gang, J. Wang, Thermal performance evaluation and optimal design of building roof with outer-layer shape-stabilized PCM,

Renewable Energy. 145 (2020) 2538–2549. doi:10.1016/J.RENENE.2019.08.026.

[9] M. Pomianowski, P. Heiselberg, R.L. Jensen, R. Cheng, Y. Zhang, A new experimental method to determine specific heat capacity of inhomogeneous concrete material with incorporated microencapsulated-PCM, Cement and Concrete Research. 55 (2014) 22–34. http://linkinghub.elsevier.com/retrieve/pii/S0008884613001981 (accessed May 2, 2018).

[10] R. Cheng, M. Pomianowski, X. Wang, P. Heiselberg, Y. Zhang, A new method to determine thermophysical properties of PCM-concrete brick, Applied Energy. 112 (2013) 988–998. doi:10.1016/j.apenergy.2013.01.046.

[11] M. Pomianowski, P. Heiselberg, R.L. Jensen, R. Lund Jensen, Dynamic heat storage and cooling capacity of a concrete deck with PCM and thermally activated building system, Energy and Buildings. 53 (2012) 96–107. doi:10.1016/j.enbuild.2012.07.007.

[12] K.A.R. Ismail, J.R. Henríquez, Parametric study on composite and PCM glass systems, Energy Conversion and Management. 43 (2002) 973–993. doi:10.1016/S0196-8904(01)00083-8.

[13] K.A.R. Ismail, C.T. Salinas, J.R. Henriquez, Comparison between PCM filled glass windows and absorbing gas filled windows, Energy and Buildings. 40 (2008) 710–719. doi:10.1016/j.enbuild.2007.05.005.

[14] H. Weinlaeder, W. Koerner, M. Heidenfelder, Monitoring results of an interior sun protection system with integrated latent heat storage, Energy and Buildings. 43 (2011) 2468–2475. doi:10.1016/J.ENBUILD.2011.06.007.

[15] H. Johra, P. Heiselberg, Influence of internal thermal mass on the indoor thermal dynamics and integration of phase change materials in furniture for building energy storage: A review, Renewable and Sustainable Energy Reviews. 69 (2017) 19–32.

doi:10.1016/J.RSER.2016.11.145.

[16] H. Johra, P. Heiselberg, J. Le Dréau, Influence of envelope, structural thermal mass and indoor content on the building heating energy flexibility, Energy and Buildings. 183 (2019) 325–339. doi:10.1016/j.enbuild.2018.11.012.

[17] H. Weinlaeder, W. Korner, B. Strieder, A ventilated cooling ceiling with integrated latent heat storage-Monitoring results, Energy and Buildings. 82 (2014) 65–72. doi:http://dx.doi.org/10.1016/j.enbuild.2014.07.013.

[18] R. Ansuini, R. Larghetti, A. Giretti, M. Lemma, Radiant floors integrated with PCM for indoor temperature control, Energy and Buildings. 43 (2011) 3019–3026. doi:10.1016/J.ENBUILD.2011.07.018.

[19] X. Jin, X. Zhang, Thermal analysis of a double layer phase change material floor, Applied Thermal Engineering. 31 (2011) 1576–1581. doi:10.1016/j.applthermaleng.2011.01.023.

[20] A. De Gracia, L. Navarro, A. Castell, L.F. Cabeza, L.F. Cabeza, Numerical study on the thermal performance of a ventilated facade with PCM, Applied Thermal Engineering. 61 (2013) 372–380. doi:10.1016/j.applthermaleng.2013.07.035.

[21] Y. Hu, P. Heiselberg, A new ventilated window with PCM heat exchanger – performance analysis and design optimization, Energy and Buildings. 169 (2018) 185–194. doi:10.1016/j.enbuild.2018.03.060.

[22] F. Motte, G. Notton, C. Lamnatou, C. Cristofari, D. Chemisana, Numerical study of PCM integration impact on overall performances of a highly building-integrated solar collector, Renewable Energy. 137 (2019) 10–19. doi:10.1016/J.RENENE.2017.12.067.

[23] J.R. Turnpenny, D.W. Etheridge, D.A. Reay, Novel ventilation cooling system for reducing air conditioning in buildings.: Part I: testing and theoretical modelling, Applied Thermal

Engineering. 20 (2000) 1019–1037. doi:10.1016/S1359-4311(99)00068-X.

[24] D.J. Morrison, S.I. Abdel-Khalik, Effects of phase-change energy storage on the performance of air-based and liquid-based solar heating systems, Solar Energy. 20 (1978) 57–67. doi:10.1016/0038-092X(78)90141-X.

[25] S. Canbazoğlu, A.S. Şahinaslan, A. Ekmekyapar, Ý. Gökhan Aksoy, F. Akarsu, Enhancement of solar thermal energy storage performance using sodium thiosulfate pentahydrate of a conventional solar water-heating system, Energy and Buildings. 37 (2005) 235–242. doi:10.1016/j.enbuild.2004.06.016.

[26] M.J. Huang, P.C. Eames, S. McCormack, P. Griffiths, N.J. Hewitt, Microencapsulated phase change slurries for thermal energy storage in a residential solar energy system, Renewable Energy. 36 (2011) 2932–2939. doi:10.1016/J.RENENE.2011.04.004.

[27] D. Appelfeld, C.S. Hansen, S. Svendsen, Development of a slim window frame made of glass fibre reinforced polyester, Energy and Buildings. (2010). doi:10.1016/j.enbuild.2010.05.028.

[28] M. Liu, P.K. Heiselberg, O.K. Larsen, L. Mortensen, J. Rose, Investigation of Different Configurations of a Ventilated Window to Optimize Both Energy Efficiency and Thermal Comfort, Energy Procedia. 132 (2017) 478–483. doi:10.1016/j.egypro.2017.09.660.

[29] J. Tanimoto, K.I. Kimura, Simulation study on an air flow window system with an integrated roll screen, Energy and Buildings. 26 (1997) 317–325. doi:10.1016/S0378-7788(97)00012-1.

[30] J. Wei, J. Zhao, Q. Chen, Optimal design for a dual-airflow window for different climate regions in China, Energy and Buildings. 42 (2010) 2200–2205. doi:10.1016/j.enbuild.2010.07.016.

[31] T. tai Chow, Z. Lin, K. fai Fong, L. shun Chan, M. miao He, Thermal performance of natural airflow window in subtropical and temperate climate zones - A comparative study, Energy Conversion and Management. 50 (2009) 1884–1890. doi:10.1016/j.enconman.2009.04.028.

[32] D. Appelfeld, S. Svendsen, Experimental analysis of energy performance of a ventilated window for heat recovery under controlled conditions, Energy and Buildings. 43 (2011) 3200–3207. doi:10.1016/J.ENBUILD.2011.08.018.

[33] J.S. Carlos, H. Corvacho, Evaluation of the performance indices of a ventilated double window through experimental and analytical procedures: SHGC-values, Energy and Buildings. 86 (2015) 886–897. doi:10.1016/j.enbuild.2014.11.002.

[34] J.S. Carlos, Optimizing the ventilated double window for solar collection, Solar Energy. 150 (2017) 454–462. doi:10.1016/j.solener.2017.04.063.

[35] J.S. Carlos, H. Corvacho, P.D. Silva, J.P. Castro-Gomes, Real climate experimental study of two double window systems with preheating of ventilation air, Energy and Buildings. 42 (2010) 928–934. https://www.sciencedirect.com/science/article/pii/S0378778810000095 (accessed August 21, 2019).

[36] Y. Hu, P. Heiselberg, R. Guo, Ventilation cooling/heating performance of a PCM enhanced ventilated window - an experimental study, Energy and Buildings. Accepted (2020) 109903. doi:10.1016/j.enbuild.2020.109903.

[37] Schild P.G., Mysen M., Technical note AIVC 65: Recommendations on Specific Fan Power and Fan System Efficiency, 2009. https://www.aivc.org/resource/tn-65-recommendations-specific-fan-power-and-fan-system-efficiency (accessed November 28, 2019).

[38] Y. Hu, P. Heiselberg, H. Johra, R. Guo, Experimental and numerical study of a PCM solar air heat exchanger and its ventilation preheating effectiveness, Renewable Energy. 145

(2019) 106–115. doi:10.1016/J.RENENE.2019.05.115.

[39] Wittchen, Kim Bjarne, Vurdering af potentialet for varmebesparelser i eksisterende boliger, 2004. https://sbi.dk/Pages/Vurdering-af-potentialet-for-varmebesparelser-i-eksisterende-boliger.aspx (accessed April 3, 2019).

[40] R. Jensen, J. Nørgaard, O. Daniels, R. Justesen, Person- og forbrugsprofiler: bygningsintegreret energiforsyning, 2011.

Appendix E. Paper 5

Y. Hu, R. Guo, H. Johra, P. Heiselberg, Temperature hysteresis of phase change materials and its impact on building modeling. Building simulation: an international journal; Submitted. Reprinted by the permission of the Editor of the Journal.

Building Simulation: an International Journal

(Under review)

Temperature hysteresis of phase change materials and its impact on building modeling

Yue Hu*, Rui Guo, Hicham Jorha, Per Kvols Heiselberg

Aalborg University, Division of Architectural Engineering, Department of Civil Engineering, Thomas Manns Vej 23, DK-9220 Aalborg Øst, Denmark

Abstract

Applying phase change material (PCM) into thermal energy storage (TES) for latent heat storage in sustainable building systems has recently gained increasing attention. However, the temperature hysteresis of the melting/solidification cycle of certain PCM has not been fully understood. As a result, the impact of this phenomenon has been mostly neglected regarding the modeling of building energy systems. This paper firstly looks into the phenomenon of hysteresis, its causes and modeling challenges associated with it. The article then analyzes the thermal and energy performance of models using PCMs with different phase transition temperatures and degrees of hysteresis for distinct summer and winter applications. A sensitivity analysis is conducted to compare which parameter has more influence on the building HVAC energy demand and indoor thermal comfort. The results show that the hysteresis degree has more influence on both the HVAC energy demand and the thermal comfort than the phase transition

temperature, for all seasons of the year. The paper ends with specific suggestions for the selection of PCM based on the purpose of the application.

Keywords: Phase Change Material, temperature hysteresis, PCM modeling, building simulation

1. Introduction

Buildings have a predominant role in our modern society. Indeed, people living in industrial countries typically spend more than 90% of their time indoors (Höppe 2002). Buildings are intended to protect the occupants from the outdoor weather conditions and provide a comfortable environment. Humans are especially sensitive to ambient temperature. They will easily experience thermal discomfort if the indoor temperature is not maintained within a narrow temperature range (U.S. Green Building Council 2005) without rapid transient change of the operative temperature (ASHRAE Standard 2004). In addition, the building sector is the largest energy end-user in the world (International Energy Agency 2013). Therefore, diminishing indoor space heating and cooling needs have been clearly identified as a key target for the reduction of global energy use and CO_2 emissions (European Parliament 2010). Moreover, buildings can modulate their energy profile to a certain extent by shifting their power load in time. The energy storage capacity of buildings or clusters of buildings can thus be employed to perform demand-side management and building energy flexibility strategies which can greatly improve the efficiency, stability and reliability of Smart Energy Grids with a large share of intermittent renewable energy sources (Jensen et al. 2017).

With regard to the aforementioned matters, phase change materials (PCM) at near-room temperatures (10 °C - 30 °C) have drawn considerable attention over the last decade (Pomianowski et al. 2013b). Unlike materials experiencing only sensible heat storage (under normal environmental conditions), a PCM operates a phase transition (change in the microstructure of the material) at near ambient temperature. This phase transition requires a considerable amount of thermal energy (latent heat) but occurs with a very limited temperature variation. The latent heat thermal energy storage (LHTES) ability of the PCM is a great asset for high-density thermal storage at a constant temperature in building systems. Indeed, PCM for building applications has volumetric heat storage capacities which are typically 5 to 14 times greater than sensible heat storage materials such as water or concrete (Sharma et al. 2009).

The primary application for PCM in buildings is to increase the effective thermal inertia of the built environment. It can greatly help to improve the indoor temperature stability, thus reducing risks of

overheating, and attenuating peaks of heating and cooling power demand. Many experimental tests have been carried out for PCM wallboards which can be easily installed on the inner surfaces of walls and ceilings (Kuznik et al. 2008) (Medina et al. 2008) (Diaconu and Cruceru 2010), or in-floor elements (Xu et al. 2005) (El Mays et al. 2017). Building components can be manufactured from stable-form PCM products incorporated in a polymer matrix (DuPontTM 2007 Data Sheet), or by mixing the PCM directly with construction materials such as concrete (Pomianowski et al. 2013a) (Pomianowski et al. 2012), plaster (Carbonaro et al. 2015) (Kusama and Ishidoya 2017), or bricks (Zhang et al. 2011) (Hichem et al. 2013). PCM can also be contained in translucent window systems (Weinläder et al. 2005), double-skin façades (de Gracia et al. 2018), or internal shutters and solar shadings (Weinlaeder et al. 2011) (Alawadhi 2012). Passive building solar collector systems such as Trombe walls can also benefit from the additional thermal energy storage capacity of the PCM (Soares et al. 2013). Some researchers suggested that PCM can be integrated into furniture elements and provide significant supplementary heat storage to the indoor space of light-weight structure buildings (Johra and Heiselberg 2017). Alternatively, LHTES can be directly incorporated in HVAC systems such as hot water storage tanks of heat pump (Pardiñas et al. 2017) and solar heating systems (Kee et al. 2018), or ventilation air conditioning units (Kabeel and Abdelgaied 2018) (Mosaffa and Garousi Farshi 2016) (Fleming et al. 2013). Additionally, it was found that the integration of PCM elements in the indoor environment of light-weight structure buildings could greatly increase their effective thermal inertia, which contributes to improving the time-shifting of the space heating needs for demand-side management and building energy flexibility strategies (Johra et al. 2018).

The large enthusiasm of the scientific community for PCM applications during the last decades has led to the development of various numerical models for simulating the thermodynamics and heat storage in LHTES systems. However, the accuracy and reliability of PCM numerical models used for building applications are usually too low for proper design and simulation purposes (Kośny 2015). The thermal properties of the materials are rarely known with precision. The latent heat of phase transition is usually derived from Differential Scanning Calorimetry (DSC) measurements of pure PCM products. However, most of the organic PCMs are difficult to purify. They are normally a mixture of the congeneric alkanes.

The main product of interest with a definite phase transition temperature is therefore associated with other alkanes that present different thermal properties and phase transition temperatures. Characterization of the pure PCM solely may thus be insufficient to model realistic materials. In addition, most of the PCM models use average thermal properties (such as specific heat capacity and thermal conductivity) of both melted and solidified phases in the case of the solid-liquid phase transition material. Unfortunately, researchers hardly ever consider, understand, or study the temperature hysteresis phenomenon occurring between the melting and the freezing processes.

The aim of this article is to take a deeper look at the hysteresis phenomenon in PCM and the influence of PCM transition temperature and hysteresis on the building energy efficiency and indoor thermal comfort performances. Firstly, a literature study of the PCM hysteresis is presented, including the causes and the modeling of PCM hysteresis. The article continues with the influence of the PCM phase transition temperature and hysteresis degree on the building energy and thermal comfort performance for both severe winter and summer conditions, and transition seasons. Based on these results, the authors suggest a selection of PCMs for ventilative heating and cooling applications respectively.

2. PCM temperature hysteresis

The thermal properties of the PCM (thermal conductivity and apparent specific heat capacity) have some discrepancies between the melting process and the freezing process (Kuznik and Virgone 2009). The temperature hysteresis is a phenomenon of PCM that characterizes those discrepancies. The properties of the PCM depend on its temperature history (temperature path) and on its occurring phase transition process: melting or freezing process. Figure 1 illustrates this temperature hysteresis phenomenon. One can clearly see that the specific heat capacity curve of the PCM is different for the cases of continuous melting and continuous freezing processes (see Figure 1(a)). The melting and freezing peaks are offset from one another, and the general shape of the two curves is different. Figure 1(b) shows the enthalpy curves of this material in relation to the temperature during similar melting and freezing processes. Here again, the enthalpy paths for melting and freezing are different.

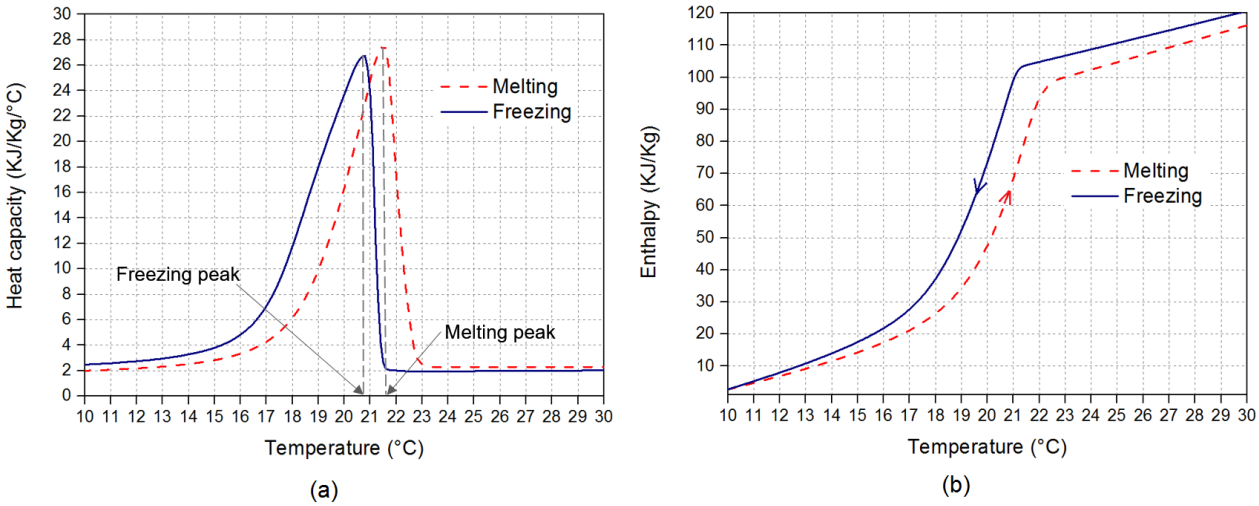

Figure 1 Example of hysteresis for melting and freezing processes. The data is from the DSC test of a paraffin wax at the heating and freezing rate of 0.5 K/min.

Subcooling is observed in the freezing process of certain PCMs. It is one cause of the hysteresis phenomenon. When cooled down, the temperature of the liquid material drops significantly below the melting temperature before any solidification process starts (Heat and cold storage with PCM 2008; Huang et al. 2010 2018). Figure 2(a) shows the temperature change as a function of time when PCM undergoes subcooling during the freezing process. The PCM temperature drops below the phase transition temperature before the freezing process actually starts. Afterward, it rises to the phase change temperature and the phase transition occurs. Figure 2(b) shows the enthalpy curve as a function of temperature during the freezing process. The enthalpy (internal energy) of the PCM is continuously decreasing as cooling is applied, but the temperature of the material drops significantly below the freezing temperature before the solidification actually starts. Figure 2(c) shows the change of heat capacity in the subcooling period. Identically, a lower temperature is reached before the phase change starts. It is therefore quite difficult to identify precisely the evolution of the PCM thermal properties when the latter is cooled down or heated up close to the temperature of phase transition. However, the enthalpy/temperature profile seems to be the best choice for good visualization of the subcooling phenomenon.

Many PCMs show negligible subcooling for macro-containment. However, in the case of micro-containment, the subcooling effect often appears to be more severe, which is due to the slow crystal

growth (Huang et al. 2010). In addition, organic PCMs are usually less susceptible to subcooling and temperature hysteresis effects than inorganic PCMs (Koschenz and Lehmann 2004).

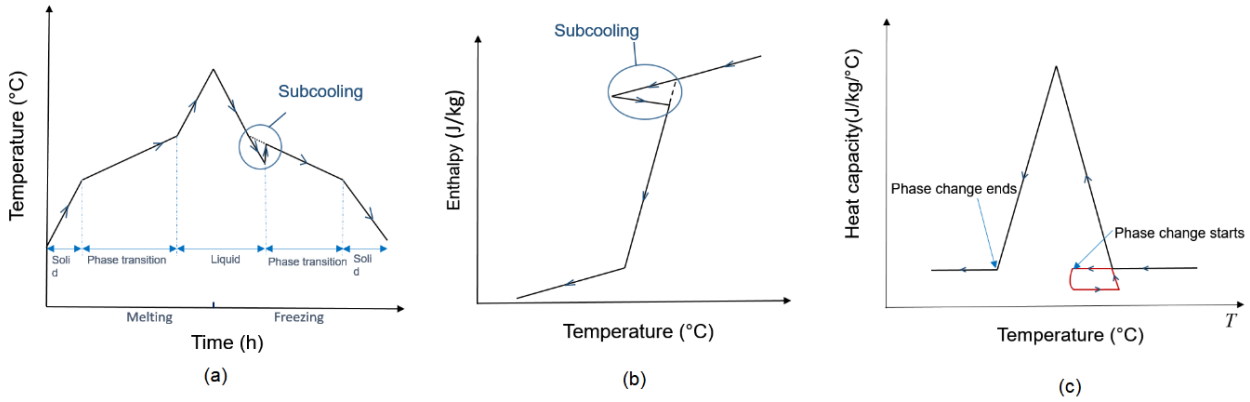

Figure 2 Example of subcooling effect in temperature curve, enthalpy curve, and heat capacity curve based on T-history measurement of mannitol.

The hysteresis, subcooling, and other complex thermal properties of PCM greatly complicate the development of reliable LHTES models for building simulations. It is important to have a better understanding of the hysteresis and subcooling phenomenon and the refinement of the numerical model dealing with these issues.

For PCM in the active building application systems, the thermal response of the PCM is usually 1-8 hours for 20 K according to (Hu and Heiselberg 2018) (Hu et al. 2019), which corresponding to a heating/cooling rate of 0.04 K/min to 0.33 K/min. For passive building applications, the thermal response time could be as long as 12 hours, which corresponding to a heating/cooling rate of 0.03 K/min.

The same PCM measured with different heating/cooling rates can get different hysteresis degrees in the measured result. Decreasing the heating/cooling rate can result in a low hysteresis degree. However, the single enthalpy curve without hysteresis cannot be achieved even with infinitely slow measurement, because of subcooling, incomplete crystallization, or polymorphic crystal structures result in different shapes of heating and cooling curves (Rathgeber et al. 2014). In certain cases, even with the smallest heating/cooling rates, the hysteresis phenomenon can still be observed due to the intrinsic hysteresis of the material.

There is abundant literature showing the hysteresis of PCM with standard measurement methods. Table 1 lists many PCMs and their properties from literature with accurate measurements from PCM manufacturers or independent laboratories. All of them show a certain degree of hysteresis regardless of the different measurement methods and measurement heat rates. For some of them, the hysteresis degree (the temperature difference between melting peak and freezing peak) is 0，but there are still differences between melting and freezing processes. This part of hysteresis should be modeled in building simulations for PCM.

Table 1 The thermal properties and measurement methods of PCMs found in the literature (the hysteresis degree is calculated by the difference between melting peak and freezing peak).

Type	Melting range (℃)	Freezing range (℃)	Melting peak (℃)	Freezing peak (℃)	Temperature hysteresis (℃)	Latent heat (kJ/kg)	Measurement method	Reference
Coconut oil	7.2-22.9	3-12	22.9	7.5	15.4	110	DSC 2 K/min	(Wi et al. 2015)
MePCMs from PG_8H_2-E	23.9-26.9	18.4-23.1	25.54	20.21	5.33	-	DSC 1K/min	(Yin et al. 2018)
Dodecanol	23.8-27.1	18.3-23.2	25.22	20.11	5.11	-	DSC 1K/min	(Yin et al. 2018)
MePCMs from PG_8H_2	23.7-27.2	18.1-22.9	25.14	20.07	5.07	-	DSC 1K/min	(Yin et al. 2018)
Paraffin	23-29	20-25	23	27.7	4.7	179	DSC 2 K/min	(Lamberg et al. 2004)
Paraffin within copolymer	15.1-28.2	9.6-24.5	22.2	17.8	4.4	107.5	DSC 0.05K/min	(Kuznik et al. 2011)
Paraffin within copolymer	12-30	11-28	22.1	17.9	4.2	72.4/71.0	DSC 0.05K/min	(Kuznik and Virgone 2009)

PCM-wallboard	16.8-19.35	16.9-22.1	21.05	16.98	4.07	35	DSC 0.2K/min	(Feldman and Banu 1996)
Q20	16-24	13-18	20	16	4	210-250	DSC	BioPCM
paraffin PCM 6	0-7	-5	3	-0.5	3.5	178	DSC 1K/min	(Sharifi and Sakulich 2015)
C24	24-27	21-23	24	27	3	140	DSC	Climator
Q27	24-30	23-27	27	24	3	210-250	DSC	BioPCM
Q29	27-32	24-27	29	26	3	210-250	DSC	BioPCM
paraffin Microtek 37 D	32-37	29-35	36	33	3	220	DSC 0.15 K/min	(Stathopoulos et al. 2016)
Paraffin hydrocarbon	23-28.5	21-24.9	25.5	22.9	2.6	75	DSC 1K/min	(Takeda et al. 2004)
paraffin PCM 28	15-28	15-22	23	20.5	2.5	161	DSC 1K/min	(Sharifi and Sakulich 2015)
gallium	29.5-30.5	26.9-29	30	27.5	2.5	80	T-history	(Lázaro et al. 2006)
Fatty acid wall board	18.5-24.2	15.0-18.6	20.3	17.9	2.4	39.1	DSC 0.2K/min	(Shilei et al. 2006)
Q23	20-26	18-24	23	21	2	210-250	DSC	BioPCM
Q25	23-28	22-25	25	23	2	210-250	DSC	BioPCM
Paraffin in gypsum board	25-28.5	24-27.5	28	26.5	1.5	75	DSC 2K/min	(Voelker et al.)
gypsum–PCM compound	21-24	20-22.5	24	22.5	1.5		DSC 0.05K/min	(Jaworski et al. 2014)
$C_{13}H_{28}$	-6.7-(-4.5)	-6.3-(-7.9)	-5.6	-7.1	1.5	210	T-history	(Gunasekara et al. 2017)

PCM-plaster compound	24.1-28.5	23.2-27.1	28.12	26.8	1.32	16.5	DSC 1~2K/min	(Weimar 2000)
Hexadecane	16.5-19.5	16.2-17.2	18	16.7	1.3	236	T-history	(Lázaro et al. 2006)
RT27	24.5-28.2	25.0-26.9	27	25.9	1.1	180	T-history	(Lázaro et al. 2006)
HS22P(inorganic)	21-25	-	23	22	1	185	T-history	SavENRG
RT27 (organic paraffin)	26.86-28.69	27.94-26.44	28.37	27.38	0.99	130.8	DSC 1K/min	(Jin et al. 2014)
Butyl stearate	16-20.9	16-20.8	20.9	20.4	0.5	30.7	DSC	(Ahmad et al. 2006)
Emerest 2326	16.69-19.75	16.51-19.6	19.57	19.45	0.12	140	DSC 0.2K/min	(Feldman and Banu 1996)
C21(salt hydrate)	21-26	18-22	21	21	0	134	DSC	Climator
Paraffin RT 25	22-26	23-26	25	25	0	-	DSC 0.2 K/min	(Iten et al. 2017)

There are mainly two approaches currently used by some researchers to model the transition between freezing and melting processes within the phase change range. Bony et al. (Bony and Citherlet 2007) proposed that the enthalpy transition line between the melting process and freezing process is a straight line that parallels to the sensible enthalpy curve. Kaushik et al. (Biswas et al. 2018) suggest that there is no hysteresis shown until the PCM completely solidifies or melts. Then the enthalpy curve changes to another one. When comparing the two models in a building energy simulation (Energy Plus), it is found that the hysteresis does not have a large influence on the annual building energy, but the impact on the surface temperature and zone temperature is considerable (Chandrasekharan 2013). However, this conclusion is only based on one study case. In the following section of this current paper, the influences of the PCM transition temperature and hysteresis degree on building modeling for summer and winter applications are investigated numerically.

3. The effect of phase transition temperature and hysteresis on building thermal and energy performance

To test the influence of the PCM hysteresis on building energy performance, 2 models of ventilated windows with an integrated PCM thermal energy storage (PCMVW) are used for summer applications and winter applications separately. The PCMVW is installed in the southwest façade of a 3-room apartment. For the summer night cooling applications, the PCM thermal energy storage is discharged by the cold outdoor air during the night time. It then pre-cools the supplied fresh air during day time. The PCM thermal energy storage is fully shaded from solar radiation, while the ventilated window is shaded by external shading when the solar radiation is higher than 200 W/m^2. The airflow rate through the PCMVW is based on the people load in the room (30 m^3/h/person). For winter solar energy storage applications, the PCM stores solar energy during the sunny day, and later releases the energy to preheat the inlet fresh air. There is no shading for the PCM thermal energy storage and the ventilated window. The airflow rate is the same as for the summer night cooling applications. The configuration of the PCMVW is shown in Figure 3 (Hu et al. 2020b).

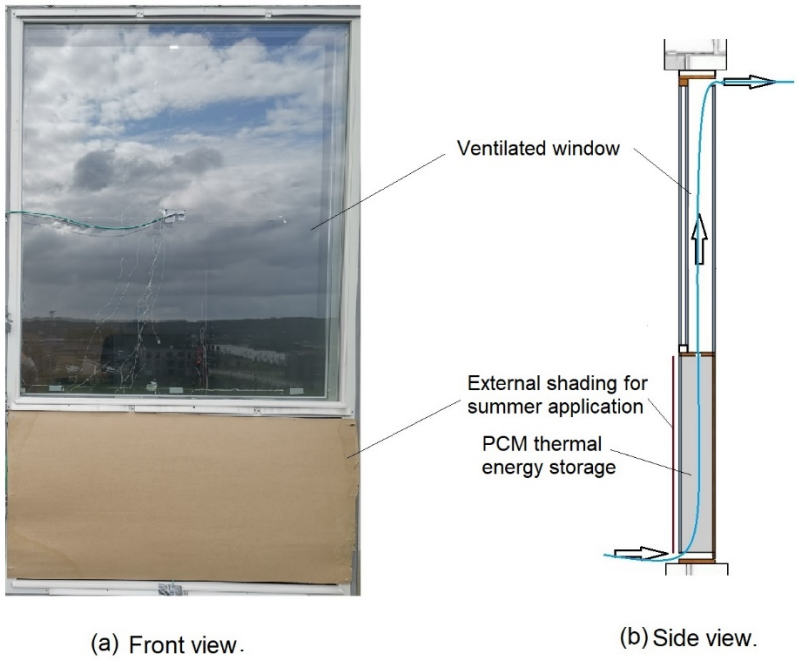

Figure 3 The PCMVW system(Hu et al. 2020).

The models have been validated by full-scale experimental results. For more details please refer to (Hu et al. 2020). In this paper, the summer application operates from 1st May to 31st October under the Danish climate, while the winter application operates from 1st November to 30th April. The air conditioning system only operates during severe summer and severe winter periods, in cases when the PCM thermal energy storage cannot provide enough pre-heated or pre-cooled air. The indoor air temperature setpoint for summer is 26 °C from 1st June to 31st August. For winter it is 22 °C from 1st November to 29th February. It is considered a transition season when there is no operating HVAC.

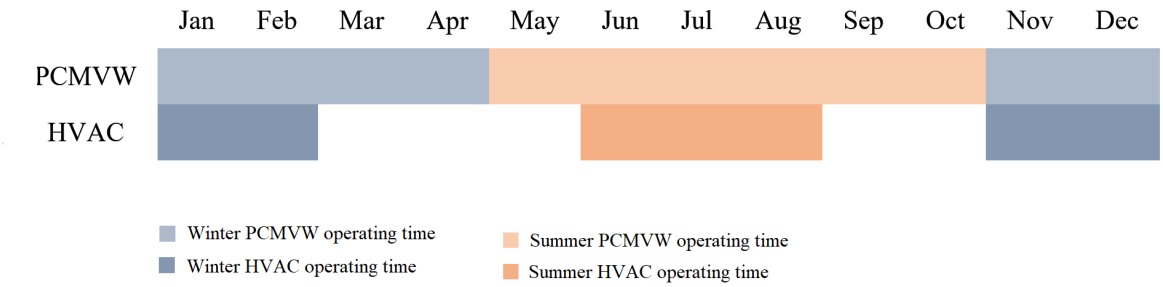

Figure 4 The PCMVW and HVAC operation schedule.

A local sensitivity analysis is conducted to determine which parameters have a higher influence on the system energy demand during the severe summer and winter periods. The sensitivity analysis is performed by the methodology (Heiselberg et al. 2009) (Silva and Ghisi 2020):

1. Define input variables with their variation ranges.
2. Set variation level m for each input variable in a discrete distribution.
3. Using a one-parameter-at-a-time (OAT) method to generate $p = m \times n$ observations, where n is the number of input variables.
4. Obtain output variables by conducting n simulations.
5. Visualize the output distribution.
6. Assess the importance of each input parameter to the output by calculating the sensitivity index, which is calculated by the equation below:

$$SI_i = \frac{E_{\max,i} - E_{\min,i}}{E_{\max}}$$

Where SI_i is the local sensitivity index; $E_{max,i}$ and $E_{min,i}$ is the maximum and minimum outputs corresponding to the ith input; E_{max} is the maximum global outputs among all the inputs of all the variables.

In this case, the input parameters are the phase transition temperature and hysteresis degree, and the outputs are the summer cooling energy demand, winter heating energy demand and total heating+cooling energy demand of the room.

For the transition seasons, the HVAC is not operating. The PCMVW is supposed to cover the heating and cooling energy demand of the model. The system's performance is then evaluated with the predicted percentage of dissatisfied (PPD) proposed by Fanger (Fanger 1972). The lower the PPD, the better is the indoor environment quality.

3.1. Severe summer and winter conditions

The study continues with the PCM phase transition temperature and hysteresis degrees and their influences on the PCM temperature and room energy demand for severe summer and winter conditions.

For summer night cooling applications during the severe summer condition, 6 PCMs with different phase transition temperatures (no hysteresis) are firstly studied. The latent heat, heat conductivity and other properties are all the same. Figure 5 shows some of the PCM temperatures from those cases. There are large differences in the PCM temperature profiles for PCMs with different phase transition temperatures. For the days with low average daily outdoor air temperature, the PCM with low phase transition temperature has a more stable temperature profile and a relatively low temperature during the daytime. For the days with high average daily outdoor air temperature, the PCM with high phase transition temperature has a more stable temperature profile and a relatively low temperature during the daytime. For PCM with a 21 °C phase transition temperature, the PCM temperature is more stable than PCM with 25 °C for most of the days. It is because the average outdoor air temperature is much closer

to 21 °C, so that the PCM with a 21 °C phase transition temperature is more activated than with a 25 °C phase transition temperature.

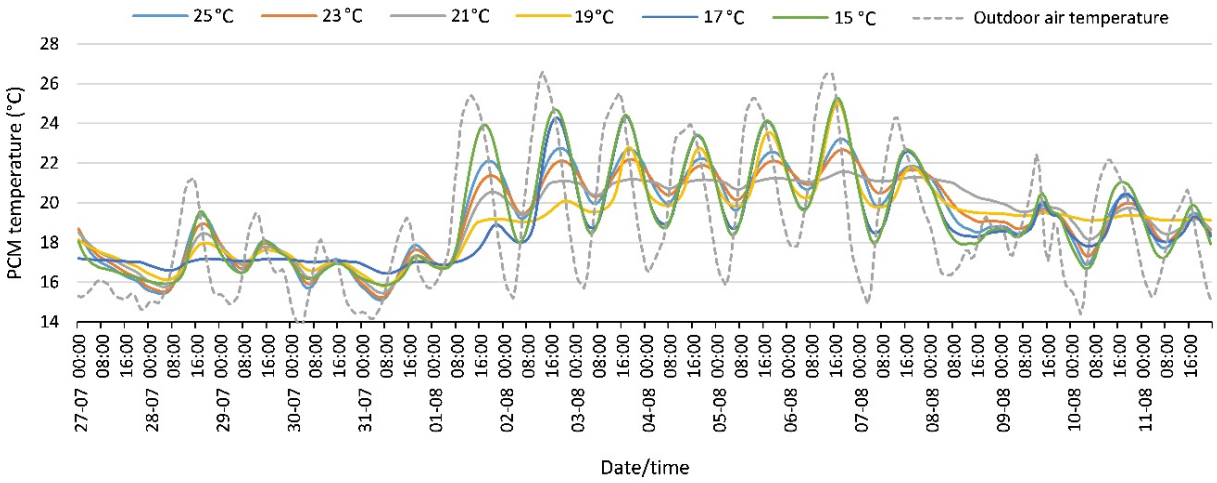

Figure 5 The PCM temperature for cases with different phase transition temperatures for summer night cooling application.

Figure 6 shows the daily energy demand from cases using PCM with different phase transition temperatures during the summer period. For some days the model with a 21 °C phase transition has the lowest energy demand, especially at the beginning of August, when the outdoor air temperature is relatively high. While for some other days the model with a 15 °C phase transition has the lowest energy demand, for example, 8th August - 10th August when the outdoor air temperature is relatively low. For the whole severe summer period (1st June - 31st August), the total energy demand presents an increasing trend with the increase of phase transition temperature. However, the increasing rate is not so high. It increases by 1% (from 365.63MJ to 369.38MJ) when the phase transition temperature increases from 15 °C to 25 °C.

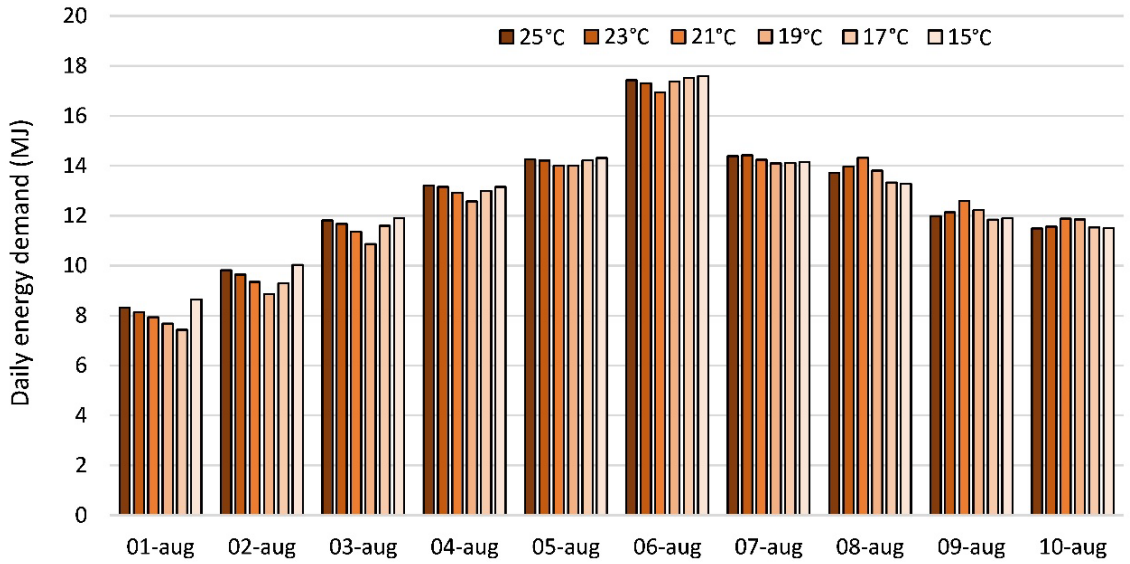

Figure 6 The daily energy demand of cases using PCMs with different phase transition temperatures for summer night cooling application.

Figure 7 shows the PCM temperature profiles for cases using PCM with different hysteresis degrees. It shows that PCM with no hysteresis has the most stable temperature profile and lowest temperature during the daytime for most of the days. PCM with a 5 °C hysteresis has the least stable temperature profile and the highest temperature during the daytime for most of the days. Figure 8 shows the daily energy demand of cases using PCMs with different hysteresis degrees. For most of the days, the case with no hysteresis has a lower energy demand than with a 5 °C hysteresis. For the total run period (1st June - 31st August), the total energy demand increased by 14.5% (from 369.09 MJ to 431.75 MJ) when the hysteresis degree increases from 0 °C to 5 °C.

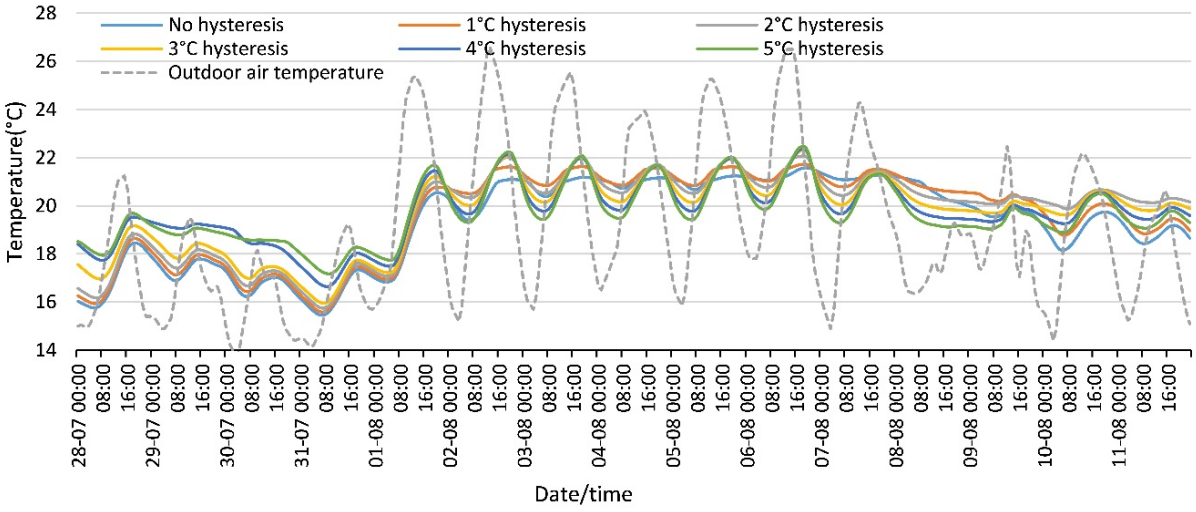

Figure 7 The PCM temperature profiles for cases using PCMs with different hysteresis degrees for summer night cooling applications.

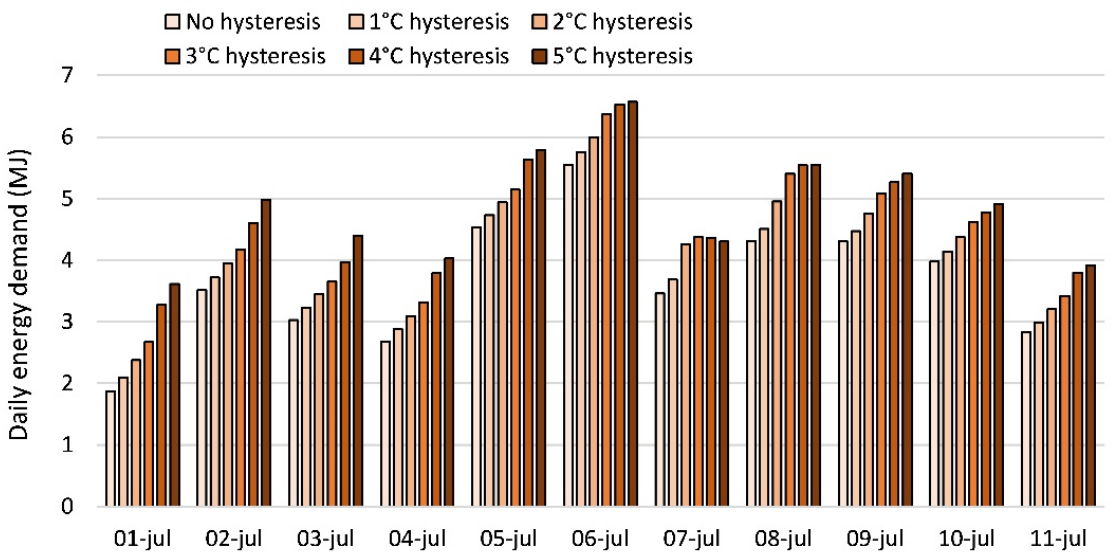

Figure 8 The daily energy demand of cases using PCMs with different hysteresis degrees for summer night cooling applications.

For winter solar energy storage applications, the influence on building energy demand of the 6 PCMs with the same latent heat but different phase transition temperatures is studied first. Next, the studies carry on with the PCMs with different hysteresis.

Figure 9 shows the PCM temperature of cases with different phase transition temperatures for winter solar energy storage applications. For the days with high solar radiation, the PCM with a higher phase transition temperature has a higher temperature during the night time. There is no significant difference regarding the PCM temperature when solar radiation is low. Figure 10 shows the daily energy demand of cases using PCMs with different phase transition temperatures for winter energy storage applications. PCM with a 15 °C phase transition temperature has the lowest energy demand for most of the days. There is no significant difference for the other days. The total energy demand increased by 1.5% (from 804.48 MJ to 817.05 MJ) when the transition temperature increases from 15 °C to 25 °C during the period 1st November – 29th February.

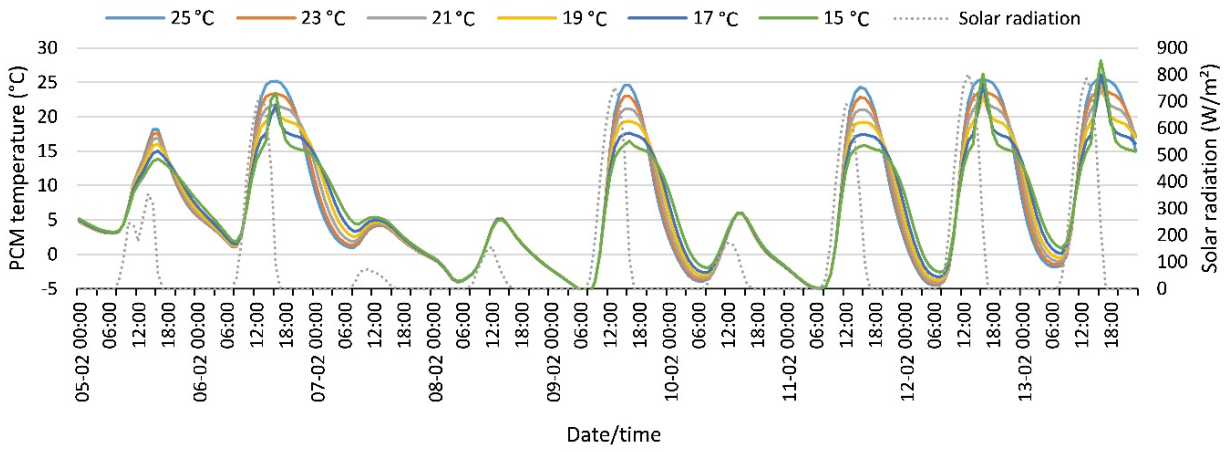

Figure 9 The PCM temperature of models with different phase transition temperatures for winter solar energy storage application.

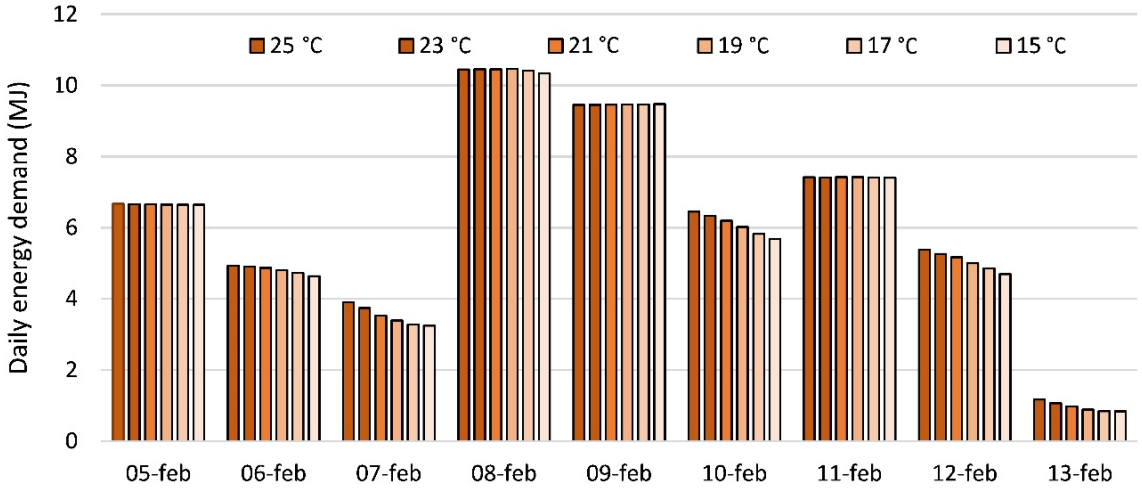

Figure 10 The daily energy demand of models using PCMs with different phase transition temperatures for winter energy storage application.

Figure 11 shows the PCM temperature profiles for cases using PCMs with different hysteresis degrees for winter solar energy storage applications. One can see that PCM with higher hysteresis has a higher temperature. Consequently, PCM with a 5 °C hysteresis has the lowest daily energy demand, as shown in Figure 12. The total energy demand decreases by 10.2% (from 812.62 MJ to 729.47 MJ) when the hysteresis degree increases from 0 °C to 5 °C during the period 1st November – 29th February.

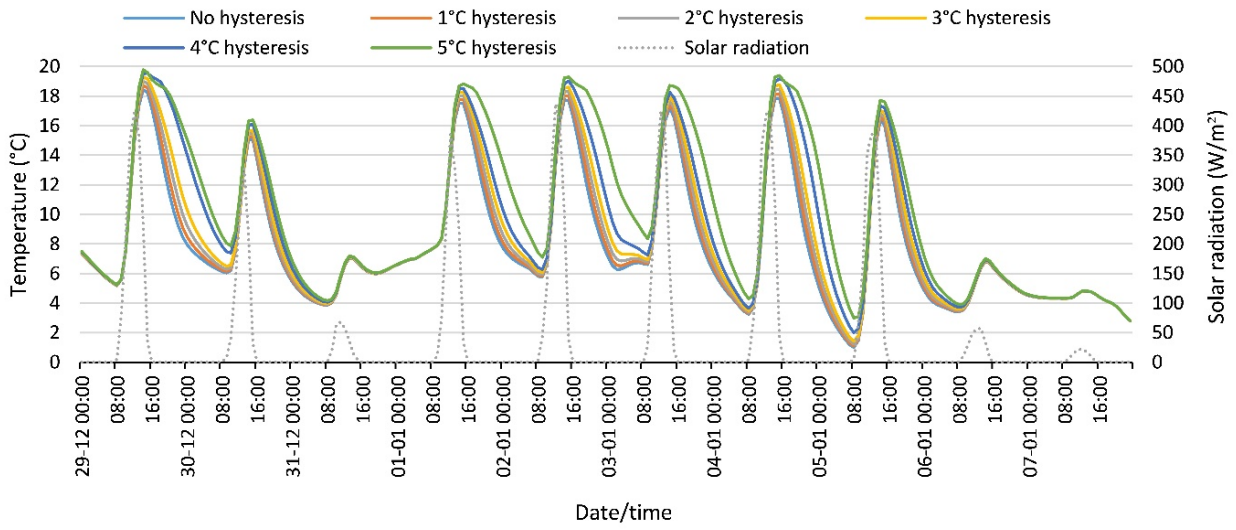

Figure 11 The PCM temperature profiles for models using PCMs with different hysteresis degrees for winter solar energy storage application.

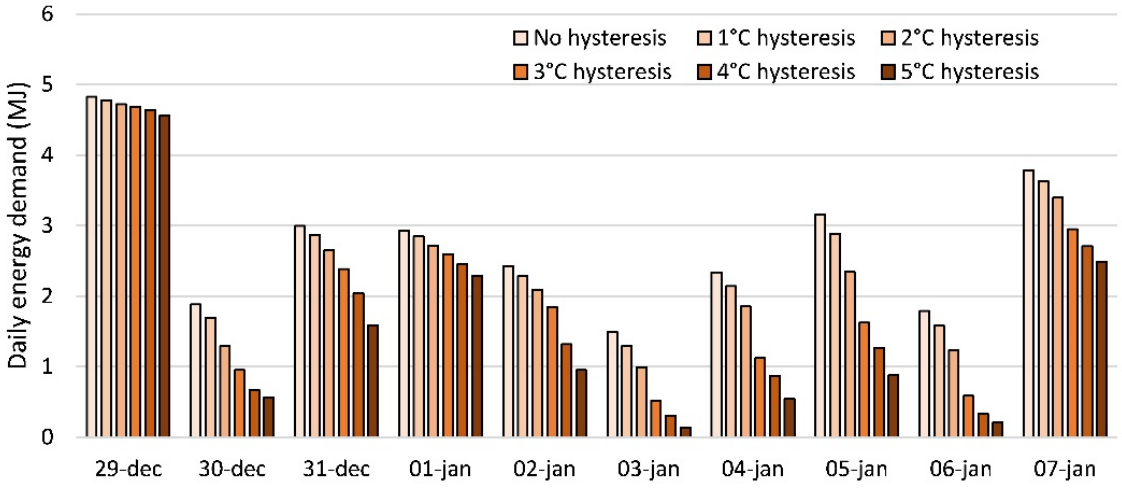

Figure 12 The daily energy demand of cases using PCMs with different hysteresis degrees for winter solar energy storage applications.

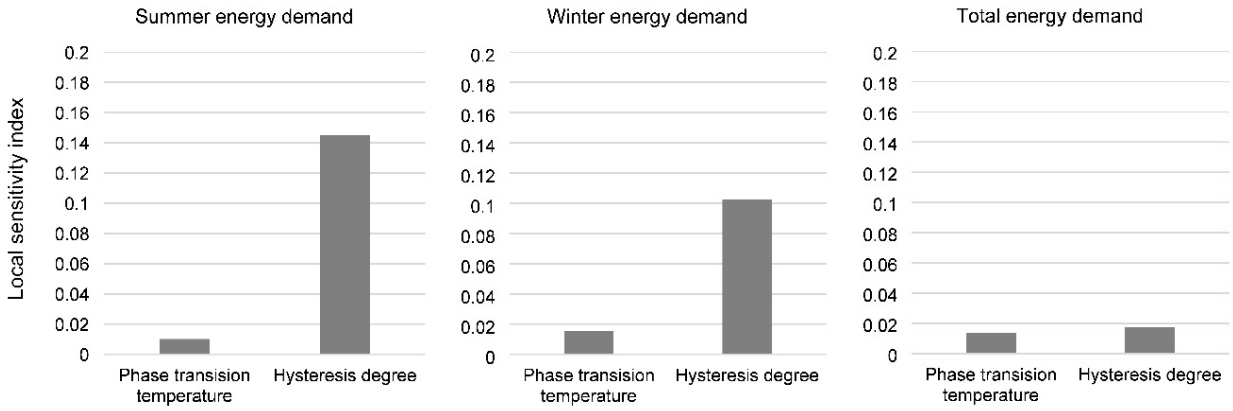

Figure 13 The sensitivity index of phase transition temperature and hysteresis degree on the HVAC energy demand.

The sensitivity analysis is done to determine which variable has a higher impact on the model energy demand. Figure 13 shows the sensitivity indexes of the 2 variables. The figure shows that the hysteresis degree has a high sensitivity index for both summer energy demand and winter energy demand, which are 0.15 and 0.10, respectively. However, for the yearly total energy demand, both phase transition temperature and hysteresis degree have small sensitivity indexes.

3.2. Transition seasons

For transition seasons, the HVAC system is not operating. The PCMVW plays an important role in the indoor thermal comfort. Figure 14 and Figure 15 show the room inlet air temperature from PCMVW using PCMs with different phase transition temperatures for summer and winter transition seasons respectively. The case using PCM with lower transition temperature has a more stable inlet air temperature for summer transition season, but a lower inlet air temperature in winter transition season. However, there is no large difference regarding the PPD for all the simulated cases, as seen in Figure 16. The reason is that the inlet air flow rate is quite low (0.0039 m^3/h).

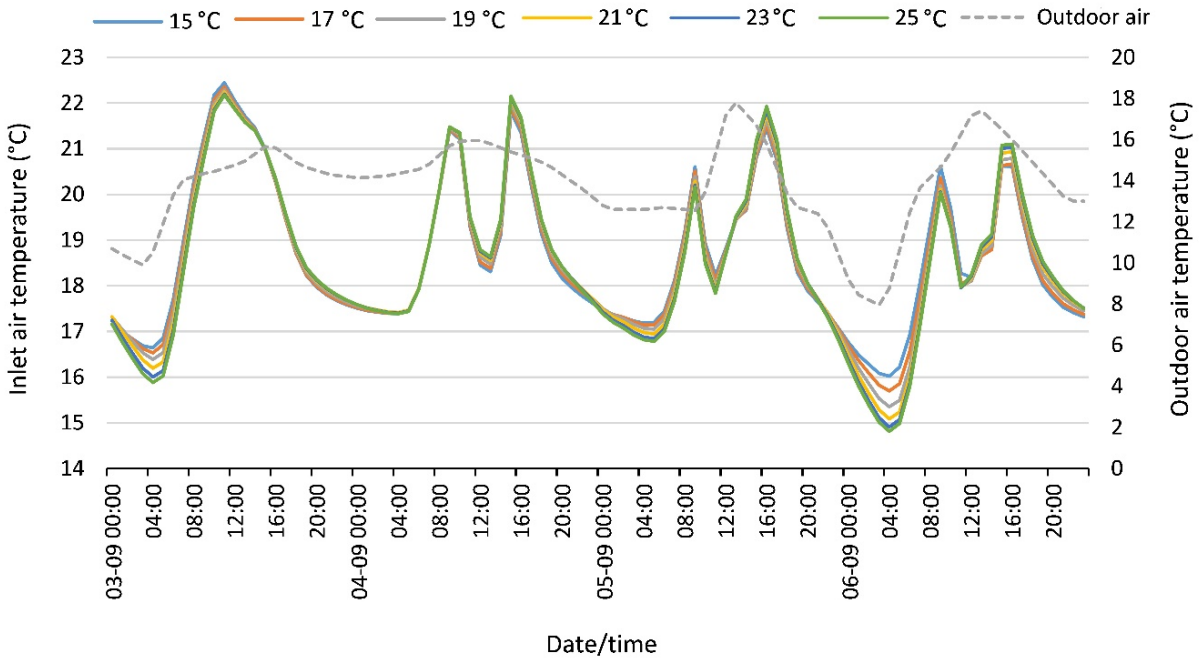

Figure 14 The room inlet air temperature from the PCMVW in relation to phase transition temperature during summer transition season.

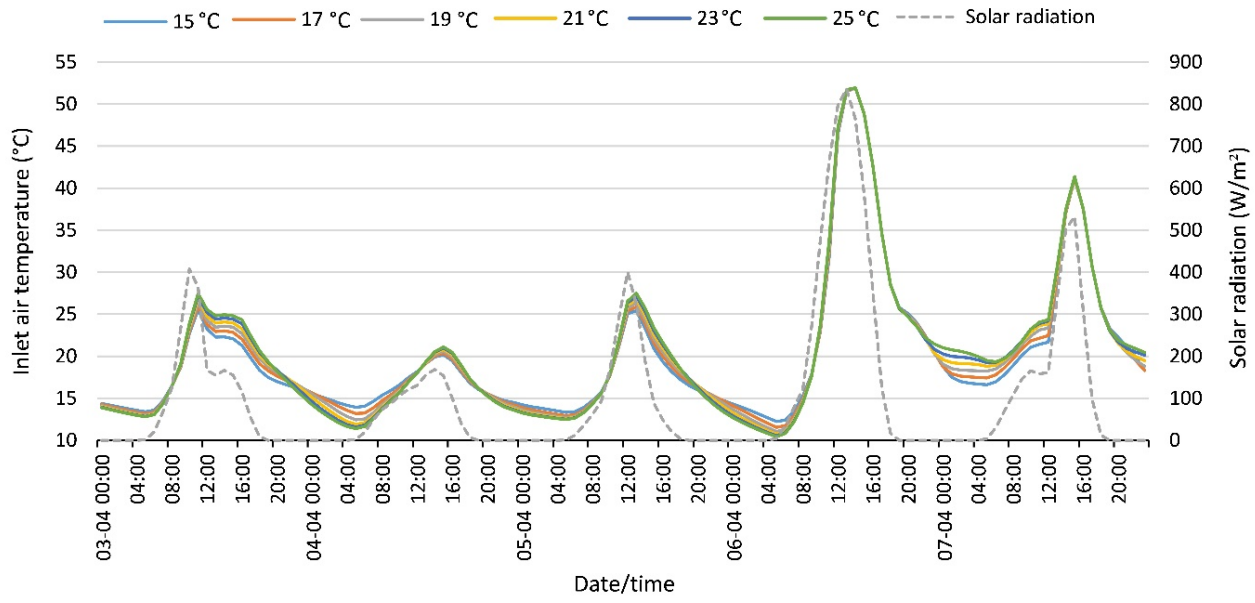

Figure 15 The room inlet air temperature from the PCMVW in relation to phase transition temperature during winter transition season.

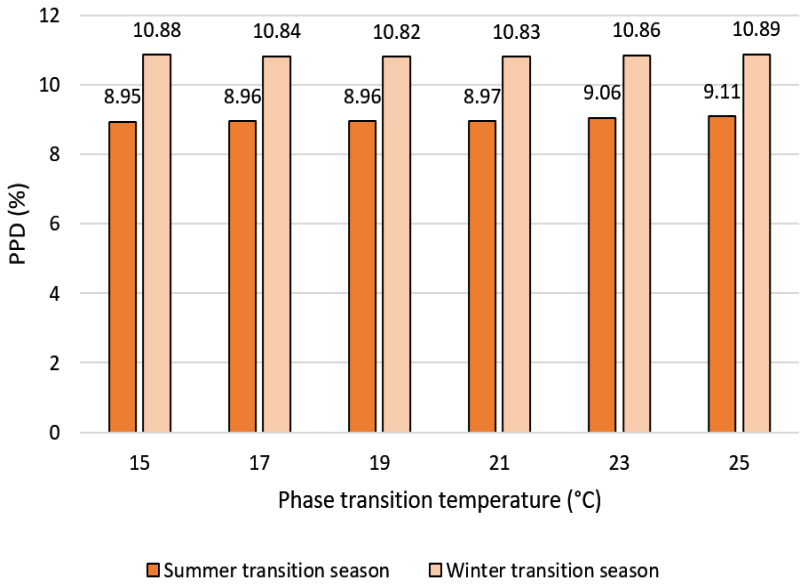

Figure 16 The Predicted Percentage of Dissatisfied (PPD) of the cases using PCMs with different phase transition temperatures in transition seasons.

For cases using PCMs with different hysteresis degrees, there are noticeable differences in the inlet air temperatures (see Figure 17 and Figure 18). Cases using PCM with higher hysteresis have higher inlet air temperatures, for both summer transition season and winter transition season. As a result, the PPD of the cases using PCMs with higher hysteresis is lower, as shown in Figure 19.

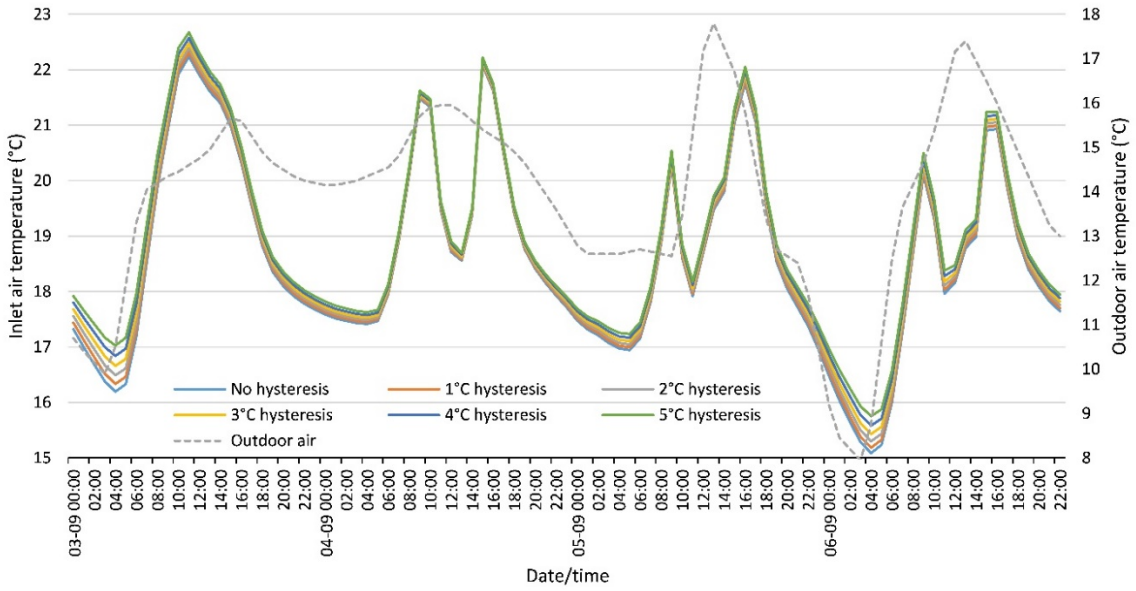

Figure 17 The room inlet air temperature from the PCMVW in relation to hysteresis degree during summer transition season.

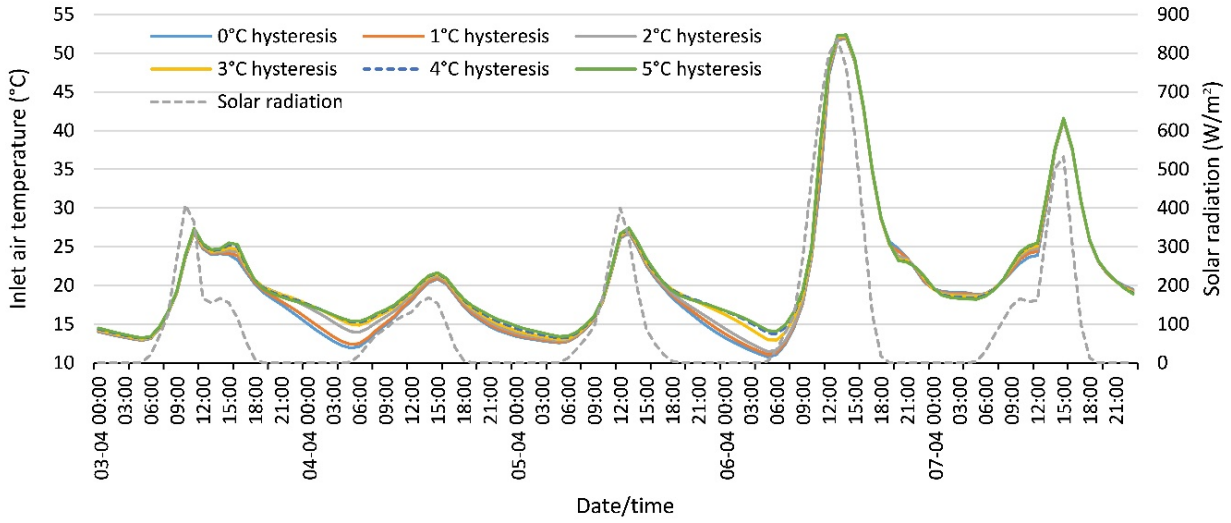

Figure 18 The room inlet air temperature from the PCMVW in relation to hysteresis degree during winter transition season.

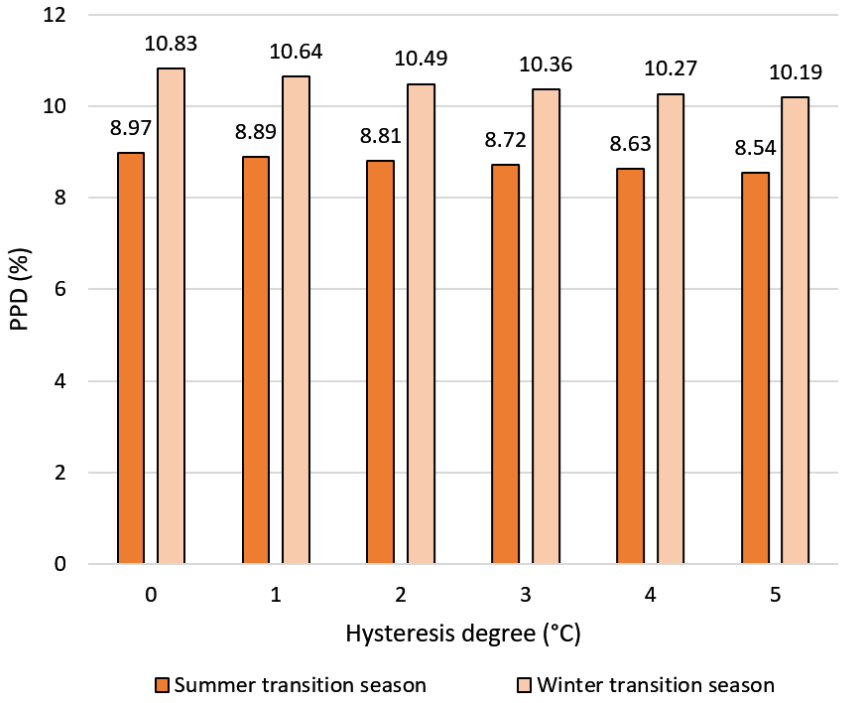

Figure 19 The Predicted Percentage of Dissatisfied (PPD) of the cases using PCMs with different hysteresis degrees in transition seasons.

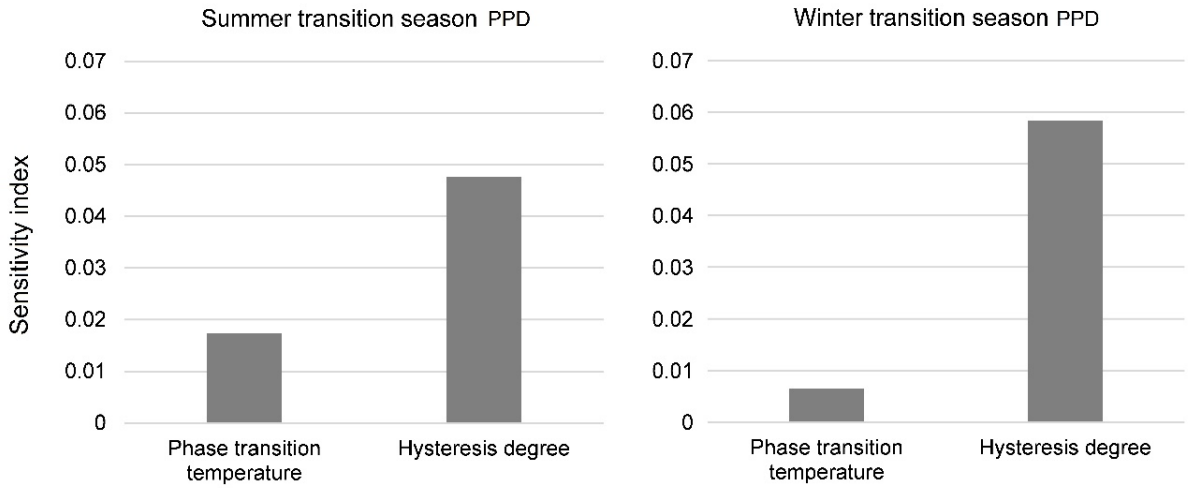

Figure 20 The sensitivity index of phase transition temperature and hysteresis degree on the PPD.

Similarly, another sensitivity analysis is done to show which parameter has a higher impact on indoor thermal comfort. The results are presented in Figure 20. It is shown that the hysteresis degree has a higher sensitivity index than phase transition temperature, especially during the winter transition season. However, the overall sensitivity indexes are not so high. One of the reasons may be the low air flow rate in the room.

4. Conclusions

Modeling of hysteresis of PCM in building simulation models is a recent trend even if the hysteresis phenomenon of PCM has long been tested and studied. This paper aims to take a deeper look into the phenomenon of PCM hysteresis, how the PCM hysteresis degree influences the building modeling works and its sensitivity compares to phase transition temperature.

PCM temperature hysteresis has been extensively observed in the literature. It is a feature of PCM, especially for the non-organic ones. However, few studies are found about the modeling of PCM hysteresis, and in those studies, the models are tested for only limited applications.

The study of PCMs with different phase transition temperature and hysteresis degree in a PCM enhanced ventilated window system for summer and winter applications during both severe seasons and transition seasons draws the conclusions below:

For severe summer season, the HVAC energy demand increases along with both increasing phase transition temperature and increasing hysteresis degree. For severe winter season, the HVAC energy demand increases with the increase of phase transition temperature, while decreases along with the increase of hysteresis degree. In total, the yearly HVAC energy demand increases with the increase of phase transition temperature, while decreases with the increase of hysteresis degree. The sensitivity analysis shows that the hysteresis degree has a high influence on the summer HVAC and winter HVAC energy demands, compared to the phase transition temperature. However, both parameters have a low influence on the yearly HVAC energy demand.

For transition seasons, the indoor thermal comfort is slightly influenced by the phase transition temperature for both summer and winter applications. The hysteresis degree, on the other hand, presents a much higher sensitivity than phase transition temperature. The indoor thermal comfort decreases along with the increasing hysteresis degree for both summer and winter applications.

Hysteresis degree should be paid more attention than phase transition temperature when selecting PCMs for a certain building application. For cooling purposes, the PCM with low hysteresis benefits more for reducing HVAC energy demand. For heating purposes, the PCM with high hysteresis is more applicable to reduce the HVAC energy demand. For transition seasons or the climate regions where the HVAC system is not necessary, the cases using PCMs with high hysteresis can have better indoor thermal comfort.

References

Ahmad M, Bontemps A, Sallée H, Quenard D (2006). Thermal testing and numerical simulation of a prototype cell using light wallboards coupling vacuum isolation panels and phase change material. Energy and Buildings 38, 673–681.

Alawadhi EM (2012). Using phase change materials in window shutter to reduce the solar heat gain. Energy and Buildings 47, 421–429. https://doi.org/10.1016/J.ENBUILD.2011.12.009

ASHRAE Standard (2004). Thermal Environmental Conditions for Human Occupancy.

Biswas K, Shukla Y, Desjarlais A, Rawal R (2018). Thermal characterization of full-scale PCM products and numerical simulations, including hysteresis, to evaluate energy impacts in an envelope application. Applied Thermal Engineering 138, 501–512. https://doi.org/10.1016/j.applthermaleng.2018.04.090

Bony J, Citherlet S (2007). Numerical model and experimental validation of heat storage with phase change materials. Energy and Buildings 39, 1065–1072. https://doi.org/10.1016/j.enbuild.2006.10.017

Carbonaro C, Cascone Y, Fantucci S, Serra V, Perino M, Dutto M (2015). Energy Assessment of A Pcm–Embedded Plaster: Embodied Energy Versus Operational Energy. Energy Procedia 78, 3210–3215. https://doi.org/10.1016/j.egypro.2015.11.782

Chandrasekharan R (2013). An Enhanced Simulation Model for Building Envelopes with Phase Change Materials. ASHRAE Transactions 119, C1–C10.

De Gracia A, Navarro L, Coma J, Serrano S, Romaní J, Pérez G, Cabeza LF (2018). Experimental set-up for testing active and passive systems for energy savings in buildings – Lessons learnt. Renewable and Sustainable Energy Reviews 82, 1014–1026.

Diaconu BM, Cruceru M (2010). Novel concept of composite phase change material wall system for year-round thermal energy savings 42, 1759–1772.

DuPontTM. (2007). Data Sheet - Measured Properties., n.d.

El Mays A, Ammar R, Hawa M, Akroush MA, Hachem F, Khaled M, Ramadan M (2017). Using phase change material in under floor heating. Energy Procedia 119, 806–811. https://doi.org/10.1016/J.EGYPRO.2017.07.101

European Parliament (2010). Directive 2010/31/EU of the European Parliament and of the Council of 19 May 2010 on the energy performance of buildings.

Fanger PO (1972). Thermal comfort: analysis and applications in environmental engineering. McGraw-Hill.

Feldman D, Banu D (1996). DSC analysis for the evaluation of an energy storing wallboard. Thermochimica Acta 272, 243–251. https://doi.org/10.1016/0040-6031(95)02456-5

Fleming E, Wen S, Shi L, da Silva AK (2013). Thermodynamic model of a thermal storage air conditioning system with dynamic behavior. Applied Energy 112, 160–169. https://doi.org/10.1016/J.APENERGY.2013.05.058

Gunasekara SN, Kumova S, Chiu JN, Martin V (2017). Experimental phase diagram of the dodecane–tridecane system as phase change material in cold storage. International Journal of Refrigeration 82, 130–140. https://doi.org/10.1016/j.ijrefrig.2017.06.003

Heat and cold storage with PCM (2008). , Heat and Mass Transfer. Springer Berlin Heidelberg, Berlin, Heidelberg. https://doi.org/10.1007/978-3-540-68557-9

Heiselberg P, Brohus H, Hesselholt A, Rasmussen H, Seinre E, Thomas S (2009). Application of sensitivity analysis in design of sustainable buildings. Renewable Energy 34, 2030–2036. https://doi.org/10.1016/J.RENENE.2009.02.016

Hichem N, Noureddine S, Nadia S, Djamila D (2013). Experimental and Numerical Study of a Usual Brick Filled with PCM to Improve the Thermal Inertia of Buildings. Energy Procedia 36, 766–775. https://doi.org/10.1016/j.egypro.2013.07.089

Hu Y, Guo R, Heiselberg P (2020). Control strategy optimization of a PCM enhanced ventilated window system by a combined experimental and numerical study. Renewable Energy Under revi.

Hu Y, Heiselberg P (2018). A new ventilated window with PCM heat exchanger – performance analysis and design optimization. Energy and Buildings. https://doi.org/10.1016/J.ENBUILD.2018.03.060

Hu Y, Heiselberg P, Guo R (2020). Ventilation cooling/heating performance of a PCM enhanced ventilated window - an experimental study. Energy and Buildings Under revi.

Hu Y, Heiselberg P, Johra H, Guo R (2019). Experimental and numerical study of a PCM solar air heat exchanger and its ventilation preheating effectiveness. Renewable Energy 145, Under review. https://doi.org/10.1016/J.RENENE.2019.05.115

Huang L, Günther E, Doetsch C, Mehling H (2010). Subcooling in PCM emulsions—Part 1: Experimental. Thermochimica Acta 509, 93–99. https://doi.org/10.1016/J.TCA.2010.06.006

Huang Z, Xie N, Luo Z, Gao X, Fang X, Fang Y, Zhang Z (2018). Characterization of medium-temperature phase change materials for solar thermal energy storage using temperature history method. Solar Energy Materials and Solar Cells 179, 152–160. https://doi.org/10.1016/j.solmat.2017.11.006

Höppe P (2002). Different aspects of assessing indoor and outdoor thermal comfort. Energy and Buildings 34, 661–665. https://doi.org/10.1016/S0378-7788(02)00017-8

International Energy Agency., Organisation for Economic Co-operation and Development. (2013). Transition to sustainable buildings : strategies and opportunities to 2050. OECD/IEA.

Iten M, Liu S, Shukla A, Silva PD (2017). Investigating the impact of Cp-T values determined by DSC on the PCM-CFD model. Applied Thermal Engineering 117, 65–75. https://doi.org/10.1016/J.APPLTHERMALENG.2017.02.021

Jaworski M, Łapka P, Furma P, Furmański P (2014). Numerical modelling and experimental studies of thermal behaviour of building integrated thermal energy storage unit in a form of a ceiling panel. Applied Energy 113, 548–557. https://doi.org/10.1016/j.apenergy.2013.07.068

Jensen SØ, Marszal-Pomianowska A, Lollini R, Pasut W, Knotzer A, Engelmann P, Stafford A, Reynders G (2017). IEA EBC Annex 67 Energy Flexible Buildings. Energy and Buildings 155, 25–34. https://doi.org/10.1016/J.ENBUILD.2017.08.044

Jin X, Xu X, Zhang X, Yin Y (2014). Determination of the PCM melting temperature range using DSC. Thermochimica Acta 595, 17–21. https://doi.org/10.1016/j.tca.2014.09.004

Johra H, Heiselberg P (2017). Influence of internal thermal mass on the indoor thermal dynamics and integration of phase change materials in furniture for building energy storage: A review. Renewable and Sustainable Energy Reviews 69, 19–32.

Johra H, Heiselberg PK, Le Dréau J, Dréau J Le (2018). Influence of envelope, structural thermal mass and indoor content on the building heating energy flexibility. Energy and Buildings 183, 325–339. https://doi.org/10.1016/j.enbuild.2018.11.012

Kabeel AE, Abdelgaied M (2018). Solar energy assisted desiccant air conditioning system with PCM as a thermal storage medium. Renewable Energy 122, 632–642. https://doi.org/10.1016/J.RENENE.2018.02.020

Kee SY, Munusamy Y, Ong KS (2018). Review of solar water heaters incorporating solid-liquid organic phase change materials as thermal storage. Applied Thermal Engineering 131, 455–471. https://doi.org/10.1016/J.APPLTHERMALENG.2017.12.032

Koschenz M, Lehmann B (2004). Development of a thermally activated ceiling panel with PCM for application in lightweight and retrofitted buildings. Energy and Buildings 36, 567–578. https://doi.org/10.1016/j.enbuild.2004.01.029

Kośny J (2015). PCM-Enhanced Building Components, Engineering Materials and Processes. Springer International Publishing, Cham. https://doi.org/10.1007/978-3-319-14286-9

Kusama Y, Ishidoya Y (2017). Thermal effects of a novel phase change material (PCM) plaster under different insulation and heating scenarios. Energy and Buildings 141, 226–237. https://doi.org/10.1016/j.enbuild.2017.02.033

Kuznik F, Virgone J (2009). Experimental investigation of wallboard containing phase change material: Data for validation of numerical modeling. Energy and Buildings 41, 561–570. https://doi.org/10.1016/J.ENBUILD.2008.11.022

Kuznik F, Virgone J, Johannes K (2011). In-situ study of thermal comfort enhancement in a renovated building equipped with phase change material wallboard. Renewable Energy 36, 1458–1462. https://doi.org/10.1016/j.renene.2010.11.008

Kuznik F, Virgone J, Roux JJ (2008). Energetic efficiency of room wall containing PCM wallboard: A full-scale experimental investigation. Energy and Buildings 40, 148–156. https://doi.org/10.1016/J.ENBUILD.2007.01.022

Lamberg P, Lehtiniemi R, Henell AM (2004). Numerical and experimental investigation of melting and freezing processes in phase change material storage. International Journal of Thermal Sciences 43, 277–287.

Lázaro A, Günther E, Mehling H, Hiebler S, Marín JM, Zalba B (2006). Verification of a T-history installation to measure enthalpy versus temperature curves of phase change materials. Measurement Science and Technology 17, 2168–2174. https://doi.org/10.1088/0957-0233/17/8/016

Medina MA, King JB, Zhang M (2008). On the heat transfer rate reduction of structural insulated panels (SIPs) outfitted with phase change materials (PCMs). Energy 33, 667–678. https://doi.org/10.1016/J.ENERGY.2007.11.003

Mosaffa AH, Garousi Farshi L (2016). Exergoeconomic and environmental analyses of an air conditioning system using thermal energy storage. Applied Energy 162, 515–526. https://doi.org/10.1016/J.APENERGY.2015.10.122

Pardiñas ÁÁ, Alonso MJ, Diz R, Kvalsvik KH, Fernández-Seara J (2017). State-of-the-art for the use of phase-change materials in tanks coupled with heat pumps. Energy and Buildings 140, 28–41. https://doi.org/10.1016/J.ENBUILD.2017.01.061

Pomianowski M, Heiselberg P, Jensen RL (2013). Full-scale investigation of the dynamic heat storage of concrete decks with PCM and enhanced heat transfer surface area. Energy and Buildings 59, 287–300. https://doi.org/10.1016/j.enbuild.2012.12.013

Pomianowski M, Heiselberg P, Jensen RL, Lund Jensen R (2012). Dynamic heat storage and cooling capacity of a concrete deck with PCM and thermally activated building system. Energy and Buildings 53, 96–107. https://doi.org/10.1016/j.enbuild.2012.07.007

Pomianowski M, Heiselberg P, Zhang Y (2013). Review of thermal energy storage technologies based on PCM application in buildings. Energy and Buildings 67, 56–69. https://doi.org/10.1016/j.enbuild.2013.08.006

Rathgeber C, Schmit H, Hennemann P, Hiebler S (2014). Calibration of a T-History calorimeter to measure enthalpy curves of phase change materials in the temperature range from 40 to 200. Measurement Science and Technology Meas. Sci. Technol 25, 35011–10. https://doi.org/10.1088/0957-0233/25/3/035011

Sharifi NP, Sakulich A (2015). Application of phase change materials to improve the thermal performance of cementitious material. Energy and Buildings 103, 83–95. https://doi.org/10.1016/J.ENBUILD.2015.06.040

Sharma A, Tyagi VV, Chen CR, Buddhi D (2009). Review on thermal energy storage with phase change materials and applications. Renewable and Sustainable Energy Reviews 13, 318–345.

Shilei L, Neng Z, Guohui F (2006). Impact of phase change wall room on indoor thermal environment in winter. Energy and Buildings 38, 18–24. https://doi.org/10.1016/J.ENBUILD.2005.02.007

Silva AS, Ghisi E (2020). Estimating the sensitivity of design variables in the thermal and energy performance of buildings through a systematic procedure. Journal of Cleaner Production 244, 118753. https://doi.org/10.1016/j.jclepro.2019.118753

Soares N, Costa JJ, Gaspar AR, Santos P (2013). Review of passive PCM latent heat thermal energy storage systems towards buildings' energy efficiency, Energy and Buildings. Elsevier. https://doi.org/10.1016/j.enbuild.2012.12.042

Stathopoulos N, El Mankibi M, Issoglio R, Michel P, Haghighat F (2016). Air–PCM heat exchanger for peak load management: Experimental and simulation. Solar Energy 132, 453–466. https://doi.org/10.1016/J.SOLENER.2016.03.030

Takeda S, Nagano K, Mochida T, Shimakura K, Shimakura K (2004). Development of a ventilation system utilizing thermal energy storage for granules containing phase change material. Solar Energy 77, 329–338. https://doi.org/10.1016/j.solener.2004.04.014

U.S. Green Building Council (2005). ISO 7730. Ergonomics of the thermal environment, Analytical determination and interpretation of thermal comfort using calculation of the PMV and PPD indices and local thermal comfort criteria.

Voelker C, Kornadt O, Ostry M (2007) Temperature reduction due to the application of phase change materials. https://doi.org/10.1016/j.enbuild.2007.07.008

Weinlaeder H, Koerner W, Heidenfelder M (2011). Monitoring results of an interior sun protection system with integrated latent heat storage. Energy and Buildings 43, 2468–2475. https://doi.org/10.1016/J.ENBUILD.2011.06.007

Weinläder H, Beck A, Fricke J (2005). PCM-facade-panel for daylighting and room heating. Solar Energy 78, 177–186. https://doi.org/10.1016/j.solener.2004.04.013

Wi S, Seo J, Jeong SG, Chang SJ, Kang Y, Kim S (2015). Thermal properties of shape-stabilized phase change materials using fatty acid ester and exfoliated graphite nanoplatelets for saving energy in buildings. Solar Energy Materials and Solar Cells 143, 168–173. https://doi.org/10.1016/j.solmat.2015.06.040

Xu X, Zhang Y, Lin K, Di H, Yang R (2005). Modeling and simulation on the thermal performance of shape-stabilized phase change material floor used in passive solar buildings. Energy and Buildings 37, 1084–1091. https://doi.org/10.1016/J.ENBUILD.2004.12.016

Yin D, Jia Y, Chen J, Zhang B (2018). Design of microencapsulated phase change material by one-step swelling polymerization in Pickering emulsion. Journal of Materials Science 53, 7249–7257.

Zhang C, Chen Y, Wu L, Shi M (2011). Thermal response of brick wall filled with phase change materials (PCM) under fluctuating outdoor temperatures. Energy and Buildings 43, 3514–3520. https://doi.org/10.1016/j.enbuild.2011.09.028

ISSN (online): 2446-1636
ISBN (online): 978-87-7210-622-9 AALBORG UNIVERSITY PRESS